University of Alberta

A Probabilistic Bottom-up Technique for Modeling and Simulation of
Residential Distributed Harmonic Sources

by

Chen Jiang

A thesis submitted to the Faculty of Graduate Studies and Research
in partial fulfillment of the requirements for the degree of

Master of Science

in

Power Engineering and Power Electronics

Electrical and Computer Engineering

©Chen Jiang
Spring 2012
Edmonton, Alberta

Abstract

The proliferation of energy-efficient appliances and modern consumer electronics has resulted in numerous power-electronic-based harmonic sources penetrating into residential households. Due to the huge number and wide adoption of these new harmonic sources, techniques for determining the cumulative harmonic impact of them are urgently needed.

A probabilistic bottom-up technique is proposed in this thesis to model aggregated harmonic sources and other linear loads. This technique not only takes into account appliances' daily usage pattern as well as household activities, but also provides the flexibility to represent future market trends and policy changes. By modeling the residential distribution systems with this technique, one can estimate how serious the harmonic impacts become when more harmonic-producing appliances penetrate into the residential loads.

The proposed technique has also been applied to evaluate the power quality impact of charging plug-in hybrid electric vehicles (PHEVs) on residential distribution systems.

Acknowledgements

First and foremost, I would like to show my deepest appreciation to my supervisor, Professor Wilsun Xu. I would have never conducted this work without his endless patience and tireless will to guide and supervise me. It has been my honor and privilege to be a student under his supervision.

As well, I should highly appreciate other professors from my M.Sc examining committee, Professor Venkata Dinavahi and Professor David Ryan, for their great support and valuable suggestions for my thesis revision.

I would like to thank all my colleagues for their friendship, and it was a great opportunity to work with them. I should express my special appreciation to Mr. Hui Wang and Mr. Diogo Salles Correa, for their selfless help during various stages of this project.

Finally, I should show my highest appreciation to my fiancée, Miss Ying Wang. She is the person who most loved and motivated me during the past two years. I would also like to express my gratitude to the love and support from my parents, Mrs. Yun Chen and Mr. Xiaobing Jiang. I dedicate this thesis to them all.

Contents

LIST OF TABLES

LIST OF FIGURES

Chapter 1

Introduction

As a power quality concern, the harmonics problem is a familiar issue in the study of power systems. Over the past two decades, because of the advent and development of power electronic technology, the electric power industry has been revolutionized. Power electronic-based devices are normally the main sources of power system harmonics, and significant efforts have been made in the field of harmonic analysis. A major concern about harmonic voltage and current distortion levels in urban distribution systems, which have the potential to exceed today's harmonic limits, is to continue to improve due to the increasing penetration of both energy-efficient and consumer electronic devices into residential loads. Therefore, a model is needed to represent these developments and to evaluate their impact. In this introductory chapter, the fundamentals of harmonics and the challenge of harmonic source evolution for harmonic analysis will be presented. At the end of this chapter, the thesis scope and outline will be provided.

1.1 The Fundamentals of Power System Harmonics

Normally, ac electric power system and its apparatuses are designed to operate with pure sinusoidal altering voltages and currents. In this ideal situation, power system will provide to the end customer a pure electricity supply with 50/60 Hz

voltage and current waveforms of the same sinusoidal shape. Hence, for most kinds of analysis, the power system is modeled as a linear system with passive elements excited by voltage sources, which are constant both in magnitude and frequency [1]. However, due to the existence of nonlinear and electronically switched loads in reality [2], the steady state ac voltage and current waveforms are no longer pure sinusoidal but distorted. These periodic distortions can be decomposed into a series of sinusoidal components called harmonics, which are with frequencies multiple times of fundamental [3]. Harmonics have existed since the adoption of ac for electricity transmission, but did not become a major concern until the widespread use of power electronic devices. As a result, harmonic studies have become an important component of power system analysis and design [4].

1.1.1 The Definition and Mathematical Basis of Harmonics

Harmonics are a mathematical expression of steady state and periodic distorted voltage or current waveforms. According to the Fourier theory, a periodic function $f(t)$ with a fundamental angular frequency w_0 can be represented by a trigonometric series as [5]:

$$f(t) = c_0 + \sum_{h=1}^{\infty} c_h \cos(h w_0 t + f_h) \tag{1.1}$$

where the angular frequency is $w_0 = 2p/T$, and T is the period of $f(t)$. The coefficients c_h, f_h and c_0 are defined as:

$$C_h = c_h \angle f_h = \frac{1}{T} \int_{-T/2}^{T/2} f(t)e^{-jhw_0t}dt \qquad (1.2)$$

$$c_0 = \frac{1}{T} \int_{-T/2}^{T/2} f(t)dt \qquad (1.3)$$

Since the function $f(t)$ has been decomposed into a series of sinusoidal components with different frequencies, hw_0 is called the *h-th* harmonic of $f(t)$. c_0 is the magnitude of the dc component, while c_h and f_h are the *h-th* order harmonic magnitude and phase angle, respectively. Under the above definition, the root mean value (RMS) of $f(t)$ is as follows:

$$RMS = \sqrt{c_0^2 + \sum_{h=1}^{\infty}\left(\frac{c_h}{\sqrt{2}}\right)^2} \qquad (1.4)$$

When harmonics combine, they cause the voltage or current waveforms to become distorted. Figure 1.1 shows an example of a distorted current waveform and its harmonic components generated by a non-linear load. In order to provide a clear understanding of this phenomenon, the decomposed fundamental and the 5th harmonic components are also shown in the waveform.

(a) Current waveform   (b) Harmonic spectrum of current waveform
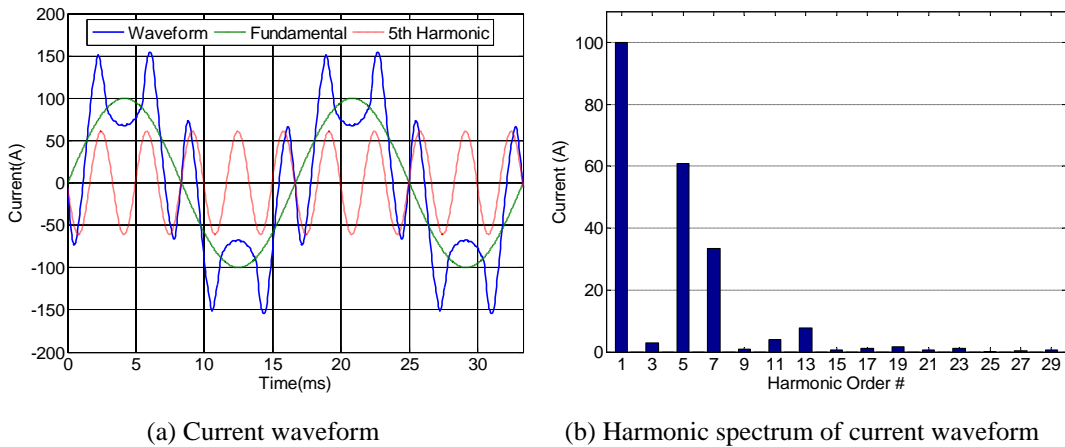
Figure 1.1 Typical distorted current waveform and its harmonic spectrum.

1.1.2 Harmonic Indices

When describing the main harmonic feature of a distorted waveform, it is inconvenient to use the coefficient series c_h defined in equation (1.2). In order to give an overall expression of the significance of the harmonic distortion in voltage or current waveform, a group of harmonic indices have been developed.

The most commonly used index to characterize the level of harmonic distortion is called the total harmonic distortion (THD), or the distortion factor [2]. The THD index is normally expressed as a percentage, and measures the relative magnitude of all harmonic components compared to that of fundamental. According to IEEE standards [6], the voltage and current THD can be determined as follows:

$$THD_V(\%) = \frac{\sqrt{\sum_{h=2}^{H} V_h^2}}{V_1} \times 100 \tag{1.5}$$

$$THD_I(\%) = \frac{\sqrt{\sum_{h=2}^{H} I_h^2}}{I_1} \times 100 \tag{1.6}$$

where V_1 and I_1 are the fundamental components of the measured voltage and current, and V_h and I_h are the corresponding *h-th* harmonic components.

However, applying the THD index to characterize harmonic current can be inappropriate in some cases, especially when fundamental current approaches zero. In this case, the resulting THD could be quite high but would not truly

4

represent the harmonic level of the measured point. Therefore, the total demand

distortion (TDD) is used specifically for harmonic currents, and is defined as [6]:

$$TDD = \frac{\sqrt{\sum_{h=2}^{H} I_h^2}}{I_L}$$ (1.7)

where I_L is the peak or maximum demand load current at the fundamental

frequency.

According to IEEE Std 519 [6], harmonic voltage distortion in power systems

with a voltage level of 69 kV or less is limited to 5% of the THD. The current

TDD limits vary based on the short circuit strength of the system injected into; the

higher the ratio of the short circuit current level to the maximum load current, the

more harmonic currents the system can handle. Generally, the TDD limitation

varies between 5% and 20%.

The transformer K-factor is the weighting of the harmonic load currents according

to their effects on transformer heating, and is based on the assumption that

transformer high-frequency harmonic winding losses are proportional to the

square of the frequency. A K-factor of 1.0 indicates a linear load (no harmonics).

The higher the K-factor, the higher is the harmonic tolerance level of the

transformer needed to supply such a load. K-factor can be calculated from

expression below [6]:

$$K = \frac{\sum_{h=1}^{H} h^2 (I_h / I_1)^2}{\sum_{h=1}^{H} (I_h / I_1)^2}$$ (1.8)

In some cases such as those involving harmonic telephone interference, instead of the THD or the TDD, the actual harmonic level is normally more useful for analysis. As a result, $V \cdot T$ or $I \cdot T$ products are introduced as a measure of harmonic interference audio circuits and are defined as follows [6]:

$$V \cdot T = \sqrt{\sum_{h=1}^{\infty}(w_h V_h)^2} \ \ or \ I \cdot T = \sqrt{\sum_{h=1}^{\infty}(w_h I_h)^2} \tag{1.9}$$

where w_h is a weighting factor accounting for the audio and inductive coupling effects at the *h-th* harmonic frequency. In addition, other indices such as the Telephone Interference Factor (TIF) have also been proposed for the same purpose as that of $V \cdot T$ and $I \cdot T$ products [6].

1.1.3 Techniques for Harmonic Modeling and Analysis

To evaluate the harmonic distortion levels at any location of a power system, certain techniques are essential. First, adequate models need to be built for the power system components, which should consider the component response characteristics at the harmonic frequency. The modeling techniques for the overhead lines, underground cables, transformers, rotating machines, and the aggregated loads are well summarized in [7]. Additionally, the modeling of residential loads for harmonic analysis will be discussed in the following chapter, as one focus of this thesis.

After models of the power system components have been built, the next step is to develop a network solution for harmonic analysis. The harmonic power flow is the appropriate solution for determining the harmonic distortion levels and checking the compliance with harmonic limits. Over the past twenty years, considerable progress has been made in conducting the harmonic power flow for a power system, and several sound techniques have been proposed in [8], [9]. A general non-iterative harmonic power flow solution is summarized as follows [7]:

Step 1: Conduct the network fundamental frequency power flow, and model the harmonic sources as constant PQ loads.

Step 2: Determine the harmonic current source models for harmonic sources based on the result of the fundamental power flow. The magnitude and phase angle of the harmonic current source can be determined by using the following formulas, respectively:

$$I_h = I_1 \frac{I_{h-spectrum}}{I_{1-spectrum}} \tag{1.10}$$

$$q_h = q_{h-spectrum} + h(q_1 - q_{1-spectrum}) \tag{1.11}$$

Step 3: Calculate the network harmonic voltages and currents by solving network nodal equations corresponding to harmonic order h:

$$[Y_h][V_h] = [I_h] \tag{1.12}$$

Equation (1.12) needs to be solved for all the harmonics of interest.

Step 4: The results of Step 1 and Step 3 jointly provide the harmonic power flow solution for the system of interest. Harmonic indices could be conducted, and the distortion levels could be evaluated based on the above results.

However, in some non-typical conditions, advanced solution algorithms for the harmonic power flow, such as the iterative harmonic method [8] or the Newton-Paphson based method [9], are necessary in order to give adequate results. Additionally, all of the solution methods mentioned above have been extended to unbalanced three-phase systems by rebuilding the system and component equations in the multi-phase domain [10]. In this thesis, a multi-phase harmonic load flow method (MHLF) will be adopted in most of the analysis, due to its ability to handle a typical North American multi-phase distribution system including neutral wire with unbalanced operating conditions.

1.2 Harmonic Source Evolution and the Challenge to Harmonic Analysis

As mentioned in the previous section, researchers have been interested in harmonic problems since almost the early 1900s. In order to meet the requirements of High Voltage Direct Current (HVDC) systems and Static Var Compensators (SVC), harmonic modeling and analysis techniques were

specialized for these applications. Since the early 1970s, researchers have been increasingly interested in power system harmonics due to the widespread use of static power converters [2]. Generally, this interest has reflected the fact that power system harmonics are produced mainly from loads which are large and concentrated in a few determined locations. Therefore, within this period, the focus has been on the network-wide harmonic power flow analysis with dominant harmonic sources.

However, harmonic sources are currently evolving from concentrated to distributed, and also from industry loads to residential loads. These distributed harmonic sources include both energy-efficient and consumer electronics devices, which are massively penetrating into residential households. Although these power-electronic-based appliances are small individually, together, they produce significant harmonics. Additionally, plug-in electric vehicles, especially plug-in hybrid electric vehicles (PHEVs), have the potential to be another main harmonic-producing load in residential households. These vehicles are normally charged by charger systems with the power-switching circuit topology shown in Figure 1.2. The typical power level of one charger system could reach up to 3.3 kW, with a THD current of around 10%.
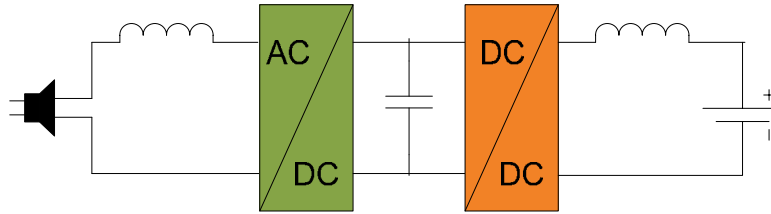
Figure 1.2 General Overview of PHEV Charger System.

The evolution of harmonic sources may create many problems and challenges for harmonic analysis, mainly due to the nature of these new sources. As mentioned in the last paragraph, the first problem results from the distributed nature of harmonic sources. Since residential harmonic sources are distributed all over an electric network, traditional harmonic analysis techniques generally have difficulty in determining the collective impact of these sources [7]. Moreover, the randomness of harmonic sources also needs to be considered and could make analysis more complicated. This complexity can be illustrated by the following scenario: numerous harmonic-producing loads are distributed at every location of a distribution system, so that, at any time instant, the harmonic summation of the system could be very different due to the random operation of the harmonic sources.

Some work has been done on using statistical methods to determine the summation impact of distributed random harmonic sources [11], [12]. Researchers agree that if a sufficiently large number of harmonic sources are present in a system, the summation of the harmonic current phasors should follow

10

the normal distribution, regardless of the distributions of individual harmonic phasors. However, what we are interested is the magnitudes of the current or voltage as well as the THD, which are functions of the harmonic current phasors. In this case, the distributions of these indices cannot necessarily be characterized by the normal distribution or any known simple distribution. Another disadvantage of these statistical methods is that their results lack time information, yet understanding the time trends of some harmonic indices in such harmonic analysis is essential.

In this thesis, a bottom-up approach is selected to model aggregated harmonic sources and other linear loads. Basically, we develop individual models for each component of an actual electric system, and every distributed harmonic source and its location are modeled. The random operation of each component including the harmonic source is modeled by the daily time of use probability functions, and will be further discussed in following chapters. By this method, we aim to build an appropriate harmonic model for residential loads and to provide a framework to evaluate the impact of all kinds of harmonic sources on residential distribution systems.

1.3 Thesis Scope and Outline

This thesis develops a method to model the residential harmonic loads, and then evaluates the impact of these harmonic sources on residential distribution

networks. Most of the past research on harmonic modeling and analysis has focused on a few large dominant harmonic sources, which are normally industrial loads. Currently, however, the mass penetration of both energy-efficient and consumer electronic devices is resulting in significant distortions to the voltage and current waveforms in residential distribution systems. The waveform distortions in urban distribution systems are also increasingly being dominated by the harmonics from distributed residential loads. For example, the 3rd harmonic has become a main contributor to the feeder voltage distortion, and the 9th harmonic has caused telephone interference in a number of cases.

The utilities and researchers are extremely concerned about this situation. Two key questions are

- Is the current distribution system capable of accepting more nonlinear loads?
- What could be the consequences of excessive harmonic loads?

A fundamental step towards answering these questions is to develop a tool that can assess and predict harmonic distortion levels for the current and future power distribution systems. In this context, the final objective of this thesis is to provide our study results and a basic understanding of the potential problems caused by the modern nonlinear residential loads. More specifically, this thesis will try to answer the following questions:

- What are the potential power quality impacts of mass distributed nonlinear loads on residential distribution systems? Sample impacts include voltage distortion, zero sequence harmonics, neutral voltage/current rise, harmonic-caused stray voltages, metering error, increased losses, and overloading of distribution transformers.

- How serious will the impacts become when more and more energy-efficient appliances and consumer electronics penetrate into the residential loads?

- What are the technical and economic implications for utilities?

This thesis is organized in six chapters as follows:

Chapter 2 presents the customer trends and electrical characteristics of common home appliances. By surveying and analyzing various consumer market research data, the adoption or usage trends of key home appliances have been established. Based on the findings of previous and additional research, harmonic models have been developed for home appliances.

A bottom-up harmonic probabilistic model for residential houses based on the information associated with the individual appliances is presented in Chapter 3. The proposed house model takes into account appliances' usage patterns as well as the number of occupants and their activities. Finally, by combining the

residential house harmonic model, a service transformer model is also derived. These models are verified by comparing their results with measurements.

Chapter 4 presents the modeling of residential distribution systems to evaluate the impact of the distributed nonlinear residential loads on the *secondary distribution system*. Next, the procedure to carry out the harmonic power flow simulations is developed. The simulation results are depicted for different study scenarios. First, a base case is evaluated to verify if the proposed modeling approaches give adequate results. Then, a load growth scenario based on the appliance penetration trends established in Chapter 2 is evaluated in order to determine how serious the impacts become when more appliances penetrate into the residential loads. Finally, a sensitivity study is carried out to evaluate the impact of the system parameters variation on the harmonic levels.

Chapter 5 is mainly about the harmonic as well as other power quality impacts of charging plug-in hybrid vehicles (PHEV) on residential distribution networks. First, the modeling of PHEV charging loads is developed based on the charging characteristics. Similar as in Chapter 3, PHEV daily charging pattern will be considered in the model. Then, the procedure to integrate the PHEV charging loads into the residential distribution network used in Chapter 4 is provided. Finally, the simulation results are conducted at different vehicle penetration levels with various charger types under different charging strategies, and conclusions are drawn.

The main conclusion from this thesis, suggestions for future studies and improvements are presented in Chapter 6.

Chapter 2

Evolution of Residential Loads and Their Electrical

Models

In order to develop a tool that can evaluate the impact of distributed nonlinear residential loads on primary and secondary power distribution systems, the initial step is to develop adequate models for those residential loads. In this chapter, we will divide such models into two aspects. One is the usage trend model and the other is the electrical model. The first model helps to predict the extent of home appliance adoptions in the future, while the second one is essential for representing the appliance in typical harmonic power flow study.

2.1 Customer Trends for Home Appliances

As many countries have placed lighting and appliance standards at a very high priority of energy policy, more and more replacement of such appliances into energy-efficient ones will happen in the next few years. Although these appliances consume considerably less power than their old counterpart, they inject relatively large amount of harmonics into the distribution feeders. In the meantime, more and more consumer electronics will be also added into household as another harmonic producing source. Due to above reasons, we need to consider

the impact of appliances replacement or increasing adoption on the residential loads harmonic penetration.

Therefore, in the following subsections, a study is conducted to estimate the usage or consumer trends of harmonic-producing home appliances, which is important for the utilities to understand how the harmonic voltage/current levels will evolve in the next 5 or 10 years. By analyzing the market survey data for key consumer electronics and home appliances, their trend models will be established.

However, since it is impossible to predict the future situation exactly based on past information, our trends models are mainly used to demonstrate the usefulness of the bottom-up modeling technique proposed later.

2.1.1 Lighting Appliances

According to a report published by IEA [13], in the year of 2002, households had an average of 1 CFL and 36 Incandescent bulbs. In 2007, a large survey comprising 34,750 households found an average of 3.37 CFLs per household [14]. Using these two data points, it is possible to estimate the past trend of CFLs penetration. Assuming that the total number of bulbs per household remains constant, one can keep track of the remaining incandescent lamps to be replaced in every year of the forecast, which is shown in Figure 2.1(a) ([15]). According to

17

the estimation, nowadays, 13.5% of the residential installed lamps are CFLs while incandescent lamps will disappear by 2020.

However, according to a report by Lawrence Berkeley National Laboratory, a bill mandating the phase out of incandescent lighting has been passed by U.S. Congress in 2007 as part of the Energy Independence and Security Act (EISA) [15]. As a result, incandescent bulbs will vanish more quickly in U.S. than above estimated. Figure 2.1(b) below indicates that part of the market of incandescent lights will be phased out each year between 2012 and 2014, until their complete ban in 2014. When CFL bulbs completely replace the incandescent bulbs, the associated lighting consumption can be reduced by 70%.

(a) Incandescent bulbs (GSIL) phase out before EISA.

(b) Incandescent bulbs (GSIL) phase out after EISA.
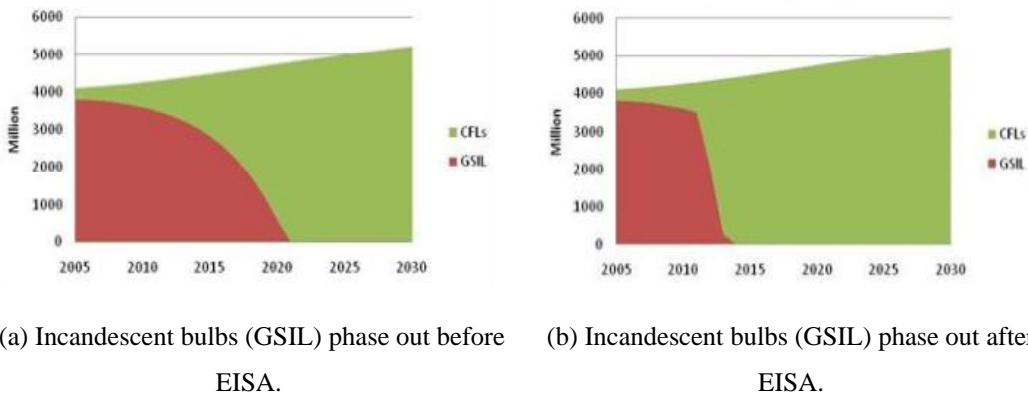
Figure 2.1 Market projection of lighting bulbs by technology type.

In this thesis, the trend of CFL adoption by homes is built from the trend shown in Figure 2.1(a) and the data from references [13], [14]. In the next 10 years, the average number of CFLs and incandescent bulbs is given by Figure 2.2 and Figure 2.3, respectively. These trends are used to represent the lighting appliance situation of a typical Canadian household.

18
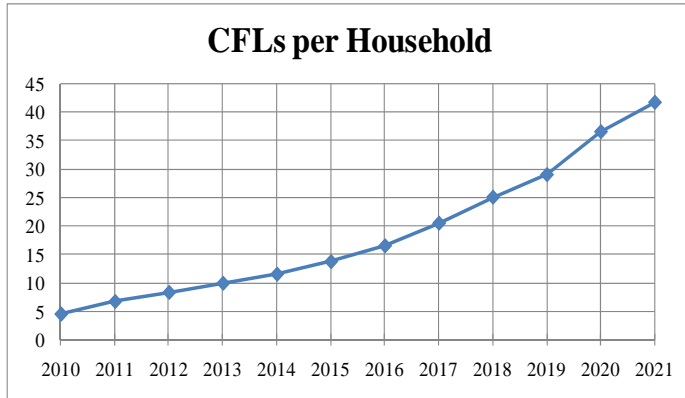
Year	CFLs per Household
2010	4.55
2011	6.73
2012	8.33
2013	9.92
2014	11.52
2015	13.70
2016	16.47
2017	20.43
2018	24.97
2019	28.93
2020	36.42
2021	41.55

Figure 2.2 Trend of CFLs per household.
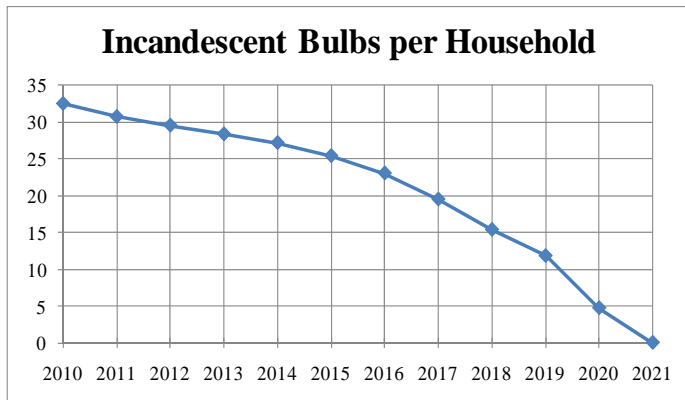
Year	Incandescent Bulbs per Household
2010	32.45
2011	30.68
2012	29.50
2013	28.32
2014	27.14
2015	25.37
2016	23.01
2017	19.47
2018	15.34
2019	11.80
2020	4.72
2021	0

Figure 2.3 Trend of incandescent light bulbs per household.

2.1.2 Televisions

Televisions have been changing rapidly in recent years as the transition from analog broadcasting to digital broadcasting accelerates. As a result, CRTs' share has been getting smaller and replaced by LCD (including LED-backlit) and Plasma (PDP) displays, which have the nature advantage of providing digital media. As shown in Figure 2.4, in the year of 2007, half of the market was

19

dominated by CRT and half by LCD and Plasma [16]. Moreover, one can observe that CRT TV will be eliminated by year 2014.
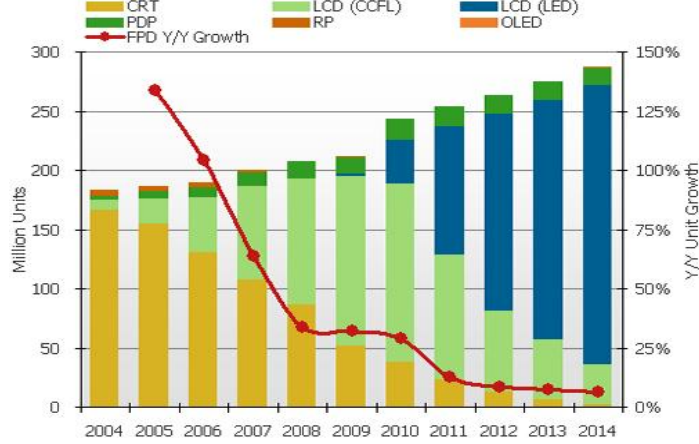
Figure 2.4 Worldwide TV market share by technology type.

The average number of TV sets in US household is 2.24, which is also the situation in Canada. The typical lifespan of television is 5 to 6 years. Assuming people would change their TV set every 6 years, the different types of TVs' penetration in one year will only be affected by the TV sales of the past 6 years. Information about the annual sales of each TV can be found on Figure 2.4. For the years after 2014, it was assumed the sales are the same as the year 2014, as predictions after this year were not found in the literature. Therefore, for each type, the number of TV per household, for year i, can be calculated as follows:

$$TVH^{typeY}(i) = \frac{SP^{typeY}(i-5) \times TS(i-5) + ... + SP^{typeY}(i) \times TS(i)}{TS(i-5) + ... + TS(i)} \times NTV \qquad (2.1)$$

where,

- TVH^{typeY} is the number of TVs of type Y per household.

20

- NTV is the average number of TVs, including all types, per household.
- SP^{typeY} is the ratio between sales of TVs of type Y and the total sales of all types of TV, which is given by TS.

Therefore, according to the above equation and assuming the average number of TVs per household (NTV) is fixed during the next 10 years, the number of LCD and CRT per household can be estimated and is shown in Figure 2.5 and Figure 2.6, respectively.

Year	LCD TV per Household
2010	1.11
2011	1.41
2012	1.68
2013	1.88
2014	2.03
2015	2.11
2016	2.18
2017	2.21
2018	2.23
2019	2.24
2020	2.24
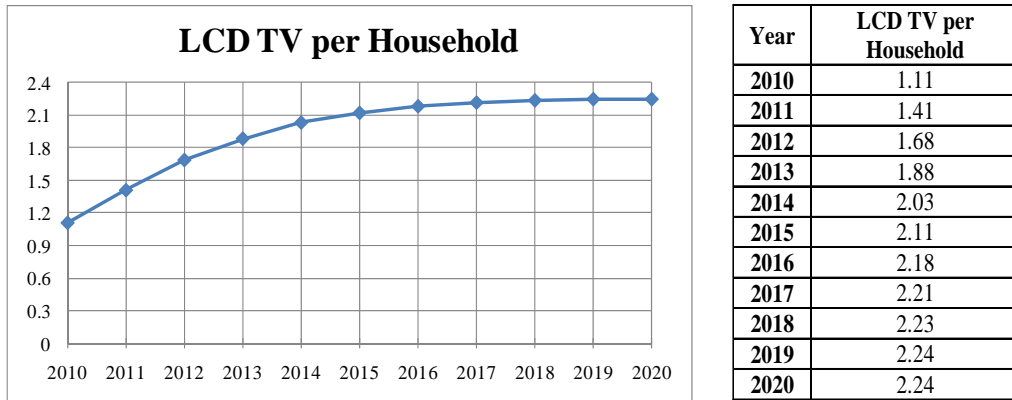
Figure 2.5 Trend of the number of LCD TV per household.

Year	CRT TV per Household
2010	1.13
2011	0.83
2012	0.55
2013	0.36
2014	0.21
2015	0.13
2016	0.06
2017	0.03
2018	0.01
2019	0
2020	0
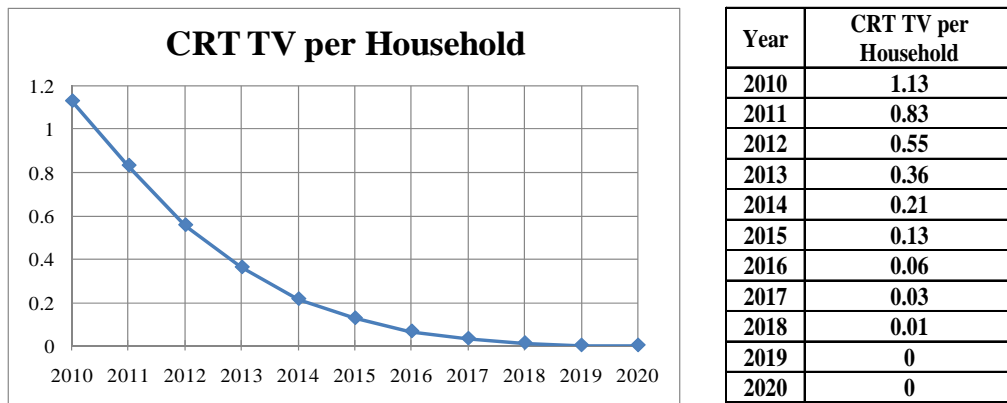
Figure 2.6 Trend on the number of CRT TV per household.

21

According to the measurement results, discussed in the next section, the current of CRT TV contains much more harmonics than that of LCD. Hence if the CRT TV is replaced by the LCD TV, the collective harmonic impact from TV appliances is expected to decrease. It is worth noting that the LCD TV also consumes less power which will also be considered in the simulation studies.

2.1.3 Personal Computers

Industry practice uses the indicator of *Computer Ownership per Person* (CP) [17], [18], instead of *Computers per Household* (CH). So in order to determine CH, the following equation can be used:

$$CH = CP \times APH \tag{2.2}$$

in which, APH is the Average Population per Household.

The Economist does a lot of marketing research over the world and its annual publication "*Pocket World in Figures*" [17] has a worldwide survey on computer ownership. In order to estimate the future trend of computers per household, the data from years 2006 and 2010 were sampled from [17], which gives:

Year 2006: Computers per Person (CP) for North America = 0.773

Average population per household (APH) for North America = 2.72

$$CH = CP \times APH = 0.773 \times 2.72 = 2.10 \text{ (computers/household)}$$

Year 2010: CP for North America = 0.98

22

APH for North America = 2.72

$$CH=CP\times APH=0.98\times 2.72=2.67 \text{ (computers/household)}$$

The above will yield an estimated annual growth rate of computers per household of 5.95%. With this rate, CH can be estimated for the next 10 years and it is illustrated at Figure 2.7.

Computers per Household

Year	Computers per Household
2010	2.67
2011	2.82
2012	2.99
2013	3.17
2014	3.36
2015	3.56
2016	3.77
2017	3.99
2018	4.23
2019	4.48
2020	4.75
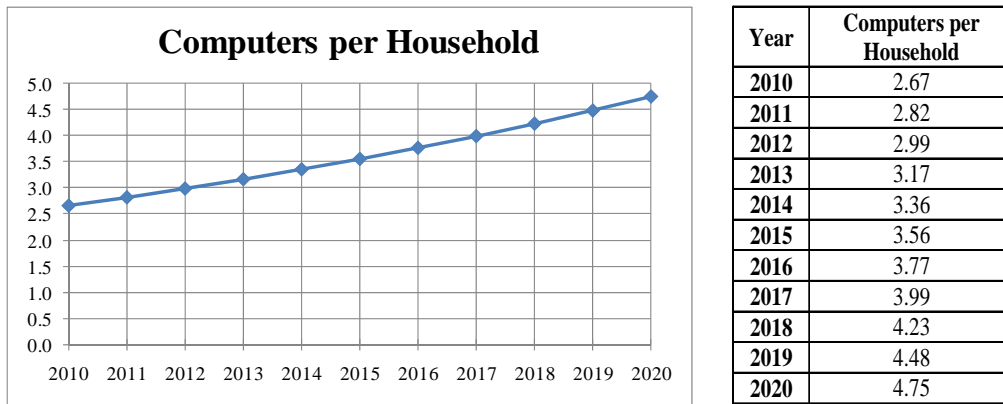
Figure 2.7 Trend on the number of computers per household.

Regarding laptop ownership, a research done by Ipsos Reid [19] showed that Canadian laptop ownership jumped from 0.43 in 2007 to 0.59 per person in 2010, which means *Laptop per Household* (LH) in 2007 was (APH in Canada is 2.5):

$$LH=LP\times APH=0.43\times 2.5=1.075 \text{ (laptops/household)}$$

LH in 2010 was:

$$LH=LP\times APH=0.59\times 2.5=1.475 \text{ (laptops/household)}$$

The corresponding annual growth rate is 11.1%. Based on this rate, the LH index can be estimated for the next 10 years and it is shown in Figure 2.8.

Laptops per Household
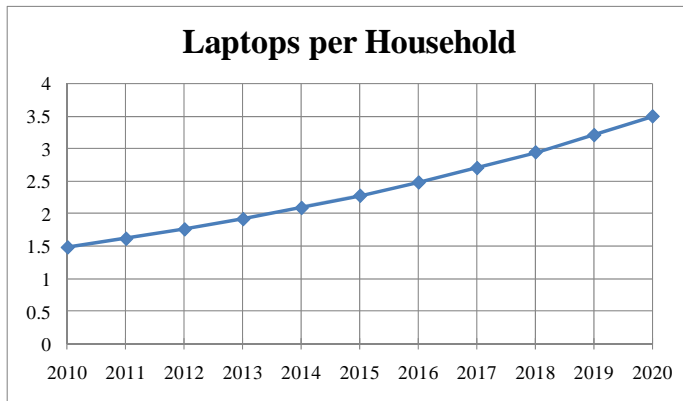
Year	Laptops per Household
2010	1.48
2011	1.61
2012	1.75
2013	1.91
2014	2.08
2015	2.27
2016	2.47
2017	2.70
2018	2.94
2019	3.20
2020	3.49

Figure 2.8 Trend on the number of laptops per household.

To calculate the number of desktops per household, the curve of Figure 2.8 is subtracted from the curve of Figure 2.7. The result is shown in Figure 2.9.

Desktops per Household
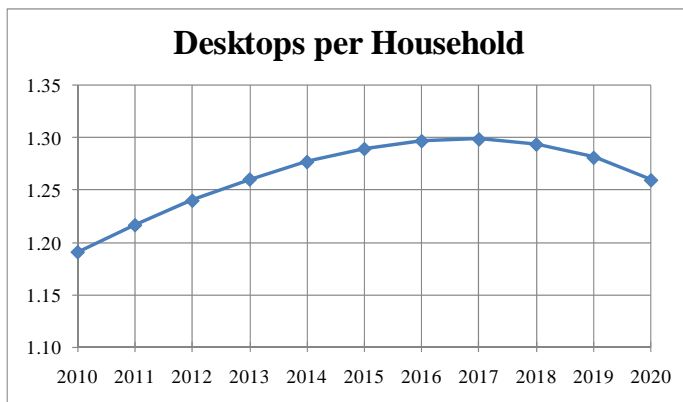
Year	Desktops per Household
2010	1.19
2011	1.22
2012	1.24
2013	1.26
2014	1.28
2015	1.29
2016	1.30
2017	1.30
2018	1.29
2019	1.28
2020	1.26

Figure 2.9 Trend on the number of desktops per household.

This indicates that desktops ownership will change slightly at around 1 per household. This result is consistent with other findings. According to an article from '*Ars Technica*' [20], industry analysts predicted that notebooks sales would

24

exceed desktop sales for the first time in 2008. By 2011, it expected laptops to represent 66% of corporate purchases, with 71% of consumers opting for a notebook instead of a desktop. The increasing demand of laptops is also fuelled by the education market — an increasingly large number of educational institutions are stimulating students to buy laptop since its cost has been decreasing significantly in the last years.

2.1.4 Home Printers

Printer ownership data has not been found on the literature. However, literature search showed that printer sales in the 2nd quarter of 2006 in US were 1,763,201. Meanwhile, the US PC sales in the 4th quarter of 2006 were 15,866,000 [21]. Hence, printers installed per computer (PPC) are:

$$PPC = \frac{Printer\ Shipment}{PC\ Shipment} = \frac{1763201}{15866000} = 0.111 \text{ (printers per PC)}$$

The above data presents a possible estimate of the printer use in homes. It is noted that printers' growth rate could be higher than PC as the above rate includes printers used for business and home. Assuming that the printers' ownership is associated with the PC ownership, the trend index *Printers per Household* (PH) is given by:

$$PH = 0.111 \times CH \tag{2.3}$$

The resulting estimation of printers per household for the next several years is illustrated in Figure 2.10.

Printers per Household

Year	Printers per Household
2010	0.30
2011	0.31
2012	0.33
2013	0.35
2014	0.37
2015	0.40
2016	0.42
2017	0.44
2018	0.47
2019	0.50
2020	0.53
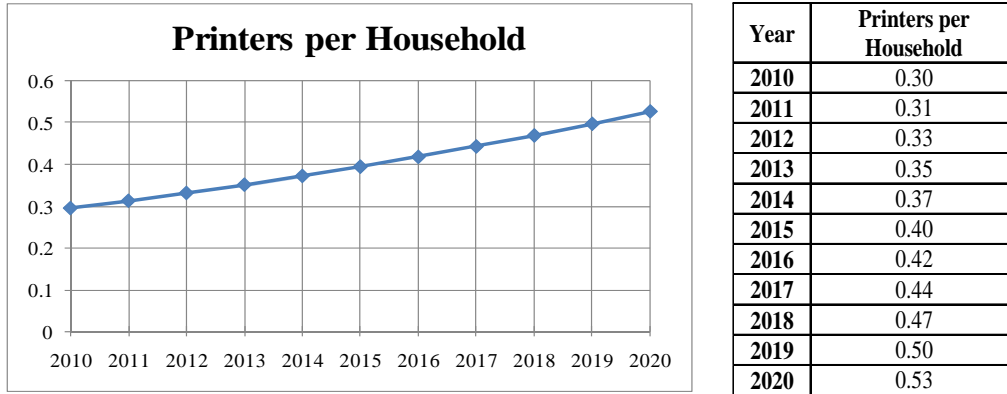
Figure 2.10 Trend on the number of printers per household.

2.1.5 Major Appliances

In this thesis, major appliances stand for fridge, freezer, clothes washer, electric cloth dryer and electric range. In Canada, these appliances are under governmental regulation, and the information regarding each appliance penetration per household can be obtained from NRCan (Nature Resources Canada) [22]. According to its report, the biggest change of major appliances between 1990 and 2006 is the significant improvement towards energy efficiency. In this thesis, electric dryer and range are treated as linear impedance load, so their replacement has no impact on the harmonic current penetration. However, if the motor based appliances, such as washers, fridges and freezers, are changed to newer models, an impact on harmonic levels is expected. Figure 2.11 shows the average number of fridges and washers per household, which is quite constant for both.
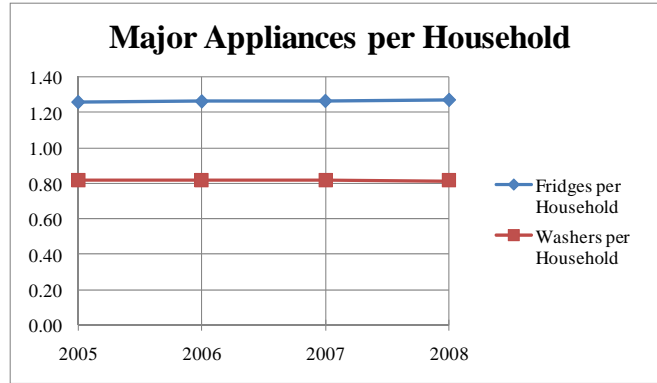
Figure 2.11 Trends on the number of fridges and washers per household.

Figure 2.12 indicates that refrigerators are tending to perform better at power consumption. In 1990, no refrigerator consumed less than 30 kWh/cu.ft. per year. By 2006, 88.6 percent of fridges consumed less than 30 kWh/cu.ft. per year and 97.1 percent consumed less than 40 kWh/cu.ft. [22]. Based on previous data, estimation for future trend is made and shown in Figure 2.13. For example, in 2008, almost all fridges on market consumed less than 30 kWh/cu.ft. per year.

Model Year	kWh/cu. ft. per year							
	<30 (%)	30–39.9 (%)	40–49.9 (%)	50–59.9 (%)	60–69.9 (%)	70–79.9 (%)	80–89.9 (%)	≥90 (%)
1990	0.0	1.5	3.9	15.3	60.2	15.4	3.0	0.7
1991	0.0	2.9	10.7	26.9	41.3	12.2	3.6	2.4
1992	0.0	4.8	26.9	33.2	16.0	10.4	4.0	4.8
1993	0.1	51.0	29.7	9.1	1.4	4.2	1.9	2.6
1994	0.4	70.9	22.4	4.0	0.0	0.0	1.7	0.6
1995	2.8	63.3	29.3	1.6	0.0	0.1	2.5	0.5
1996	6.6	60.0	31.2	0.9	0.1	0.0	0.7	0.4
1997	6.9	60.4	31.4	0.9	0.1	0.0	0.2	0.1
1998	5.9	62.4	27.1	0.8	0.0	0.6	2.9	0.2
1999	8.4	61.2	25.0	0.6	0.2	0.7	3.4	0.6
2000	12.2	57.4	23.6	0.9	0.4	0.7	3.6	1.2
2001	44.5	34.5	12.7	1.3	0.8	4.0	0.7	1.5
2002	64.3	26.6	3.1	0.2	0.0	3.9	0.2	1.7
2003	78.4	15.5	1.6	0.2	0.2	2.8	0.2	1.0
2004	82.6	11.0	1.3	0.2	0.2	1.2	3.0	0.7
2005	86.7	6.5	0.2	0.2	0.6	3.3	1.8	0.7
2006	88.6	8.5	0.9	0.3	0.2	0.9	0.1	0.5
Total Change	88.6	7.0	3.0	15.0	60.0	14.5	2.9	0.2

Figure 2.12 Average annual unit energy consumption per cubic foot of fridges.
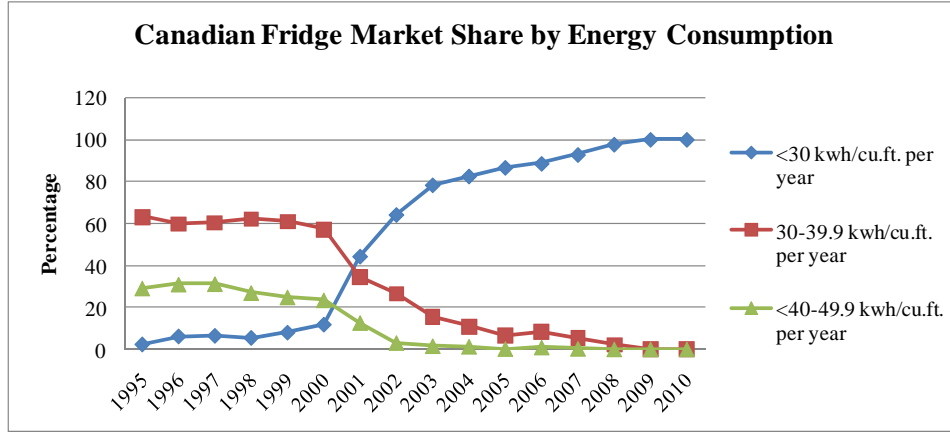
Figure 2.13 Canadian fridge market share by energy consumption.

With the increased usage of ASD-based (Adjustable Speed Drive) fridges, there will be a significant change in harmonic current producing due to the power electronic based drive. According to [23], the THD of current can reach as high as 136% when operated at reduced speed. If ASD-based fridge is replaced, it is expected that significant incremental harmonic currents will be injected into the distribution system.

The typical lifespan of fridge is 15 years, which means that the different types of fridges' penetration in household in a certain year is related to the last 15 years:

$$FRIH^{typeY}(i) = \frac{SP^{typeY}(i-15) \times TS(i-15) + ... + SP^{typeY}(i) \times TS(i)}{TS(i-15) + ... + TS(i)} \times NFRI \qquad (2.4)$$

where,

- $FRIH^{typeY}$ is the number of fridges of type Y per household.
- $NFRI$ is the average number of fridges, including all types, per household

28

- SP^{typeY} is the ratio between sales of fridges of type Y and the total sales of all types of fridges, which is given by TS

It is assumed that the total fridge sales every year is fixed. If fridges with energy consumption less than 30 kwh/cu.ft. per year are categorized as energy conservation type, the estimated fridge household penetration for energy conservation ones and regular ones is shown in Figure 2.14 and Figure 2.15, respectively.

Energy Conservation Fridge per Household
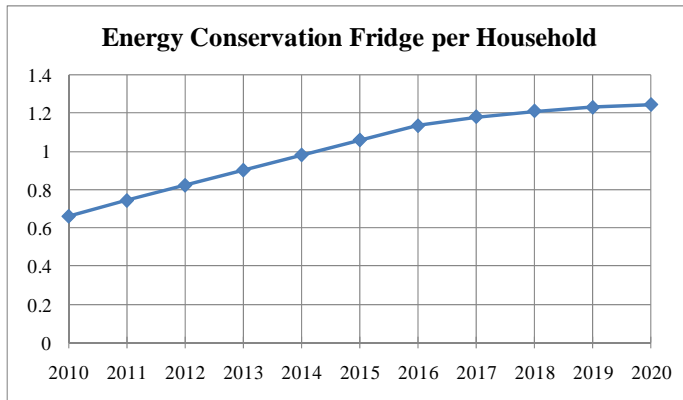
Year	Energy Cons. Fridges per Household
2010	0.66
2011	0.74
2012	0.82
2013	0.90
2014	0.98
2015	1.06
2016	1.13
2017	1.18
2018	1.21
2019	1.23
2020	1.24

Figure 2.14 Trend on the number of energy conservation fridges per household.

Regular Fridge per Household
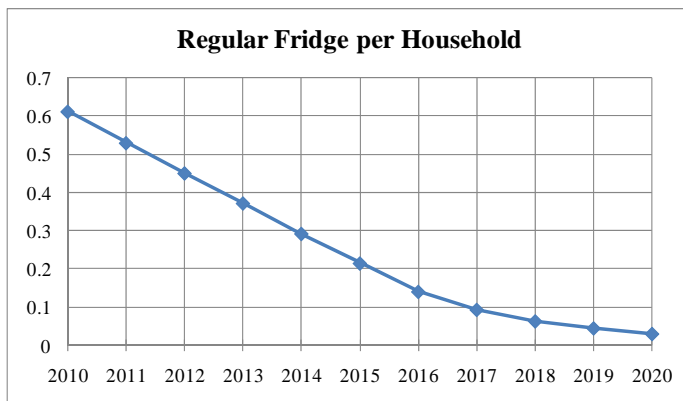
Year	Regular Fridges per Household
2010	0.61
2011	0.53
2012	0.45
2013	0.37
2014	0.29
2015	0.21
2016	0.14
2017	0.09
2018	0.06
2019	0.04
2020	0.03

Figure 2.15 Trend on the number of regular fridges per household.

Currently there are two types of washers available in Canada, front-loading and top-loading. In 2006, 46.9% of the clothes washers shipped in Canada were front-loading units, and they are generally more efficient. The shipment-weighted average annual unit energy consumption (UEC) of front-loading clothes washers was 203 kilowatt hours (kWh), compared with 555 kWh for top-loading ones. Figure 2.16 ([22]) illustrates the increase in popularity of front-loading models versus top-loading ones since 2001, and the annual growth rate for front-loading is around 6.3%. Based on the trend of Figure 2.16, the future market is estimated and shown in Figure 2.17. In this figure, it is possible to observe that the front-loading clothes washer dominated the market from 2007.

Model Year	Clothes Washer Type	
	Front-Loading Clothes Washers (%)	Top-Loading Clothes Washers (%)
2001	15.7	84.3
2002	16.8	83.2
2003	21.5	78.5
2004	29.2	70.8
2005	42.3	57.7
2006	46.9	53.1
Total Change	31.2	31.2

Figure 2.16 Distribution of clothes washer by type.
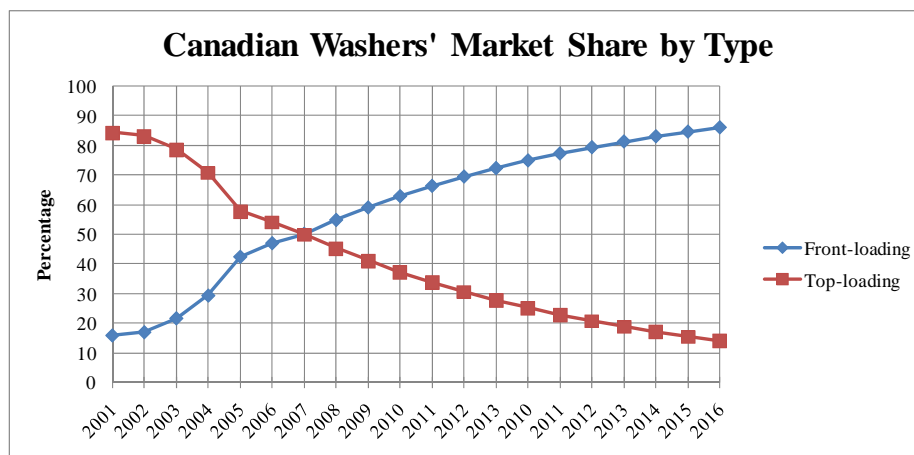
Figure 2.17 Canadian washer market share by type.

Assuming the lifespan of washer is 10 years, which means that the different types of washers' penetration in household in a certain year is related to the last 10 years:

$$WASH^{typeY}(i) = \frac{SP^{typeY}(i-10) \times TS(i-10) + ... + SP^{typeY}(i) \times TS(i)}{TS(i-10) + ... + TS(i)} \times NWASH$$

(2.5)

where,

- $WASH^{typeY}$ is the number of washers of type Y per household.
- $NWASH$ is the average number of washers, including all types, per household
- SP^{typeY} is the ratio between sales of washers of type Y and the total sales of all types of washers, which is given by TS

From equation (2.5), it is possible to estimate for the coming years the number of washers of each type per household. The results for front-loading and top-loading washers are shown in Figure 2.18 and Figure 2.19, respectively.

Year	Front Washers per Household
2010	0.40
2011	0.45
2012	0.50
2013	0.55
2014	0.60
2015	0.63
2016	0.67
2017	0.70
2018	0.73
2019	0.75
2020	0.77
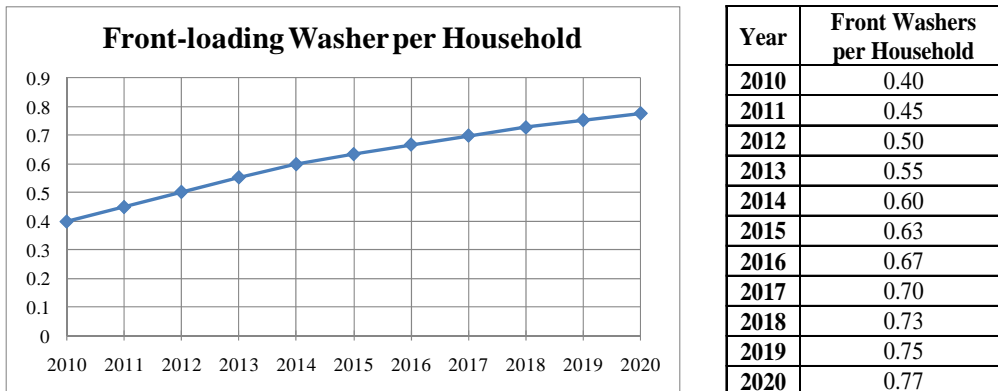
Figure 2.18 Trend on the number of front-loading washers per household.

Year	Top Washers per Household
2010	0.60
2011	0.55
2012	0.50
2013	0.45
2014	0.40
2015	0.37
2016	0.33
2017	0.30
2018	0.27
2019	0.25
2020	0.23
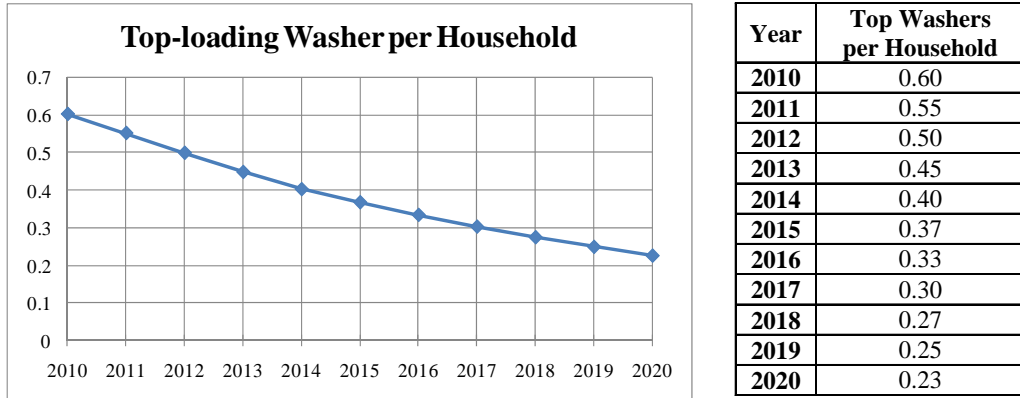
Figure 2.19 Trend on the number of top-loading washers per household.

2.1.6 Other Appliances

There are many other harmonic producing appliances in homes, such as microwave ovens and electronic gadgets. Due to the lack of market data, the usage trend of these appliances is assumed to be constant over the next several years. A list of appliances considered in this thesis is shown in Table 2.1.

The residential load model adopted by this thesis is based on the situation in Alberta, Canada. In Alberta, three types of electric loads, air-conditioning units, electric furnaces and electric space heating are not present. However, these appliances can be included using the techniques developed by this thesis.

2.2 Characteristics of Current Residential Loads

This section presents the characteristics of currents drawn by common home appliances obtained from measurements conducted in Alberta, Canada. Air-conditioner and electric heater are not included since they are quite rare in this province. The measured appliances are listed in Table 2.1. Codes are assigned to them for easy identification in the figures and tables shown later. This table also identifies the number of measured appliances of each type. In total, 31 types of common appliances are measured and listed. Some appliances have different operating cycles that exhibit different power consumption and harmonic current characteristics. For example, a washing machine can have washing, rinsing and spinning cycles. Other appliances, such as TVs, exhibit almost constant power consumption. In order to provide representative results, various operating cycles were measured. Detailed data about each appliance are shown in Appendix A.

Table 2.1 Measured home appliances.

Group	Code	Appliance Type	Number Tested
Lighting	CFL	Compact Fluorescent Lamp	12
	EBL	Electric-Ballast Fluorescent Lamp	3
	MBL	Magnetic-Ballast Fluorescent Lamp	1
	INC	Incandescent Lamp	1
Entertainment	PC	Desktop PC	3
	LCD	LCD Computer Monitor	3
	LAP	Laptop	3
	LCD TV	LCD Television	3
	CRT TV	CRT Television	2
Major Appliances	R FR	Regular Fridge	2
	ASD FR	ASD-based Fridge	3
	FRE	Freezer	1
	WSH	ASD-based Washer	1
	DRY	Regular Dryer	1

Major Appliances	ASD DRY	ASD-based Dryer	1
	RAN	Electric Range	3
	OVE	Electric Oven	1
Kitchen	MW	Microwave Oven	3
	TOA	Toaster	1
	COF	Coffee Maker	1
	GRI	Griddle	1
	WAF	Waffle Iron	1
	BRE	Bread Maker	1
	BLE	Blender	2
	FOO	Food Processor	1
Office	PRIN	Printer	1
	COP	Copier	1
Others	KET	Electric Kettle	2
	FUR	Furnace	1
	GAR	Garage Door	1
	VAC	Vacuum Cleaner	2

2.2.1 Linear and Nonlinear Appliances

The first step to develop an adequate model for each appliance is to verify if it is a linear or nonlinear load. In general, power electronic-based home appliances are nonlinear harmonic sources while resistive or motive appliances are linear loads. However, it is not a simple task to determine if an appliance is linear or not by only checking the current harmonic spectrum. In a distorted supply voltage scenario, even a resistive appliance could have distorted current waveform, appearing as a nonlinear source. In this thesis, we use the correlation of the current and voltage waveforms of an appliance to determine its linear or nonlinear characteristics. The method is illustrated in Figure 2.20 and Figure 2.21. If an

appliance is linear, the voltage versus current plot is shaped either as a straight line (resistive load) or as a ring (reactive load).

The V x I plot for all appliances under analysis in this thesis is shown in Appendix B. Based on this analysis, each appliance is categorized as linear or nonlinear load, as shown in Table 2.2.

(a) Griddle V x I plot

(b) Griddle V and I waveforms.

(c) Dryer V x I plot

(d) Dryer V and I waveforms.
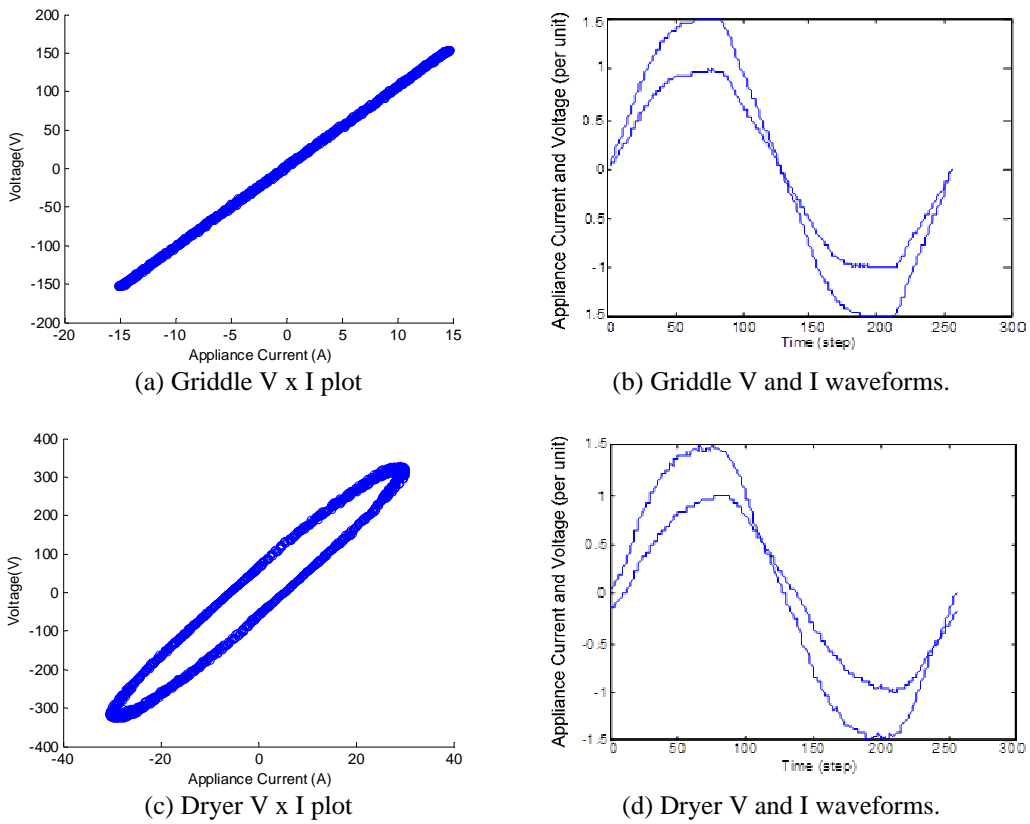
Figure 2.20 Correlation between V and I of linear appliances.
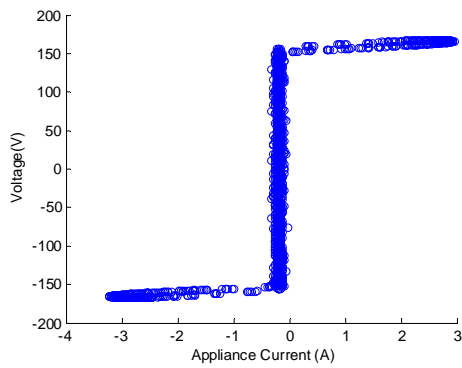
(a) CRT TV V x I plot
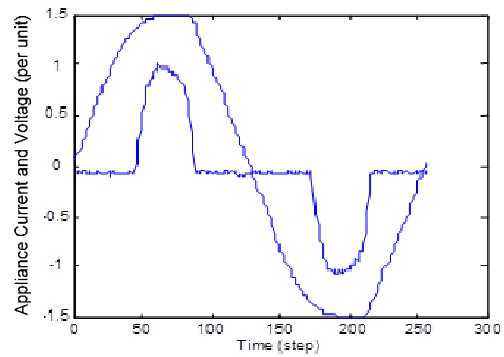
(b) CRT TV V and I waveforms.
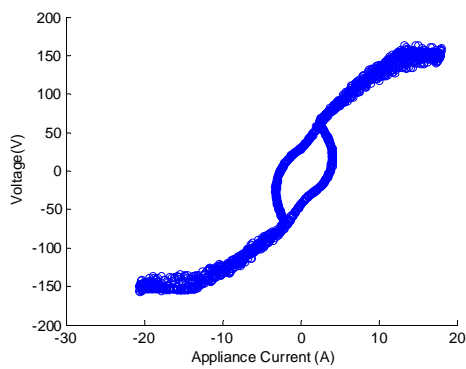
(c) Microwave V x I plot
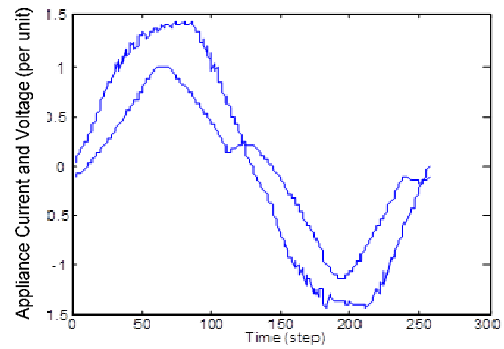
(d) Microwave V and I waveforms.

Figure 2.21 Correlation between V and I of nonlinear appliances.

Table 2.2 Linear and nonlinear appliances.

Appliance Name	Characteristic of Appliance
Compact Fluorescent Lamp	Non-linear
Electric-Ballast Fluorescent Lamp	Non-linear
Magnetic-Ballast Fluorescent Lamp	Linear
Incandescent Lamp	Linear
Desktop PC	Non-linear
LCD Computer Monitor	Non-linear
Laptop	Non-linear
LCD Television	Non-linear
CRT Television	Non-linear
Fridge	Non-linear
Freezer	Non-linear
Washer	Non-linear

Dryer	**Linear**
Electric Range	**Linear**
Electric Oven	**Linear**
Microwave Oven	Non-linear
Toaster	**Linear**
Coffee Maker	**Linear**
Griddle	**Linear**
Waffle Iron	**Linear**
Bread Maker	Non-linear
Blender	Non-linear
Food Processor	Non-linear
Printer	Non-linear
Copier	Non-linear
Electric Kettle	**Linear**
Furnace	Non-linear
Garage Door	Non-linear
Vacuum Cleaner	Non-linear

2.2.2 Harmonic Magnitude Characteristics of Nonlinear Appliances

Table 2.3 shows the main electric results obtained for some of the main home appliances. Those results include the fundamental current Total Harmonic Distortion (THD_I), power factor (FPF) and total power factor (PF) and, which were calculated by using the IEEE definition [24].

Table 2.3 Harmonic magnitude characteristics of home appliances.

Appliance	THD_I [%]	FPF	PF	Operating power [W]	I_{rms} [A]	I_1 [A]
CFL	120	0.9*	0.6	15	0.24	0.15
EBL	140	0.96*	0.56	15	0.24	0.14
MBL	8	0.38	0.38	33	0.73	0.73
PC	112	1	0.69	100	1.30	0.88

LCD	110	0.96*	0.64	40	0.48	0.34
LAP	130	0.96*	0.58	75	1.14	0.68
LCD TV	10	0.99*	0.98	300	2.59	2.58
CRT TV	145	1	0.56	70	1.00	0.57
MW	41	0.99*	0.9	1200	11.08	10.49
ASD FR	7	0.92	0.91	170	1.6	1.6
R FR	16	0.94	0.93	150	1.30	1.27
WSH	75	0.45	0.35	180	4.20	3.36
ASD DRY	55	0.98	0.86	1000	4.90	4.30
FUR	11	0.84	0.84	500	4.85	4.82

In order to compare the harmonic impact of various home appliances, an index called Equivalent-CFL is proposed. This index quantifies each appliance in terms of its harmonic impact expressed as the number of CFLs it is equivalent to. This index is defined as follows. For each harmonic order h, the ratio of the appliance's current to that of the representative CFL current is determined by using the following equation:

$$Ratio_{h\_appliance} = \frac{I_{h\_appliance}}{I_{h\_CFL}} \tag{2.6}$$

where $I_{h\_appliance}$ is the appliance's harmonic current at order h, and I_{h_CFL} is the representative CFL harmonic current at order h. For example, a $Ratio_{h\_appliance}$ of 2 implies that the appliance generates twice as much harmonic current at order h as the representative CFL. In order to obtain a single index and compare the appliance with a representative CFL, the ratios of different harmonic orders are aggregated into one value by using a weighted average as follows:

$$\text{Equivalent-CFL}_{Appliance} = \sqrt{\sum_{h=3}^{H}\left(w_h \times Ratio_{h\_Appliance}\right)^2} = \sqrt{\frac{\sum_{h=3}^{H}I_{h\_Appliance}^2}{\sum_{h=3}^{H}I_{h\_CFL}^2}} \tag{2.7}$$

The weighting factor w_h is the individual harmonic distortion of the CFL current. This weighting factor is used because if a CFL produces more harmonic at h, the harmonics from other appliances will also be treated with more significance at the same order.

The results obtained from the calculated individual Equivalent-CFL index of all appliances are presented in Table 2.4. The results are arranged in the ascending order of the index. This table shows that a desktop PC is equivalent to 7 CFLs in terms of harmonic current injection. A microwave oven has a harmonic impact equivalent to 26.4 CFLs, and a laundry washer has a harmonic impact equivalent to 16 CFLs. The table also lists the power ratios with respect to the CFL and the harmonic current ratios from the 3rd to the 9th harmonics.

Table 2.4 Comparing the harmonic impact of one unit of home appliances.

Appliance Type	Operating Power [W]	Power Ratio	Equivalent CFL	$Ratio_3$	$Ratio_5$	$Ratio_7$	$Ratio_9$
MBL	30	2	0.42	0.56	0.02	0.11	0.08
CFL	15	1	1.00	1.00	1.00	1.00	1.00
ASD FR	170	11.3	1.14	1.03	0.28	2.74	1.23
EBL	18	1.2	1.15	0.99	1.39	1.69	0.60
LCD TV	300	20	1.32	1.34	1.56	0.88	0.89
R FR	150	10	1.35	1.22	1.33	1.44	1.92
LCD	40	2.67	2.35	2.04	3.30	1.24	0.23
FUR	500	33.33	2.53	2.68	2.72	1.71	1.26
CRT TV	70	4.67	5.81	4.93	6.77	7.02	7.37
LAP	75	5	6.15	5.37	5.66	5.57	7.97
PC	100	6.67	7.05	7.32	8.02	5.47	2.43
ASD DRY	1000	66.67	12.58	15.23	8.26	5.90	10.85
WSH	180	12	16.09	12.80	17.83	20.16	22.74
MW	1200	80	26.42	33.09	16.72	9.14	7.20

2.2.3 Harmonic Phase Characteristics of Nonlinear Appliances

The appliances' current phasors at harmonic orders 3rd-13th are shown in Figure 2.22([25]). The phasors use the supply voltage angle as a reference, setting the phase angle of the fundamental frequency voltage to zero. The currents are normalized to emphasize the current harmonic angles and to improve visualization. This figure reveals the potential harmonic cancellation that might occur when 2 or more appliances are operated together. For example, the 3rd harmonic current of the LCD monitor is about 180° out of phase with that of the furnace. Conversely, the 3rd harmonic of the desktop PC is almost in phase (0°) with that of the CRT TV.
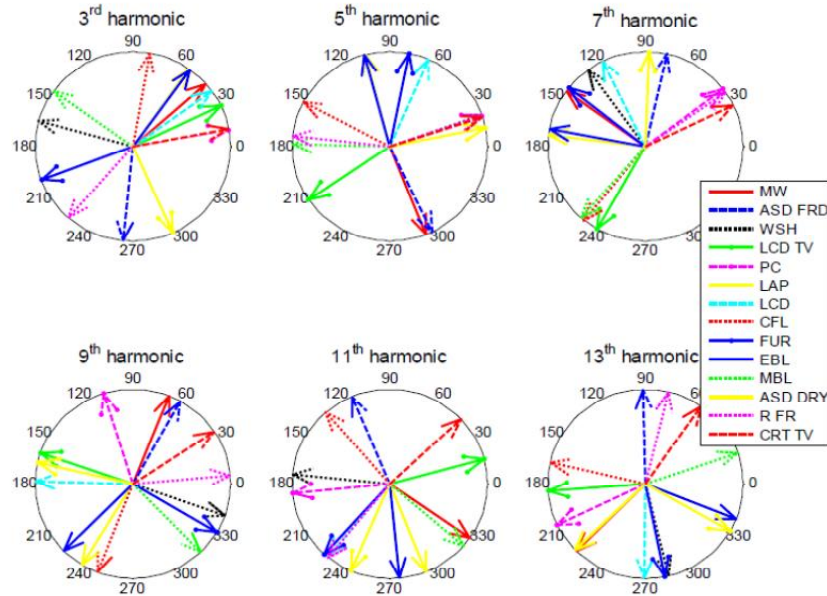
Figure 2.22 Harmonic phase characteristics of home appliances.

An index called harmonic compatibility index (CI_h) is proposed to characterize the angle diversity of home appliances. The harmonic current phase angles are important because they indicate how the harmonics from various home appliances will either add to or cancel out each other. This index also used the CFL harmonic current as a reference. For each harmonic order h, the phasor relationship of the appliance's current to that of the representative CFL current is determined by using the following equation:

$$CI_{h\_appliance} = \frac{\left|\dot{I}_{h\_appliance} + \dot{I}_{h\_CFL\_eq}\right|}{\left|\dot{I}_{h\_appliance}\right| + \left|\dot{I}_{h\_CFL\_eq}\right|} = \frac{\sqrt{I^2 + I^2 + 2I^2\cos(q)}}{2I} = \left|\cos(\frac{q_h}{2})\right| \qquad (2.8)$$

where

$$\dot{I}_{h\_CFL\_eq} = \dot{I}_{h\_CFL} \times Ratio_{h\_appliance} \qquad (2.9)$$

and

$$q_h = \left|ang(\dot{I}_{h\_appliance}) - ang(\dot{I}_{h\_CFL})\right| \qquad (2.10)$$

Figure 2.23 explains the meaning of the above index. Assume the CFL is being compared with Appliance 1, Appliance 2, Appliance 3 and Appliance 4. Figure 2.23(a) reveals that the index calculated for Appliance 1 means solely harmonic addition, resulting in $CI_{h\_Appliance1} = 1$ because both components are in phase; i.e., $\theta = 0^o$. Conversely, the index calculated for Appliance 2 (Figure 2.23(b)) is $CI_{h\_Appliance2} = 1/\sqrt{2}$ because $\theta = 90^o$. The index calculated for Appliance 3 (Figure 2.23(c)) is found to be $CI_{h\_Appliance3} = 1/2$ because the value of CI_h is the

41

same of that of the magnitudes of the individual phasors; i.e., $\theta = 120^o$. Finally, the index calculated for Appliance 4 (Figure 2.23(d)) is $CI_{h\_Appliance4} = 0$ because both components are in opposite phase angles; i.e., $\theta = 180^o$.
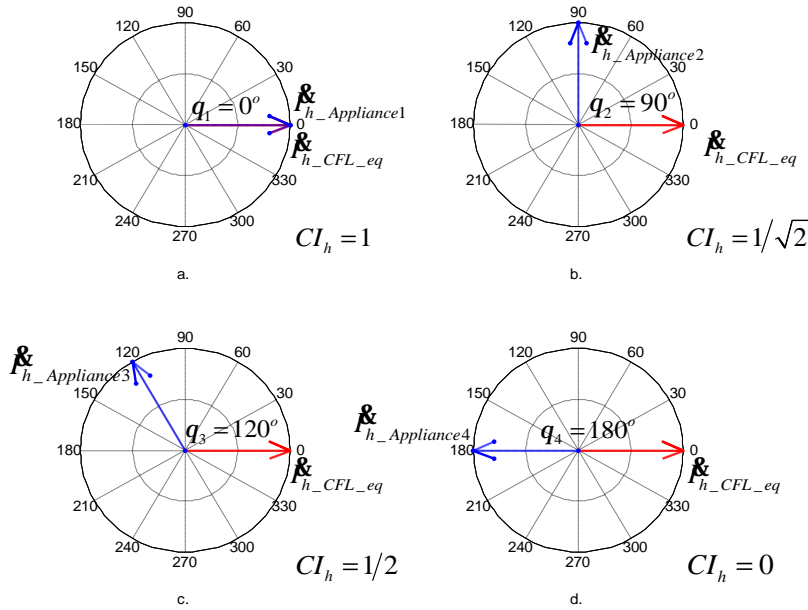
Figure 2.23 Phasor diagram to illustrate the compatibility index.

An aggregation similar to that proposed for the magnitude-based Equivalent-CFL index is used for the harmonic compatibility indices, also by using the same weighting factor, which results in the following aggregated index:

$$CI_{appliance} = \sqrt{\sum (w_h \times CI_{h\_appliance})^2} \qquad (2.11)$$

The phase angle-based harmonic compatibility index can reflect the degree of harmonic cancellation between two appliances should there be no difference in magnitude. In other words, if both appliances' current harmonics were of the same magnitude, the index $CI_{h\_Appliance}$ would reflect the amount of harmonic

cancellation. Suppose the cases (1) $\theta_h = 0$, resulting in $CI_{h\_Appliance} = 100\%$. This result means zero harmonic cancellation, and (2) $\theta_h = \pi/2$ and $CI_{h\_Appliance} = 71\%$. This result means 29% harmonic cancellation as compared to the first case. The results for the compatibility index for all appliances are calculated and presented in Table 2.5, in ascending order of $CI_{Appliance}$.

Table 2.5 Harmonic compatibility index results using CFL as a template.

Appliance	$CI_{Appliance}$	CI_3	CI_5	CI_7	CI_9	CI_{11}	CI_{13}
ASD FR	0.27	0.03	0.31	0.23	0.07	0.99	0.79
ASD DRY	0.35	0.29	0.34	0.32	0.75	0.53	0.15
R FR	0.61	0.27	0.98	0.14	0.53	0.64	0.7
CRT TV	0.63	0.82	0.39	0.22	0.3	0.72	0.56
WSH	0.64	0.74	0.4	0.61	0.7	0.93	0.53
PC	0.64	0.82	0.39	0.12	0.33	0.89	0.94
FUR	0.65	0.5	0.8	0.71	0.76	0.66	0.54
MW	0.74	0.94	0.34	0.73	0.01	0.13	0.87
LCD	0.81	0.93	0.73	0.54	0.82	0.65	0.63
LCD TV	0.88	0.89	0.86	1.00	0.72	0.53	0.99
MBL	0.89	0.85	0.97	1.00	0.84	0.07	0.27
EBL	0.92	0.97	0.92	0.86	0.98	0.3	0.08
LAP	0.93	0.98	0.91	0.87	1.00	0.16	0.88
CFL	1.00	1.00	1.00	1.00	1.00	1.00	1.00

2.3 Electrical Modeling of Home Appliances

As discussed earlier, home appliances are classified as two types, linear and nonlinear. In this thesis, the linear loads are modeled as constant power loads at the fundamental frequency (60Hz) and as impedance at harmonic frequencies, as shown in Figure 2.24([2]).

(a) Model at fundamental frequency   (b) Model at harmonic frequency

Figure 2.24 Model for linear appliances.

The parameters for the model of each linear appliance can be obtained from the measurements according to the following equations:

$$P + jQ = V_1 \times conj(I_1)$$

$$R = \frac{V_1^2}{P}$$

$$X_h = h \times \frac{V_1^2}{Q}$$

(2.12)

Table 2.6 presents the active and reactive power consumed by different linear appliances. As it can be seen, the appliances are mainly resistive (excluding dryer and magnetic-ballast fluorescent lamp). The symbol '*' means that the appliance is supplied by 240V.

Table 2.6 Fundamental active and reactive power of the linear appliances.

Device	Brands	P (W)	Q (Var)
Magnetic-ballast Fluorescent	1	33.69	80.96
Incandescent Lamp	1	59.28	0.05
Dryer*	1	1262.70	257.15
Range*	1	993.06	6.84
Oven*	1	381.75	1.82
Toaster	1	902.68	11.31
Coffee Maker	1	919.39	11.74

44

Griddle	1	1384.60	7.98
Waffle Iron	1	972.27	6.56
Electric Kettle	1	1518.80	16.02
	2	1490.50	15.43

The nonlinear loads are modeled as constant power loads at the fundamental frequency (60Hz) and as current sources at harmonic frequencies, as shown in Figure 2.25([2]). The magnitude and phase of the source is calculated from the harmonic current spectrum of the appliance using the following procedure:

(a) Model at fundamental frequency   (b) Model at harmonic frequency

Figure 2.25 Model for nonlinear appliances.

1) The harmonic-producing load is treated as a constant power load at the fundamental frequency, and the fundamental frequency power flow of the system is solved

2) The current injected from the load to the system is then calculated and is denoted as $I_h = I_1 \angle q_1$

3) The magnitude and phase angle of the harmonic current source representing the load are determined as follows:

$$I_h = I_1 \times \frac{I_{h-spectrum}}{I_{1-spectrum}}$$

45

$$q_h = q_{h-spectrum} + h \times \left(q_1 - q_{h-spectrum}\right) \qquad (2.13)$$

where subscript "spectrum" stands for the typical harmonic current spectrum of the load, which can be found in Appendix A. The meaning of the magnitude formula is to scale up the typical harmonic current spectrum to match the fundamental frequency power flow result (I_1). The phase formula shifts the spectrum waveform to match the phase angle of θ_1. Since the *h*-th harmonic has h-times higher frequency, its phase angle is shifted by *h* times of the fundamental frequency shift. This spectrum-based current source model is the most common one used in commercial power system harmonic analysis programs. The input data requirement is minimal.

2.4 Summary

The objective of this chapter has been to investigate the main characteristics of typical residential home appliances so that a proper modeling method for harmonic analysis could be developed. In summary, the following studies have been conducted in this chapter:

1) In Section 2.1, the customer trend of home appliances usage was investigated and the results provide estimation about the number of appliances adoption per household in the future.

2) In Section 2.2, it was discussed the main electrical characteristics of each appliance. Several indices, such as THD_I, operating power, *FPF*, *PF*, *Eq-CFL*, *CI* were employed to compare different appliances.

3) From the main electrical characteristics, two approaches were presented in Section 2.3 to model linear and nonlinear appliances for harmonic analysis.

So far, we have an approach to model each appliance individually. The next step consists in developing an aggregated house model so it can be connected to the service transformer and primary distribution system and the harmonic analysis can be conducted.

Chapter 3

Modeling of Residential Houses[1]

Load modeling plays a critical role on power systems operation and studies, since the results of important analysis functions are strongly dependent on the models assumed. Basically, there are two main approaches in load modeling: the bottom-up and the top-down approaches [26]. In this thesis, the modeling of residential houses is done through the bottom-up approach, which, basically, builds up the load model based on on the operating conditions (On and Off) of each home appliance, which in turn is a function of the habits and population of a household. In order to assess the harmonic impact of various home appliances adequately, it is very important to establish the model of appliance operating activities in a home.

3.1 Introduction

In a general way, the bottom-up approach is based on the determination of individual models for each component of the actual system. In this thesis, the model uses the appliance as the basic building block, where "appliance" refers to any individual domestic electricity load, such as a television, washing machine or vacuum cleaner. The individual appliances are aggregated so as to produce an individual household harmonic profile [27], [28].

---

[1] A version of this chapter has been submitted for publication: D. Sales, C. Jiang, W. Xu etc. "*Assessing the Collective Harmonic Impact of Modern Residential Loads – Part I: Method*", IEEE Transactions on Power Delivery.

The structure of the bottom-up model is shown in Figure 3.1([28]). On the left of the diagram, there is a set of daily activity profiles, which represent the likelihood of people performing different activities at different times during a day; these profiles are the same for all households. To the right of the diagram is an individual household. The household is assigned an active occupancy data series and a set of installed appliances. The actual operating status of each appliance is determined from its corresponding daily activity profiles. When an appliance switch-on occurs, it will be included as an operating load. The whole household load is a random collection of operating loads, linear or nonlinear, as a function of time. For the purpose of studying the impact on the secondary distribution systems, the loads are grouped according to the phases they are connected: phase A (120 V), phase B (120 V) and phase-to-phase (240 V).
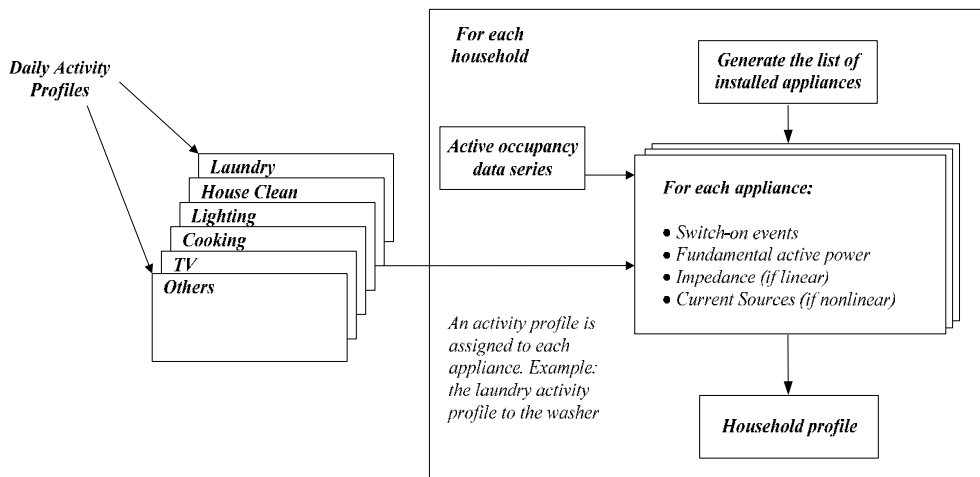
Figure 3.1 Structure of the bottom-up model for a residential house.

In the next subsections, the steps to obtain the appliances profile, the final model for single house and multiple houses is presented along with validation results.

49

3.2 Home Load Profile Modeling

Considerable research efforts have been made in the past on the subject of developing detailed residential electrical load profiles from limited sources of data, which normally reconstruct the expected daily electrical loads of a household based on appliance sets, occupancy patterns, and statistical data. Based on the published works [27], [28], the basic idea of home load profile modeling is to address three factors: 1) When an appliance will be turned on. This can be simulated using the *Daily Time of Use Probability Profile*s of the appliances, 2) How long an appliance will stay on. The duration is determined from measured data and other information collected. 3) How to include the impact of the habits and population of a household. A load profile is created by combining these factors according to established theories developed by load researchers.

3.2.1 Daily Time of Use Probability Profiles

In 1985, Walker and Pokoski [29] constructed electric load profiles from individual appliances by introducing the concept of 'proclivity' functions. The idea is predict the tendency of the occupants to switch on an appliance at any given time. Since then many researchers have investigated how to quantify the probability of the specified activity being undertaken as a function of time-of-day, which is termed as the Time of Use Probability Profiles. It represents the probability of a household performing a specific activity during a 24 hour period.

For example, the reference *UK 2000 Time Use Survey* [30] finds that the number of dwellings that have one active occupant between 08:00 and 08:10 is 2082. The number of dwellings where the occupant is performing a cooking related activity is 288. The probability of cooking event occurs at the time between 08:00 and 08:10 is 288/2082 = 0.138. In this thesis, the profile data are collected from the UK 2000 Time Use Survey (TUS) [30] and the Building America Research Benchmark Definition [31].

3.2.1.1 Cooking Activity Profile

Most of the kitchen appliances are related to cooking events. They share the same probability of switching on at a given time. As shown in Figure 3.2, the curves are applied to predict the occupants' cooking related actions and to establish the probability of an event occurring, such as using microwave, blender and griddle etc [32]. The probability profile is on 1-min resolution and the higher the value in the profile, the higher the probability that the event occurs. For example, a microwave event would be far more likely to occur at 17:00 than at 4:00. The profile on weekend is more flattened than that on weekday because people are cooking more randomly on weekends.
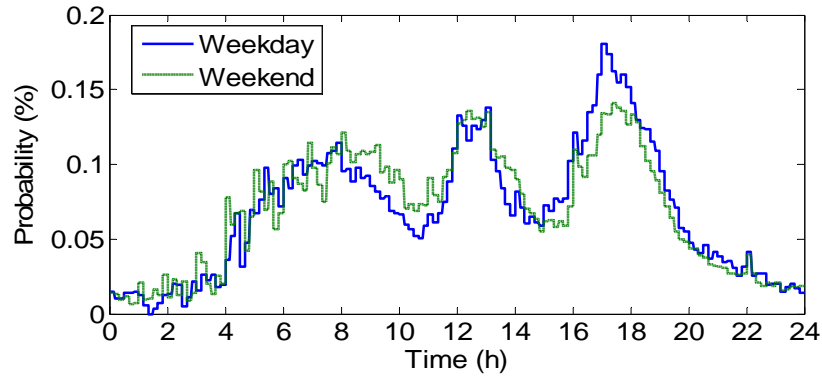
Figure 3.2 Time of use probability profile for cooking activity.

Additionally, people are more likely to use toaster and waffle iron in the morning, and range at noon and in the evening. Specific profiles for these appliances, like the ones shown in Figure 3.3, are also utilized in this thesis.
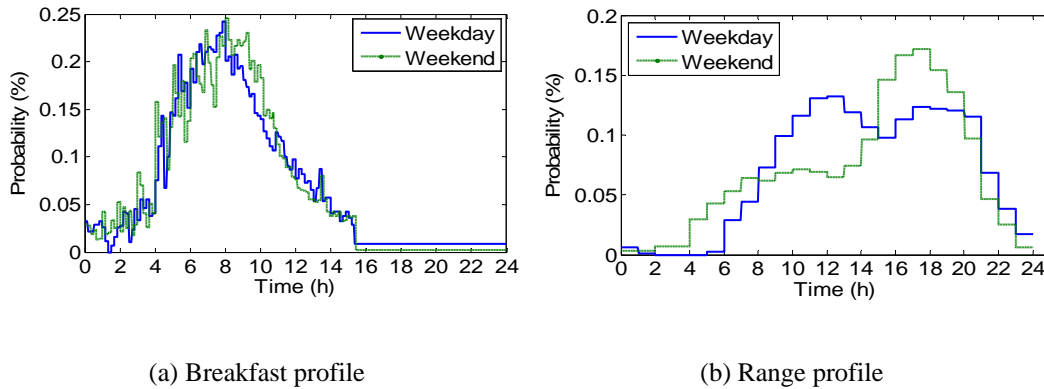
(a) Breakfast profile   (b) Range profile

Figure 3.3 Time of use probability profile for two specific cooking activities.

3.2.1.2 Laundry Activity Profile

Washer event is determined by laundry activity profile, however, since the time of use profiles for the dryer was the same shape and offset from the time of use

profile for the washer, dryer events were coupled to washer operation [32]. Dryer cycles were allowed to trigger between 10 and 30 minutes following the end of the washer cycle.
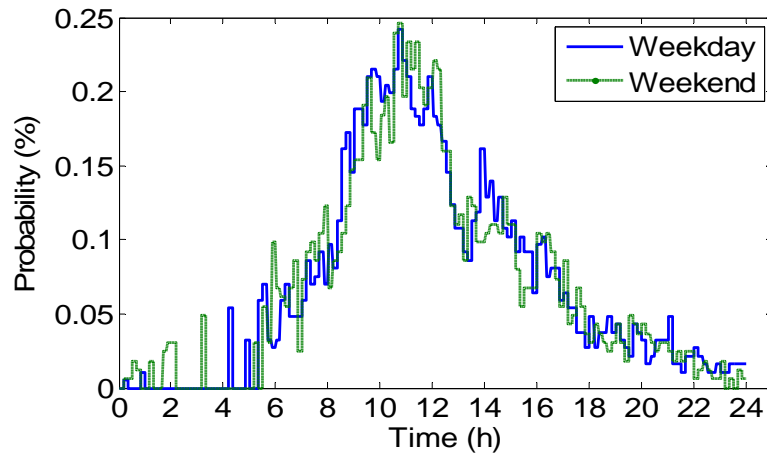
Figure 3.4 Time of use probability profile for laundry activity.

3.2.1.3 TV and PC Profile

The probability profiles of TV and PC are shown in Figure 3.5.
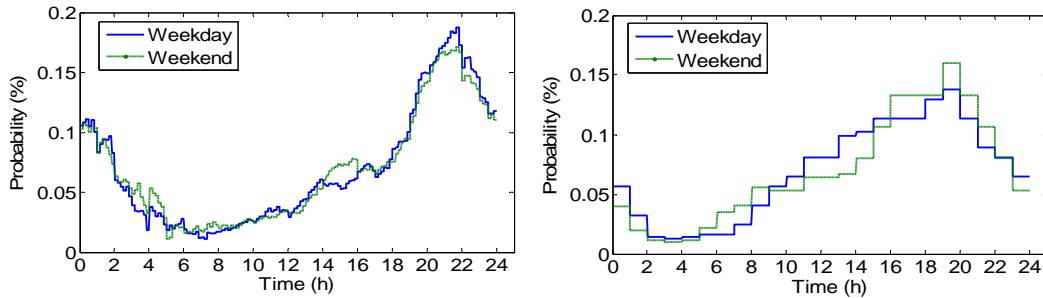
(a) Television profile   (b) PC profile

Figure 3.5 Time of use probability profile for television and PC.

3.2.1.4 Lighting Profile

Lighting can be divided into three basic categories: living room and bedroom lighting, kitchen lighting and bathroom lighting. Living room and bedroom lighting is associated with people's occupancy, while kitchen lighting is related to cooking activity (the kitchen lighting turns on with the beginning of cooking and it turns off after some time of the ending of cooking). Bathroom lighting can also be determined from people's occupancy; however it is more random if compared to living and bedroom lighting profiles. Bathroom lighting profile is given in Figure 3.6.
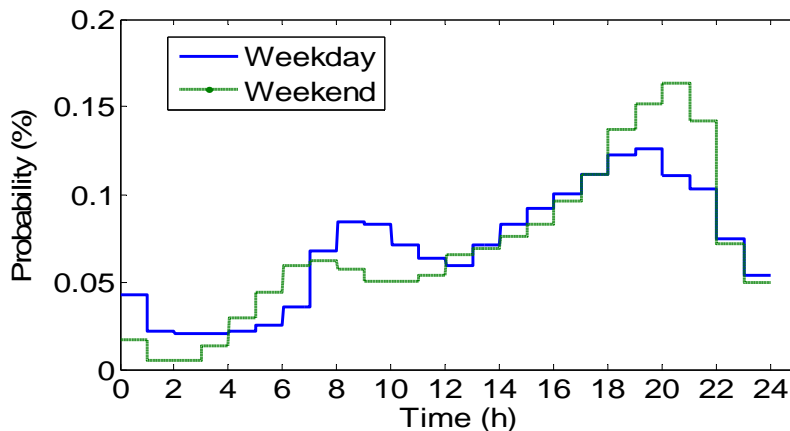
Figure 3.6 Time of use probability profile for bathroom lighting.

3.2.1.5 House Cleaning

The time of use probability profile of house cleaning devices such as vacuum cleaners can be determined from Figure 3.7. Normally, the house cleaning activity is carried out from 8:00 a.m. to 6:00 p.m.
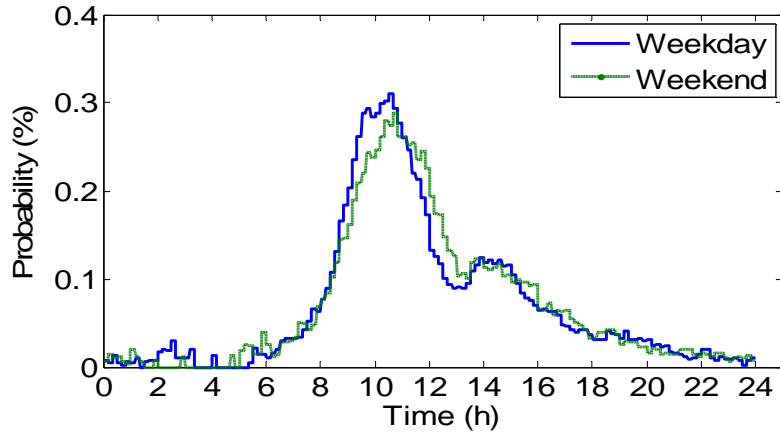
Figure 3.7 Time of use probability profile for house clean activity.

3.2.1.6 Occasional Event Profile

The occasional event time of use profile establishes the probability of a number of appliances which activate occasionally. The operating of electric kettle, motor of garage door and furnace etc. are defined as occasional event.
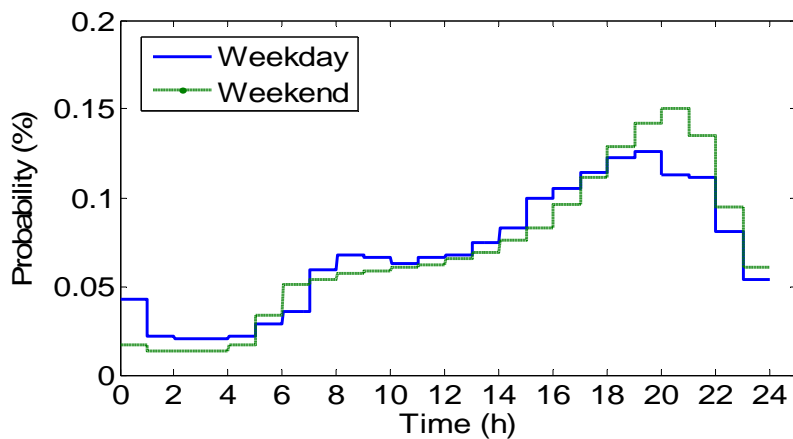
Figure 3.8 Time of use probability profile for occasional events.

3.2.2 Appliance Duration Characteristics

For major appliances, the cycle duration can be established according to the measurement data from *Canadian Center for Housing Technology* (CCHT) [33]. At the CCHT, a simulated occupancy system triggers daily lighting and appliance events in a real single detached home. The average cycles per year is derived from standard appliance test methods of the Canadian Standards Association (CAN/CSA-C373-92, CAN/CSA-C361-92 and CAN/CSA-C360 - 98) [33], [34], [35]. Details of appliance loads and cycles are presented in Table 3.1.

Table 3.1 Appliance usage pattern for major appliances.

Appliance	Power (W)	Cycle Duration (min)	Cycles per year	Annual Consumption (kWh/year)
Dishwasher	467	30 to 45	200 (low) 322 (medium) 418 (high)	58 (low) 94 (medium) 122 (high)
Washer	505	30 (two 15-minute cycles)	242 (low) 392 (medium) 601 (high)	61 (low) 99 (medium) 152 (high)
Dryer	4115	30 to 60	192 (low) 416 (medium) 640 (high)	593 (low) 1284 (medium) 1976 (high)
Range	1600	15 to 70	678 (low) 678 (medium) 950 (high)	769 (low) 769 (medium) 1077 (high)
Refrigerator	265 (peak)	----	----	801 (low), 801 (medium) 1602 (high: 2 fridges)
Freezer	202 (peak) 263 (peak)	----	----	0 (low), 614 (medium) 798 (high)

Information regarding the other appliances analyzed in this thesis was extracted from a series of buyers guides published by Natural Resources Canada [36], [37].

This list of appliances with their power rating and expected hours of operation per month is presented in Table 3.2.

Table 3.2 Average appliance usage pattern for other appliances.

	Appliances	Power Rating (W)	Average Hours per month
Kitchen	Blender	350	3
	Coffee Maker	900	12
	Deep Fryer	1500	8
	Exhaust fan	250	30
	Electric kettle	1500	15
	Hot plate (one burner)	1250	14
	Microwave oven	1500	10
	Mixer	175	6
	Toaster	1200	4
Laundry	Iron	1000	12
Comfort &Health	Electric blanket	180	180
	Fan	120	6
	Hair dryer	1000	5
Entertainment	Computer (desktop)	250	240
	Computer (laptop)	30	240
	Laptop charger	100	240
	Radio	5	120
	Stereo	120	120
	Television	100	125
	VCR	40	100
Outdoors	Lawn mower	1000	10
Tools	Drill	250	4
	Circular saw	1000	6
	Table saw	1000	4
	Lathe	460	2
Other	Sewing Machine	100	10
	Vacuum cleaner	800	10

The above data only includes the total working hours per month. The duration and the number of operations per day are determined as follow. The average working hours for electric kettle is 15 per month per the above table. If its duration is 3

min per operation, one can get m = (15×60)/(30×3) = 10 operations per day. Most of the operating durations of appliances are based on measurements obtained from previous project [25].

3.2.3 Size and Occupancy Pattern of Household

The size of household has a significant impact on daily electricity demand. The appliance usage characteristics described in the previous section are tested and derived based on average household size. According to the 2006 census data of Statistics Canada [38], the average number of people per household is 2.5, and the composition of households in Canada is listed in Table 3.3.

Table 3.3 Composition of Households in Canada (2006 Census).

Number of people in the household	1	2	3	4	5	6 or more
Proportion of households with the specified number of people	27%	33%	16%	15%	6%	3%

In order to include the impact of different household sizes, a household size factor k is introduced here. When modeling a residential house with specified number of n occupants, k is equal to the ratio between n and the average number of people per household (assumed to be 2.5 in this study). The value of average hours per month for each appliance provided in Table 3.2 cannot be used directly for different household sizes since, for example, a house with more people will lead to an increase in the appliance usage. In order to take this into account, the usage times provided in Table 3.2 will be multiplied by the household size factor k.

58

Appliance usage within a residential house is also naturally related to the number of occupants who are at home and awake, or called *occupied period*. For example, most of the appliances will not be used when people are not at home. This occupancy pattern is associated with personal life style, which is a random factor. However, the common factors influencing the occupancy pattern are as follows:

1. The time of first person getting up in the morning and last person go to sleep.
2. The period of the house unoccupied during working hours.

In view of lacking of information about house occupancy pattern, we propose 5 most typical scenarios of household occupancy pattern in Canada. Table 3.4 lists these possible scenarios.

Table 3.4 Occupancy pattern for a typical household.

Type of Day	No.	Work Type	Time of Waking up	Working Time	Time of Going to Bed
Weekday	1	Full-time	6:00 - 7:30	8:00 - 17:00	22:00 - 00:00
	2	Part-time Morning	6:00 - 7:30	8:00 - 12:00	22:00 - 00:00
	3	Part-time Afternoon	6:00 - 8:00	13:00 - 17:00	22:00 - 00:00
	4	No Working	6:00 - 8:00	N/A	22:00 - 00:00
Weekend	5	N/A	7:00 - 9:00	N/A	22:00 - 00:00

3.2.4 Probabilistic Modeling of Switch-on Event of Appliances

Based on the usage pattern of appliances discussed in the previous sections and the method of [28], a procedure to determine appliance switch-on events at a given time of a day (which is also called a simulation step) has been established by this thesis. The procedure is a form of Monte Carlo simulation and implemented in a computer program. At each simulation step, a list of appliances that are in operation is generated, which forms the load profile at that step. The simulation procedure is shown Figure 3.10 and explained below:

- The time of use probability profile is selected according to chosen appliance and whether it is a weekend or not; the occupancy pattern is also selected according to the working type and whether it is a weekend or not.

- When the simulation starts, the probability of appliance activation (P_r) can be read from its activity profile.

- The number of appliance switch-on (m) are modified by considering household size, $m^* = m \times k$, where k is the household size factor discussed in the previous section.

- The probability of appliance switch-on at current instant (P) is equal to the previous probability P_r multiplied by the modified number of appliance switch-on in simulation time period (m^*) and calibration scalar (c), $P = P_r \times m^* \times c$. A discussion of how the calibration scalar is derived is presented below.

- The result of previous step is compared to a random number (*n*) between 0 and 1.

- If *P* is larger than *n*, then a switch-on event occurs and that appliance would not switch on again during its operation cycle, directly go to the appliance end time step and go back to step 2.

- If *P* is smaller than *n*, the appliance remains off, go to next step and go back to step 2.

In step 4, the calibration scalar (c) is introduced to reflect the influence of household occupancy pattern [28]. This thesis uses occupancy function, as follows, to represent occupancy pattern.

$$OF(n) = \begin{cases} 1 & \textbf{L L} \text{ when house is occupied (e.g., early in the morning, evening)} \\ 0 & \textbf{L L} \text{ when house is unoccupied (e.g., daytime, midnight)} \end{cases}$$

If OF(n) = 0, the calibration scalar *c* is also made 0 for most appliances, which makes the probability of certain appliance switch-on to be zero when nobody is at home or awake. If OF(n) = 1, the calibration scalar *c* is introduced so as to make the mean probability of an activity taking place, when multiplied by the calibration scalar, equal the mean probability of an appliance switch-on event. As shown in Figure 3.9, before calibration, we have:

$$\sum_{n=1}^{N} Pr(n) = 1 \tag{3.1}$$

$$\sum_{n=1}^{N} Pr_C(n) = \sum_{n=1}^{N} c \times Pr(n) \times OF(n) = 1$$

$$c = \frac{1}{\sum_{n=1}^{N} Pr(n) \times OF(n)} \qquad (3.2)$$

$$\text{Hence} \qquad c = \begin{cases} 0 & \mathbf{L}\,\mathbf{L}\ OF(n) = 0 \\ \dfrac{1}{\sum_{n=1}^{N} Pr(n) \times OF(n)} \mathbf{L}\,\mathbf{L}\ OF(n) = 1 \end{cases}$$
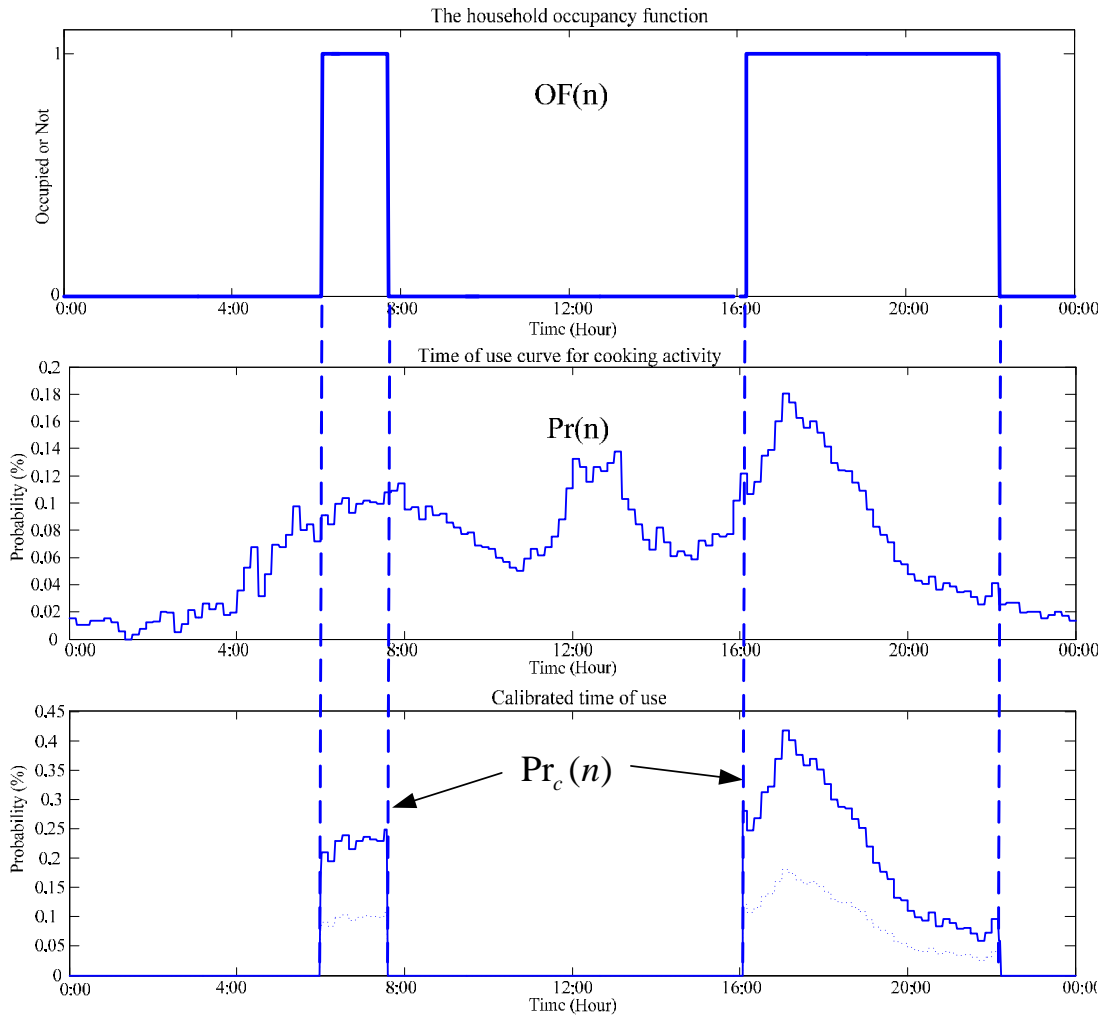
Figure 3.9 Time of use probability profile calibration with occupancy function.

Initialisation

| Size of Household | Weekday or Weekend | Working Type |

Appliance Choosing

Household Calibration Factor (**k**)

| Times of Usages per day | Time of Use Probability Profile | Household Occupancy Pattern (**OF(n)**) |

One Step

Times (**m**)

Activity Probability (**Pr**)

Calibration Scalar (**c**)

X

X

X

Probability of appliance switch-on (**P**)

Go to next Step

Compare against a random number (**n**)

Yes ← **If P>n** → **No**

Switch On the appliance and go to next D Step

Figure 3.10 Procedure to determine switch-on events of appliances.

63

The simulation of microwave usage is used as an example to illustrate the above procedure (Figure 3.11). The simulated household is set to have an average size and is full-time work type. The day of interest is weekday. The simulation resolution is 1-min, which means 1440 steps in one day. As we can see from Figure 3.11(a), the time of first person waking up is 05:40, unoccupied period during work is 7:28-16:58, and the time of last person going to bed is 22:36 for this randomly generated instance. If the simulation runs to the first step (00:01), the value of occupancy function is 0 and calibration scalar c=0, the resulting probability of microwave switch-on (P) at this time step is 0, which means the microwave has no chance to switch on. However, if the time step is equal to 1200 (20:00), the value of occupancy function is 1, and calibration scalar is

$$c = \frac{1}{\sum_{n=1}^{N} \Pr(n) \times OF(n)} = \frac{1}{0.43} = 2.33$$

The probability of microwave read from time of use profile at this step is $P_r = 0.0552\%$. According to appliance usage characteristic, the average operation duration and the average working hours per month of a microwave are equal to 4 minutes and 10 hours (Table 3.2). So the number of operations per day of the microwave is equal to m = (10×60)/(30×4) = 5 operations per day. Hence, $P = P_r \times m^* \times c = P_r \times m \times k \times c = 0.0552\% \times 5 \times 1 \times 2.33 = 0.64\%$ which means probability of microwave switch-on at current time step is 0.64%. When the simulation finishes the 1440 steps, i.e. covering the 24 hour period, results like

those shown in Figure 3.11(b) will be obtained. For this day of simulation, microwave is used for 5 times, 2 usages are at around 17:00, and 2 at around 20:00. The usage duration for one time is 4 to 5 min, and total usage time is 21 min per day, which is roughly equal to the characteristic average usage time (10 hours per month = 20 min per day), listed in Table 3.2.
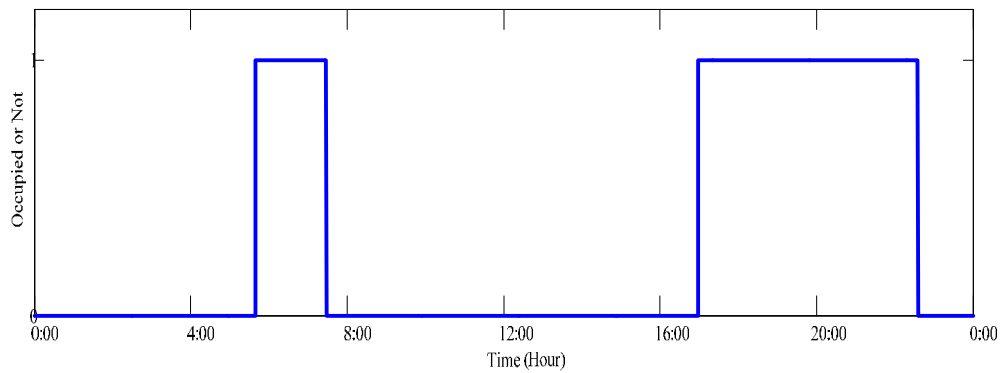
(a) The household occupancy function
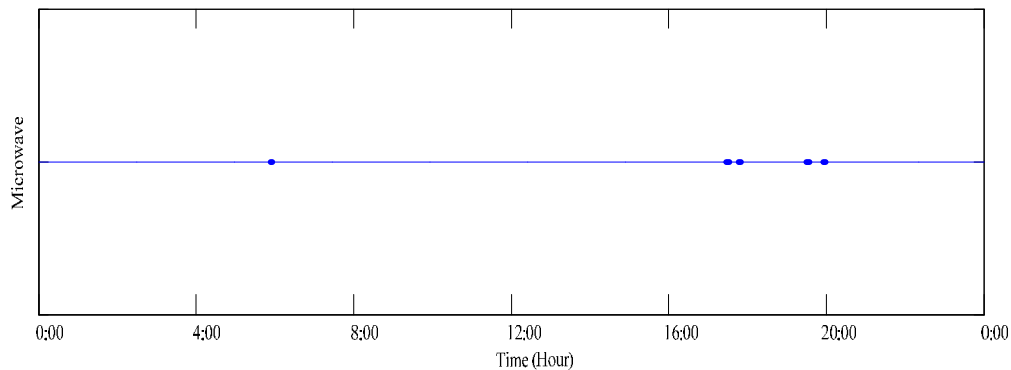
(b) Microwave usage time

Figure 3.11 Time of use probability profile for microwave.

The same procedure is conducted for each installed appliances at each simulation step. An example use pattern of some appliances as simulated by the procedure is showed in Figure 3.12. One can observe that the PC is used between 17:00 and 24:00 and washer and dryer are not used throughout the day. In the bottom of

Figure 3.12, the fridge and freezer are activated periodically throughout the whole day and not associated with household occupancy pattern. The simulated power demand in the form of current drawn by a house is shown in Figure 3.13.
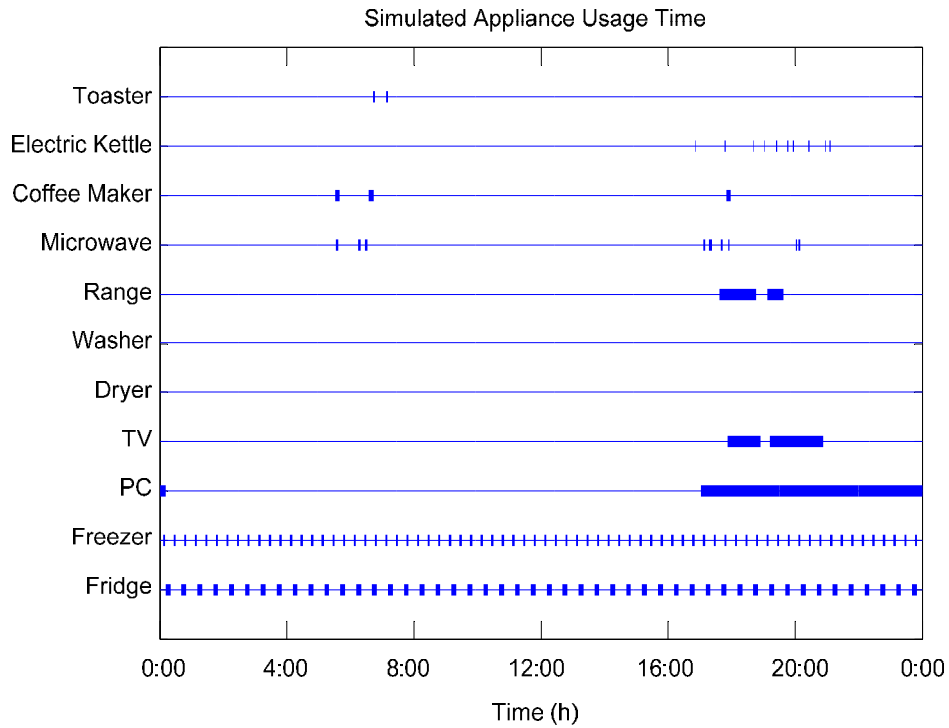
Figure 3.12 The simulated multiple-appliances usage time.
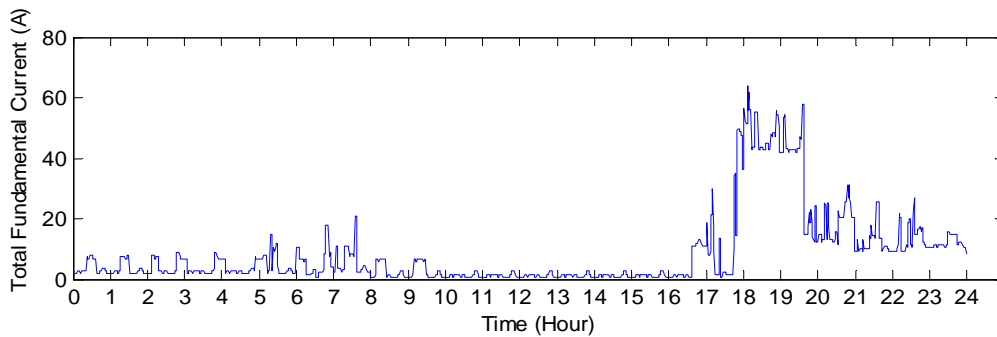
Figure 3.13 The simulated household power demand.

3.3 Single House Harmonic Load Model

Once the multiple-appliances usage time information is derived, the next step is to connect corresponding appliance models to the house circuit. In North America, residential and commercial customers are usually supplied through three-wire single-phase distribution transformers. Loads are supplied with a neutral and two hot phases carrying 120V with respect to the neutral and 240V with respect to themselves, as shown in Figure 3.14.
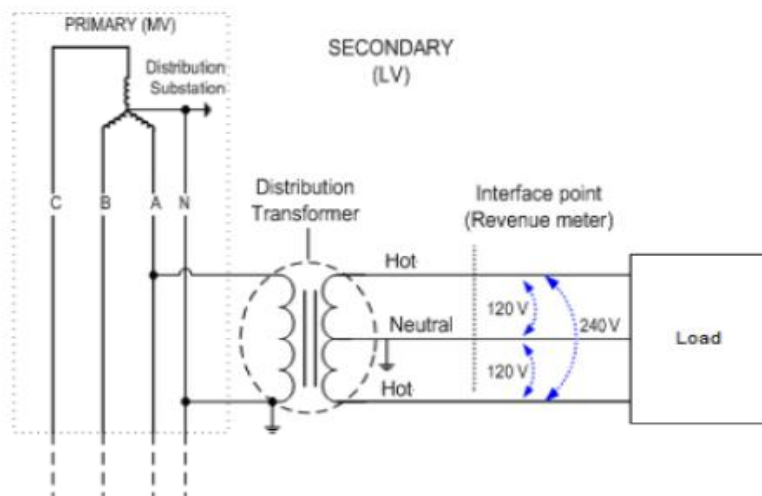
Figure 3.14 Power distribution system for three-wire single-phase feeding systems.

The appliances are essentially connected in a random fashion in the circuits, and this arrangement makes it difficult to model a house. Since this thesis is interested in the impact of appliance on utility systems, an equivalent circuit can be developed for a house. Based on the theoretical analysis shown in Appendix C, the model of Figure 3.15 has been established.

$I_{total}(h)$ $I_{NL}(h)$

System

$Z_{total}(h)$

Non-linear
Current Source
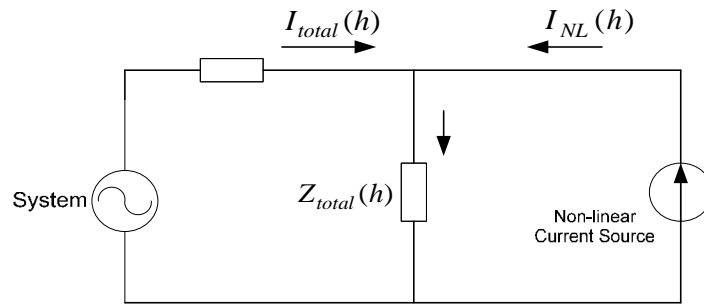
Figure 3.15 Equivalent circuit model to represent a residential house.

In each simulation step, the impedance $Z_{total}(h)$ and current source $I_{NL}(h)$ are established randomly based on the procedure described early. Impedance $Z_{total}(h)$ represents the linear loads in a house and current source $I_{NL}(h)$ represents the nonlinear loads. An example simulation output is shown in Figure 3.16.

Additionally, the result of seven days simulation, which contains 5 weekdays and 2 weekends is shown in Table 3.5. In order to validate the simulation results, field measurements were conducted for a typical residential house and the results are shown in Table 3.6. Both the tables list the mean value and standard deviation of the data on each day. The measured sample house has some occupants that do not need to go to work, so *"no working"* type occupancy pattern is chosen for simulation. Comparing Table 3.5 against Table 3.6, the mean values of fundamental and each harmonic current matched quite well.
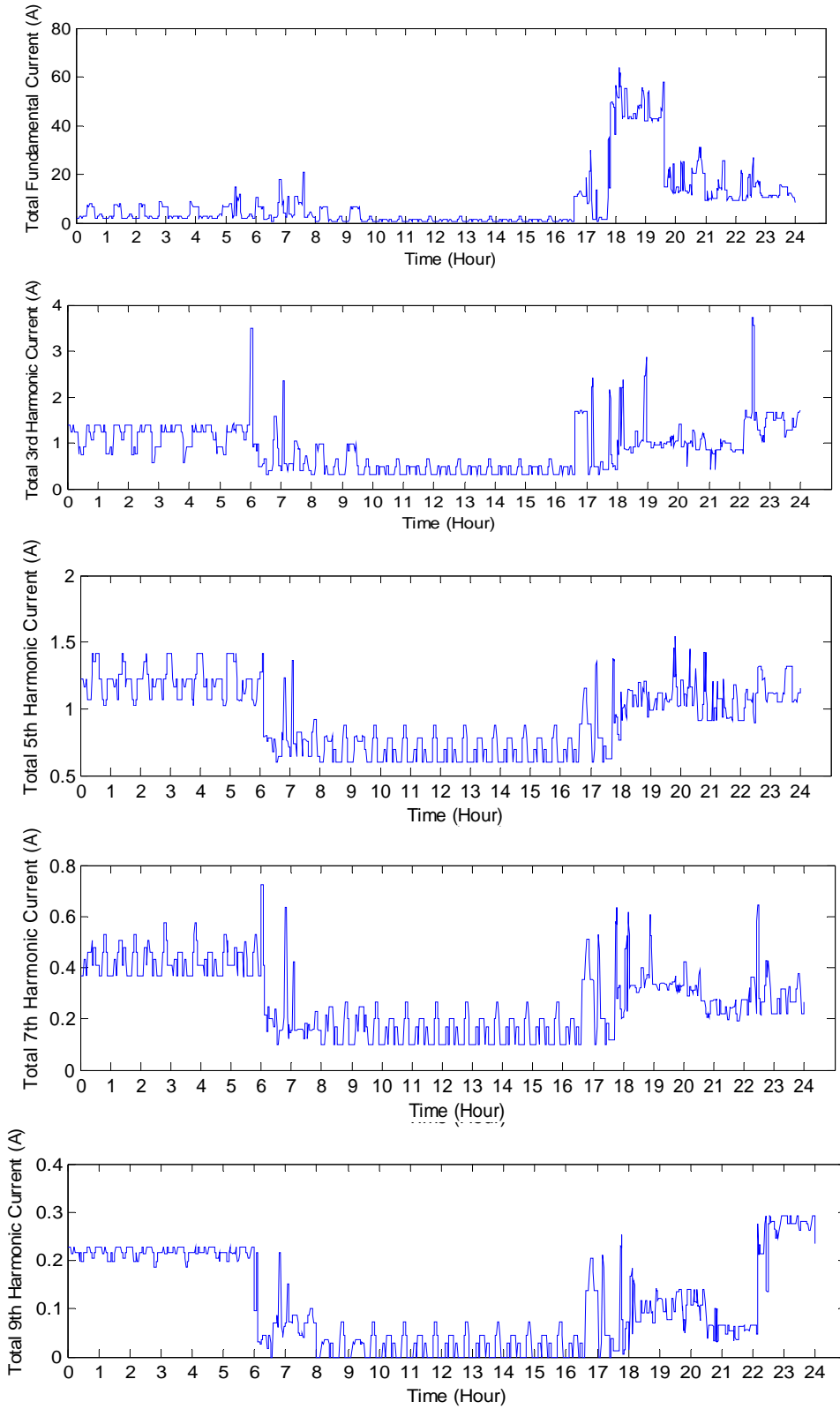
Figure 3.16 The simulation output $I_{total}(h)$ of house during one day.

Table 3.5 Simulation results of a residential house.

	Cases	Fundamental		3rd		5th	
		Mean	Std.	Mean	Std.	Mean	Std.
Weekday	Case 1	7.4255	8.4936	1.4206	0.9767	1.1325	0.4134
	Case 2	12.0936	14.1378	0.9727	0.5012	1.0008	0.2513
	Case 3	6.3924	7.5214	1.3608	0.7513	1.0672	0.2648
	Case 4	5.9725	7.6786	1.0318	0.7756	0.9515	0.3326
	Case 5	9.6551	13.6628	1.0408	0.7182	0.9447	0.2982
	Average	8.3078	10.7166	1.1653	0.7599	1.0193	0.3174
Weekend	Case 6	7.2618	9.5808	1.2442	0.8669	1.047	0.3285
	Case 7	8.2197	9.7457	1.5898	0.8434	1.0189	0.2168
	Average	7.7408	9.6636	1.417	0.8552	1.033	0.2783

Table 3.6 Measured results of a residential house.

	Date	Fundamental		3rd		5th	
		Mean	Std.	Mean	Std.	Mean	Std.
Weekday	April, 02 2010 Friday	7.6203	6.1043	1.4647	0.6793	1.0056	0.281
	April, 05 2010 Monday	7.6898	4.8839	1.3404	0.6299	0.9733	0.2486
	April, 06 2010 Tuesday	11.3668	13.3124	1.195	0.555	0.9467	0.2483
	April, 07 2010 Wednesday	7.7067	6.8004	1.0466	0.5225	0.9215	0.1896
	Average	8.5959	8.4348	1.2617	0.5998	0.9618	0.2441
Weekend	April, 03 2010 Saturday	7.5689	4.9492	1.2367	0.5807	0.9793	0.2392
	April, 04 2010 Sunday	9.2585	8.4477	1.5668	0.772	1.072	0.2744
	Average	8.4137	6.9231	1.4018	0.6831	1.0257	0.2574

Figure 3.17 shows the impedance $Z_{total}(h=1)$ obtained for the simulated house. In this figure, the impedance is not shown if linear loads are not in operation. From the profile, the operation of several significant appliances can be identified. Since the impedance represents the harmonic absorption capability of a house, it is examined in more detail. Figure 3.18 shows the cumulative distribution function of the parallel impedance during one month. The results show that the impedance is lower than 40 ohms for around 39% of the time.
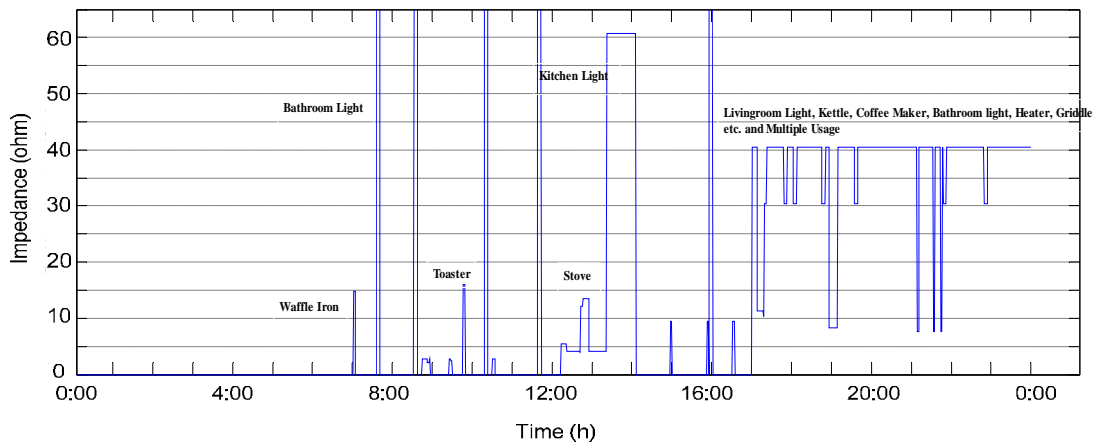
Figure 3.17 Parallel impedance of the house model.
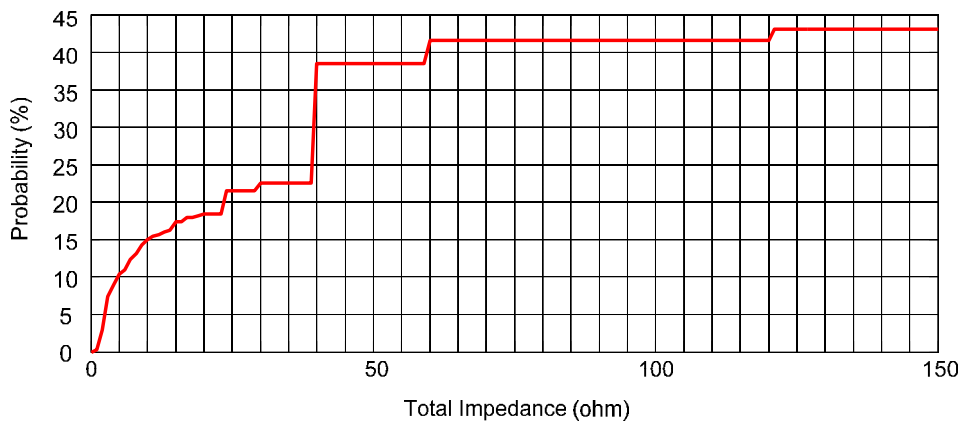
Figure 3.18 Cumulative distribution of the parallel impedance (30 days).

71

3.4 Multi-House Harmonic Load Model

As shown in Figure 3.19, residential houses are supplied through single-phase service transformers connecting the primary to the secondary system. The secondary is a 120/240 V three-wire service. Each distribution transformer normally supplies ten to twenty houses. The loads are modeled collectively as one load connected to the secondary side of the service transformer, the result is called service transformer model. This model will be used for studying the harmonic impact on primary distribution systems. The steps for conducting such model are as follows:

- Harmonic models of 10-20 house are randomly generated;
- Connect the house models into the circuit shown in Figure 3.20;
- The circuit is equivalenced into the form shown in Figure 3.21.
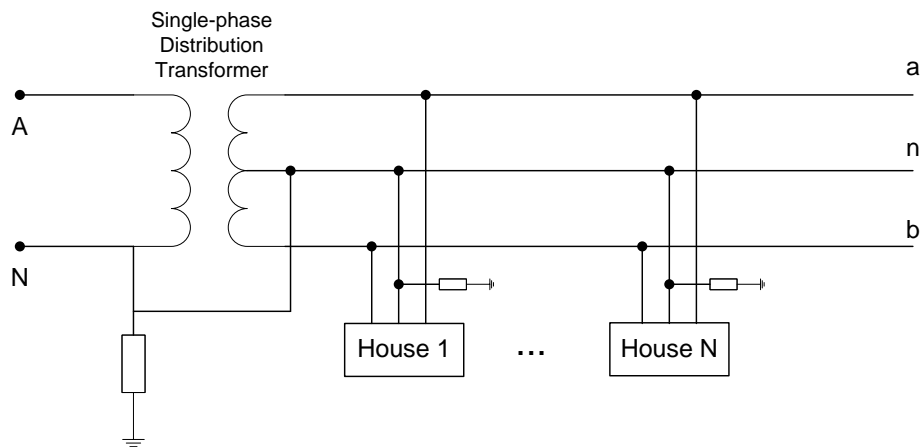
Figure 3.19 Typical service transformer connected to N houses.
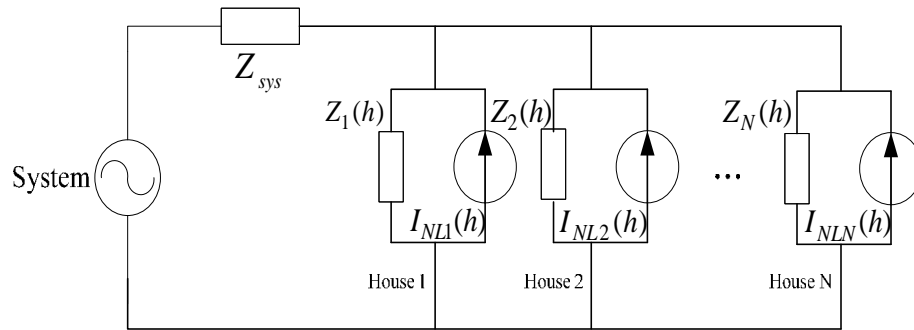
Figure 3.20 Multi-house equivalent model.
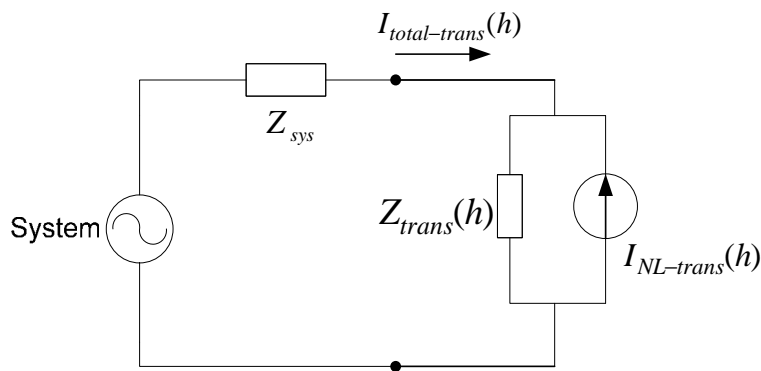
Figure 3.21 The multi-house load model.

The above multi-house or service transformer model was verified by comparing its results against those from field measurements. Load and harmonic current data of some service transformers were collected in Edmonton in winter 2008. All transformers are mainly supplying residential loads, and there are totally 55 days measurement data of 10 different transformers (Some measurement results are presented in Appendix D). The current variation of each transformer is unique, so it is not easy to compare the results with those obtained from simulation which also exhibit random characteristics. The approach adopted by this thesis is to extract and compare the principal components of the current profiles.
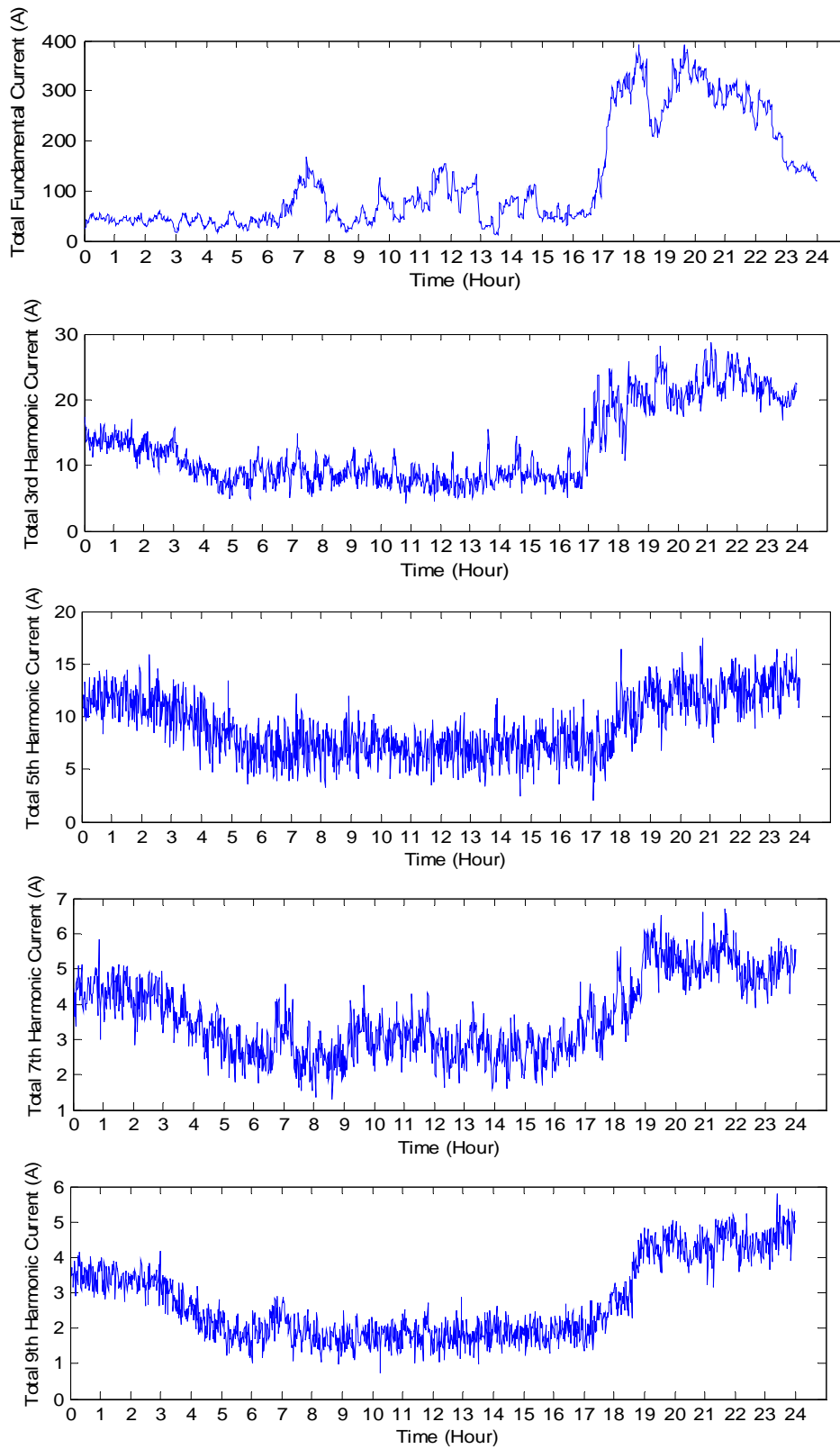
Figure 3.22 Example simulation output of transformer current during one weekday.

The Principal Component Analysis (PCA) involves a mathematical procedure that transforms a number of possibly correlated variables into a smaller number of uncorrelated variables called principal components. The first principal component accounts for as much of the variability in the data as possible, and each succeeding component accounts for as much of the remaining variability as possible. It's mathematically defined as follows:

$$X_{(m \times n)} = T_{(m \times m)} \times V_{(m \times n)}$$

$$X_{(m \times n)} = \begin{bmatrix} t_{1,1} \\ ... \\ t_{m,1} \end{bmatrix} \times (v_{1,1}...v_{1,n}) + \begin{bmatrix} t_{1,2} \\ ... \\ t_{m,2} \end{bmatrix} \times (v_{2,1}...v_{2,n}) + ... + \begin{bmatrix} t_{1,m} \\ ... \\ t_{m,m} \end{bmatrix} \times (v_{m,1}...v_{m,n}) \qquad (3.3)$$

where *X* is a matrix, which consists of m variables and n set of observation values. The above PCA formula splits the original data into several components, which is represented by *V*. *T* is the coordinate of the original data in the new frame composed by n components. Normally, the first principal component contains much of the information in original data [39].

The variance given by the corresponding principal component is used to estimate how much variance has been included by principle components. Table 3.7 lists the variance given by the first principal components for the magnitudes of measured transformers. Data are grouped into weekday and weekend. As it can be seen, for fundamental and 3rd harmonic current, first principal components can represent almost 60% of the original data; however, for higher harmonics these percentages

drop to 20-30%. The reason is that higher harmonics are more random and seem not show similar trend.

Table 3.7 Percentage of variance of the first principal component of transformer current.

Data Group	Fundamental	3rd Harmonic	5th Harmonic	7th Harmonic	9th Harmonic
Mixed Data	53.60	59.90	25.43	32.68	39.56
Weekend Data	60.03	62.15	26.04	32.01	38.71
Weekday Data	54.87	60.76	27.73	36.21	42.06

Based on the above analysis, two methods are adopted for the transformer model verification:

1. For fundamental and 3rd harmonic current, the verification method is to extract the first principal components from the measurement data and the simulation results respectively. The components are then correlated to verify their consistency.

2. For higher order harmonic currents, the verification is to compare the normalized probability distribution of the measured and calculated data.

Figure 3.23 shows the daily variation of the first components of the fundamental and 3rd harmonic currents from both measurement and simulation on weekdays. The first component of simulated fundamental current fits quite well with that of measured one. The correlation factor is 0.94. There is an acceptable difference between the first components of 3rd harmonic current from simulation and measurements. The correlation factor is 0.7.

76
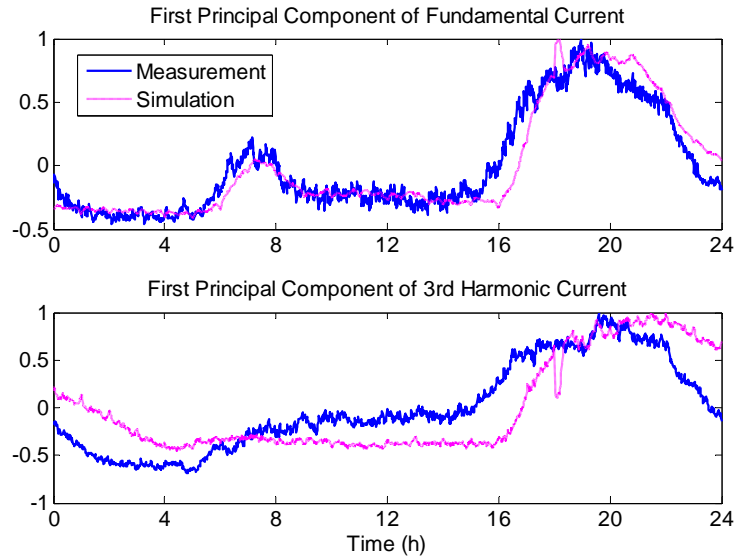
Figure 3.23 Comparison of the first principal components (weekdays).

The remaining part of the fundamental and 3rd harmonic components contains almost 40% of the original data. A comparison is made in the form of statistical distributions in Figure 3.24. The distributions exhibit similar characteristics.
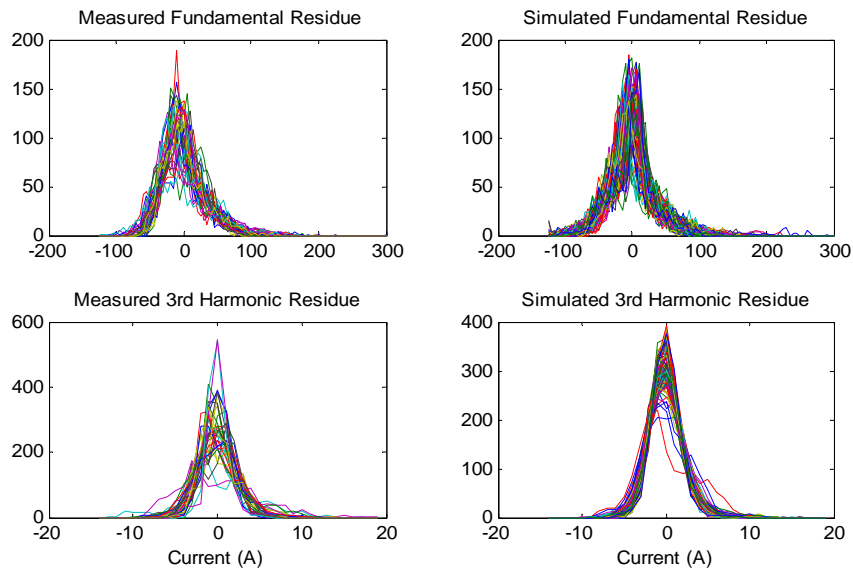
Figure 3.24 Probability distribution of measured and simulated residue part on weekday.

For higher order harmonics, the principal components are lot more random and comparison using the principal components cannot be made. Therefore, normalized harmonic distributions are used for comparison. Figure 3.25 shows the results. Table 3.8 shows the standard deviation of the harmonics. The results show some form of consistency. Based these analysis, we conclude that the proposed residential house and service transformer model is generally acceptable.
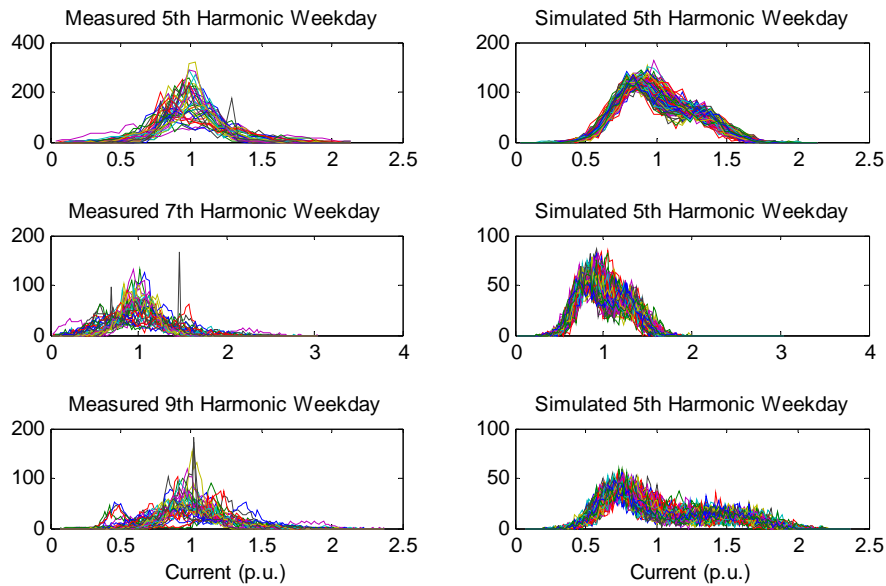
Figure 3.25 Probability distribution curves of higher harmonics.

Table 3.8 The standard deviation of higher order harmonic currents.

Data Group	5th Harmonic		7th Harmonic		9th Harmonic	
	measurements	simulation	measurements	simulation	measurements	simulation
Weekend Data	0.22	0.26	0.31	0.27	0.30	0.39
Weekday Data	0.21	0.24	0.30	0.28	0.28	0.35

3.5 Summary

This chapter presented a bottom-up harmonic model for residential houses based on the information associated to the individual appliances.

In Section 3.2, the modeling of the operating condition of each appliance was developed, considering the appliances usage pattern as well as the number of occupants and their activities. The results allows to determine what appliances are in operation, how long it will last and how many times on average it will be use in the simulation period

Then, in Section 3.3, individual appliances were aggregated so as to produce an individual residential house harmonic profile during a certain time. The single house model was validated by comparing its output current against real field measurements.

Finally, by combining residential house harmonic model, a service transformer model was derived in Section 3.4. This transformer model has been verified with the field measurement data using PCA and statistical analysis.

Chapter 4

Harmonic Modeling and Simulation of Secondary Distribution Systems[2]

A typical distribution substation will serve one or more feeder circuits, while a typical feeder circuit may serve numerous loads of all types. Industrial customer may take service directly from the distribution feeder circuit primary and all other customers, including residential and commercial, are typically served from the secondary of service transformers that are connected to the feeder.

As one can observe in Figure 4.1, distribution power networks are composed of the *primary system* and the *secondary system*. Depending on the type of study and on the location of interest, each system can be modeled differently. Since our concerned nonlinear residential loads are distributed all over the secondary system, it is a natural need for us to evaluate this impact on secondary distribution system. For the study in that purpose, the primary system will be modeled as an equivalent circuit. The service transformer will be modeled explicitly and the loads (individual houses) will be modeled as equivalent circuits in the form of one house per equivalent circuit.
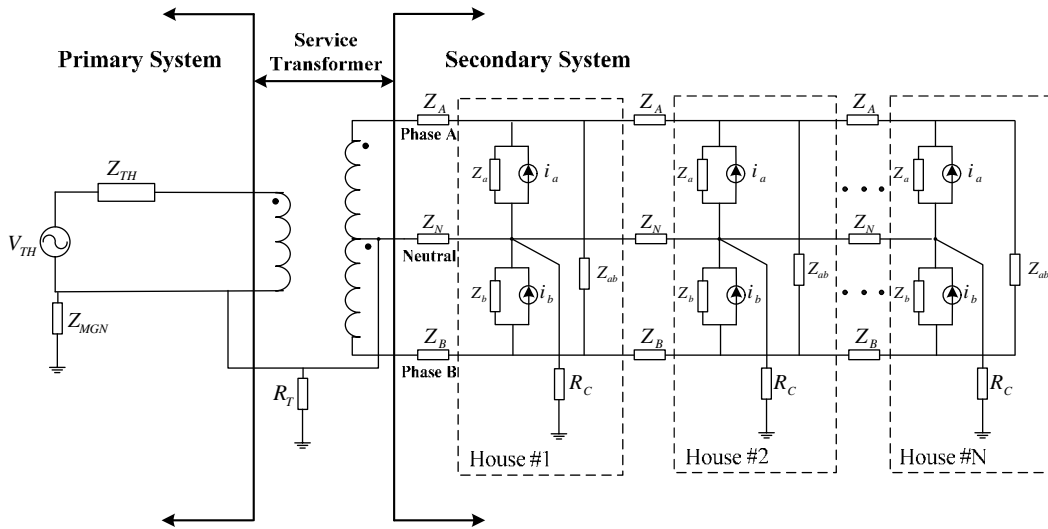
Figure 4.1 Secondary distribution network with its supply system.

4.1 The Modeling Approach for Distribution System

In this section, the modeling approach for three components of typical distribution system will be introduced and studied, which are primary system model, service transformer model and secondary system model.

4.1.1 Primary System Model

The primary system is a four-wire multi-grounded neutral (MGN) system in North America. A general layout of a MGN distribution system is shown in Figure 4.2(a). The neutral of the primary feeder is grounded at regular intervals with identical resistances. For this reason, the system is called the multi-grounded

81

neutral (MGN) system. In order to reduce the complexity of the harmonic power flow simulations, an equivalent circuit model for the primary system is adopted, as shown in Figure 4.2(b). Because of the phase-to-neutral connection of the service transformer, the supply system (substation) and the primary distribution feeder are modeled as a single-phase Thevenin circuit which consists of voltage source behind a series (*RL*) system impedance. The neutral is modeled as equivalent neutral impedance. Based on the theory represented in [40], the neutral impedance can be estimated using equation (4.1) and (4.2):
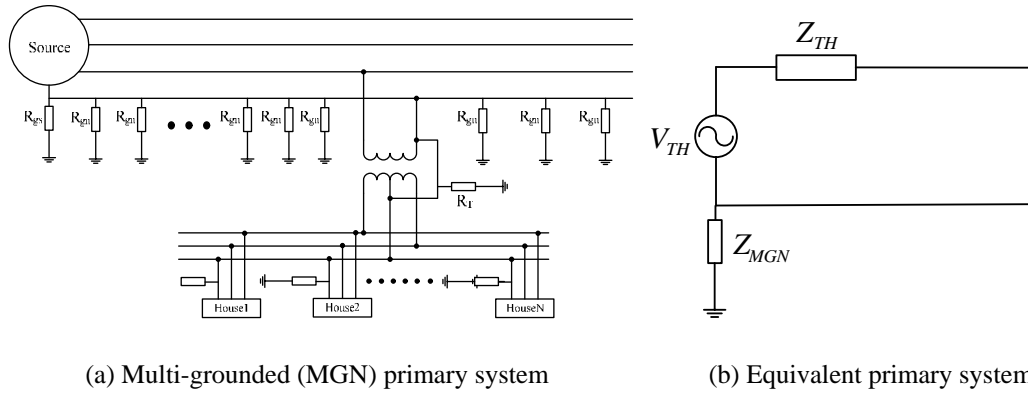
(a) Multi-grounded (MGN) primary system   (b) Equivalent primary system

Figure 4.2 Layout of a MGN distribution system.

$$Z_{MGN} \approx Z_{lad\,1} \,//\, Z_{lad\,2} = \frac{1}{2}\sqrt{z_{nn}R_{gn}s} \qquad (4.1)$$

$$Z_{lad} \approx \sqrt{z_{nn}R_{gn}s} \qquad (4.2)$$

where z_{nn} is the self impedance of the neutral wire (Ω/km), R_{gn} is the neutral grounding resistance and s is the distance (km) between the grounding resistance (R_{gn}), as shown in Figure 4.3.
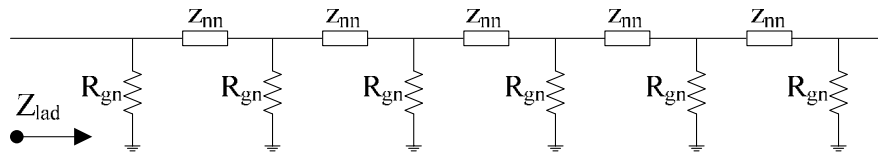
Figure 4.3 Multi-grounded neutral ladder network.

The parallel of Z_{lad1} with Z_{lad2} is due to the fact that there is an upstream and a downstream ladder at the point of the service transformer.

4.1.2 Service Transformer Model

The standard secondary load service is a 120/240 V three-wire service in North America. This is accomplished with a single-phase, three-winding service transformers connecting the primary to the secondary system [41]. The model for this transformer is shown in Figure 4.4.
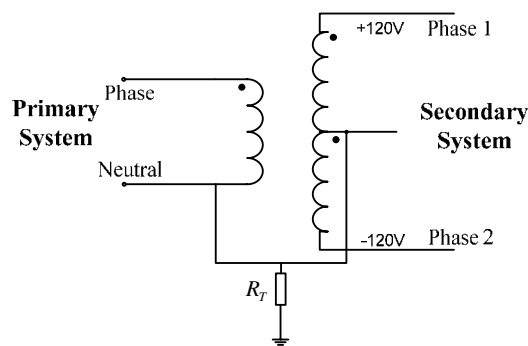
Figure 4.4 Single-phase service transformer.

Normally, the nameplate impedance of a single-phase transformer is the full-winding impedance, the impedance seen from the primary when the full

83

secondary winding is shorted from *Phase 1* to *Phase 2*. If the full-winding nameplate impedance for the transformer is $R + jX$, the primary (Z_A) and secondary impedances (Z_1 and Z_2), as shown in Figure 4.5, can be obtained through equation (4.3) ([41], [42]):
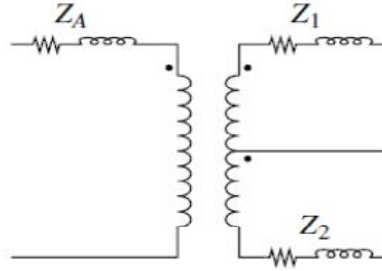
Figure 4.5 Model of a 120/240-V secondary winding with all impedances.

$$Z_A = 0.5R + j0.8X$$
$$Z_1 = Z_2 = R + j0.4X$$

(4.3)

It is common practice to interconnect the primary and secondary neutrals and to use a single ground for these neutrals, which provides lower grounding resistance for both the primary and secondary systems as well as surge protection. A disadvantage of this practice is the occurrence of stray voltage on the secondary system, emanating from the high neutral-to-earth voltage (NEV) of the primary system [43].

4.1.3 Secondary System Model

The secondary system of the power distribution networks consists of several houses (and other low voltage loads) connected to the secondary of the service transformer. The houses contain multiple appliances that are linear or nonlinear. In Chapter 2 and 3, a probabilistic bottom-up technique has been developed to model typical appliances of a house, which led to an aggregated harmonic model for each house. Important parameters were taken into account to determine the type and number of appliances in operation at a given time, such as daily time of use probability profiles and appliance usage characteristics. The technique developed to build the harmonic aggregated house model and the secondary system is summarized as follows:

- Determine the type appliances per household
- From the load trend data, determine the number of appliances per household
- Build the model for linear and nonlinear loads
- Obtain the daily usage pattern for each appliance
- Model the single harmonic house aggregated model (Z_a, i_a, Z_b, i_b and Z_{ab}), as shown in Figure 4.6
- Connect each house model to the secondary side of the service transformer
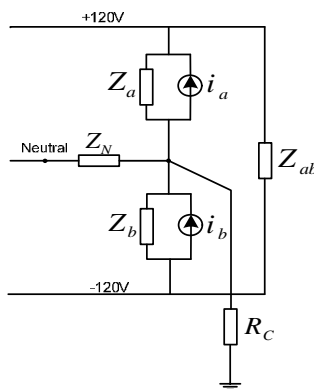
Figure 4.6 Single house model.

85

As mentioned in Chapter 3, only linear appliances are connected to both phases (240 V) so that, in this thesis, there are no nonlinear 240 V loads.

4.2 Technique and Model Parameters Used for Simulation Studies

A Multiphase Harmonic Power Flow program is used for simulation studies [10]. The system must be modeled in multiphases due to the inclusion of the neutral conductor, grounding points and two-phase conductors. The procedure to perform the harmonic power flow simulations is shown in Figure 4.7 and is summarized as follows:

1) Determine the type of appliances per household
2) From the load trend data, determine the number of appliances per household
3) Generate the model for the linear and nonlinear appliances
4) Determine each appliance daily usage pattern and build the harmonic houses model
5) For time snapshot T1, connect the fundamental frequency component of the houses model to the service transformer and the primary system and run power flow
6) Set up the harmonic current source models for the nonlinear loads based on the load flow results
7) Connect the harmonic current sources into the study system and run harmonic power flow. Save the results
8) Go back to Step 5, and repeat it for another time snapshot (T2), until last snapshot
9) Go back to Step 2 for another load penetration level (load growth)
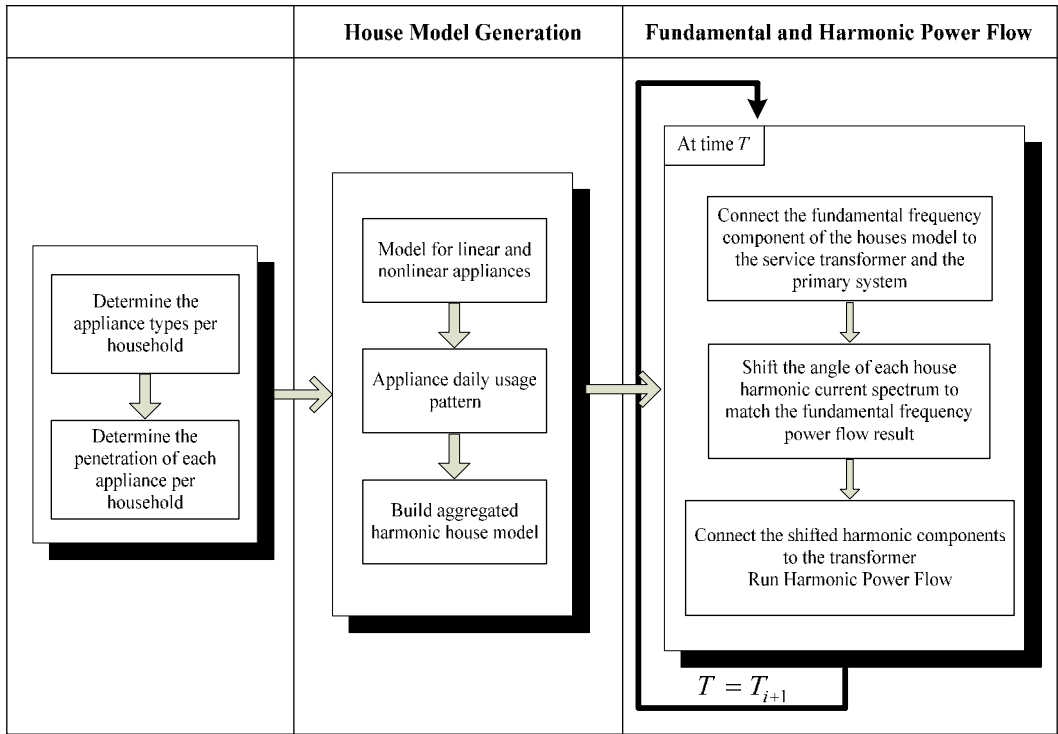
Figure 4.7 Harmonic power flow simulation procedure for the secondary system.

Figure 4.8 shows the secondary distribution network employed for case studies.

Parameters of this study are summarized in Table 4.1.
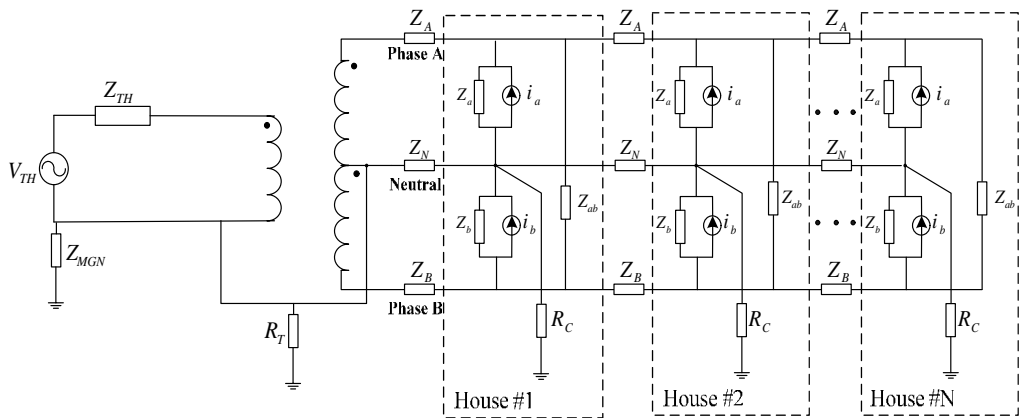
Figure 4.8 Distribution network model for secondary system analysis.

Table 4.1 Base case system parameters.

Base Case System Parameters		Values
Primary System	MGN grounding resistance (R_{gn})	15 ohms
	Grounding span of the MGN neutral (s)	75 m
	Impedance of MGN neutral (z_{nn})	0.397 + j0.912 ohm/km
	Voltage Source (V_{TH})	14400 V (@ 60 Hz)
Service Transformer	Voltage (V_H/V_L) rating	14400/120 V
	KVA rating	37.5 kVA
	Impedance	2 %
	Resistance	1.293 %
	Grounding resistance (R_T)	12 ohms
Secondary System	Customer grounding resistance (R_C)	1 ohm
	Neutral impedance (Z_N)	0.55 + j0.365 ohm/km
	Phase impedance (Z_A and Z_B)	0.21 + j0.094 ohm/km
	Number of houses (N)	10
	Typical house load	1 kW
	Distance between houses	20 m

4.3 Simulation Study Scenarios

As the goal of this thesis is to determine the impact of nonlinear home appliances into the future, the studies are conducted for each year over the next several years considering the market trends established in Chapter 2. The following study scenarios are evaluated:

- **Base Case**: The base case scenario uses a current year nonlinear load penetration situation. Its results are used to check if there are any inconsistencies in the simulation results and to serve as the baseline results for comparative studies.

- **Load Evolution Cases**: The appliance loads are "evolved" or "grown" according to the market data. Four load evolution cases are studied:

Case 1: Natural Load Evolution. This case considers the evolution or change of all home appliances per the market trend.

Case 2: CFL Load Evolution. This case considers the replacement of lighting loads by the CFL only. The other loads remain the same as the base case. This is a hypothetical case that helps to understand the impact of CFL.

Case 3: PC Load Evolution. This case considers the situation where only PC related appliances are changed. Again this is a hypothetical case useful to understand the specific impact of PC loads.

Case 4: TV Load Evolution. This case considers the situation where only TVs are changed. The results help to understand the specific impact of TV loads.

It shall be noted that the same distribution network is used for all case studies. The number of customers remains the same as in the base case. Only thing that is changed is the appliances under study. The appliances are changed according to the market trend. A sensitivity study is also conducted to verify the impact of different market trends on load evolution study results, which is shown in Appendix E.

- **System Parameters Sensitivity Study**: The objective is to evaluate what is the impact of changing the system parameters on the secondary system harmonic distortion levels. The following system parameters are considered for the sensitivity analysis:

    o Customer house grounding
    o Distance between houses
    o Houses distribution (parallel and series)
    o MGN primary system neutral grounding resistance
    o Distorted supply system

4.4 Secondary System Harmonic Simulation Results

The harmonic power flow simulations yield massive amount of results for each time snapshot, feeder location, and power quality indices. For secondary system analysis, the following results are analyzed by this thesis:

ꟷ Voltage and current distortions in the secondary system:

- Harmonic spectrum

- Individual Harmonic Voltage Distortion (IHD$_V$)

- Total Harmonic Voltage Distortion (THD$_V$):

  This index can be calculated from equation (1.5)

- Individual Demand Distortion of Current (IDD):

$$IDD(\%) = \frac{I_h}{I_L} \times 100 \qquad (4.4)$$

- Total Demand Distortion of Current (TDD):

  This index can be calculated from equation (1.7)

ꟷ Neutral conductor current/voltage rise:

- Neutral current and voltage harmonic spectrum

- Neutral voltage RMS:

$$V_{RMS} = \sqrt{\sum_{h=1}^{H} V_h^2} \qquad (4.5)$$

ꟷ Impact of harmonics on the secondary system losses:

- Fundamental and harmonic power losses at phases, neutral and grounding circuits

90

$$P_h = R(\,h\,) \times I_h^2 \qquad\qquad (4.6)$$

ı   Impact of harmonics on revenue meter errors

  • Harmonic influence on the accuracy of residential revenue meter. This study is based on reference [44].

ı   Overloading of the distribution transformer:

  • Distribution transformer windings I²R losses for fundamental and harmonics

  • K-Factor: this index is a weighting of the harmonic load currents according to their effects on transformer heating. A K-factor of 1.0 indicates a linear load (no harmonics). The higher the K-factor, the greater the harmonic heating effects. It can be calculated from equation (1.8).

The above results can be quite different at different times of a day due to the random nature of the loads. Therefore massive amount of results are available for analysis. In order to facilitate the interpretation of results, further processing is needed to produce summary information. The time variation of the results can be condensed using histograms and cumulative distribution curves. For example, instead of providing the 24 hours profile of a harmonic result, a single index showing the average value or the value that is not exceeded by 95% of the time (called the "95% index") can be more useful. The results obtained at different locations can also be condensed through averaging. In this thesis, the "95% index" is adopted. This index is explained using Figure 4.9. In this case, the simulation

studies will yield the 3rd harmonic voltage profiles for different houses (i.e. nodes in the simulation model) over a 24 hour period. These profiles are averaged over houses first to create a 3rd harmonic voltage profile representing the secondary system. The average profile is then transformed into an accumulative probability curve. This curve helps to identify a 3rd harmonic voltage value that will not be exceeded by 95% of the time. This value (showed as 0.81V in the Figure) is the "95% index" value of interest.
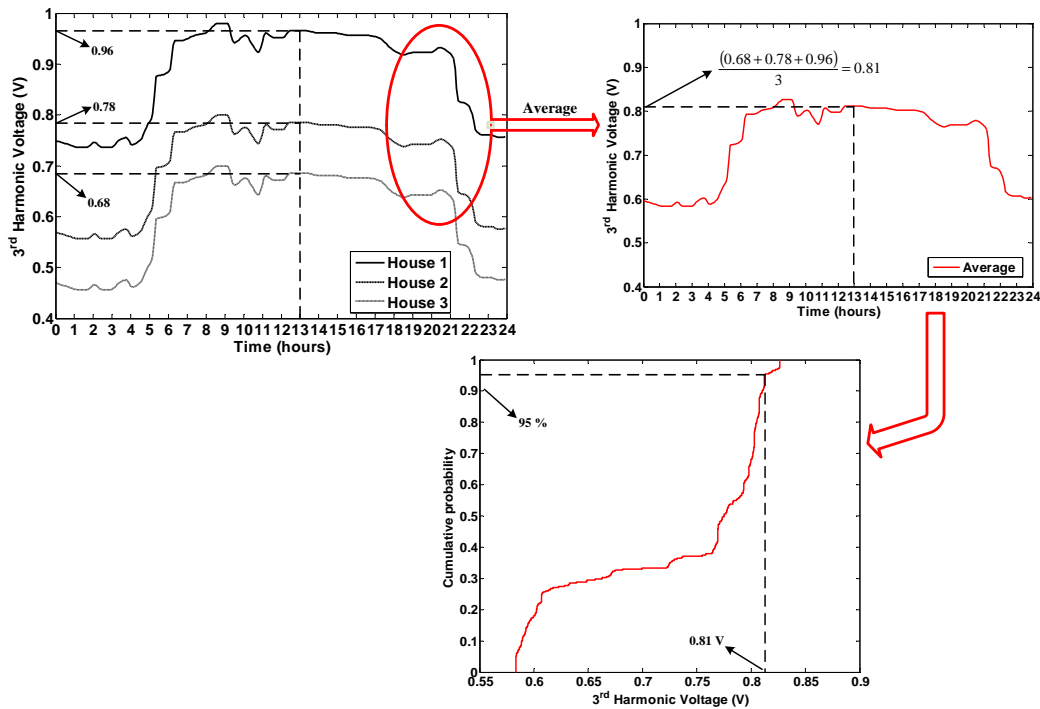
Figure 4.9 Definition of and procedure to determine the "95% index".

Based on the simulation scenarios defined in Section 4.3, the following subsections present the results for the base case, load growth and system sensitivity studies.

4.4.1 Base Case Results

4.4.1.1 Voltage and Current Distortions in the Secondary System

The harmonic phase-to-neutral voltages for all houses connected to Phase A of the secondary system are obtained. For simplicity, phase-to-neutral voltage will be referred to as phase voltage. The daily average profile include THD_V is determined and shown in Figure 4.10(a). The "95% index" of the phase voltage is shown in Figure 4.10(b). The results associated to Phase B are not shown because they are similar to Phase A.
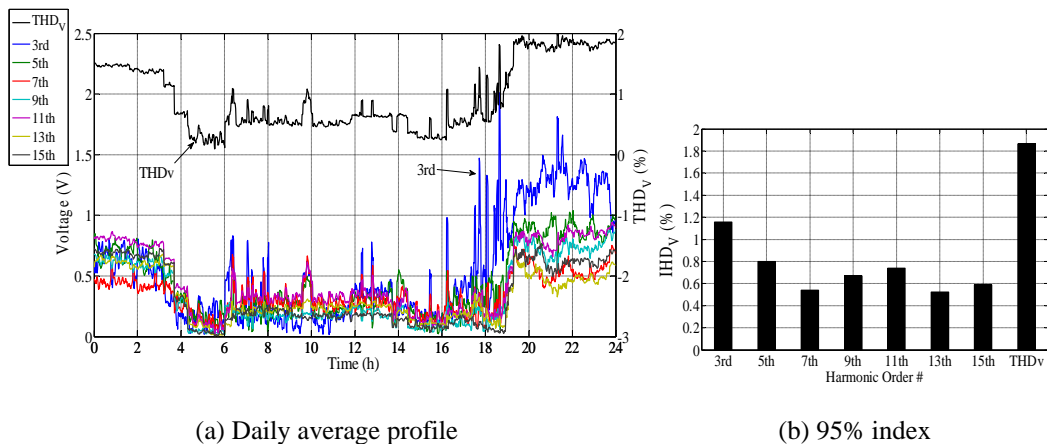
(a) Daily average profile   (b) 95% index

Figure 4.10 Average harmonic phase voltages of all houses.

Likewise, the harmonic phase A currents between the houses are obtained. Then, the daily average profile is determined and shown in Figure 4.11(a). The daily average profile of the TDD is shown as well. Finally, from Figure 4.11(a), the 95% index of the individual demand distortion (IDD) and TDD are be determined and are shown in Figure 4.11(b).

93
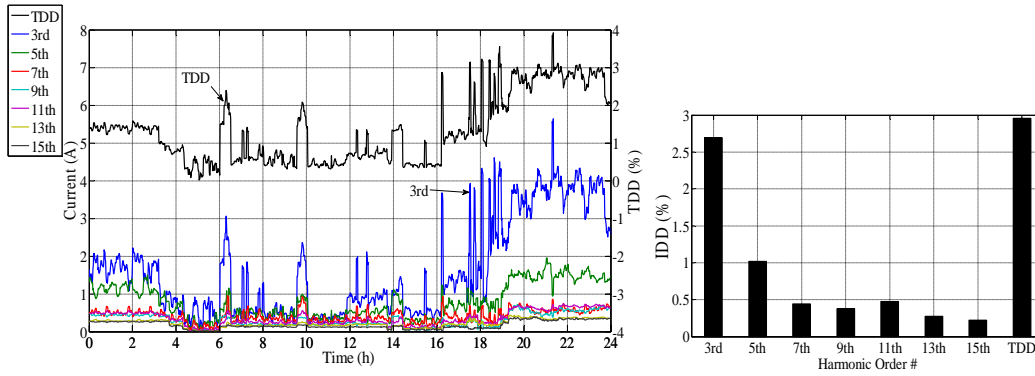
(a) Daily average profile   (b) 95% index

Figure 4.11 Average harmonic phase current of all houses.

The results show that the 3rd harmonic is the most dominant component, which is then followed by the 5th and 7th components. This is consistent with the field measurement results. The period at which the harmonic levels are the highest is between 18:00 and 24:00 since most nonlinear appliance usage is observed during this time, such as PC, TV and CFL etc. During the period between 00:00 and 05:00, residential loads are dominated by other nonlinear appliances, such as fridge, freezer and furnace.

From Figure 4.10(b), one can observe that the voltage total harmonic distortion (THD_V) is below the limits defined by the IEEE Standard 519-1992 [6]. This standard also recommends limits related to the total demand distortion (TDD), which is defined by equation (1.7). Figure 4.11(b) show that the TDD remained below the strictest limit ($TDD < 5\%$) defined by the standard.

4.4.1.2 Neutral Conductor Current & Voltage Rise

Figure 4.12(a) shows the daily profile of the neutral to ground harmonic voltage averaged over all the secondary system houses. Figure 4.12 (b) shows the 95% index of the neutral harmonic voltage and its RMS value. Figure 4.13(a) shows the daily profile of the average harmonic neutral current circulating between the houses of the secondary system. Figure 4.13(b) shows the 95% index of the harmonic neutral current. The fundamental component daily profile is not shown so that the figures do not become too crowded.
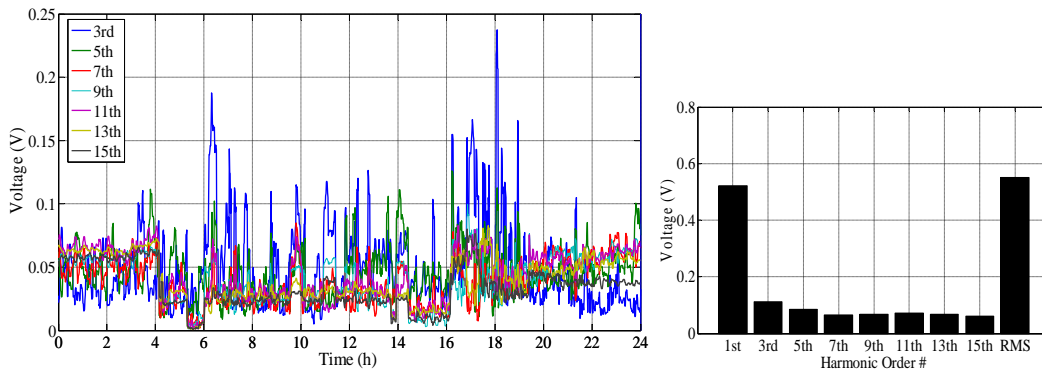
(a) Neutral voltage daily average profile.   (b) 95% index
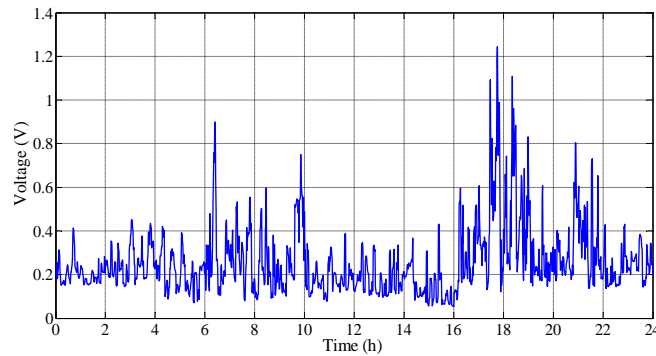
(c) RMS neutral voltage daily average profile

Figure 4.12 Average neutral to ground voltage.

(a) Daily average profile

(b) 95% index (fundamental and RMS divided by 10)
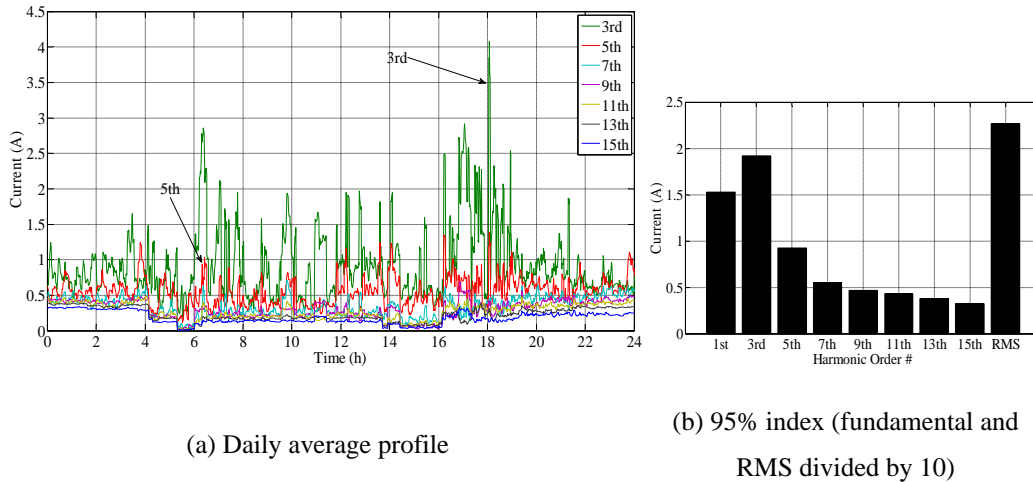
Figure 4.13 Average neutral current circulating between the houses.

The results show that the neutral voltage is still dominated by the fundamental frequency component. These are caused by the load imbalance between the two phases. The implication is that the harmonics produced by nonlinear loads don't have a major impact on neutral-to-earth voltage rise (a major component of stray voltage). The results also show that the neutral current contains more 3rd harmonic components.

4.4.1.3 Impact of Harmonics on the Secondary System Losses

Figure 4.14 shows the daily total fundamental and harmonic losses of the phase and neutral circuits of the secondary distribution system. The 95% index over the daily phase and neutral losses is also provided. The main finding is that the majority of losses are caused by the fundamental frequency component and they occur at the phase conductors. The conclusion is that harmonic caused losses in the secondary system shall not be a concern to utility companies.

96
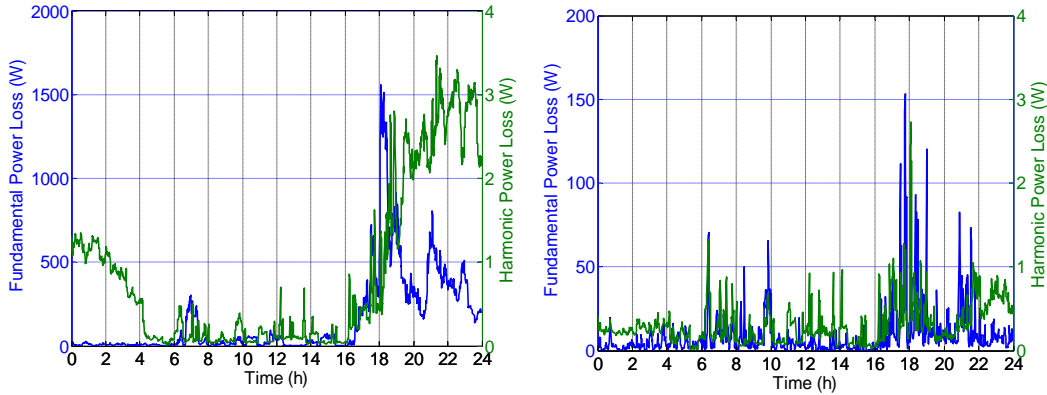
| | (a) Phases conductors power loss | | (b) Neutral conductor power loss |

Time 95% Index Power Loss			
Conductor	Fundamental	Harmonic	Total
Phases	618.16 W	2.91 W	621.07 W
Neutral	35.22 W	0.83 W	36.05 W
Total	656.77 W	4.35 W	661.12 W

Figure 4.14 Secondary system power losses.

4.4.1.4 Overloading of Distribution Transformers

Losses in transformers are due to stray magnetic losses in the core, and eddy current and resistive losses in the windings. Of these, eddy current losses are of most concern when harmonics are present, because they increase approximately with the square of the frequency. One approach to account for this increased eddy current loss in selecting a transformer is to calculate the factor increase in eddy current loss and specify a transformer designed to cope; this is known as *K-Factor* and is defined by *IEEE Std C57.110-1998* [45].

Figure 4.15(a) shows that the K-Factor is high between 00:00 a.m. to 04:00 a.m., which is due to the fact that mainly nonlinear appliances are operating, such as fridge and freezer, and also the transformer loading (fundamental component) is

very low during this period, which makes the K-Factor very high, as can be seen from equation (1.8). On the other hand, beyond this period, the K-Factor is around 1.2 showing that harmonic heating effect is lower. Figure 4.15(a) also shows the daily *K-Factor* profile of the service transformer calculated from the base case. This figure shows that for the 95% of the time the *K-Factor* is lower than 6. This result indicates that the service transformers take more (equivalent) loads than what are calculated from the load flow results. Since most service transformers are oversized, the harmonic impact may not be as high as indicated by the K-Factor results. Here the factor is used as an indicator to assess the increased loading on the service transformers. How to include harmonics in estimating the total loading of a service transformer needs more research.

The winding losses shown in Figure 4.15(b) reveal that the fundamental frequency winding loss is still much higher than the harmonic loss.

(a) Service transformer K-Factor   (b) Service transformer winding losses
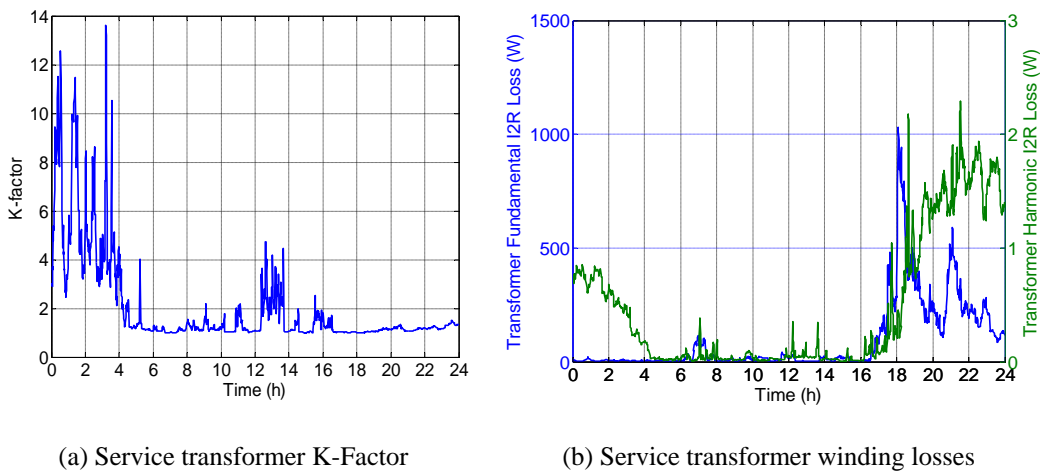
Figure 4.15 Service transformer power losses.

4.4.2 Load Evolution Results

The load evolution studies are done using the market trend data. In order to facilitate the interpretation and comparison of the results, all the results are represented by their "95% index" values. Two different charts are provided. The first type of charts shows the index values over the study period (5 years). The second type of charts shows the average annual growth rate of the indices. The annual growth rate is the most useful parameter to predict the future harmonic conditions of a residential feeder.

4.4.2.1 Harmonic Voltage and Current Distortions

Figure 4.16(a) shows harmonic voltage in the next 5 years. From the curves, one can calculate the average annual growth rate associated to the index, which is shown in Figure 4.16 (c). For example, the 3rd harmonic index will grow at the rate of 15% per year. Figure 4.16 (c) also shows the individual impact of CFL, PC and TV loads on the annual harmonic growth rate. The harmonic current results are shown in Figure 4.17. The main findings are

- The harmonic current and harmonic voltages have similar growth rates.
- The harmonic growth rates are generally high (above 10%). Among them, the 3rd, 5th, 13th and 15th harmonics have the highest growth rates.
- The CFLs have more contributions to the harmonic increase. The LCD TVs has insignificant impact on harmonic increases.
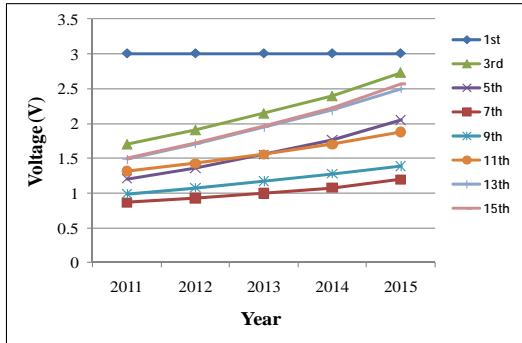
(a) Natural load evolution (fundamental is divided by 40)
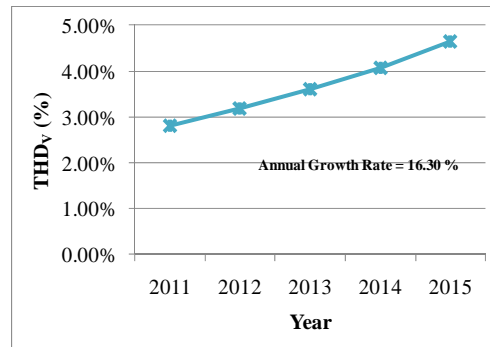
(b) Natural load evolution
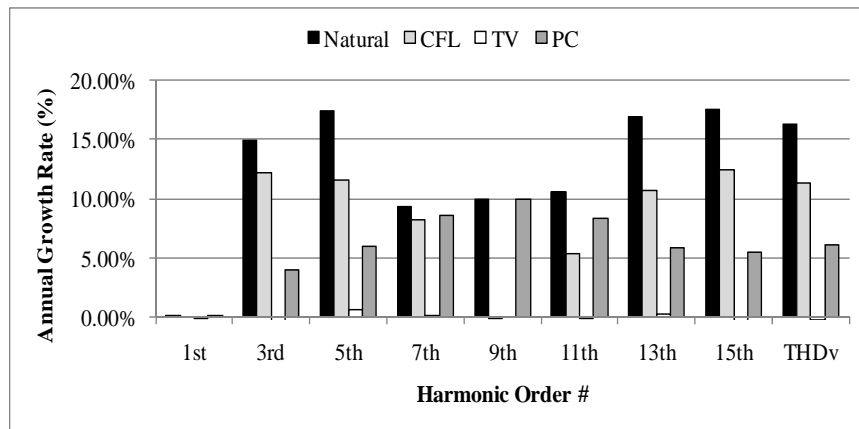
(c) Average annual growth rate

Figure 4.16 Average phase A voltage.
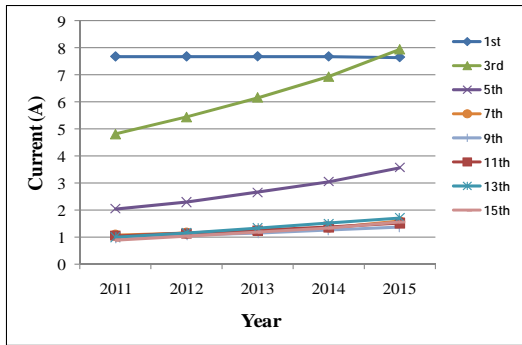
(a) Natural load evolution (fundamental is divided by 10)
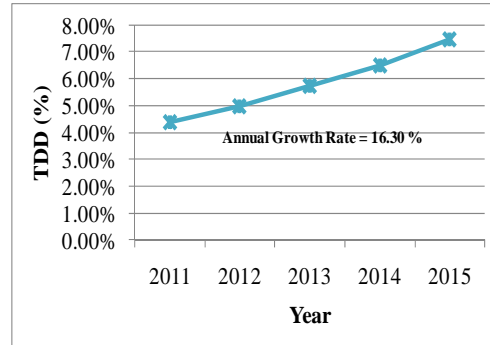
(b) Natural load evolution
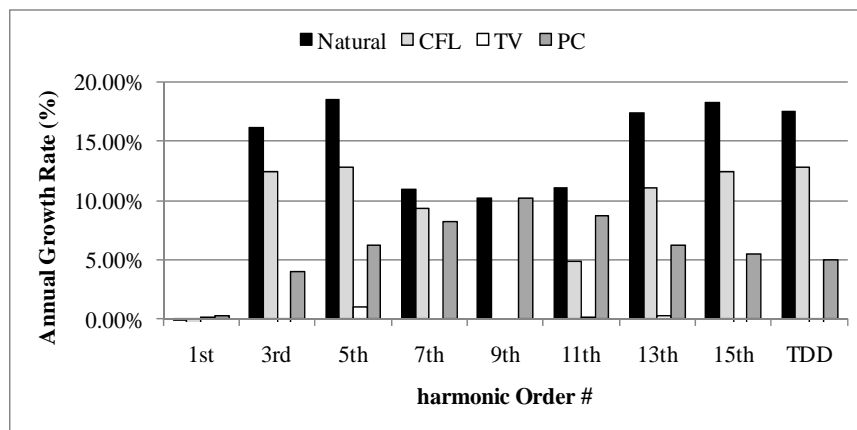
(c) Average annual growth rate

Figure 4.17 Average phase A current.

4.4.2.2 Neutral Harmonic Voltage and Current

Figure 4.18 shows the average neutral to ground voltage in the next 5 years and the associated average annual growth rate. The results of neutral current are shown in Figure 4.19. The main findings are as follows:

- The neutral voltage and current harmonics have similar growth rates. They are generally lower than that of the phase harmonics.

- The PCs and CFLs are the main contributors for the increase of the neutral harmonics in the coming years. From 3rd to 5th harmonic component, the CFLs are the main sources and for higher harmonics PCs devices are more influential.

- The neutral RMS voltage levels still remain very low and its average annual growth rate is less than 3%, so home appliances are not expected to create problems associated with neutral voltages. Similar behavior can be noticed for the RMS current levels, shown in Figure 4.19 (b), in which the average growth rate is also less than 3%. This means the increasing penetration usage of nonlinear appliances is not expected to create problems associated to neutral currents, including neutral losses.
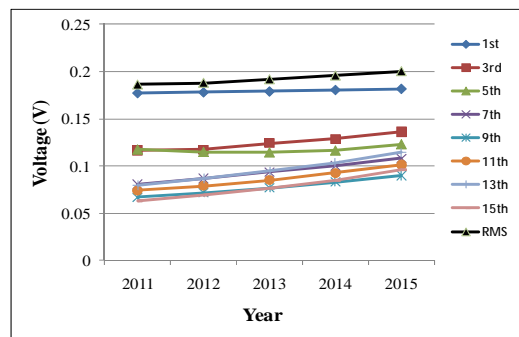
(a) Natural load evolution (fundamental and RMS divided by 3)
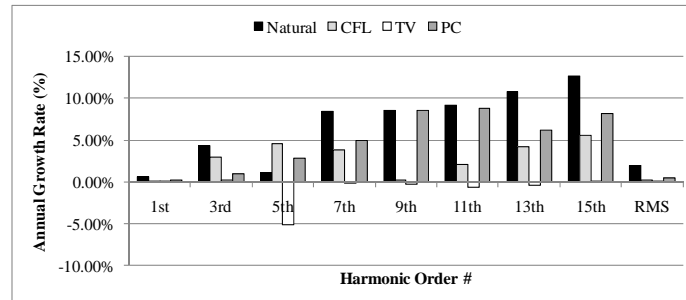
(b) Average annual growth rate

Figure 4.18 Average neutral voltage level.
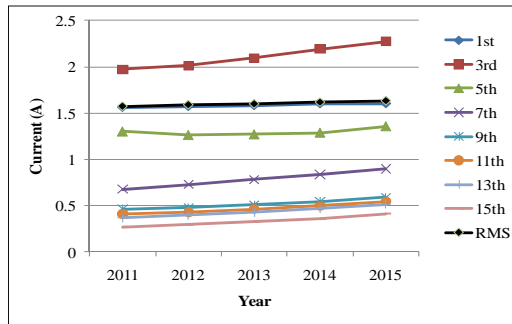
(a) Natural load evolution (fundamental and RMS divided by 3)
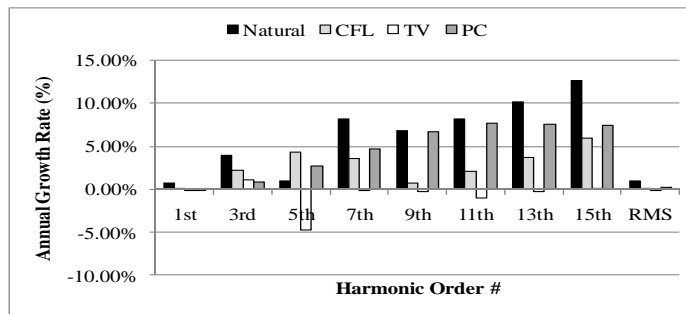
(b) Average annual growth rate

Figure 4.19 Average neutral current circulating between the houses.

4.4.2.3 Power Losses

Figure 4.20 and Figure 4.21 show the total fundamental and harmonic power losses, respectively, on the phases and neutral circuits of the secondary system for the next five years and correspondent average annual growth rate. Figure 4.20 shows a small decrease on the fundamental power losses, which is caused by the use for of more energy efficient appliances, such as CFLs. Although Figure 4.21 shows a relatively higher growth rate of harmonic power losses, it does not represent a concern because the harmonic power losses are very low in comparison with those caused by the fundamental frequency component.

Natural Load Evolution
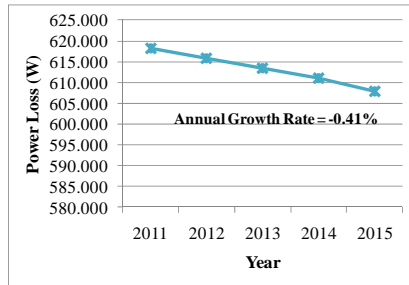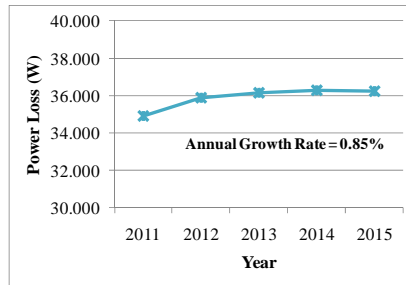
(a) Phases conductors power loss

(b) Neutral conductors power loss
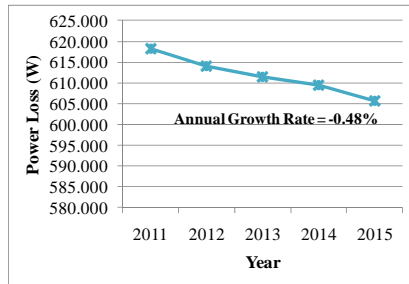
CFL Load Evolution

(c) Phases conductors power loss
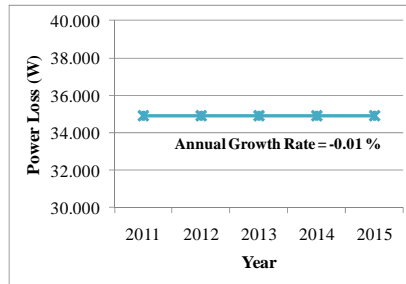
(d) Neutral conductors power loss
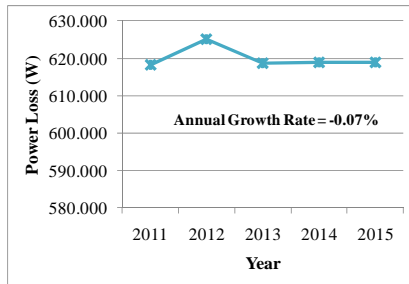
TV Load Evolution

(e) Phases conductors power loss
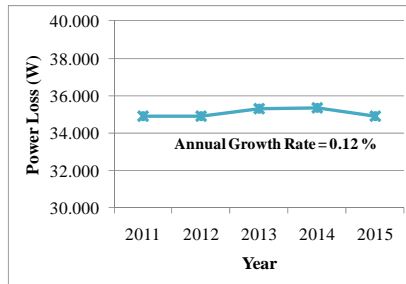
(f) Neutral conductors power loss
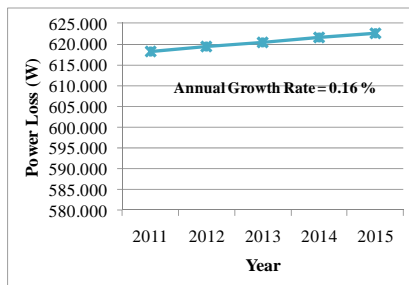
PC Load Evolution

(g) Phases conductors power loss
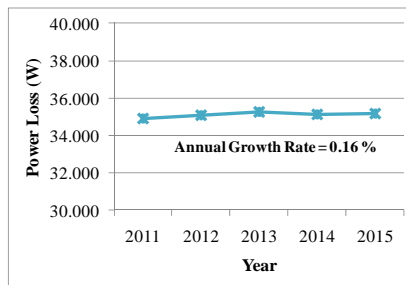
(h) Neutral conductors power loss

Figure 4.20 Total fundamental power losses at the secondary system.

Natural Load Evolution
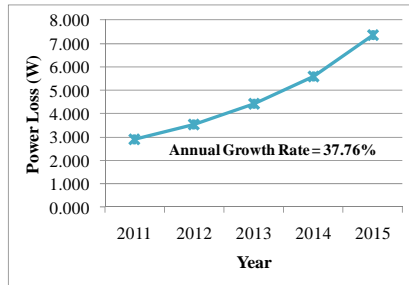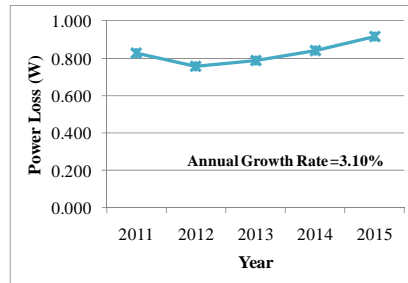
(a) Phases conductors power loss

(b) Neutral conductors power loss
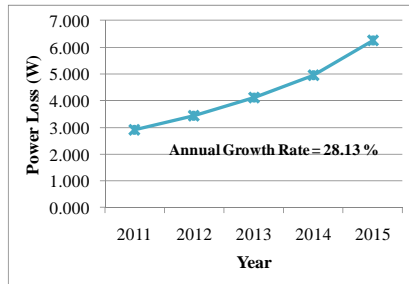
CFL Load Evolution

(c) Phases conductors power loss
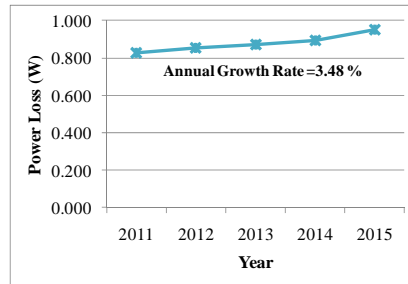
(d) Neutral conductors power loss
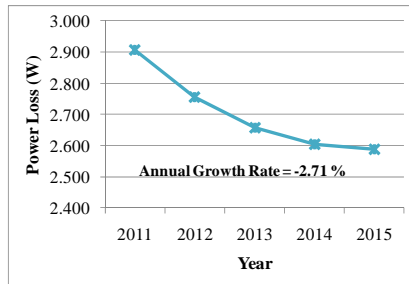
TV Load Evolution

(e) Phases conductors power loss
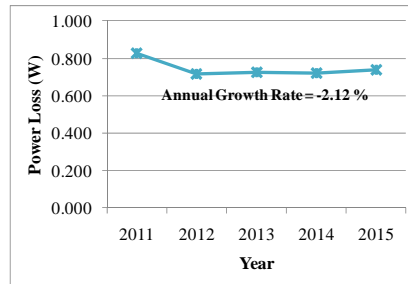
(f) Neutral conductors power loss

PC Load Evolution
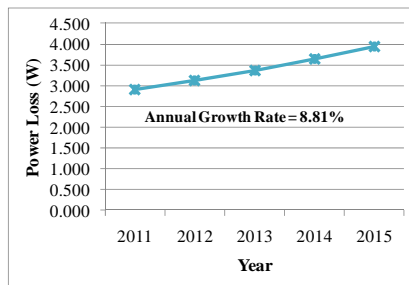
(g) Phases conductors power loss
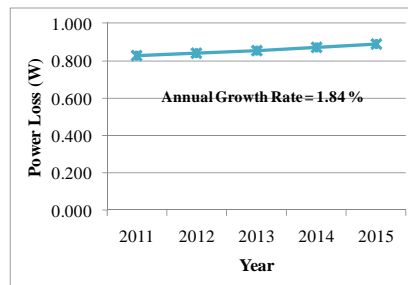
(h) Neutral conductors power loss

Figure 4.21 Total harmonic power losses at the secondary system.

4.4.2.4 Impact of Harmonics on Revenue Meter Errors

Reference [44] investigated the billing accuracy of three residential revenue meters of different designs (inductive, digital sampling and time division) under both sinusoidal and distorted conditions. The results indicated that if the voltage distortion limits of IEEE Standard 519-1992 ([6], limit of 5% THD_V) are not violated, the harmonic power of the load is small and does not significantly affect the overall accuracy of the energy meters. Six conditions with different harmonic levels were considered in the analysis. Even with the worst condition of THD_V =4.1% and TDD_I =28.8%, the energy measured by each meter was very accurate.

Our field measurements of some residential houses in Canada showed that the 95% index of THD_V at the metering point is between 4.3% and 4.5%. If these levels are compared to the analysis of [44], one can conclude that the harmonic levels would not affect the accuracy of the energy meters at present. However, according to the results shown in Figure 4.16, i.e., the average growth rate of THD_V is about 16% per year, the THD_V could exceed the IEEE limit of 5% in two years. The implication is that the assurance on revenue meter accuracy may disappear soon. This situation not only applies to existing mechanical revenue meters, it may also apply to the low end smart meters if the meters are designed without considering the impact of harmonics on the errors of energy calculation.

4.4.2.5 Impact on Service Transformer

Natural Load Evolution
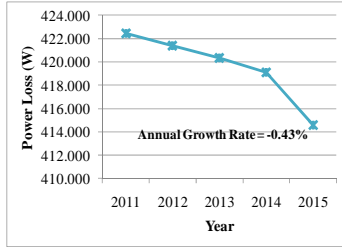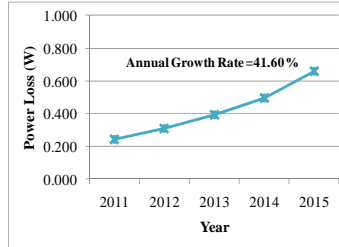
(a) Transformer fundamental power   (b) Transformer harmonic power loss   (c) Transformer K-factor
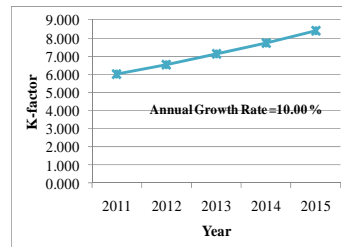
CFL Load Evolution
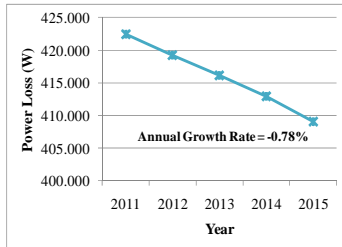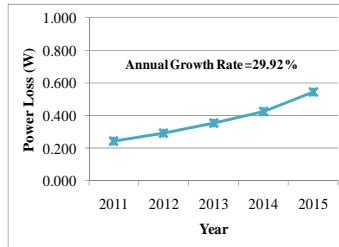
(d) Transformer fundamental power loss   (e) Transformer harmonic power loss   (f) Transformer K-factor
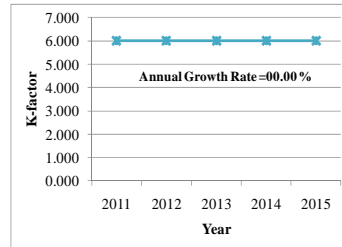
TV Load Growth
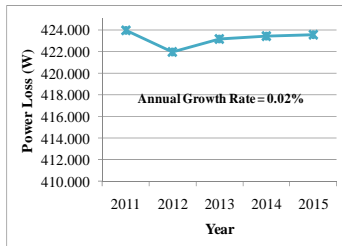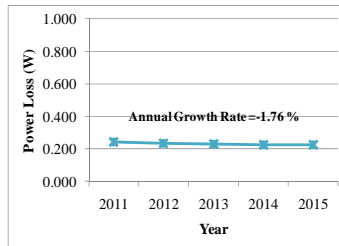
(g) Transformer fundamental power loss   (h) Transformer harmonic power loss   (i) Transformer K-factor
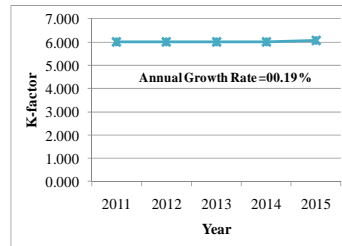
PC Load Growth
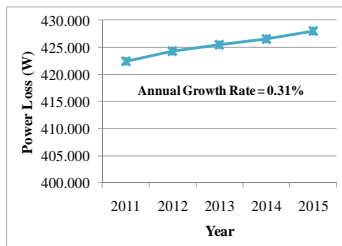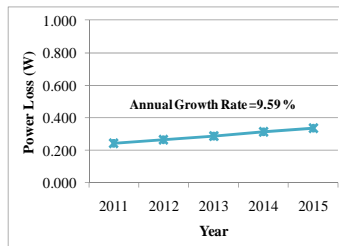
(j) Transformer fundamental power loss   (k) Transformer harmonic power loss   (l) Transformer K-factor
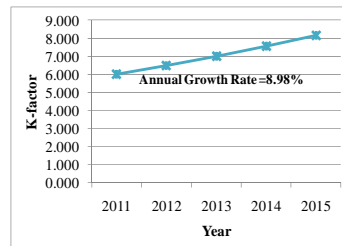
Figure 4.22 Power loss and K-factor of service transformer.

Figure 4.22 shows the fundamental, harmonic power losses and the K-Factor of the service transformer on the next five years and correspondent average annual growth rate. It is noted that the Personal Computers (PC) are the responsible for most of the K-factor increase in the coming years. The Natural Load Evolution case reveals that the K-factor will increase at the rate of 10% per year. This is one area that needs the attention by utility companies. The results also show the harmonic caused losses in service transformers are insignificant in comparison with those produced by the 60Hz component.

4.4.2.6 Summary of Load Evolution Study

Figure 4.23 shows a summary of the load evolution results for the various indices. The value between parenthesis and the one without above each bar refer to index level at the year 2011 and the average annual growth rate, respectively. The main findings are summarized below:
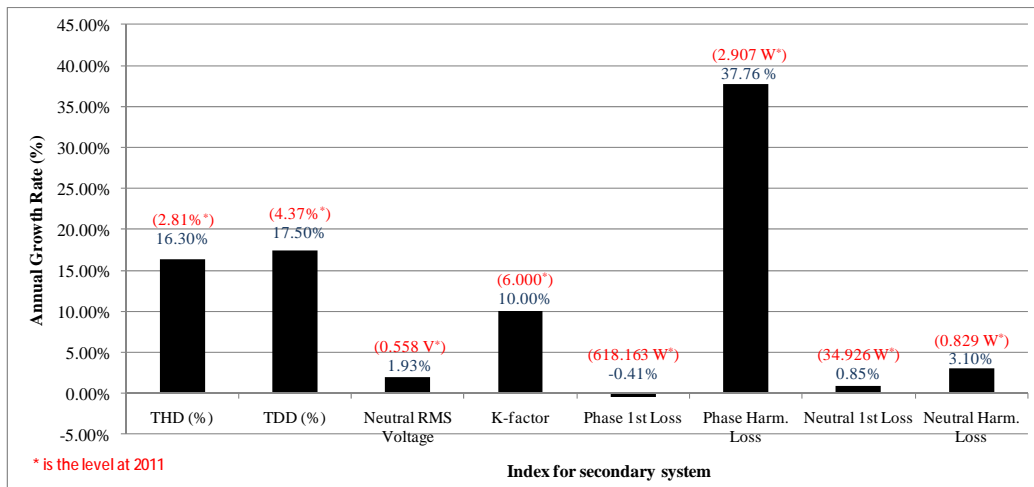
Figure 4.23 Average annual growth for main power quality indices.

108

- The increased use of electronic home appliances is likely to create concerns in the following areas: (1) increased phase voltage and current harmonics, (2) increased loading on service transformers, and (3) revenue meter errors. The following areas are not of significant concern: (1) harmonic-caused neutral voltage and current rises (2) harmonic-caused losses.

- The typical annual growth rates of the indices of concern are in the range of 10% to 15%. The main harmonic components that are of concerns are: 3rd, 5th, 13th and 15th due to their relatively high growth rate.

- In terms of major home appliances, CFLs and computing devices are major sources of harmonic increase while the CFL as the most significant. The new generation TVs (LCD TV) are not a concern since they don't contribute to harmonic increase in the system.

4.4.3 System Sensitivity Study

Several system sensitivity studies are conducted in this section to evaluate what is the impact of changing the system parameters on the secondary system harmonic distortion levels. The system parameters evaluated on the studies are outlined below (the numbers in bold represent the base case). It must be noticed that the parameters values are based on several standards and technical guides [46], [47]. The results are presented in the next subsections.

- Customer house grounding (R_C):
  - $R_C = \{0.5\ \Omega,\ \mathbf{1\ \Omega},\ 2\ \Omega\}$
- Distance between houses (s):
  - $s = \{10m,\ 15m,\ \mathbf{20m}\}$
- Houses distribution configuration

- MGN primary system neutral grounding resistance (R_{gn}):
  - $R_{gn} = \{5\ \Omega,\ 10\ \Omega,\ \mathbf{15\ \Omega},\ 20\ \Omega\}$
- Distorted supply system

In the same manner as the base case and the load evolution study case, all the results are represented by the time 95% cdf value over the average of the index of interest.

4.4.3.1 Customer Grounding Resistor R_C

This case study considers the impact of different house grounding resistor (R_C) on the harmonic levels of the secondary system. $R_C = 1\ \Omega$ represents the base case. The other system parameters remain the same as the base case. The results reveal that:

- Customer grounding resistance practically has no impact on phase current, voltage, related phase conductor power loss, service transformer power loss as well as K-factor.
- However, as shown by Figure 4.24(a), when secondary customer grounding resistance increases, less current goes to the ground circuit, which increases the current on neutral conductor. As a consequence the neutral power losses increase, but still the neutral losses are very low and do not represent a concern.
- Figure 4.24(b) shows the neutral to ground voltage behavior as the R_C increases. The neutral to ground voltage is one of the components for stray voltage problems, which has become a wider concern in North America.
- Table 4.2 shows that the *THD$_V$* and *TDD* practically remain unchanged compared to the base case ($R_C = 1\ \Omega$), which also would not affect the revenue meter energy measurement accuracy [44].

110

| (a) Neutral current | (b) Neutral to ground RMS voltage |
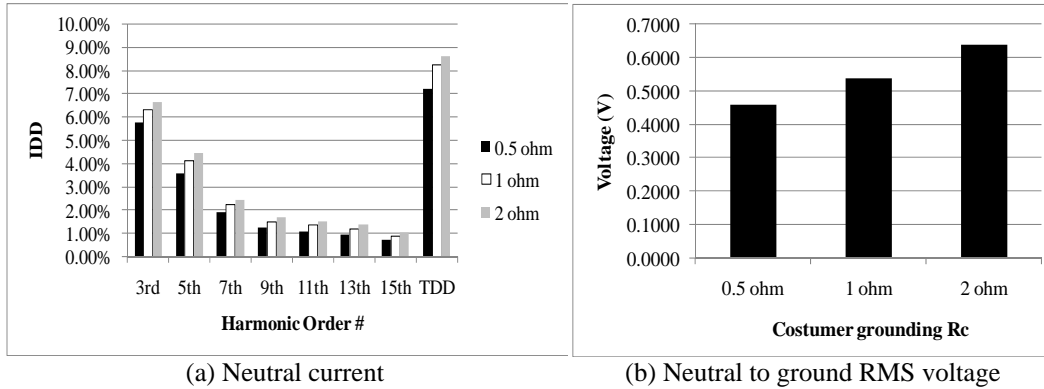
Figure 4.24 Impact of house grounding (R_C) on the neutral circuit of the secondary system (base case $R_C = 1\ \Omega$).

Table 4.2 Impact of house grounding (R_C).

	R_C			Diff. (%)	Diff. (%)	Impact
	1 Ω (base case)	0.5 Ω	2 Ω	0.5 Ω	2 Ω	
Phase A THD$_V$ (%)	2.22	2.25	2.22	1.26	-0.27	NO
Phase A TDD (%)	4.21	4.20	4.21	-0.24	0.00	NO
Transformer K-factor	8.12	8.12	8.12	0.00	0.00	NO

4.4.3.2 Distance between Houses

In this case study, the distance between the houses (s) is varied in order to verify the impact on the secondary system. The distance of 20 meters represents the base case. The findings are as follows:

- Secondary neutral impedance practically has no impact on phase voltage and current, related phase conductor power loss, service transformer power loss as well as K-factor.

- The longer the distance between the houses, the higher is the neutral impedance and, consequently, less current circulates on the neutral circuit, as can be observed on Figure 4.25(a). Also for the same reason, neutral to

111

ground voltage increases with the growth of distance as shown on Figure 4.25(b).

(a) Neutral current   (b) Neutral to ground RMS voltage
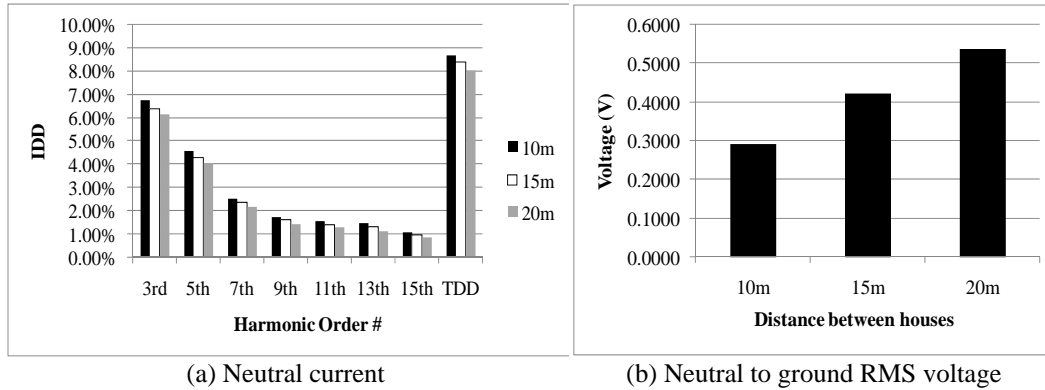
Figure 4.25 Impact of distance between houses (s) on the neutral circuit of the secondary system (base case s = 20 m).

Table 4.3 Impact of distance between houses (s).

	s			Diff. (%) 15 m	Diff. (%) 10 m	Impact
	20 m (Base Case)	15 m	10 m			
Phase A THD$_V$ (%)	2.22	2.26	2.32	1.71	4.32	NO
Phase A TDD$_I$ (%)	4.21	4.22	4.23	0.24	0.48	NO
Transformer K-factor	8.12	8.12	8.12	0.00	0.00	NO

4.4.3.3 Houses Distribution

In this sensitivity study, two different physical distributions of the houses along the secondary system are evaluated. The first one is the same like the base case shown in Figure 4.1. The second configuration is changed into a way the service transformer is no longer directly connected to the first house, but between the fifth and sixth house. For simplicity, the base case configuration is referred to as "Series" and the latter configuration as "Parallel".

112

- As shown by Figure 4.26, the impact of different houses configuration is significant on the phase (similar for phase voltage) and neutral current. There is also a significant decrease on neutral to ground voltage when changing from the series (base case) to the parallel configuration.

- However, changing the houses configuration would not affect the total phase and neutral current fed into the service transformer; hence the transformer winding loss and K-factor did not change.

(a) Phase A current

(b) Neutral current

(c) Neutral to ground RMS voltage
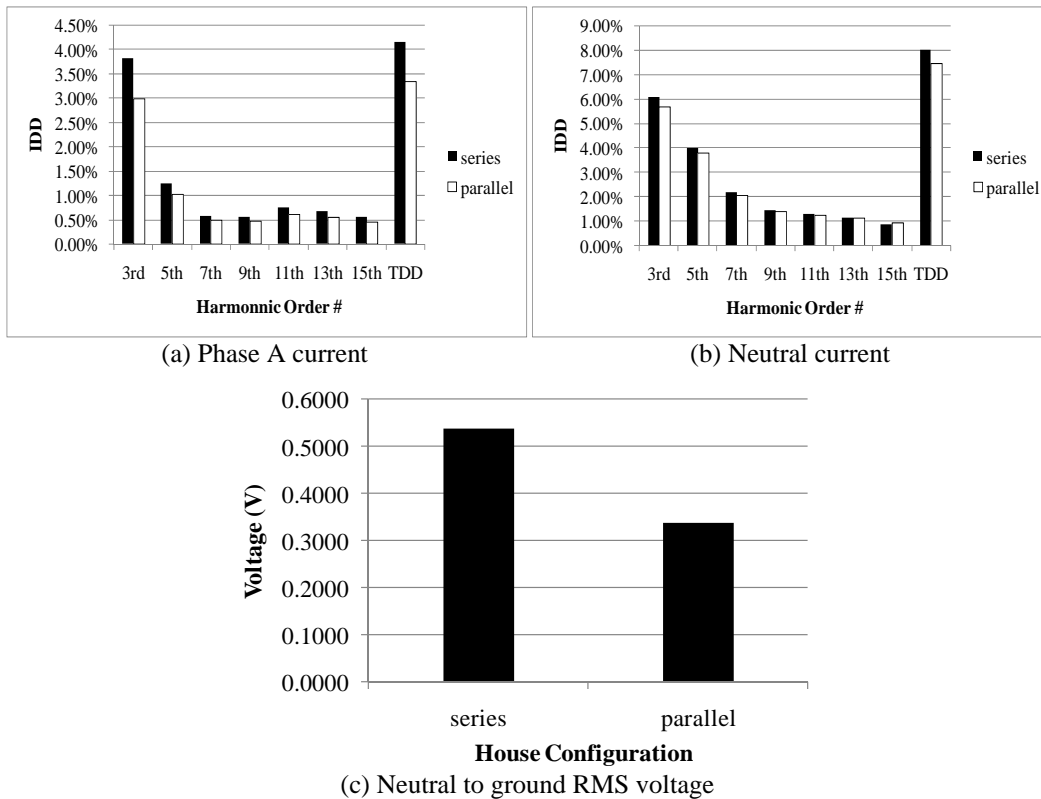
Figure 4.26 Impact of different houses configuration on the secondary system (base case "Series").

Table 4.4 : Impact of different houses configuration.

	Configuration		Diff. (%)	Impact
	Series (Base Case)	Parallel		
Phase A THD$_V$ (%)	2.22	2.31	3.82	NO
Phase A TDD (%)	4.21	3.34	-20.67	YES
Transformer K-factor	8.12	8.13	0.17	NO

4.4.3.4 MGN System Grounding Resistance (R$_{gn}$)

MGN system grounding resistance (R$_{gn}$) variation has practically no impact on the secondary system distribution system. The secondary system phases, neutral and grounding losses are not influenced as well.

4.4.3.5 Distorted Supply System

In this sensitivity study, the objective is to verify the impact of a distorted supply system on the secondary distribution system. Three case studies are analyzed; purely sinusoidal (60 Hz) supply system and two cases are based on real field measurements (Case 1 and Case 2) at two different service transformers. The voltage harmonic spectra associated to Case 1 and Case 2 are shown in Figure 4.27.

- As expected, when changing the primary side voltage source from pure sinusoidal to distorted voltage source, the phase harmonic voltage at houses increased dramatically, as shown by Figure 4.28(a).
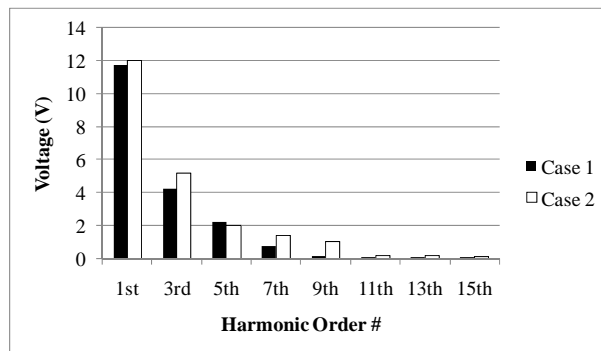
Figure 4.27 Harmonic spectrum of voltage measured from two different service transformers (fundamental divided by 10).

(a) Phase A voltage

(b) Phase A current

(c) Neutral current

(d) Neutral to ground RMS voltage
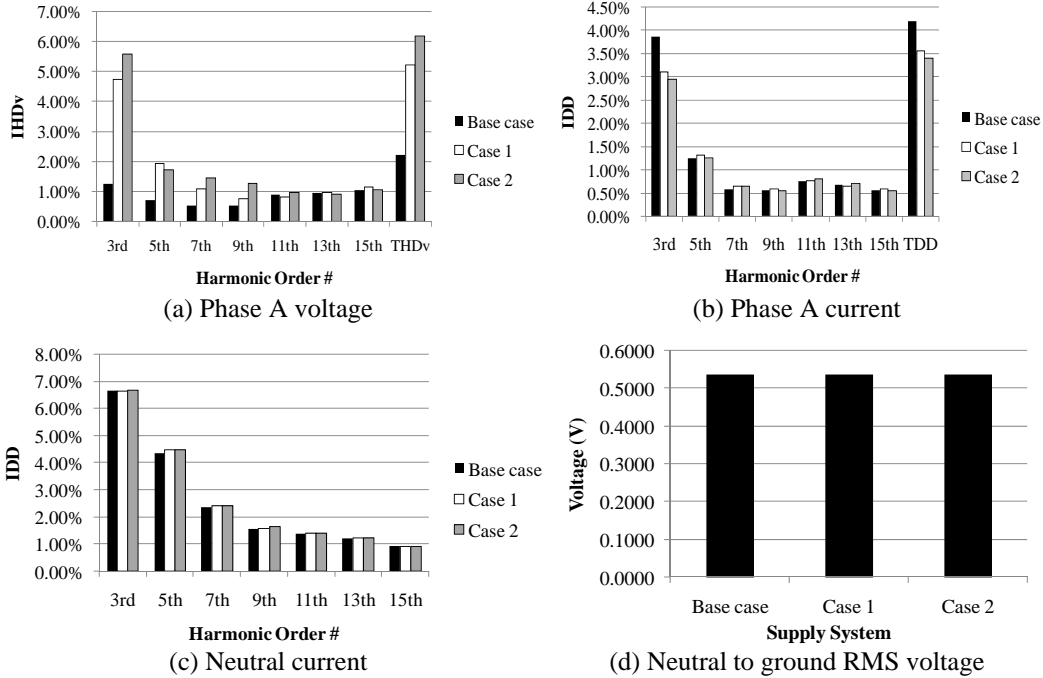
Figure 4.28 Impact of a distorted supply system on secondary system.

- Because of the highly distorted voltage, the harmonic current from linear appliances can either add up or cancel harmonic currents from the nonlinear loads, this cause the slight decrease of phase 3rd harmonic current and significant increase of other harmonic current.

- The harmonic components of phase current exhibit a random behavior as the distortion of supply system is changed, as shown by Figure 4.28(b). This can also be caused by the cancelation effect between the harmonic currents.

- The changing of primary side voltage source has little effect on neutral system, particularly on the neutral to ground voltage.

- As shown by Table 4.5, the THD_V changes significantly, which might affect the revenue meters energy measurement accuracy. According to reference [44], as the THD_V increases above the limits defined by the standards the more inaccurate is the energy measured by the inductive watthour meter.

115

Table 4.5 Impact of distorted voltage supply.

	Supply system			Diff. (%)	Diff. (%)	Impact
	Base Case	Case 1	Case 2	Case 1	Case 2	
Phase A THD$_V$ (%)	2.22	5.22	6.19	134.68	178.63	YES
Phase A TDD (%)	4.21	3.56	3.39	-15.44	-19.48	YES
Transformer K-factor	8.12	8.12	8.12	0.00	0.00	NO

4.4.3.6 Conclusions of System Sensitivity Study

Five system parameters are evaluated in above subsections to check their impact on the harmonic levels of the secondary system, and Table 4.6 shows the effect of each system parameter analyzed.

Table 4.6 The impact of each system parameter on the harmonic levels of the secondary system.

	Factor	Effect
1	Customer house grounding resistance	This might represent a concern regarding stray voltage but it is not a concern in term of neutral losses.
2	Distance between houses	Same behavior as Factor 1. Stray voltage might be a concern.
3	Houses distribution configuration	This factor affects both phase and neutral voltage/current levels. The "Parallel" configuration leads to lower harmonic levels. Service transformer indices are not affected.
4	Primary MGN grounding resistance	Different MGN grounding resistance has practically no affect in any of the indices evaluate.
5	Distorted supply system	It affects the THD$_V$ levels, however neutral and phase harmonic currents do not change significantly.

4.5 Summary

This chapter presents a methodology to investigate the potential impact of modern residential loads on the power quality of secondary distribution systems, which is based on the residential house model developed in Chapter 3.

In Section 4.1, the modeling approach for three components of typical distribution system are introduced and studied, which are primary system model, service transformer model and secondary system model. Generally, the primary system is modeled as an equivalent circuit. The service transformer is modeled explicitly and the secondary loads are modeled as equivalent circuits in the form of one house per equivalent circuit.

In Section 4.2, the technique and model parameters used for secondary system simulation are developed and presented. Several study scenarios are defined in Section 4.3 for secondary system harmonic simulation in different purposes.

Finally, the harmonic simulation results for secondary distribution system are shown and analyzed in Section 4.4. First, a base case study was conducted, which uses a current year nonlinear load penetration situation. Then, a load evolution study was conducted in order to assess the impact of nonlinear loads into the future. Moreover, a sensitivity study was performed to investigate how the secondary systems parameters affect the harmonic levels on the secondary system.

The conclusions drawn from these studies could be quite essential for utilities to understand the power quality problems encountered in secondary distribution system caused by residential nonlinear loads.

Chapter 5

The Power Quality Impact of PHEVs on Residential Distribution System

In recent years, hybrid electric vehicles (HEVs), battery electric vehicles (BEVs) and plug-in hybrid electric vehicles (PHEVs) are becoming more welcome in the market for their low energy cost and near zero-emission. Amongst all above types of EVs, PHEVs are the most promising alternatives for conventional internal combustion engine based vehicles, thanks to their capability for charging their battery packs by plugging into standard electric outlets.

While we all recognize the potential environmental and economic benefits of PHEVs, reliable and efficient operation of the electrical network is still a concern after the widespread of PHEV adoption. Many studies [48], [49], [50] have shown that no additional generation capacity would be required for a relatively large penetration of PHEVs when charging cycles start in the off-peak periods. However, the other important aspect of PHEV integration study which needs to be addressed is the impact on distribution systems level. Unlike the system-wide study, a micro level analysis that considers the possible variations in location diversity of the PHEVs plugged in and time diversity in their charging patterns is needed for distribution system level PHEV integration study [51]. In the following sections, the model of PHEV charging loads is built based on above

considerations, and hence its impact on distribution system is evaluated on the same frameworks used in previous chapters.

5.1 The Modeling of PHEV Charging Load

This section identifies and characterizes the factors necessary to develop a proper load modeling for PHEVs. Initially, a realistic scenario is used to help identify these factors, as follows. As shown in Figure 5.1, the customers connected to a typical secondary distribution network might possess one or more PHEVs which could be connected and charged at their own houses. Obviously, the average vehicle number under each service transformer is determined by the *penetration level*. However, at any time instant, the number of vehicles plugged in is not necessarily equal to the total vehicle number. This time diversity could be modeled by the *charging start time* as well as *charging duration*, which, in turn, is determined by *vehicle driving pattern and battery state of charge (SOC)*. Moreover, individual electrical *charging characteristic* of different vehicle chargers also needs to be considered.

The above four aspects has been discussed in many papers on modeling of PHEV charging load so that the proper ones are chosen for our model after thorough literature analysis. Moreover, real field measurement data and simulation results are used to represent the chargers charging electrical characteristics, which are essential part of the proposed PHEV load model.
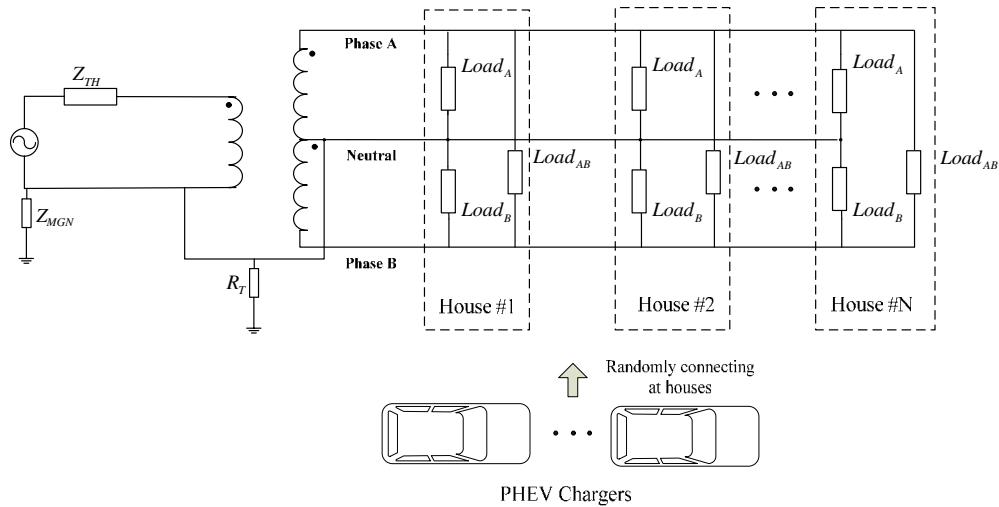
Figure 5.1 PHEV charging on residential distribution system.

5.1.1 PHEVs Penetration Level

Due to environment concerns and government incentives the increasing penetration level of PHEV will definitely have a drastic impact on distribution system [52]. Until recently, many auto manufactures have announced they will put on sale their plug-in hybrid models in 2011 and 2012. The detailed information is listed in Table 5.1. Since most of PHEV models still are not commercially available or have been released recently, it is not easy to estimate their real market penetration. However, multiple studies use similar and realistic statistics to determine the market share and penetration of PHEVs while other studies are based on mathematical models.

A report by Oak Ridge National Laboratory in 2006 [50] estimates that PHEV-20 (with 20 miles all-electric range) vehicles will make up over 25% of new sales in

the entire car and light-truck market in 2018, as shown in Figure 5.2(a). According to an EPRI report [53], [54], PHEVs could reach a maximum of 50% new vehicle market share by 2030, as shown in Figure 5.2(b). Reference [55] predicts that the maximum penetration level for PHEV will be 30% by 2030 in Belgium. European countries are more interested in conventional EVs and fuel cell vehicles (FCVs) so that the predicted PHEV penetration is lower.
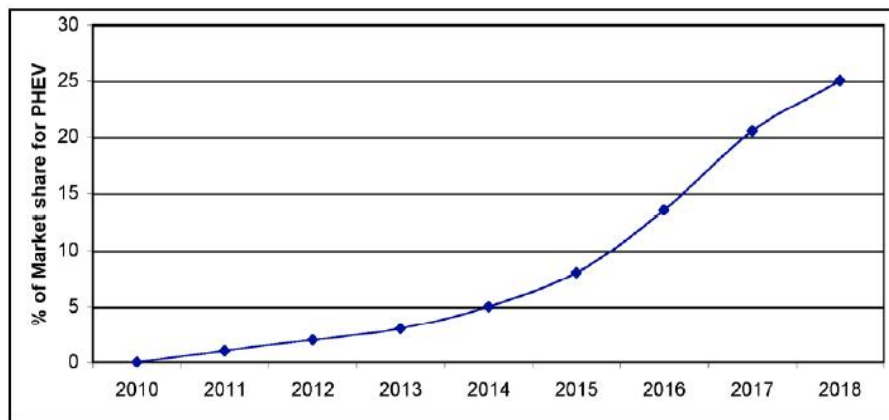
(a) PHEV-20 market share estimated by Oak Ridge National Laboratory [50]
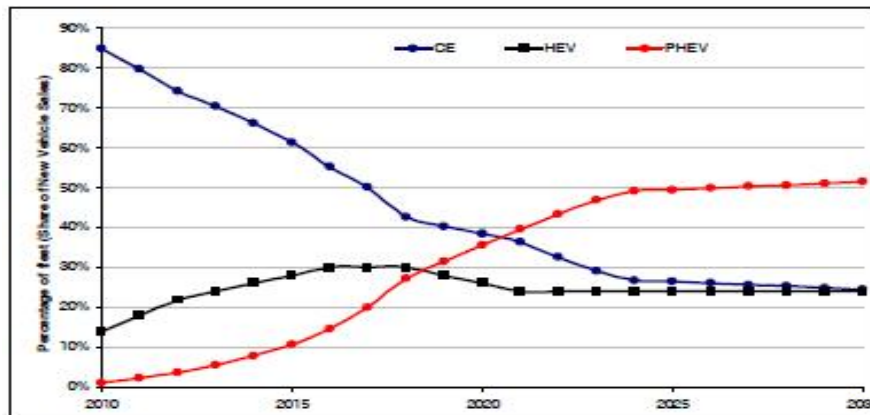
(b) PHEV market share estimated by EPRI [53-54]

Figure 5.2 The estimated penetration level for PHEVs.

Table 5.1 The detailed information of announced PHEV models.

Company	Model	Battery Capacity (kwh)	Release Date
BYD	F3DM	16	2012 in US
GM	Chevrolet Volt	16	Mid-December 2010 in US Q3 or Q4 2011 in Canada
Toyota	Prius Plug-in	5.2	Q2 2012
Ford	Escape Plug-in	10	2012
Volvo	V70	11.3	2012
Suzuki	Swift Plug-in	2.66	2012
Ford	C-Max Hybrid	N/A	2012 in North America

Same effort as in Chapter 2 is needed to translate PHEVs market share level into expected penetration level across utility customers or households. The analysis of PHEV penetration in [51] calculates the probability that a certain household will have multiple PHEVs in their home, which is quite interesting and innovative. They use the data from U.S. Department of Transportation to generate projections of the number of PHEVs per household as a function of market penetration, and an example is shown in Table 5.2. However, as the probability of household has more than 1 PHEV is relatively small, we assume the maximum number of PHEV a household could have is 1, which is quite true especially for low and medium PHEV market share.

Table 5.2 Penetration of PHEV per household.

Market Penetration	PHEV per Household		
	0	1	2
2%	96.9%	3.1%	0.0%
4%	93.8%	6.1%	0.1%
8%	87.8%	11.6%	0.5%

Since the data in Table 5.2 only provides partial information, the estimation method mentioned in [56] is used to calculate PHEV penetration level in this chapter. The number of cars sold every year in the U.S. is about constant at 20 million [50], considering the PHEV market share level in Figure 5.2 as well as the assumption of average 12 years vehicle lifespan [57], the total number of PHEV for 2010 to 2030 is shown in Figure 5.3(a). According to the linear regression analysis using the data [58] from 1990 to 2008, the total projected number of passenger vehicles for 2010 to 2030 is calculated and plotted in Figure 5.3(b). Since the average number of vehicles per household is 2 [56], the penetration level across households is calculated as follows:

$$PHEVH\left(i\right) = \frac{NPHEV\left(i\right)}{NPV\left(i\right)} \times PVH \qquad (5.1)$$

where,

- *PHEVH* is the number of PHEVs per household.
- *NPHEV* is the total number of PHEVs shown in Figure 5.3(a), while *NPV* is the total number of passenger vehicles shown in Figure 5.3(b).
- *PVH* is the average number of vehicles per household, which is equal to 2.
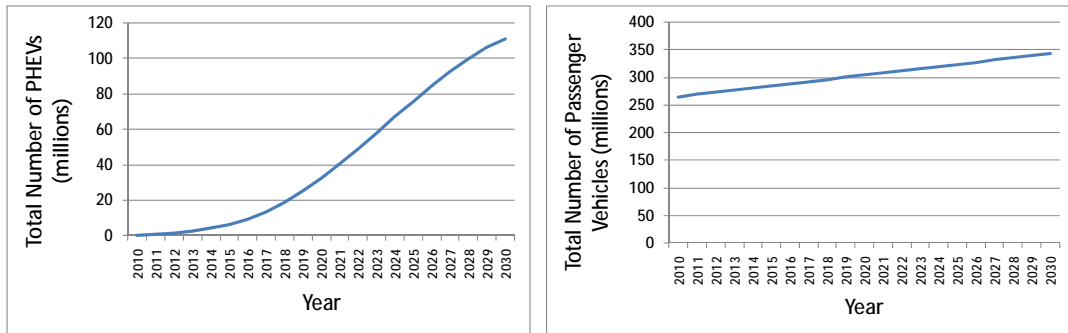
(a) Total estimated number of PHEVs for 2010 to 2030

(b) Total estimated vehicle number for 2010 to 2030

Figure 5.3 The estimated total number of PHEVs and passenger vehicles.

Therefore, from equation (5.1), the final expected PHEV penetration level per household is determined and shown in Figure 5.4. From this figure, the average number of PHEVs per household in 2020 is 0.2, which shows good consistency with the estimation in [56].
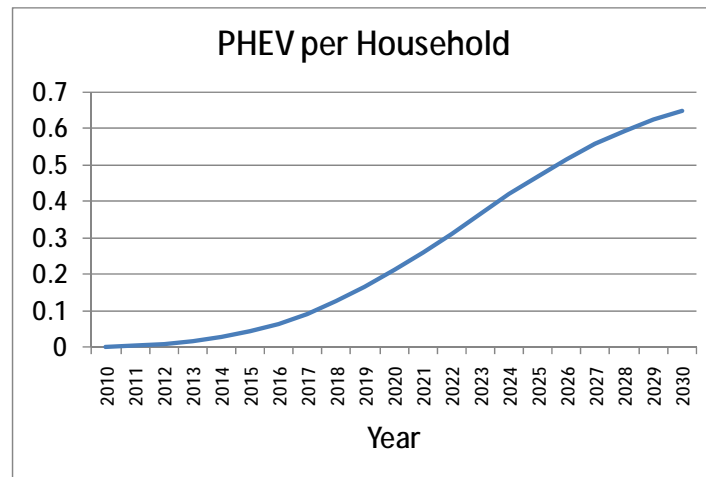
Figure 5.4 The estimated number of PHEVs per household for 2010 to 2030.

5.1.2 PHEV Charging Time

Another important aspect that needs to be considered in the PHEVs load modeling is when vehicles will be recharged during a day, commonly denominated daily charging tendency in [52]. Because all PHEVs will not begin charging simultaneously, it is more suitable to treat the start time of charger as random variable based upon daily charge pattern. There are many options can be found in references, and the charging time is strongly related to the charging strategy implemented. The simplest charging plan is the uncontrolled charging, which means PHEVs could start charging any time they are plugged in. In other words, most people will immediately charge their vehicles preparing for next trip just

when they arrive home from work. Obviously, uncontrolled charging tendency is strongly associated with people's travelling behavior. The Federal Highway Administration maintains records of both forecast and historical traffic patterns [59], which are represented as daily vehicle traffic pattern for commuting purpose, as shown in Figure 5.5(a). Two obvious peaks are observed in the figure, the morning peak (6:00-9:00) and early evening peak (16:00-18:00), which are exactly the time when people go to work and return home. As such reason, most references consider the worst case, and choose 18:00 as the starting time. However, as shown in [60], a uniform distribution with a narrow range around 18:00 is more close to reality.
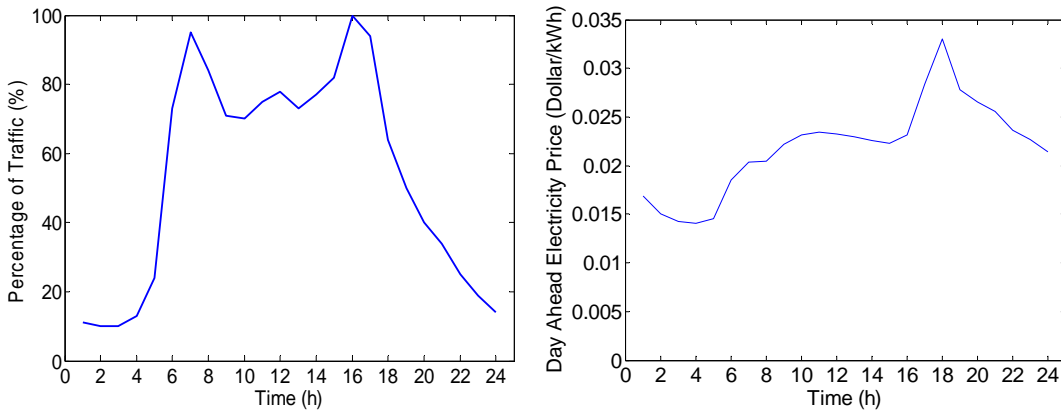
(a) Daily vehicle traffic for commuting [59]   (b) Day ahead real-time electricity price [61]

Figure 5.5 Daily vehicle traffic pattern and real-time electricity price.

Once PHEV adoption rate reach to certain level, because of the consistency with early evening system peak, uncontrolled charging plan could significantly increase this peak. In such case, both new peak generation capacity and burden on transmission and distribution will be of concern, hence it is likely that utilities

126

would use either time of use pricing or direct control method such as in-home delay devices to shift PHEV charging load to off-peak time. This charging strategy is defined as controlled charging. Normally, the peak load time is defined as from 7:00 pm to 8:59 pm, while off-peak load time is from 9:00 pm to 6:59 am. By shifting PHEV charging load to after 9:00 pm, another uniform distribution of start time ranging from 9:00 pm to 11:59 pm could also be found in [60].

Incorporation smart technology into the charging system and distribution grid, smart charging strategy is the most advanced approach for EV charging. Reference [56] uses Advanced Metering Infrastructure (AMI) together with PHEV control unit and remote switches to imply stagger charging which limits the charging based upon pre-determined power levels communicated through the grid. This method will help smooth the PHEV charging load seen by service transformer, especially for high PHEV penetration. As a result, no additional peaks due to PHEV will be created on transformer load, either in the early evening or midnight. Similarly, reference [62] and [63] use the same technology to coordinate PHEV charging in order to minimize distribution system losses, while the aim in [60] is to minimize the charging cost.

For example, assuming the total PHEV charging load to be $p_1, p_2, \ldots, p_n$ at $t=1, 2, \ldots, n$, respectively, smart charging based on minimization charging cost becomes an optimization problem, as expressed in equation (5.2):

$$min\left(\sum_{t=1}^{n} c_t \cdot p_t\right) \qquad (5.2)$$

subject to

$$\sum_{t=1}^{n}(p_t \cdot \mathbf{V}t) = E_{total}$$

$$S_j \leq S_j^{max}$$

Where c_t is the day ahead real time electricity rate shown in Figure 5.5(b), p_t represents PHEV charging load, at any time instant t, respectively. E_{total} is the total energy needed for charging all PHEVs in distribution system for one day. S_j is the apparent power flowing at branch j and it should be under the limit of S_j^{max}. Similar objective function and constraints with other aim such as minimization of distribution system losses or load variance etc. could be found in [62] and [63].

However, considering the complexity of employing various smart charging optimization algorithms, we use a simple distribution of start time to represent all smart charging strategies. This distribution is derived by plotting the reciprocal of the product of distribution of daily vehicle traffic pattern shown in Figure 5.5(a) and real-time electricity shown in Figure 5.5(b) [60], which ensures PHEV chargers have higher possibility to switch on at the time real-time electricity rate or total load demand is low. This distribution is roughly bell-shaped and it can be fitted by a Gaussian distribution with 1:00 am mean value.

Based on above three different charging strategies, three corresponding daily charging start time pattern is proposed for our modeling: (1) uncontrolled

charging; (2) controlled charging; (3) smart charging. The detailed information is

shown both in Table 5.3 and Figure 5.6.

Table 5.3 The proposed three charge strategies and daily charge patterns.

PHEV Charging Strategy	Daily Charge Pattern Distribution Type	Probability Density Function
Uncontrolled	Uniform	$f(x) = \dfrac{1}{b-a}, a \le x \le b,$ $a = 18, b = 19$
Controlled	Uniform	$f(x) = \dfrac{1}{b-a}, a \le x \le b,$ $a = 21, b = 24$
Smart	Gaussian	$f(x) = \dfrac{1}{s\sqrt{p}} e^{\left(-\frac{1}{2}\left(\frac{x-m}{s}\right)^2\right)},$ $m = 1, s = 3$
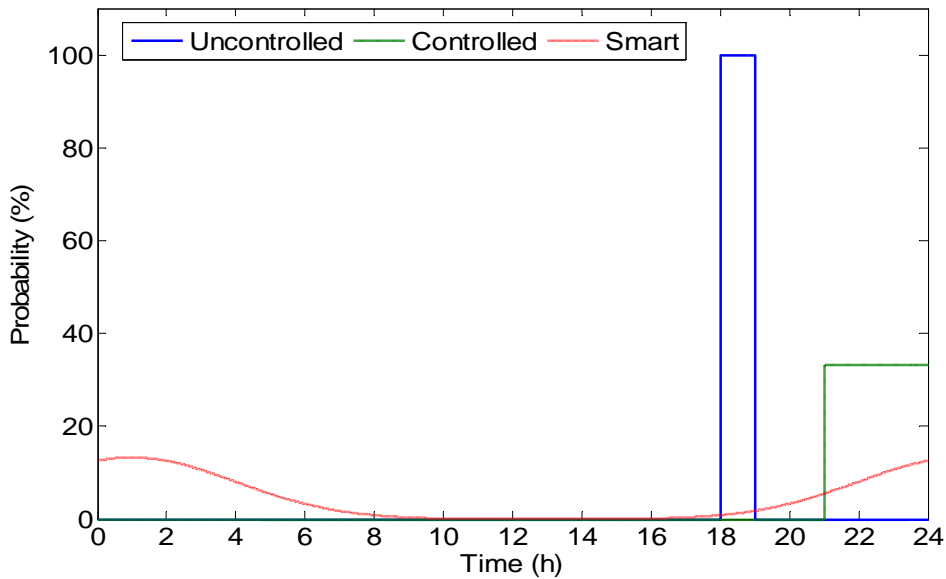
Figure 5.6 The proposed PHEV charging start time pattern.

5.1.3 PHEV Driving Pattern and Battery State of Charge (SOC)

Since charging start time can be derived from daily charge pattern, the next important charging parameter is the charging duration. Charging duration will be not only determined by the power level of charger and the capacity of battery (Kwh), but also by the initial battery state of charge (SOC), which corresponds to the remaining energy on the vehicle's battery. The parameter SOC is better represented as a random variable, however very little actual data on its probability distribution is available, simply because quite few PHEVs are now available in households. However, from general vehicles driving pattern, a probability distribution of daily distance driven has been derived in [64]. The distribution is found to be log-normal type, but with zero probability at all negative distances. The mean of the distribution is 34.2 miles and the standard deviation is 21.1 miles, at the year of 1983. The probability function is as follows:

$$d(m) = \frac{1}{ms\sqrt{p}} e^{-\frac{(ln(m)-m)^2}{2s^2}}, m > 0 \tag{5.3}$$

where,

$$m = \ln(E[M]) - \frac{1}{2}\ln\left(1 + \frac{Var[M]}{E[M]^2}\right)$$

$$s^2 = \ln\left(1 + \frac{Var[M]}{E[M]^2}\right)$$

Where m is the random variable of daily distance travelled in miles, E [M] and Var [M] stand for the mean value and variance of m.

According to [50], daily average vehicle miles travelled is 33 miles in 2008, to account for this change, we scale the standard deviation to 20.4 miles with constant ratio. Figure 5.7 shows the probability density function of daily distance driven in 2008.

Assuming that each PHEV is recharged only once a day, with m miles travelled in one day, which can be obtained from the distribution defined in equation (5.3) and Figure 5.7, the initial SOC can be determined in the following equations:

$$SOC = \begin{cases} \dfrac{R-m}{R} \times 100\% & 0 \leq m \leq R \\ 0 & m > R \end{cases} \tag{5.4}$$

Where R is the all-electric range (maximum miles that the PHEV can run from the electric battery only) of PHEV in miles.
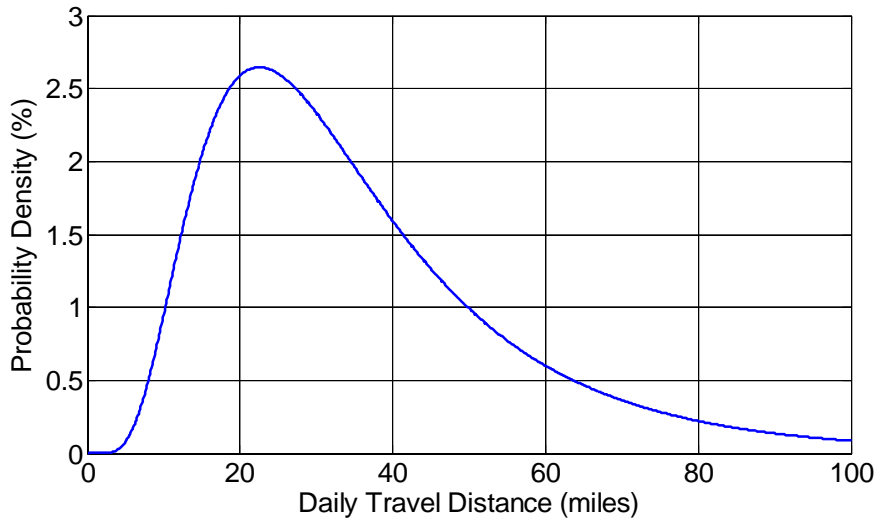
Figure 5.7 The probability density function of daily travel distance in 2008.

Once the battery state of charge (SOC) is generated from above distribution, charging duration D can be obtained as follows:

$$D = \frac{C \times (1 - SOC) \times DOD}{P \times h} \qquad (5.5)$$

Where *C* is battery capacity, *DOD* stands for the depth of discharge rating that could be used for battery charging, *P* is the power level of charger, which is determined by charger level, and is the efficiency of charger. In our model, *C* is 16 kWh, a typical *DOD* of 65% and 88% charger efficiency [62] is assumed.

5.1.4 PHEV Charging Characteristics

One of the most important factors to understand about PHEV is its charging characteristics. In [51], [52], [56], charging characteristics are simply defined as power demand as a function of time. General physical, electrical, and performance requirements for the electric vehicle conductive charging system and coupler for use in North America are proposed in SAE J1772 [65]. Based on voltage and power levels, three levels of charging are indentified in SAE J1772, which are shown in Table 5.4.

Table 5.4 PHEV charging characteristics defined in SAE J1772 [65].

Type	Power Level
Level 1: 120 VAC	1.2-2.0 kW
Level 2 (low):208-240 VAC	2.8-3.8 kW
Level 2 (high):208-240 VAC	6-15 kW
Level 3: 208-240 VAC	>15 kW-96kW
Level 3:DC Charging: 600 VDC	>15 kW-240kW

Because of different battery PHEV uses, and also because of different charger types, charging characteristics are varying. Moreover, in our research, charging characteristics need to be extended to harmonic levels for the harmonic related impact study on distribution systems. Charging characteristics of Level 1 and Level 2 chargers are essential, because these charger levels are most probably adopted in households.

In this thesis, the harmonic characteristics of five different PHEV chargers are obtained from real measurements data. Three of them (named Charger A[3], Charger B and Charger C) are Level 1 and two (named Charger D[1] and Charger E) are Level 2 chargers. These chargers are all used for vehicles with 16 kWh lithium-ion batteries, which equals to 40 miles all-electric range. The characteristics of the above mentioned chargers are detailed as follows.

5.1.4.1 Level 1 Charger Charging Characteristics

Level 1 charger can be drawn from a standard 120V/15A outlet, and its power level is around 1.5 kW. The fundamental and harmonic characteristics for measured Level 1 chargers are recoded and processed.

---

[3] Due to the limitation of measurement data, only magnitude information of each harmonic current is available for Charger A and D. In that case, typical charging systems are built and simulated in Simulink/Matlab to provide angle information for them.

According to the measurement data, charging characteristics of both chargers such as demand power, power factor, THD_I as well as each input harmonic currents are almost constant over time, which means we can use constant model to represent the whole charging procedure. The reason is that most PHEVs only use the middle band of battery`s total capacity, which makes the recharging procedure linear. Table 5.5 lists all charging characteristics during the whole charging procedure.

Table 5.5 Charging characteristics for measured Level 1 chargers.

Charging Characteristics	Charger A	Charger B	Charger C
Demand Power	1.355 KW	1.262 KW	1.272 KW
Power Factor	0.991	0.991	0.999
Input AC Voltage	100.35 V	112.30 V	111.50 V
Input AC Current	13.73 A	11.36 A	11.48 A
THD_I	10.1 %	10.2 %	3.9 %

5.1.4.2 Level 2 Charger Charging Characteristics

Most of Level 2 chargers need to be hard wired and drawn from 240 V circuit. Currently, many Level 2 charger systems such as Chevy Volt and Nissan Leaf run on 16 Amps wire and have a maximum output at around 3.3 KW. The measurement based models Charger D and Charger E are exactly of this type. The fundamental and harmonic characteristics of measured Level 2 chargers are recoded and processed.

Because of higher power level, the charging duration is cut to half. With the same consistency during the charging, we can still use constant model to represent this procedure. Table 5.6 lists all the charging characteristics for Level 2 chargers during the whole charging procedure.

Table 5.6 Charging characteristics for measured Level 2 chargers.

Charging Characteristics	Charger D	Charger E
Demand Power	2.774 KW	2.24 KW
Power Factor	0.98	0.994
Input AC Voltage	196.84 V	201.3 V
Input AC Current	14.38 A	11.23 A
THD_I	9.8 %	9.7 %

5.1.4.3 Harmonic Phase Characteristics of Level 1 and Level 2 chargers

Figure 5.8 illustrates the phase angles of different harmonic current components for all Level 1 and Level 2 chargers. Similar as before, it should be noted that the phasors use the supply voltage angle as a reference, setting the phase angle of the fundamental frequency voltage to zero. The currents are normalized to emphasize the current harmonic angles and to improve visualization. This figure shows that for some harmonics such as 3rd, 5th, 7th and 9th, the harmonic cancellation effect is quite significant.

Based on the definition of harmonic compatibility index (CI_h) shown in equation (2.8), the results for all chargers and some major appliances are calculated and

presented in Table 5.7, in ascending order of $CI_{Appliance}$. The results also confirmed

chargers may occur great harmonic cancellation when plugged in together.
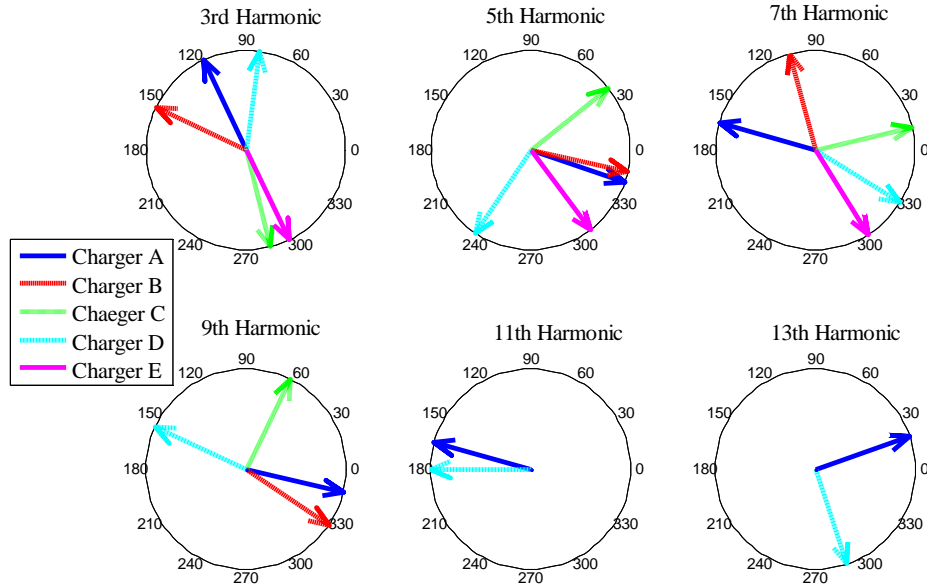
Figure 5.8 Normalized harmonic currents of all PHEV chargers using the
fundamental voltage phase angle as a reference

Table 5.7 Harmonic Compatibility Index Results for PHEV chargers using CFL
as a Template

Appliance	$CI_{Appliance}$	CI_3	CI_5	CI_7	CI_9	CI_{11}	CI_{13}
ASD FRIDGE	0.27	0.03	0.31	0.23	0.07	0.99	0.79
CHARGER C	0.31	0.23	0.60	0.21	0.21	0.92	0.96
CHARGER E	0.33	0.16	0.74	0.70	0.92	0.96	0.73
R FRIDGE	0.61	0.27	0.98	0.14	0.53	0.64	0.7
CRT TV	0.63	0.82	0.39	0.22	0.3	0.72	0.56
PC	0.64	0.82	0.39	0.12	0.33	0.89	0.94
CHARGER B	0.73	0.78	0.20	0.56	0.88	0.92	0.96
LCD	0.81	0.93	0.73	0.54	0.82	0.65	0.63
LCD TV	0.88	0.89	0.86	1	0.72	0.53	0.99
CHARGER A	0.88	0.95	0.14	0.89	0.78	0.27	0.99
LAPTOP	0.93	0.98	0.91	0.87	1.00	0.16	0.88
CHARGER D	0.97	1.00	0.70	0.56	0.55	0.40	0.63
CFL	1	1	1	1	1	1	1

5.1.4.4 Electrical Modeling of Level 1 and Level 2 chargers

Both Level 1 and Level 2 chargers measured will be modeled by a constant $P+jQ$ for the fundamental frequency and current source for the harmonic frequencies, as shown in Figure 5.9. The procedure to establish the current source model also follows equation (2.2). The only difference between Level 1 and Level 2 models is that Level 1 is connected to 120 V circuit at Phase A or Phase B to neutral line, while Level 2 should connected to 240 V circuit at Phase A to Phase B.

(a) Model at fundamental frequency   (b) Model at harmonic frequency
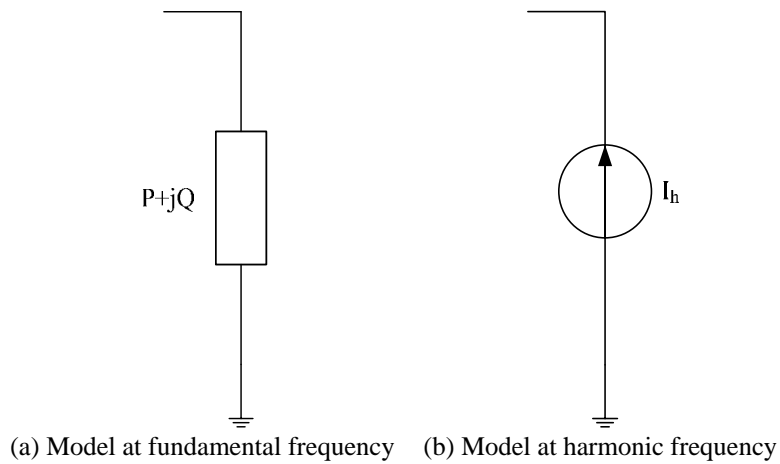
Figure 5.9 Model for PHEV chargers.

5.2 PHEV Simulation Procedure

This section describes the steps necessary to perform simulations to analyze the impact of PHEV charging on distribution system. From the simulation results, it

will be possible to analyze the impact of PHEV charging on both secondary and primary distribution systems.

The procedure to perform PHEV charging load simulations is as follows:

Step 1: Determine global variables such as the number of PHEVs in distribution system, charging strategy, battery capacity and charger level in initialization.

Step 2: For one PHEV, randomly generate the charging start time T according to the probability density function f(x) in Table 5.3 with corresponding charging strategy.

Step 3: Randomly generate current PHEV daily travel distance M according to the probability density function d(m) in equation (5.3) , then determine initial state of charge (SOC) for this PHEV battery with equation (5.4).

Step 4: PHEV charging duration D in hour is determined by battery capacity, charger level and initial SOC through equation (5.5).

Step 5: Choose corresponding charger current source model according to the charger level, output individual PHEV charging load including harmonic components based on charging start time T and duration D.

Step 6: Go back to Step 2 and repeat the procedure for another PHEV, until last PHEV plugged in distribution system.

Figure 5.10 shows a flowchart illustrating these steps.
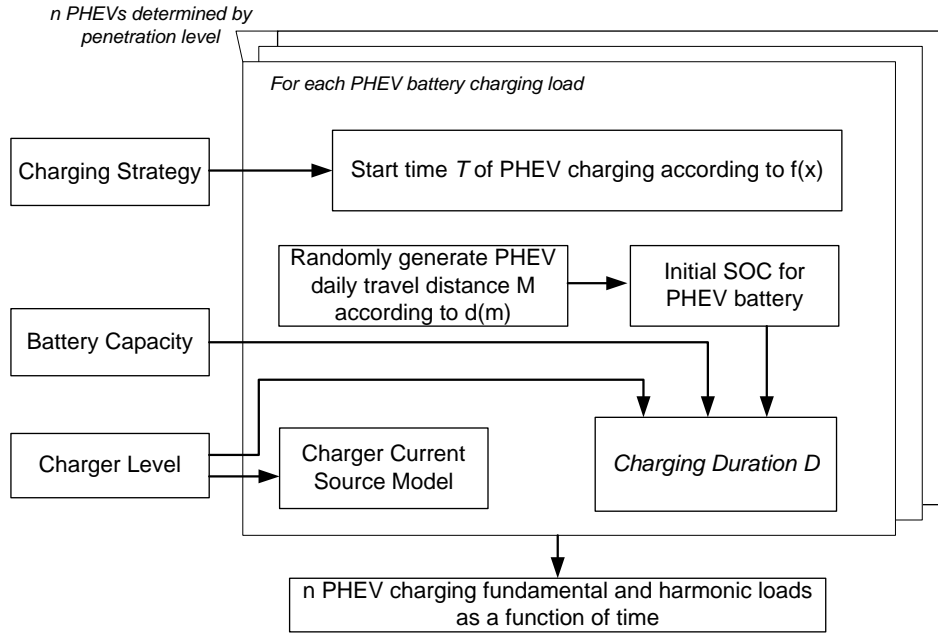
Figure 5.10 Simulation procedure for overall PHEV charging load.

5.2.1 Simulation Procedure for Secondary System with PHEV Load

The PHEV charging loads are firstly integrated into the secondary distribution system described in Chapter 4, which has the system parameters shown in Table 4.1. As each PHEV charging load is modeled as constant $P + jQ$ for fundamental frequency and constant current source for harmonic frequency, the integration of PHEV charging load is simply connecting the model at the certain node (house) of the secondary system shown in Figure 5.11 during corresponding charging duration. The detailed procedure for secondary system integrating with PHEV loads simulation is as follows:
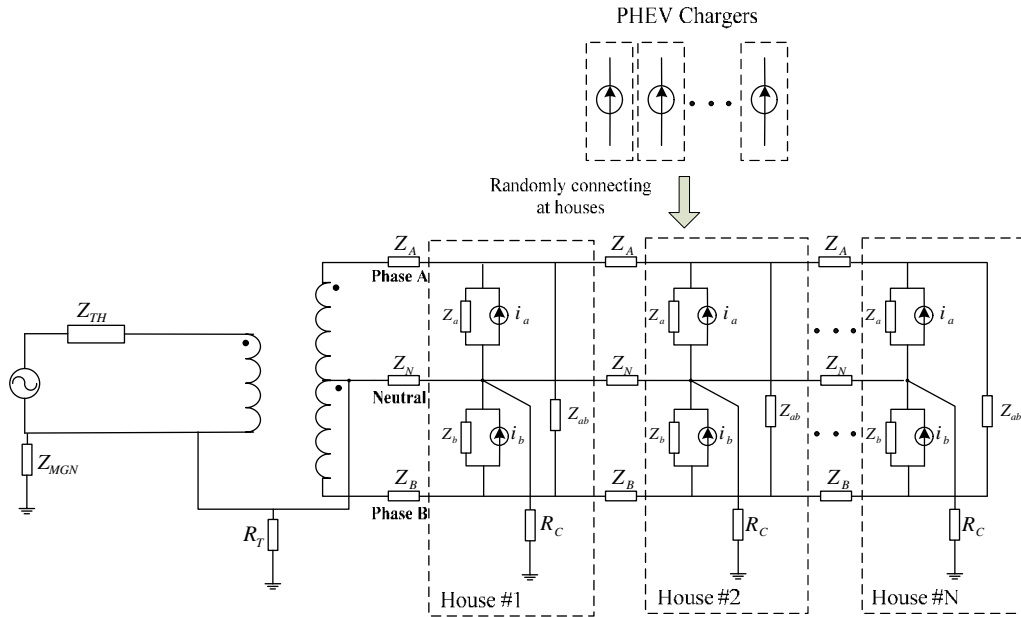
Figure 5.11 Integrating PHEV charging load into secondary distribution network.

Step 1: Build aggregated harmonic house model based on different appliances and their usage pattern following the procedure shown in Chapter 3.

Step 2: Generate PHEV charging fundamental and harmonic model following Figure 5.10 according to PHEV penetration level.

Step 3: Randomly integrate PHEV charger model into house model, connecting charger model to random phase (Phase A or B) if Level 1 chargers are employed.

Step 4: For time snapshot T1, connect the fundamental frequency component of the houses model to the service transformer and the simplified primary system and run power flow.

Step 5: Shift the angle of each house harmonic current spectrum to match the fundamental frequency power flow result.

Step 6: Connect the shifted harmonic components of the houses and run harmonic power flow. Save the results.

Step 7: Go back to Step 4, and repeat it for another time snapshot (T_2), until last snapshot.

Step 8: Go back to Step 2, and repeat it for another Monte Carlo run, until last run.

Step 9: Derive the average of all Monte Carlo running results.

These steps are also illustrated in Figure 5.12.
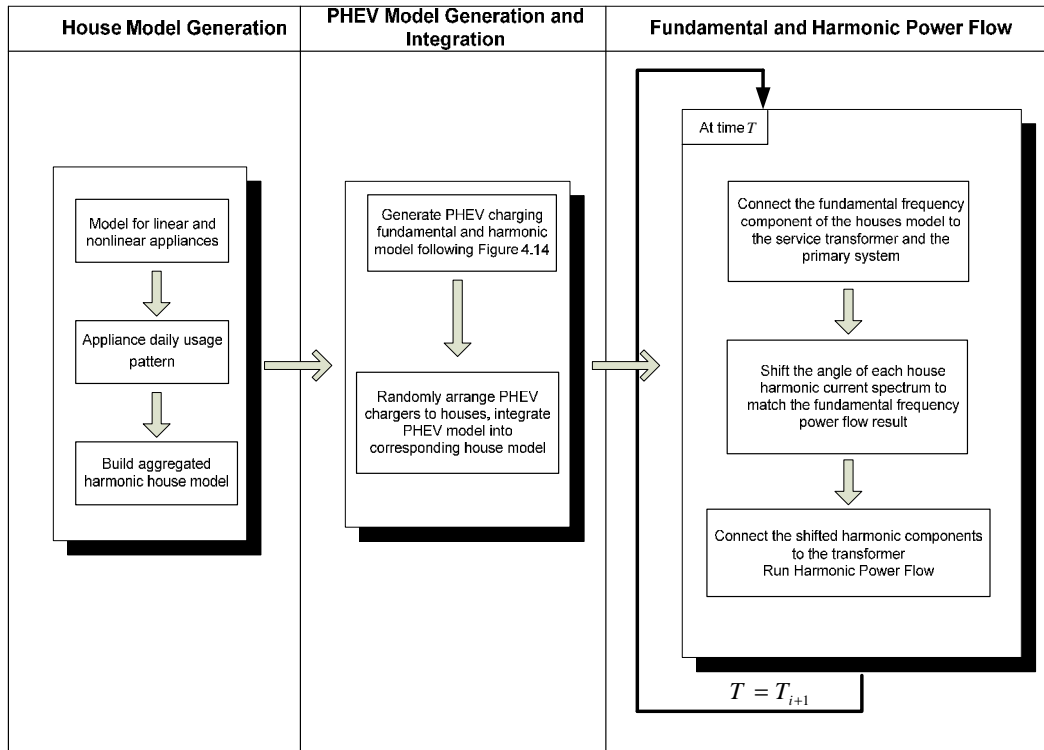
Figure 5.12 Simulation procedure for integrating PHEV charging load into secondary distribution network.

During the integration of the PHEV charging loads, because of the random fashion of several parameters such as charging start time, battery SOC as well as the location of charger, and considering the fact that the total number of PHEVs at the secondary system level is low, the simulation result could be different from

one run to another. Monte Carlo method is introduced to solve this problem, and the average result derived from different Monte Carlo runs is finally used. However, it is very important to determine the number of Monte Carlo runs needed to achieve the steady state solution. As illustrated in Figure 5.13, both the average fundamental and harmonic current result of one sample PHEV charger at one time instant stabilized around 200 runs, therefore 200 is selected to be the upper limit of the Monte Carlo running number for Step 8 in the above procedure.
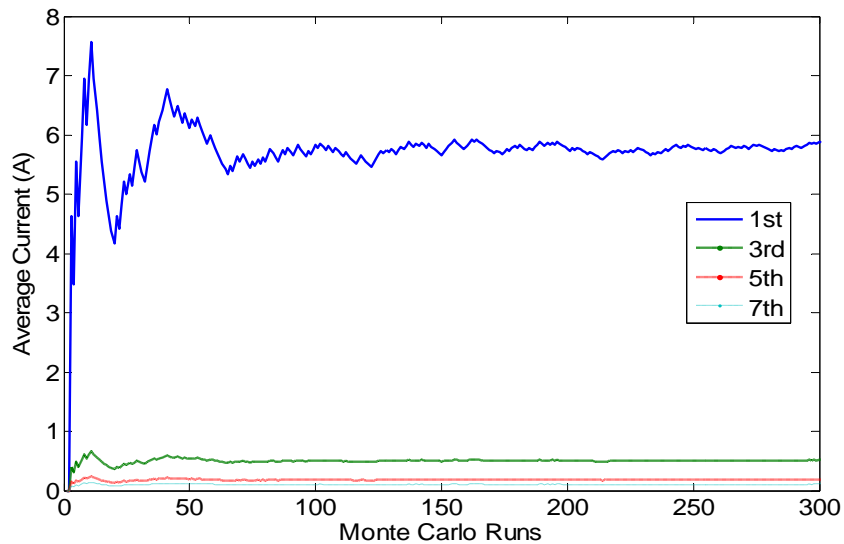
Figure 5.13 Average fundamental and harmonic current for one charger at 1:00 am vs. Monte Carlo runs.

5.2.2 Simulation Procedure for Primary System with PHEV Load

As discussed in Chapter 4, depending on the type of the study and on the location of interest, the primary and the secondary distribution systems can be modeled differently. In this subsection, the objective is to analyze the impact of PHEV

charging load on the primary system so that a detailed model for this system is necessary.

The network adopted for our primary system analysis is shown in Figure 5.14, and its general configuration is a four-wire, multi-grounded system (three-phase conductors plus a multi-grounded neutral). In this figure, the portion of the network inside the dashed rectangle represents one or more single-phase service transformers connected between each phase of the primary conductor and neutral conductor, and each service transformer could be represented by the secondary system configuration shown in Figure 5.11. In this study, we assume the service transformers are evenly distributed, which means transformers are only connected at certain points of three phase conductors, and the interval between points are the same.
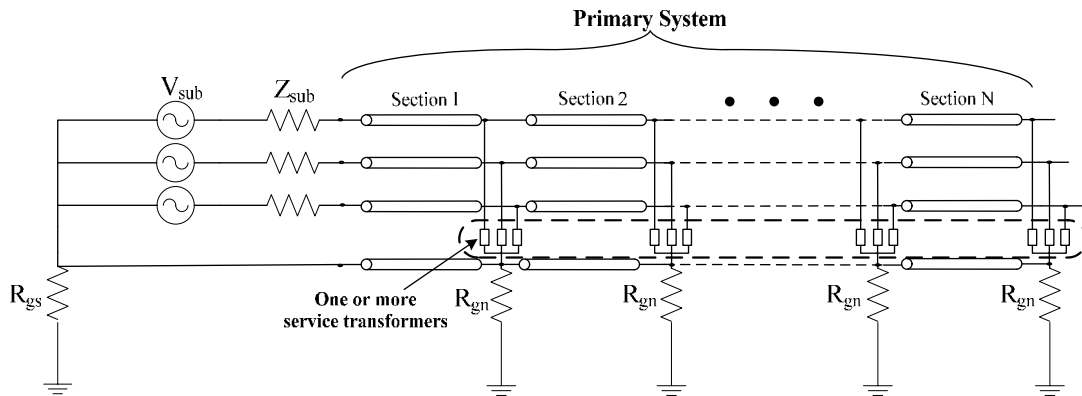
Figure 5.14 Distribution network model to study the impact of PHEV charging loads on the primary system.

Table 5.8 shows the primary and secondary system parameters employed in the distribution network shown in Figure 5.14. It shows that this feeder under

analysis has 10 transformers at each kilometer and for each phase so that the total

number of service transformers is 10 x 3 phases x 15 km = 450, and the total

residential customer supplied by this feeder is 4500 for each transformer supplies

10 houses.

Table 5.8 Primary and secondary system parameters used for study.

Base Case System Parameters		Values
Primary System	Supply system voltage	14400 V @ 60 Hz
	Substation MVA level	242 MVA
	Substation positive sequence impedance	0.688 + j2.470 ohms
	Substation zero sequence impedance	0.065 + j2.814 ohms
	Substation grounding (R_{gs})	0.15 ohms
	MGN grounding resistance (R_{gn})	15 ohms
	Grounding span of the MGN neutral (s)	75 m
	Feeder length	15 km
	Feeder conductor type	4 - 336.4 ACSR
Services Transformer	Number of transformers per phase	12 per km
	Voltage (V_H/V_L) rating	14400/120 V
	KVA rating	37.5 kVA
	Impedance	2 %
	Resistance	1.293 %
	Grounding resistance (R_T)	12 ohms
Secondary System	Customer grounding resistance (R_C)	1 ohm
	Neutral impedance (Z_N)	0.55 + j0.365 ohm/km
	Phase impedance (Z_A and Z_B)	0.21 + j0.094 ohm/km
	Number of houses (N)	10
	Distance between houses	20 m

The simulation procedure for PHEV charging load integrating into this

distribution network is as follows:

Step 1: Build aggregated harmonic house models based on different appliances
and their usage pattern following the procedure shown in Chapter 3.

Step 2: Generate PHEV charging fundamental and harmonic models following
the procedure presented in Figure 5.10 according to PHEV penetration
level.

Step 3: Randomly integrate PHEV charger model into house model, connecting charger model to random phase (Phase A or B) if Level 1 chargers are employed.

Step 4: Randomly choose 10 houses, connect them to secondary system to form service transformer models. Note that for the houses with PHEV are randomly chose, the number of PHEVs at each service transformer may be different, but around total penetration level.

Step 5: For time snapshot T1, connect the fundamental frequency component of the service transformer models to the primary system and run power flow.

Step 6: Shift the angle of each service transformer harmonic current spectrum to match the fundamental frequency power flow result.

Step 7: Connect the shifted harmonic components of the service transformer models and run harmonic power flow. Save the results.

Step 8: Go back to Step 5, and repeat it for another time snapshot (T_2), until last snapshot.

Figure 5.15 shows a flowchart illustrating these steps.
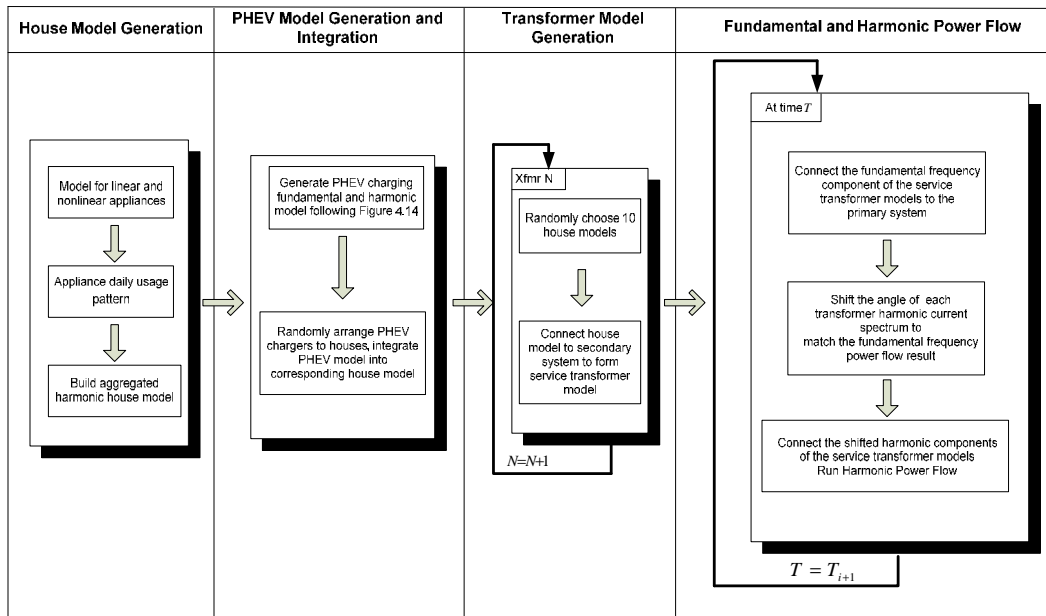
Figure 5.15 Simulation procedure for integrating PHEV charging load into primary distribution network.

5.3   PHEV Simulation Study Scenarios

As the goal of this thesis is to determine the impact of PHEV into the future, the studies are conducted for each year over the next several years considering the market trends established in Figure 5.4. The following study scenarios are evaluated:

- **Base Case**: The base case scenario is defined as integrating mixed chargers types under uncontrolled charging strategy with 30% PHEV penetration level into system. Mixed chargers include Level 1 and Level 2 chargers at a ratio of 1:1. This case is used to give an overview of the situation when the highest level of PHEVs penetrates into system with the most common charging strategy and chargers composition. The objective of this base case study is to address the following issues:

  - ∨ **Identify the power quality indices of concern**?
  - ∨ **How does these impacts compare with those of other nonlinear appliances**?

The "30% PHEV" base case is compared to three other scenarios analyzed in the previous chapters, which considered only home appliances:

- o "Pure Loads": This scenario considers only nonlinear appliances and the respective penetration rates refer to year 2011 market data;
- o "CFL 2015": All home appliances loads remain the same as the "Pure Load" scenario, except that the penetration of lighting related appliances refers to year 2015 market data.

146

o "PC 2015": All home appliances loads remain the same as the "Pure Load" scenario, except that the penetration of PC related appliances refers to year 2015 market data.

- **Sensitivity Study:** The object is to evaluate what is the impact of changing charging strategies and charger types on the PHEV simulation. The scenarios are outlined below:

   ∨ *Charging strategies*: Studies are conducted under three different charging strategies as defined in Table 5.3, which are "uncontrolled charging", "controlled charging" as well as "smart charging". In these cases, mixed chargers are employed and 30% PHEV penetration level is supposed.

   ∨ *Charger types:* Besides *mixed chargers*, *Level 1 charger only* and *Level 2 charger only* are employed separately in the study to evaluate the impact of charger types on distribution system.

- **PHEV Load Growth Study:** In this case study the penetration of PHEV loads is increased according to PHEV market data. From the PHEV trend data shown in Figure 5.4, penetration levels of 0, 10%, 20%, and **30%** (base case) are chosen, which are equal to 0, 0.2, 0.4 and 0.6 PHEVs per household, respectively. Charger type is fixed to mixed chargers. Regarding charging strategy, both controlled and uncontrolled strategies are considered in the analysis.

5.4 PHEV Simulation Results

The indices of interest to quantify the impact of PHEV charging loads on both secondary and primary distribution system are presented in this subsection. In this thesis, only odd harmonics from 3rd to 15th order are considered.

The following indices are analyzed according to each issue associated with integrating PHEV charging loads into **both secondary and primary distribution system**, most of them are similar to Section 4.4:

- Voltage and current distortion levels:
  - Harmonic spectrum
  - Voltage Total Harmonic Distortion (THD_V):
  - Total Demand Distortion (TDD):
- Neutral conductor current/voltage rise:
  - Neutral current and voltage harmonic spectrum
  - Neutral voltage RMS:
- Secondary/Primary distribution system power losses:
  - Fundamental and harmonic power losses at phases and neutral circuits
- The loading of service transformer:
  - The maximum loading of service transformer is investigated at different scenarios
- Voltage violation at secondary/primary distribution system:
  - The minimum node voltage at secondary/primary distribution system is recorded

The following indices are specified for **secondary distribution system** analysis:

- Impact of harmonics on service transformer K-factor:

The following indices are specified for **primary distribution system** analysis:

- Telephone interference in the form of IT factors:
  - Total IT product:

$$IT_{total} = \sqrt{\sum_{h=1}^{H} \left(w_h I_h^0 \right)^2}$$ (5.6)

  - Contribution of each harmonic to the IT:

$$IT_h = w_h I_h^0$$ (5.7)

where w_h is the C-message weighting ([6]), used in the USA and Canada. I_h^0 is the zero sequence current at harmonic h (only odd harmonics), H is the maximum harmonic order (in this thesis, $H = 15$).

As discussed in Chapter 4, in order to facilitate the interpretation of results, further processing is needed to produce summary information. Instead of providing the 24 hours profile of a harmonic result, a single index showing the average value or the value that is not exceeded by 95% of the time (called "95% index") can be more useful. The results obtained at different locations can also be condensed through averaging. For example, the simulation studies will yield the 3rd harmonic voltage profiles for different houses (i.e. nodes in the simulation model) over a 24 hour period. More explanations of this index can be found in Section 4.4.

5.4.1 Simulation Results for Secondary System with PHEV Load

This section presents the harmonic study results with respect to the impact of PHEV loads on secondary distribution systems. Several study scenarios mentioned in the previous section are investigated.

5.4.1.1 Secondary System Base Case Results

I. Voltage and Current Distortion in the Secondary System

From harmonic power flow results, the harmonic phase voltages for all houses connected to Phase A of the secondary system are obtained. The daily house average profile include THD_V is determined and shown in Figure 5.16(a). The "95% index" of the phase voltage is shown in Figure 5.16(b). The results associated to Phase B are not shown because they are similar to Phase A.

Likewise, the daily house average harmonic current profile for Phase A is determined and shown in Figure 5.17(a). The daily average profile of the TDD is shown as well. Finally, from Figure 5.17 (a), the "95% index" of the individual demand distortion (IDD) and TDD are be determined and are shown in Figure 5.17 (b). The results show that the 3rd harmonic is the most dominant component, which is then followed by the 5th component. The period at which the harmonic levels are the highest is after 18:00 since this is the usual time people will come

home from work and plug in their PHEVs for charging and the fact that more nonlinear appliance usage is observed during this time.

Figure 5.16(b) and Figure 5.17(b) also show the "95% index" of harmonic phase voltage and current associated to the scenarios that consider only home appliances ("Pure Load", "CFL 2015", "PC 2015"). The results indicate that even with 30% penetration level, the harmonic distortion caused by PHEV is not significant since both IHD and IDD levels are comparable to those of "Pure Load" case study. The main reason is that PHEV chargers normally have lower THD_I (<10%) than other nonlinear home appliances. Moreover, one can observe from "CFL 2015" and "PC 2015" that the increasing penetration of CFL and PC loads should be more of concern to utilities in terms of harmonic distortion in secondary systems compared to increasing usage of PHEVs.

(a) Daily average profile   (b) 95% index
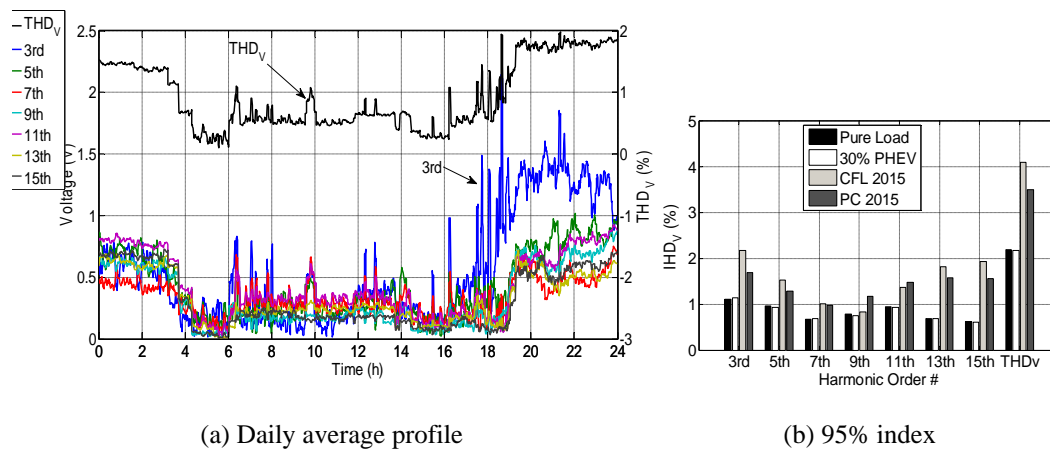
Figure 5.16 Average harmonic phase voltages of all houses under PHEV base case.

(a) Daily average profile   (b) 95% index
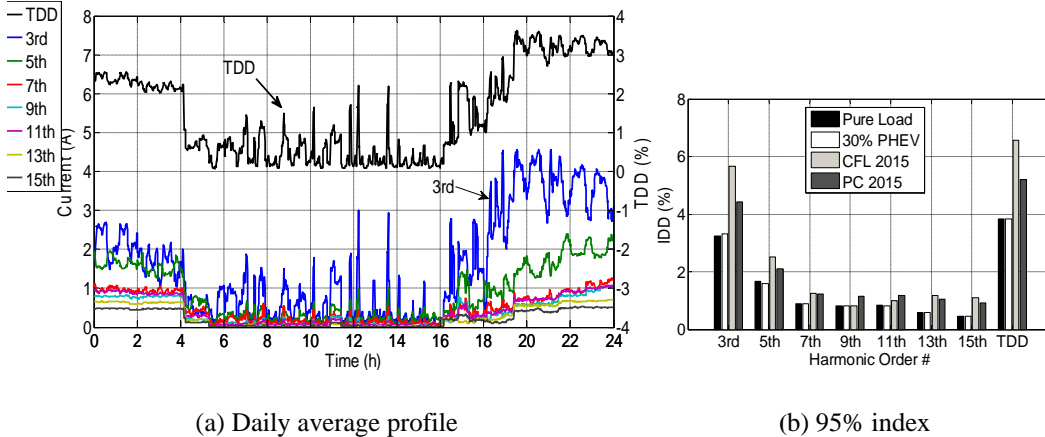
Figure 5.17 Average harmonic phase current of all houses under PHEV base case.

II. Neutral Conductor Current & Voltage Rise

Figure 5.18(a) shows the daily profile of the neutral to ground harmonic voltage averaged over all the secondary system houses under 30% PHEV base case. Figure 5.18(c) shows the daily profile of the neutral RMS voltage. Figure 5.18(b) shows the 95% index of the neutral harmonic voltage and its RMS value caused by PHEV and other additional nonlinear loads. Figure 5.19(a) and Figure 5.19(b) show the corresponding contents for the average harmonic neutral current circulating between the houses.

After integrating PHEV charging loads (30% PHEV case study), there is a significant increase on both fundamental and RMS neutral voltage/current compared to other scenarios. This phenomenon is caused by the load imbalance between the two phases, with more impact coming from the integration of Level 1 chargers. On the other hand, the harmonics produced by PHEVs loads do not have

152

major impact on the neutral voltage rise, since the harmonic levels are similar to scenarios CFL 2015 and PC 2015. Furthermore, Figure 5.19(b) shows that the neutral current contains more fundamental component for the 30% PHEV scenario; however for the other scenarios the 3rd harmonic components are more dominant. This observation corroborates the fact the harmonics injected by PHEV will not have an impact on both neutral voltage and current levels.
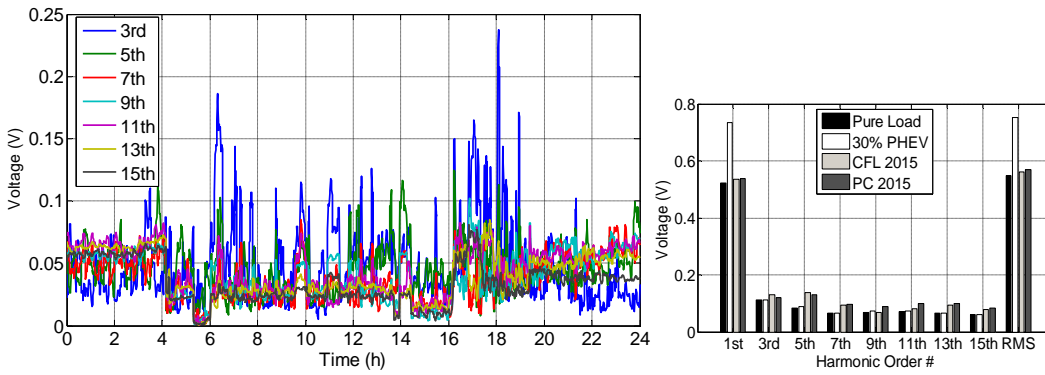
(a) Neutral voltage daily average profile.

(b) 95% index
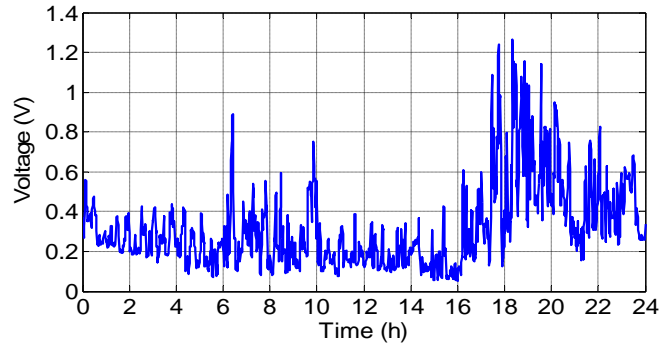
(c) RMS neutral voltage daily average profile

Figure 5.18 Average neutral to ground voltage under PHEV base case.

(a) Daily average profile

(b) 95% index (fundamental and RMS divided by 10)
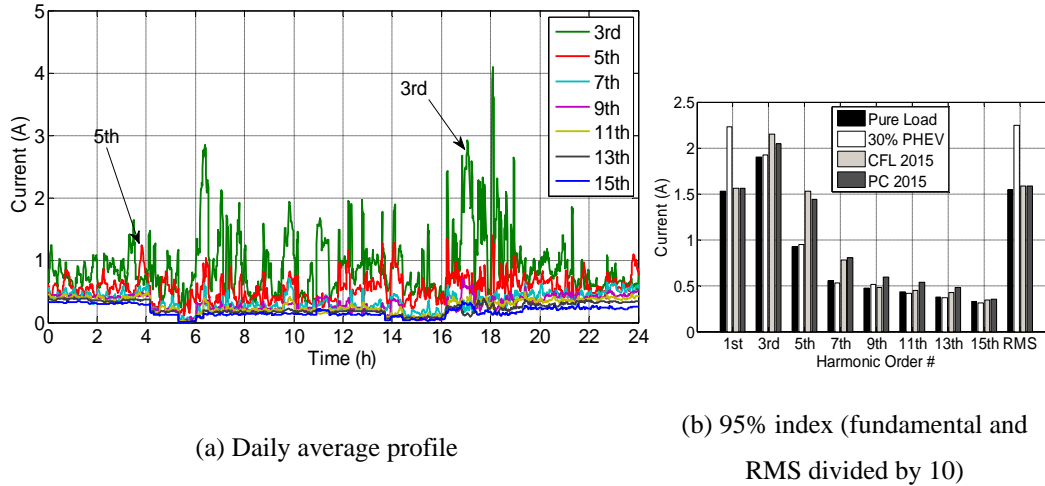
Figure 5.19 Average neutral current circulating between the houses under PHEV base case.

III. Impact on Secondary System Losses

Figure 5.20 shows the daily total fundamental and harmonic losses of the phase and neutral circuits of the secondary distribution system under PHEV base case. The daily average phase and neutral losses with and without PHEV loads are also provided in Table 5.9. The main finding is that PHEV loads will cause a notable increase of both phase and neutral conductor fundamental power loss. Since the majority of losses are caused by the fundamental frequency component, hence the conclusion is that PHEV caused losses in the secondary system shall be a great concern to utility companies.
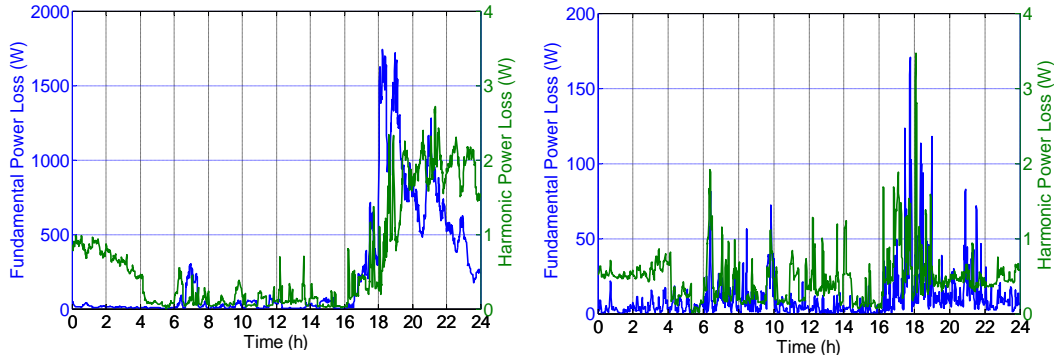
(a) Phases conductors power loss   (b) Neutral conductor power loss

Figure 5.20 Secondary system power losses under PHEV base case.

Table 5.9 Secondary system power losses with and without PHEV loads.

Daily Average Power Loss in Secondary System							
No PHEV	Phases	Neutral	Total	*30% PHEV*	Phases	Neutral	Total
Fundamental	149.68 W	9.10 W	158.77 W	**Fundamental**	231.37 W	18.03 W	249.40 W
Harmonic	0.65 W	0.26 W	0.91 W	**Harmonic**	0.65 W	0.29 W	0.94 W
Total	150.32 W	9.36 W	159.68 W	**Total**	232.02 W	18.32 W	250.34 W

IV. Overloading of Service Transformer

Figure 5.21(a) shows that the K-Factor is significantly decreased between 00:00 a.m. to 03:00 a.m. comparing with our previous results without PHEV. The reason is that most of Level 1 chargers will be operating during that period, which increases transformer loading (fundamental component) greatly but with only slight harmonic growth. Due to this reason, the "95% index" of *K-Factor* is decreased to 3.36.

155

The service transformer loading shown in Figure 5.21(b) reveals that uncontrolled charging PHEV would add peak load, which causes service transformer overloading problems. Supplying 30% penetration level of PHEV with uncontrolled charging strategy, the service transformer loading will remain beyond its rated level (37.5 KVA) for almost 30 minutes.

(a) Service transformer K-Factor   (b) Service transformer loading
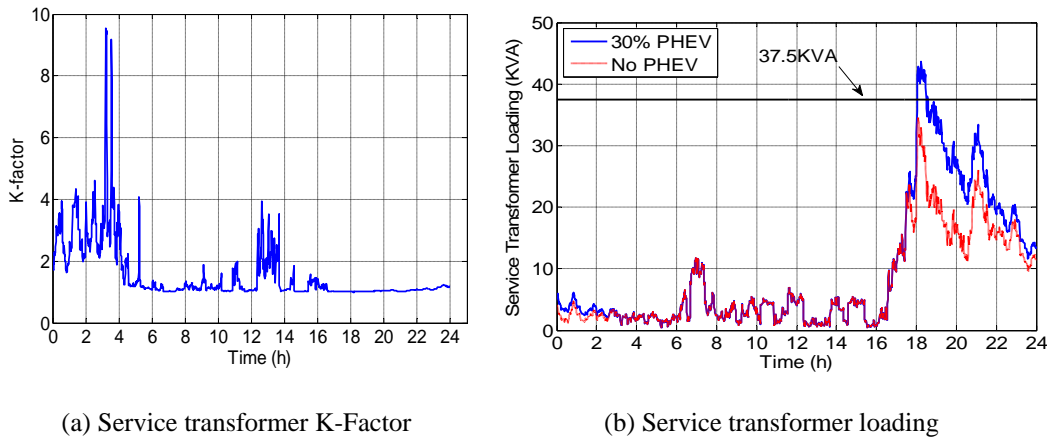
Figure 5.21 Service transformer K-factor and loading under PHEV base case.

V. Voltage Violation at Secondary System

Voltage profile for all houses connected to Phase A of the secondary system are obtained and recorded. Figure 5.22 shows the voltage profile for "House 10" located at the end of the secondary distribution branch where the voltage drop is the greatest. The result indicates that uncontrolled charging PHEV could make customer voltage drop to an unacceptable level[4]. It can also be observed that the highest voltage drop occurs around 18:00, which is the regular time people come home from work.

---

[4] According to "CSA Standard CAN3 C235-83: Preferred Voltage Levels for AC Systems 0 to 50,000 V" [51], the limits for operational steady-state voltages are 0.94 pu (112.8 V) and 1.06 pu (127.2 V).
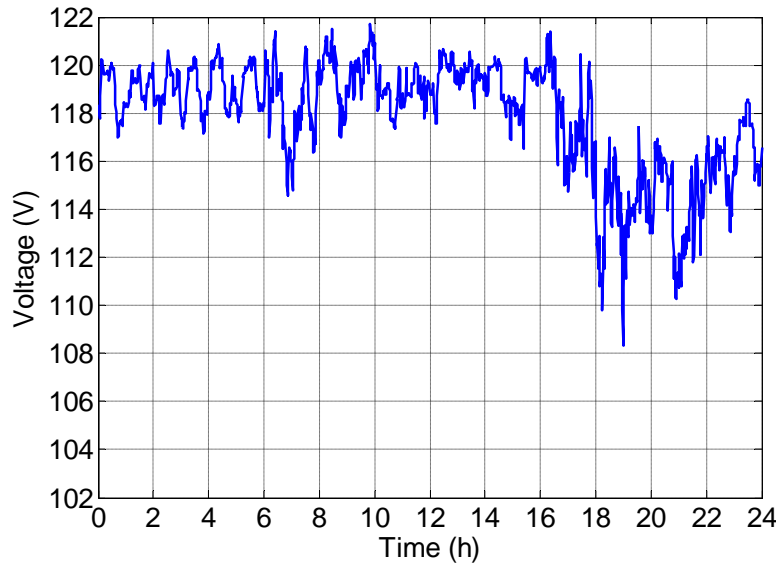
Figure 5.22 Voltage profile of House 10 under PHEV base case.

5.4.1.2 Secondary System Sensitivity Study

Several sensitivity studies are conducted in this section to evaluate what is the impact of changing charging strategies and charger types on the voltage and current levels of secondary distribution systems.

I. The Impact of Charging Strategies

This case study considers the impact of different charging strategies on the power quality indices of the secondary system. The penetration level of PHEV is fixed to 30%, mixed chargers are used, and the other system parameters including base load remain unchanged. Figure 5.23(a) and Figure 5.23(b) show the 95% index associated to the average phase harmonic voltages and currents, respectively, including the associated THD and TDD, for different charging strategies. Figure

157

5.24(a) and Figure 5.24(b) show the 95% index of the average neutral to ground voltage and neutral current, respectively.

(a) 95% index for phase voltage

(b) 95% index for phase current

Figure 5.23 Average harmonic phase voltage and current of all houses under different charging strategies.

(a) 95% index for neutral voltage

(b) 95% index for neutral current (fundamental and RMS divided by 10)
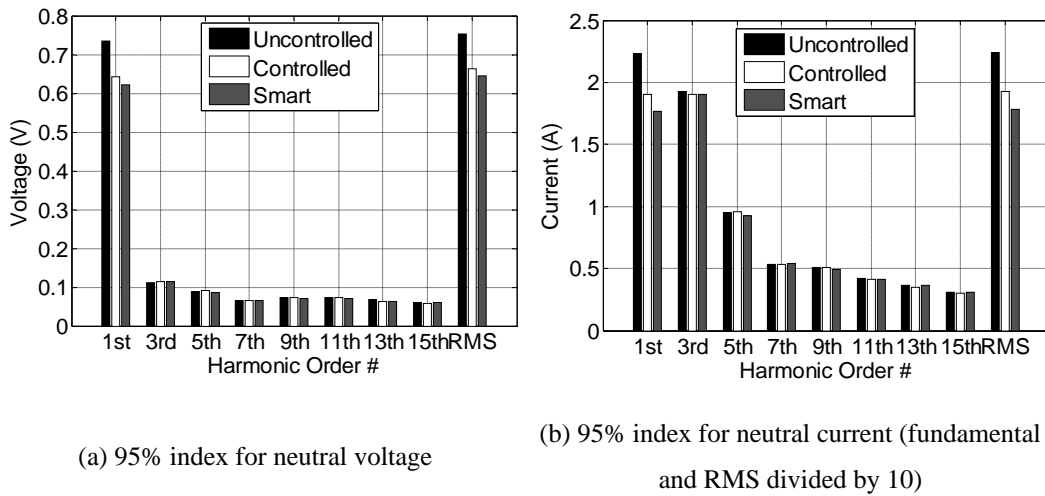
Figure 5.24 Average neutral to ground voltage and neutral current circulating between the houses under different charging strategies.

Figure 5.25 shows the daily service transformer load profile under different charging strategies at 30% PHEV penetration level with mixed chargers. Table 5.10 shows the daily average phase and neutral losses, 95% index of K-Factor as well as the minimum voltage along the secondary distribution system.
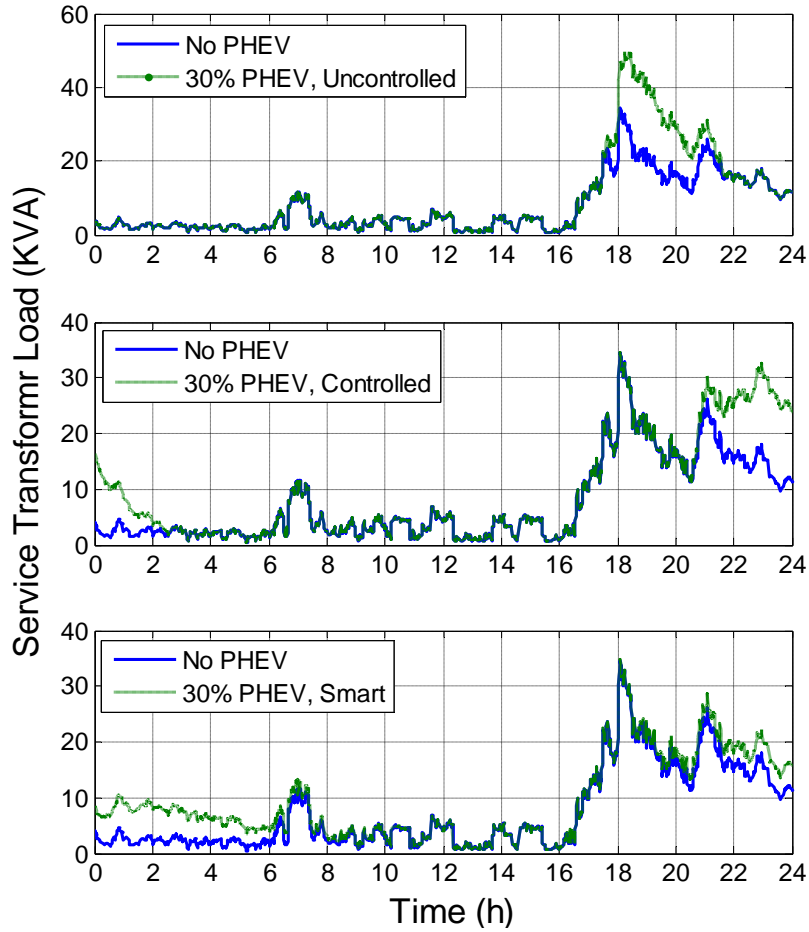
Figure 5.25 Service transformer loading under different charging strategies

Table 5.10 Impact of charging strategies on secondary system simulation results

30 % PHEV Mixed Chargers	Charging Strategy		
	Uncontrolled	Controlled	Smart
Phase Fundamental Loss (w)	231.37	191.56	176.32
Phase Harmonic Loss (w)	0.646	0.669	0.657
Neutral Fundamental Loss (w)	18.03	17.17	14.44
Neutral Harmonic Loss (w)	0.288	0.288	0.281
Transformer K-factor	3.42	1.85	1.95
Transformer Max. Loading (KVA)	43.62	34.63	34.80
Min. Customer Voltage (p.u.)	0.903	0.920	0.920

The main findings are:

- The results shown in Figure 5.23(a) and Figure 5.23(b) indicate that chargers which works under controlled charging strategy would cause the most severe harmonic voltage and current distortion. The reason is that the charging time of controlled charging is mainly in evening, which is coincidentally the period of higher harmonic background current due to frequently nonlinear appliance usage.

- Due to more concentrated charging time, uncontrolled charging causes the highest neutral voltage and current rise (mainly fundamental component), as shown in Figure 5.24(a) and Figure 5.24(b). On the contrary, smart charging is the best with controlling neutral voltage and current rise problem.

- Figure 5.25 shows the daily service transformer load profile under different charging strategies at 30% PHEV penetration level with mixed charger. As expected, uncontrolled charging could result in severe overloading problems for service transformer. Both controlled charging and smart charging strategy are able to shift charging load off daily peak to avoid service transformer loading problem. However, controlled charging could also create a new peak during the evening.

- Charging strategy has a significant impact on secondary system power losses. As shown in Table 5.10, power losses under uncontrolled charging are the largest, whilst smart charging has the smallest power losses. The reduction in total losses from uncontrolled case by controlled charging and smart charging are 18% and 27%, respectively.

- Similar as service transformer loading issue, controlled charging and smart charging strategies have less impact on the voltage drop compared to uncontrolled charging.

II. The Impact of Charger Types

In this case study, the charger types are changed in order to verify the impact on the secondary system. The penetration level of PHEV is fixed to 30%, and the other system parameters including base load remain the same as base case. Figure 5.26(a) and Figure 5.26(b) show the 95% index associated to the average phase harmonic voltages and currents, respectively, including the associated THD and TDD, for different chargers types. Figure 5.27(a) and Figure 5.27(b) show the 95% index of the average 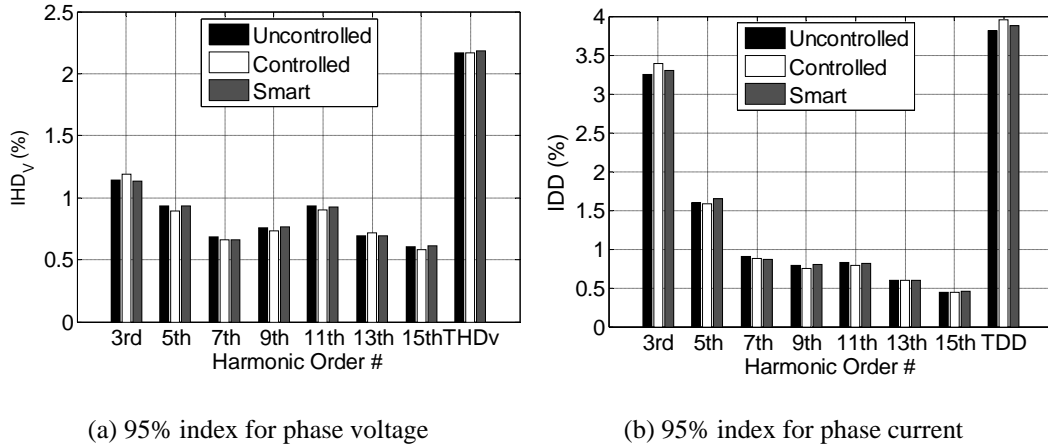neutral to ground voltage and neutral current, respectively. Table 5.11 summarizes the daily average phase and neutral losses, 95% index of K-Factor as well as the minimum voltage along the secondary distribution system. The findings are as follows:

- According to Figure 5.26, Level 2 charger, which has larger power level and connects to two phases of the secondary system, has the most severe harmonic distortion in phase voltage and current. However, since the impact of PHEV loads on harmonic level is not big overall, the effect of different charger types is not significant, either.
- Figure 5.27(a) and Figure 5.27(b) reveal that Level 1 charger would cause the most neutral voltage/current rise due to load imbalance level increase.
- As shown in Table 5.11, Level 2 charger has the most phase conductor losses due to its higher power level.
- Level 2 charger is more challenging to service transformer loading than Level 1 charger as well as mixed chargers, since it will create more than 10 KVA additional peak load for our testing 37.5 KVA service transformer.

161

- All types of chargers have unacceptable customer voltage drops under uncontrolled charging.

(a) 95% index for phase voltage

(b) 95% index for phase current
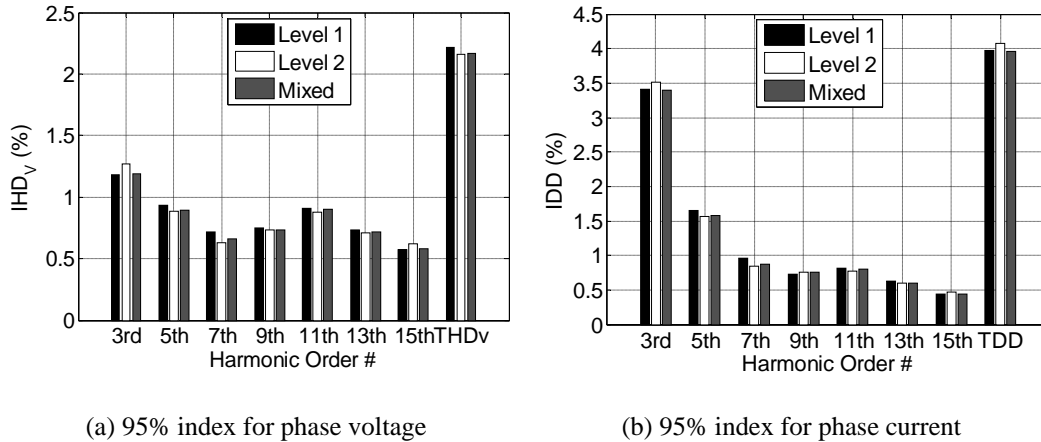
Figure 5.26 Average harmonic phase voltage and current of all houses under controlled charging strategy with different charger types.

(a) 95% index for neutral voltage

(b) 95% index for neutral current (fundamental and RMS divided by 10)
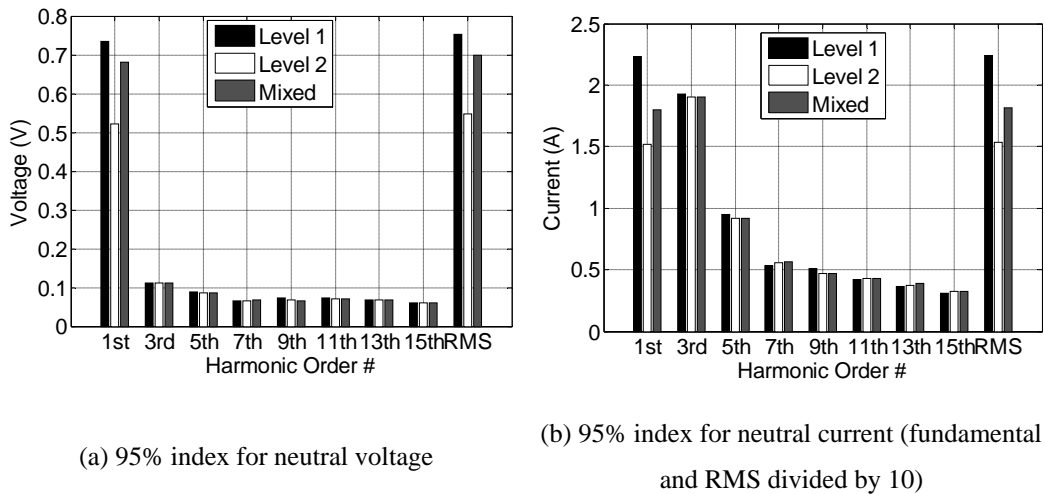
Figure 5.27 Average neutral to ground voltage and neutral current circulating between the houses under uncontrolled charging strategy with different charger types.

Table 5.11 Impact of charger types on secondary system simulation results

30 % PHEV Uncontrolled Charging	Charger Types		
	Level 1	Level 2	Mixed
Phase Fundamental Loss (w)	220.95	246.53	231.37
Phase Harmonic Loss (w)	0.676	0.695	0.646
Neutral Fundamental Loss (w)	18.03	9.06	13.24
Neutral Harmonic Loss (w)	0.288	0.265	0.276
Transformer K-factor	2.86	4.51	3.42
Transformer Max. Loading (KVA)	39.90	47.66	43.62
Min. Customer Voltage (p.u.)	0.896	0.897	0.903

5.4.1.3 Secondary System PHEV Load Growth Study

PHEV load growth studies are done using the estimated penetration trend data shown in Figure 5.4. As it has been done in the previous sections, most of the indices (such as harmonic voltage/ current, neutral voltage/current rise, as well as service transformer K-factor) are represented by its associated "95% index" in order to facilitate comparison of the results. Two different charts are provided. The first type of charts shows the index values respect to the increasing PHEV penetration level. The second type of charts shows the average growth rate per 10% PHEV increment for each index. The latter can be very useful parameter to predict the future power quality conditions of with more PHEV loads.

Charger type is fixed to mixed chargers during the study, which is a more realistic configuration. Since previous results showed that the harmonic distortion is more

severe under controlled strategy, all harmonic related results are conducted under controlled strategy. However, for other issues, like voltage drop, the uncontrolled strategy is applied.

I. Voltage and Current Distortion in the Secondary System

Figure 5.28(a) shows harmonic voltage respect to the increasing PHEV penetration level under controlled charging strategy. From the curves, one can calculate the average growth rate associated to the index, which is shown in Figure 5.28(c). For example, the 3rd harmonic index will grow at the rate of 2.41% per 10% PHEV increment. The harmonic current results are shown in Figure 5.29.
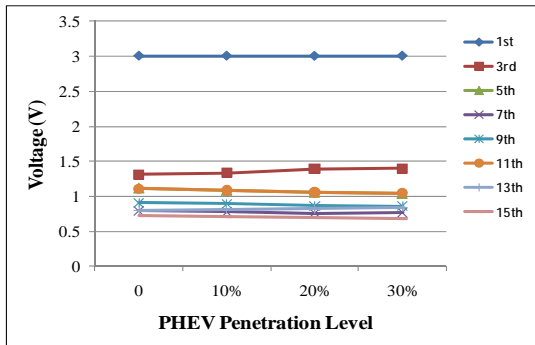
(a) Harmonic voltage (fundamental is divided by 40)
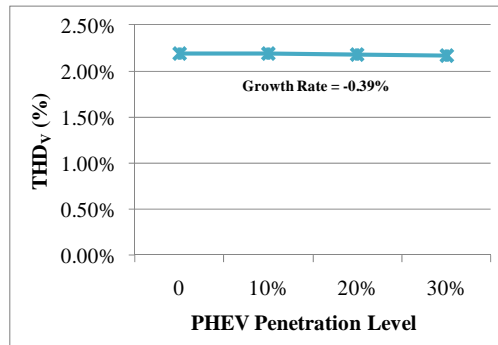
(b) THD$_V$
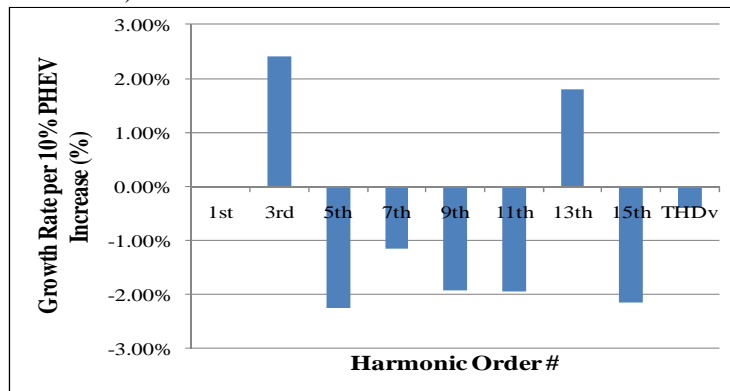
(c) Average growth rate per 10% PHEV increase

Figure 5.28 PHEV Growth characteristics of average phase A voltage in the secondary system.
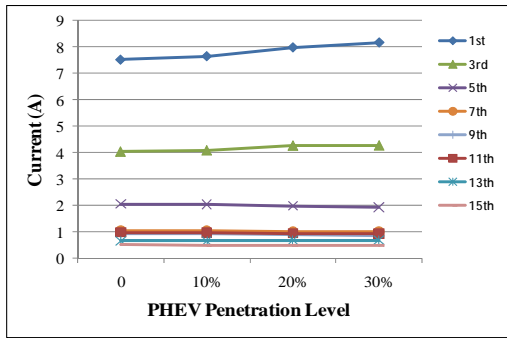
(a) Harmonic current (fundamental divided by 10)
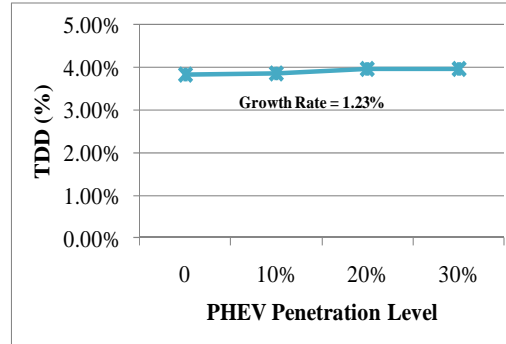
(b) TDD
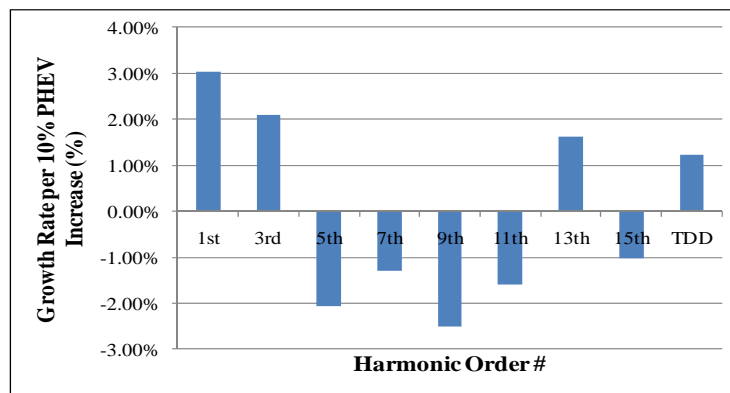
(c) Average growth rate per 10% PHEV increase

Figure 5.29 PHEV Growth characteristics of average phase A current in the secondary system.

The main findings are:

- The harmonic current and harmonic voltage have similar growth (decrease) rate for individual harmonic component.

- The harmonic growth rate is not significant. Depending on the angle of harmonic spectrum for individual charger, PHEV chargers may decrease the harmonic voltage/current levels due to cancellation with the household background harmonics. The TDD growth rate is 1.23%, which means the harmonic growth issue caused by PHEV could be ignored at most of time.

165

II. Neutral Conductor Current & Voltage Rise

Figure 5.30 shows the average neutral to ground voltage respect to the increasing PHEV penetration level and the associated average growth rate per 10% PHEV increment under uncontrolled charging. The results of neutral current are shown in Figure 5.31. The main findings are as follows:

- The increasing penetration of Level 1 chargers would cause neutral fundamental voltage/current growth due to load imbalance level increase.
- Due to this reason, RMS neutral voltage will increase at a notable growth rate. However, the most severe situation for neutral to ground voltage would be increasing from 0.549 V to 0.698 V at 30% PHEV penetration level, which is still less than 1 V.

(a) Neutral harmonic voltage (fundamental and RMS divided by 3)

(b) Average growth rate per 10% PHEV increase
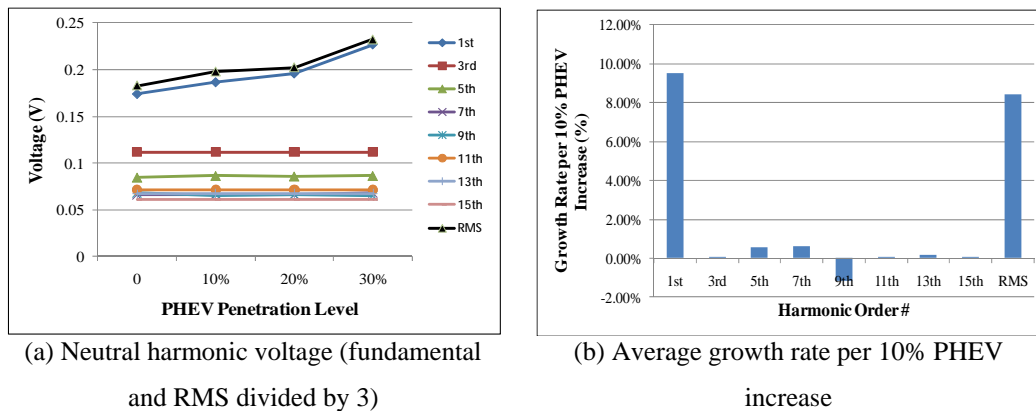
Figure 5.30 PHEV Growth characteristics of average neutral voltage level in the secondary system.
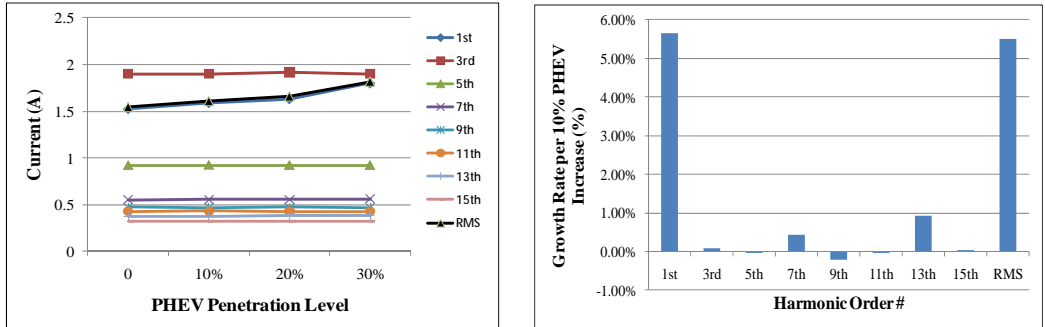
(a)) Neutral harmonic current (fundamental and RMS divided by 10)

(b) Average growth rate per 10% PHEV increase

Figure 5.31 PHEV Growth characteristics of average neutral current level in the secondary system.

III. Secondary System Power Losses

Figure 5.32 and Figure 5.33 show the total fundamental and harmonic power losses, respectively, on the phases and neutral circuits of the secondary system respect to increasing PHEV penetration level and correspondent average growth rate under uncontrolled charging. Figure 5.32 shows a significantly high growth rate of fundamental power losses for both phase and neutral conductors. Since the majority of power losses are caused by the fundamental ones, the results indicate that there would be almost 20% additional total power losses when increasing PHEV penetration level with 10%, which is a great concern to distribution system operation.
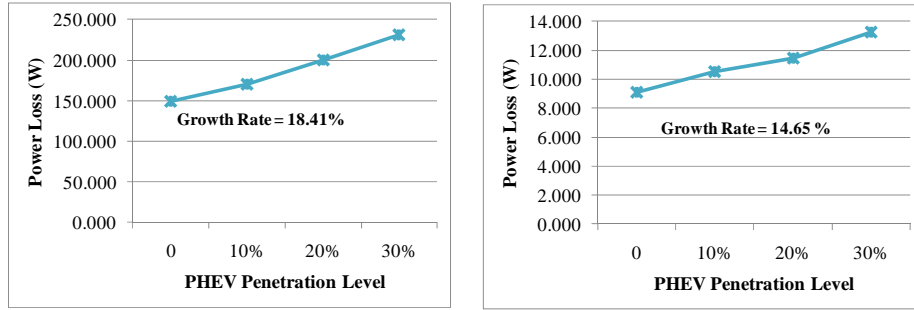
(a) Phases conductors power loss   (b) Neutral conductors power loss

Figure 5.32 Daily average fundamental power losses at secondary system respect to increasing PHEV penetration.
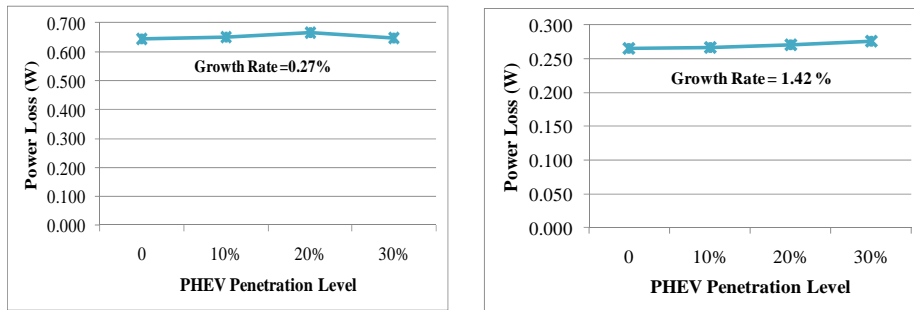
(a) Phases conductors power loss   (b) Neutral conductors power loss

Figure 5.33 Daily average harmonic power losses at secondary system respect to increasing PHEV penetration.

IV. Impact on Service Transformer

Figure 5.34 shows the K-Factor and maximum loading of the service transformer respect to increasing PHEV penetration level and correspondent average growth rate. As discussed in base case, K-factor will decrease with the integration of PHEV loads. Figure 5.34(b) shows that additional 3 KVA will be added to transformer peak load every 10% PHEV penetration increase. Our testing 37.5 KVA service transformer can support roughly 10% PHEV penetration without causing overloading problems.

(a) Service transformer K-factor   (b) Service transformer max. loading
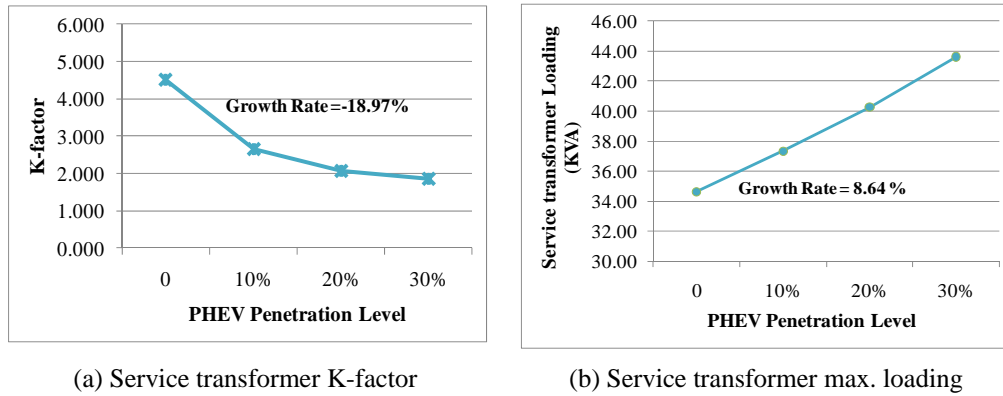
Figure 5.34 Service transformer K-factor and maximum loading respect to increasing PHEV penetration.

V. Voltage Violation at Secondary System

Figure 5.35 shows the minimum voltage at House 10, which is also the minimum costumer voltage in the secondary distribution system, respect to increasing PHEV penetration level under uncontrolled charging. The minimum customer voltage would drop linearly with increasing PHEV penetration, and the most severe voltage drop is 9.7% at 30% PHEV penetration.
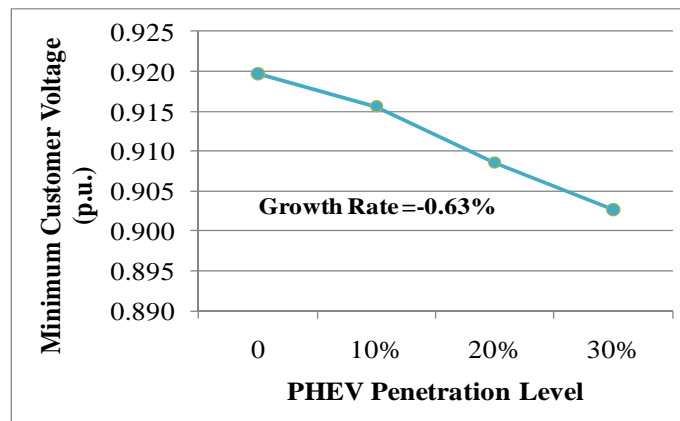
Figure 5.35 Minimum customer voltage respect to increasing PHEV penetration.

169

5.4.2 Simulation Results for Primary System with PHEV Load

The following subsections present the simulation results for primary distribution system integration with PHEV loads considering the case studies presented on Section 5.3.

5.4.2.1 Primary System Base Case Results

I. Voltage and Current Distortion in the Primary System

For quantifying the harmonic distortions, the three phase voltages at every 1 km along the primary feeder are obtained first. The sequence components are calculated and for each harmonic the dominant sequence is determined. The procedure of condensing the data as secondary system results is then applied. The daily average profile associated to the dominant sequence voltage of each harmonic is determined and shown in Figure 5.36(a). The daily average profile of the THD_V is shown as well. The dominant sequence voltage individual harmonic distortion (IHD_V) and THD_V can be determined and are shown in Figure 5.36(b).

Likewise, the harmonic phase currents at each section of the primary feeder and the respective sequence components are obtained. Then, the daily average profile associated to the dominant sequence current of each harmonic is determined and shown in Figure 5.37(a). The daily average profile of the TDD is shown as well. Finally, from Figure 5.37(a), the time 95% index of the individual demand

distortion (IDD) and TDD can be determined and are shown in Figure 5.37(b). Figure 5.36(b) and Figure 5.37(b) also show the "95% index" of harmonic dominant voltage and current of "pure" loads excluding any additional nonlinear loads as well as the loads with additional CFL and PC loads 5 years later (2015), which are used to compare the effect on primary system voltage/current harmonic distortion among different residential loads.

(a) Daily average profile

(b) 95% index
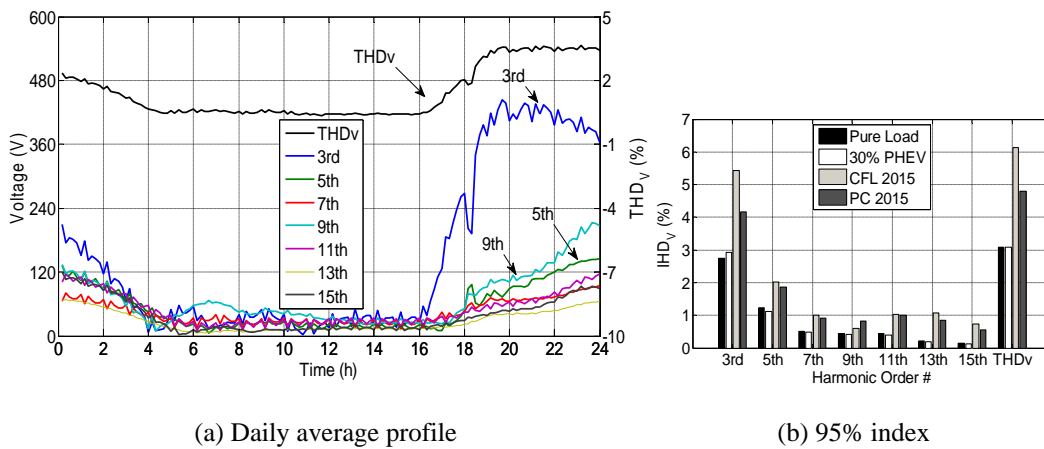
Figure 5.36 Average dominant sequence voltage of all nodes under PHEV base case.

(a) Daily average profile

(b) 95% index
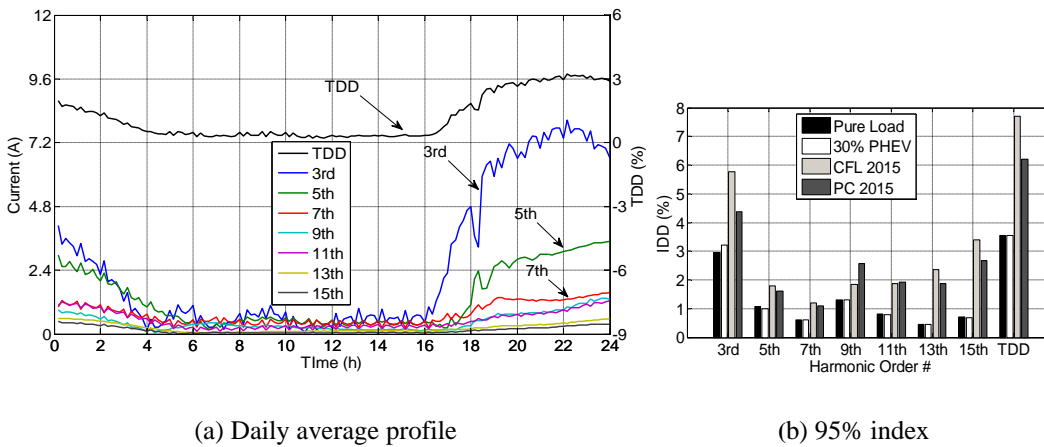
Figure 5.37 Average dominant sequence current of all sections under PHEV base case.

Comparing to our previous base case results without PHEV loads, the impact of PHEV on voltage and current distortion is not significant. Moreover, Figure 5.36(b) and Figure 5.37(b) indicate that even with 30% penetration level, the harmonic distortion caused by PHEV loads are less severe than that by future incoming CFL and PC loads. The reason is the same as explained in secondary system results.

II. Telephone interference level

One of the consequences of increasing harmonic current levels is audible noise on telephones lines that run in parallel with distribution feeders. The impact on the telephone line is normally measured by calculating the IT factors given in equation (5.6). The results are shown in Figure 5.38.

(a) Daily average profile   (b) 95% index
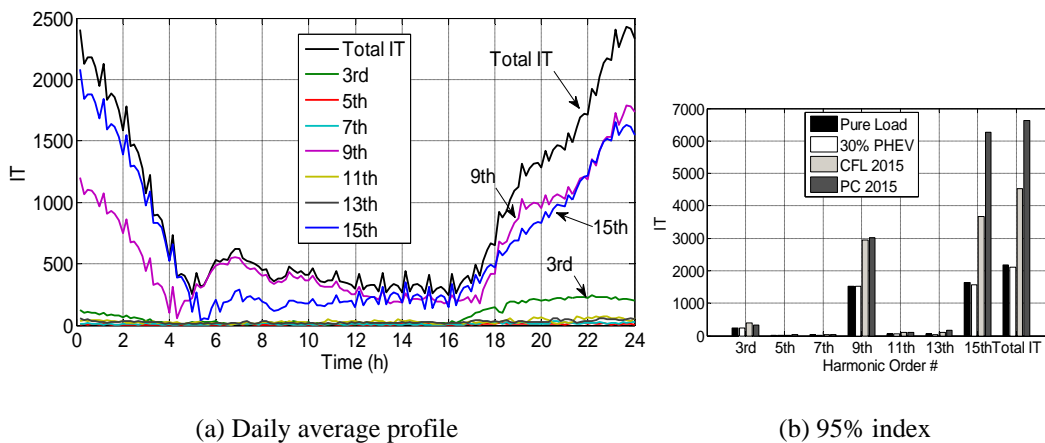
Figure 5.38: Average individual and total IT levels at the primary system under PHEV base case.

The voltage induced at the end of a (75m) conductor parallel to the primary feeder is also determined, as shown in Figure 5.39. This voltage is a more useful indicator on the telephone interference level since the effect of neutral current is included. The results are shown in Figure 5.40. Both Figure 5.38(b) and Figure 5.40(b) reveal that the impacts due to PHEV on IT level and induced voltage are very small since the levels of these indices are comparable for both "30% PHEV" and "Pure Load" case studies.
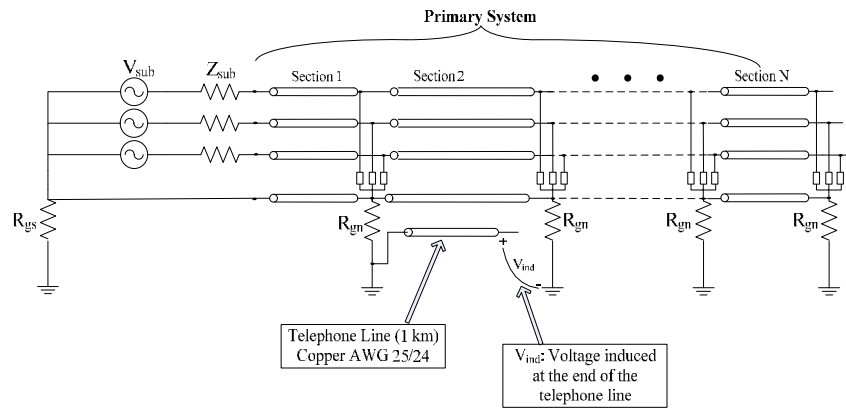
Figure 5.39 Schematic representation of the telephone line in parallel to the primary system.

(a) Daily profile	(b) 95% index
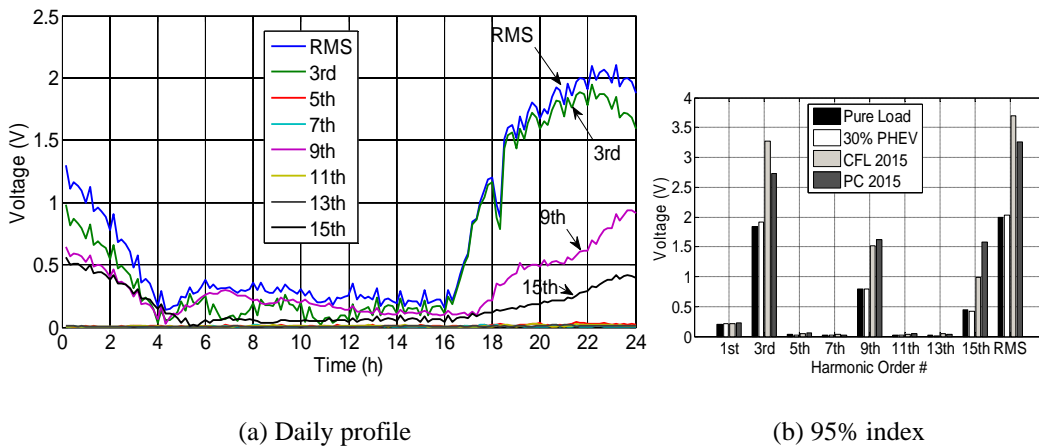
Figure 5.40 Voltage induced at the end of a telephone line under PHEV base case.

III. Neutral Conductor Current & Voltage Rise

The impact of the nonlinear residential loads on the average neutral current and voltage levels at the primary distribution system has been investigated. The results are shown in Figure 5.41 and Figure 5.42.

For primary system, adding PHEV loads has almost no impact on both fundamental and harmonic neutral voltage/current. Since there is harmonic caused neutral to ground voltage rise for additional CFL or PC loads, PHEV seems to cause the lowest RMS neutral to ground voltage among these loads.

(a) Neutral voltage daily average profile   (b) 95% index
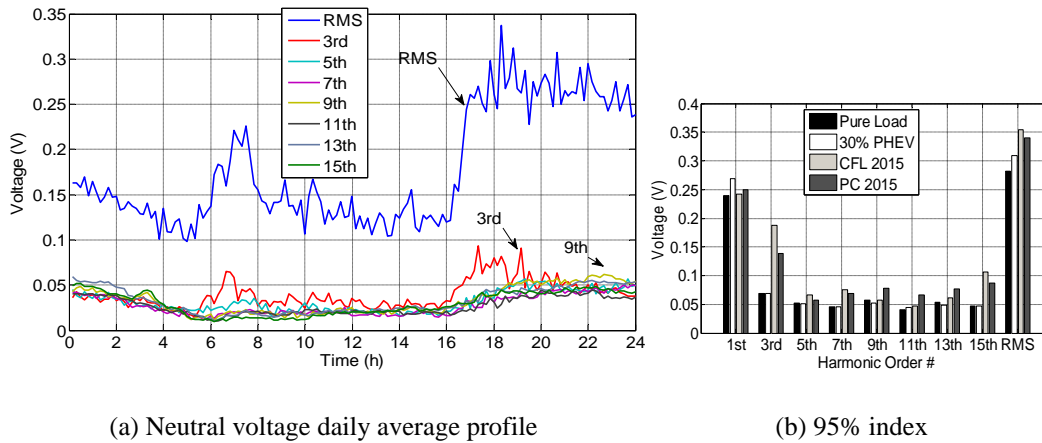
Figure 5.41 Average neutral voltage level at the primary system under PHEV base case.

(a) Daily average profile   (b) 95% index
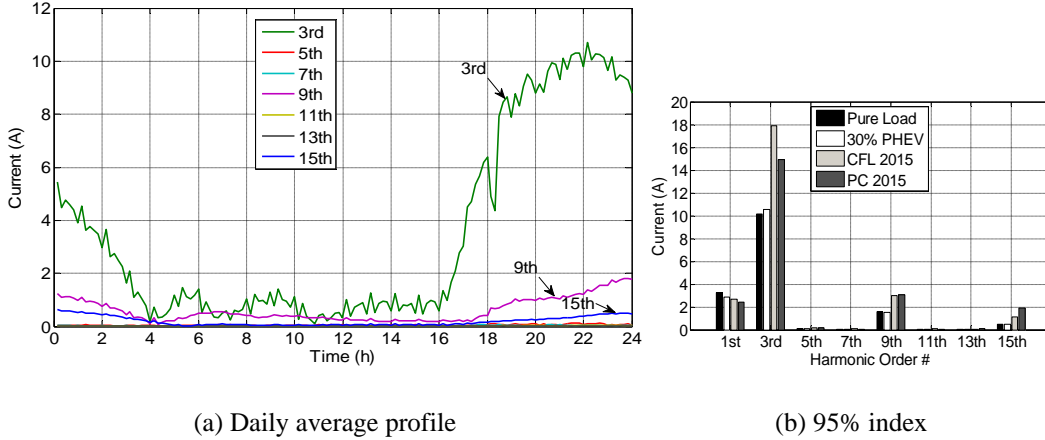
Figure 5.42 Average neutral current level at the primary system under PHEV base case.

IV. Impact on Primary System Losses

The impact of PHEVs on primary system losses are shown in Figure 5.43. The daily average phase and neutral losses with and without PHEV loads are also provided in Table 5.12. The losses shown are total losses of the study feeder. The results show a good consistency with secondary system results, PHEV loads will cause a notable increase of phase conductor fundamental power loss. Since fundamental frequency current caused losses are much higher than that caused by the harmonic currents for the phase conductors, hence the conclusion is that PHEV caused losses in the primary system is also a challenging issue to utility companies.

175
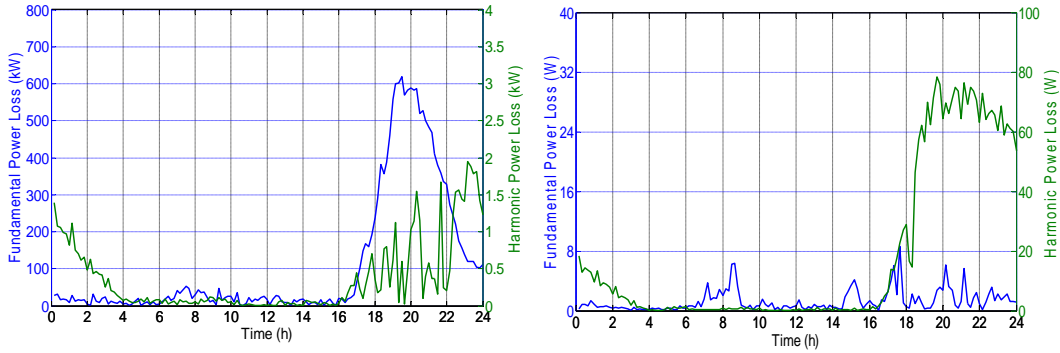
(a) Phases conductors power loss   (b) Neutral conductor power loss

Figure 5.43 Primary system power losses under PHEV base case.

Table 5.12 Primary system power losses with and without PHEV loads.

Daily Average Power Loss in Primary System							
No PHEV	Phases	Neutral	Total	*30% PHEV*	Phases	Neutral	Total
Fundamental	88.65 kW	0.001 kW	88.65 kW	Fundamental	111.68 kW	0.001 kW	111.68 kW
Harmonic	1.66 kW	0.02 kW	1.68 kW	Harmonic	0.37 kW	0.02 kW	0.39 kW
Total	90.31 kW	0.021 k W	90.3 kW	Total	112.05 kW	0.021 kW	112.07 kW

V. Voltage Violation at Primary System

Voltage profiles for all nodes at Phase A of the primary system are also investigated. However, for Node 15 locates at the end of distribution branch where the voltage drop is the greatest as expected, its voltage profile is chosen to be shown in Figure 5.44. The result confirms that uncontrolled charging PHEV could also make node voltage drop to an unacceptable level.

176
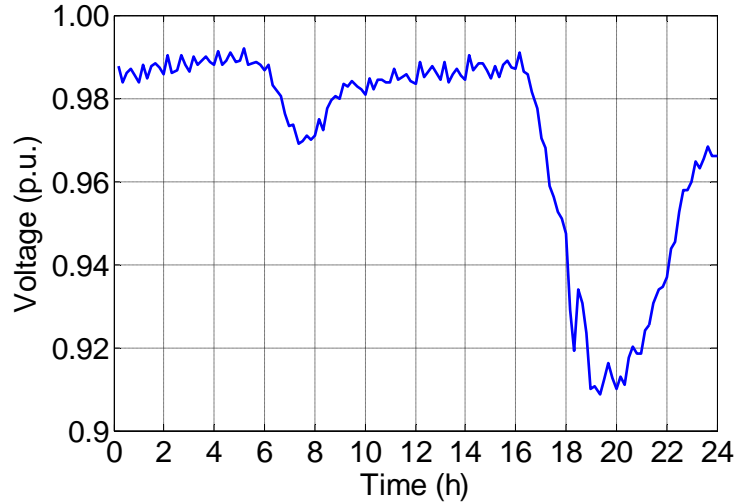
Figure 5.44 Voltage profile of Node 15 under PHEV base case.

5.4.2.2 Primary System Sensitivity Study

Several sensitivity studies are conducted in this section to evaluate what is the impact of changing charging strategies and charger types on the primary system PHEV simulation.

I. The Impact of Charging Strategies

This case study considers the impact of different charging strategies on the power quality indices of the primary system. The penetration level of PHEV is fixed to 30%, mixed chargers are used, and the other system parameters including base load remain unchanged. The results reveal that:

- The results shown in Figure 5.45(a) and Figure 5.45 (b) indicate that chargers which works under controlled charging strategy would cause the most severe harmonic voltage and current distortion in primary system. The results are consistent with our secondary system results.

177

- Similar as harmonic distortion level, controlled charging causes the highest IT levels as well as induced voltage at the end of a telephone line, as shown in Figure 5.46(a) and Figure 5.46 (b).

- Charging strategy has almost no impact on the RMS value of primary neutral to ground voltage.

- Charging strategy has a significant impact on primary system power losses. As shown in Table 5.13, power losses under uncontrolled charging are the largest, whilst smart charging has the smallest power losses. The reduction in total losses from uncontrolled case by controlled charging and smart charging are 15% and 20%, respectively.

- Similar as secondary system results, controlled charging and smart charging strategy would not bring out unacceptable voltage violations while uncontrolled charging would.
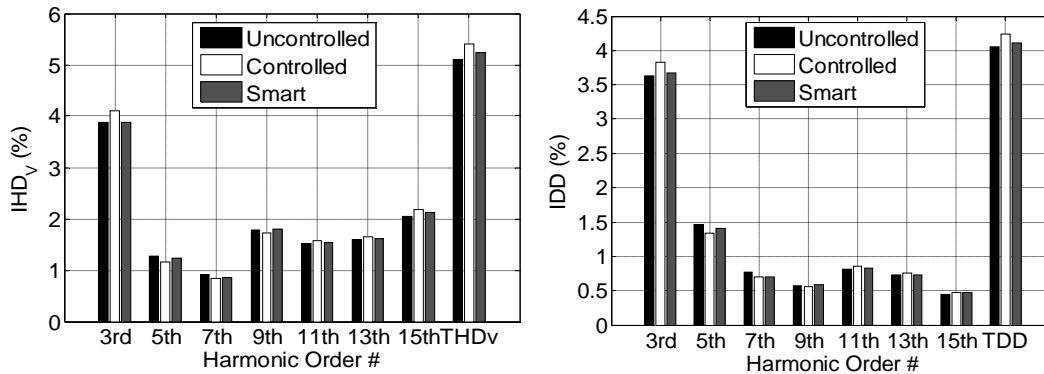
(a) 95% index for phase voltage (b) 95% index for phase current

Figure 5.45 Average dominant sequence harmonic voltage and current of all nodes at primary feeders under different charging strategies.
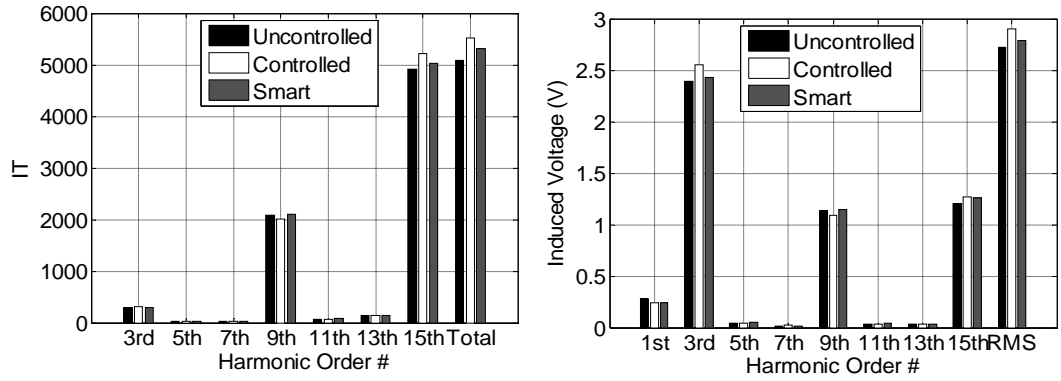
(a) 95% index for individual and total IT   (b) 95% index for induced voltage

Figure 5.46 Average IT levels and induced voltage at telephone line at the
primary system under different charging strategies.

Table 5.13 Impact of charging strategies on primary system simulation results

30 % PHEV Mixed Chargers	Charging Strategy		
	Uncontrolled	Controlled	Smart
RMS Neutral Voltage (V)	0.374	0.383	0.344
Phase Fundamental Loss (kw)	130.69	110.95	105.72
Phase Harmonic Loss (kw)	0.88	0.80	0.92
Neutral Fundamental Loss (kw)	0.002	0.002	0.002
Neutral Harmonic Loss (kw)	0.03	0.03	0.03
Min. Node Voltage (p.u.)	0.898	0.916	0.916

II. The Impact of Charger Types

In this case study, the charger types are changed in order to verify the impact on
the primary system. The penetration level of PHEV is fixed to 30%, and the other
system parameters including base load remain the same as base case. The findings
are very similar to those of secondary system:

- According to Figure 5.47, Level 2 charger has the most severe harmonic distortion in phase voltage and current. Additionally, as shown in Figure 5.48, IT levels and telephone line induced voltage are also the highest with Level 2 chargers.

- Table 5.14 reveals that Level 1 charger would cause the most neutral to ground voltage rise due to load imbalance level increase.

- As shown in Table 5.14, Level 2 charger has the most phase conductor losses due to its higher power level.

- All types of chargers have unacceptable node voltage violations under uncontrolled charging.
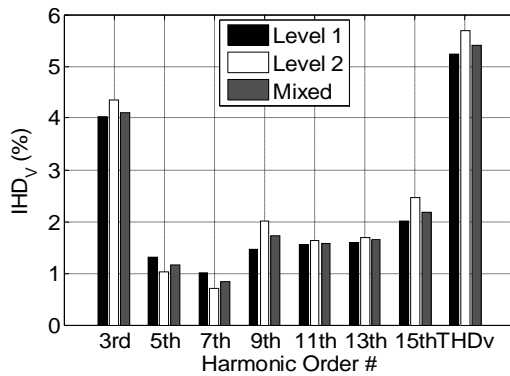
(a) 95% index for phase voltage
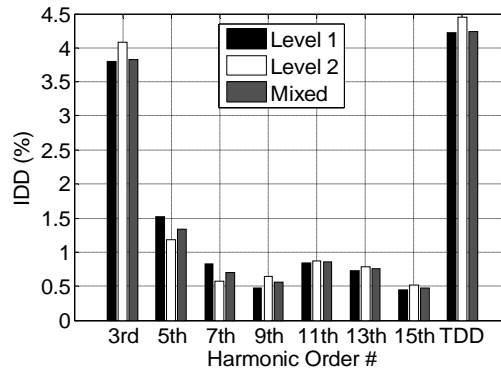
(b) 95% index for phase current

Figure 5.47 Average dominant sequence harmonic voltage and current of all nodes at primary feeders under controlled charging with different charger types.
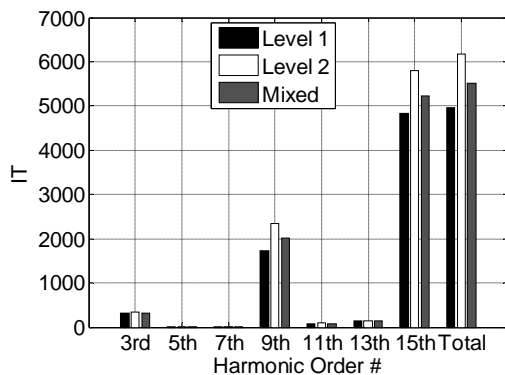
(a) 95% index for individual and total IT
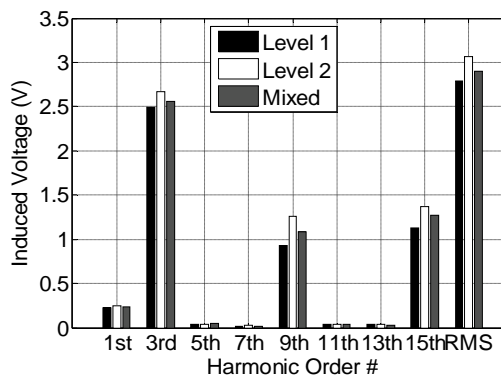
(b) 95% index for induced voltage

Figure 5.48 Average IT levels and induced voltage at telephone line at the primary system under uncontrolled charging with different charger types.

Table 5.14 Impact of charger types on primary system simulation results

30 % PHEV Uncontrolled Charging	Charger Types		
	Level 1	Level 2	Mixed
RMS Neutral Voltage (V)	0.430	0.326	0.374
Phase Fundamental Loss (kw)	124.74	135.34	130.69
Phase Harmonic Loss (kw)	0.87	1.39	0.88
Neutral Fundamental Loss (kw)	0.002	0.001	0.002
Neutral Harmonic Loss (kw)	0.03	0.03	0.03
Min. Node Voltage (p.u.)	0.907	0.892	0.898

5.4.2.3 Primary System PHEV Load Growth Study

Same as secondary system, PHEV load growth studies at primary system are also done using the estimated penetration trend data shown in Figure 5.4. In order to facilitate and comparison of the results, most of the indices (such as harmonic voltage/current, IT level/induced voltage as well as neutral voltage/current rise) are represented by its associated "95% index". Two different charts are provided. The first type of charts shows the index values respect to the increasing PHEV penetration level. The second type of charts shows the average growth rate per 10% PHEV increment for each index.

Charger type is also fixed to mixed chargers during the study. For harmonic distortion situation is the most severe under controlled strategy, all harmonic related results are conducted under controlled strategy. However, the other results are done under uncontrolled strategy.

I. *Voltage and Current Distortion in the Primary System*

Figure 5.49(a) shows the 95% index of the harmonic dominant sequence voltages respect to the increasing PHEV penetration level under controlled charging strategy. From the data provided in Figure 5.49(a), it is possible to calculate the average growth rate per 10% PHEV increment associated to the phase voltage index, which is shown in Figure 5.49(c). Similarly, Figure 5.51 and Figure 5.55 show the 95% index associated to the dominant and zero sequences of the average current along the primary feeder and the associated average growth rate.

(a) Dominant sequence harmonic voltage
(fundamental divided by 100)

(b) THD$_V$

(c) Average growth rate per 10% PHEV increase
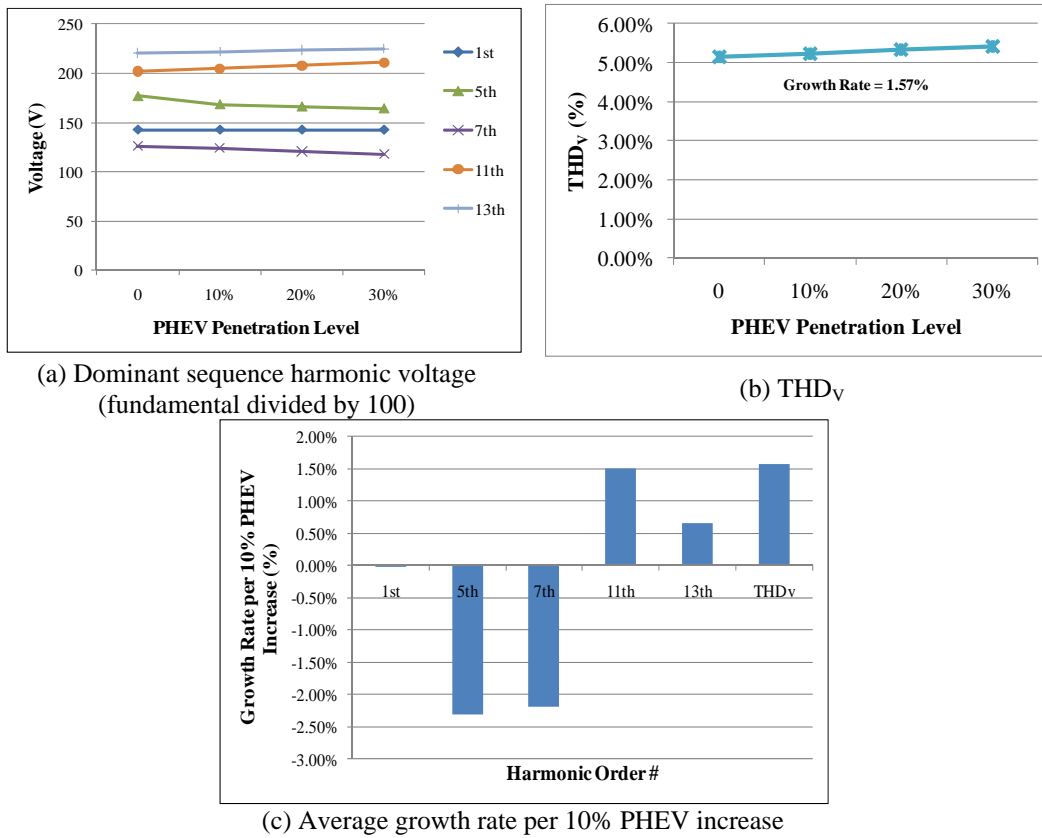
Figure 5.49 PHEV Growth characteristics of dominant sequence voltages in the primary system.
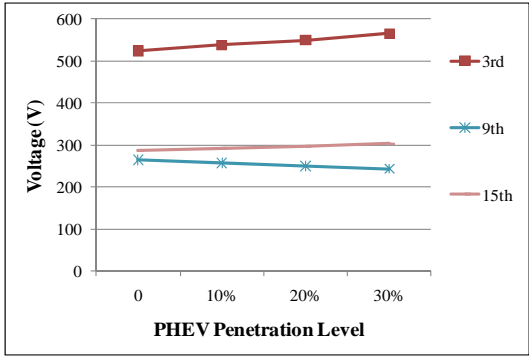
(a) Zero sequence harmonic voltage
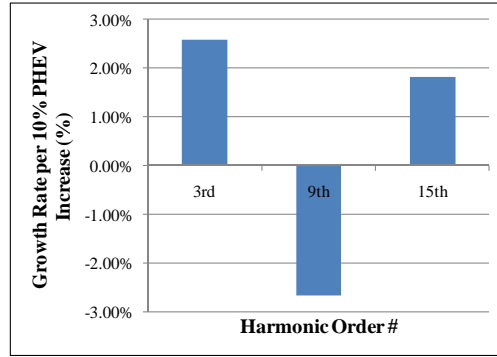
(b) Average growth rate per 10% PHEV increase

Figure 5.50 PHEV Growth characteristics of zero sequence voltages in the primary system.
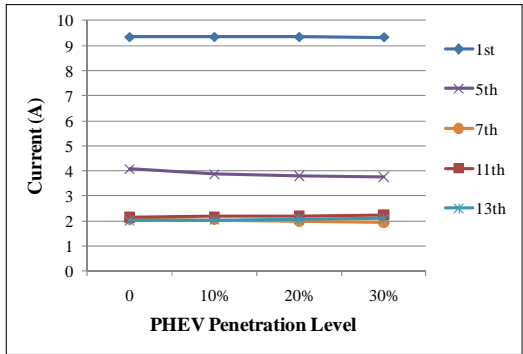
(a) Dominant sequence harmonic current (fundamental divided by 20)
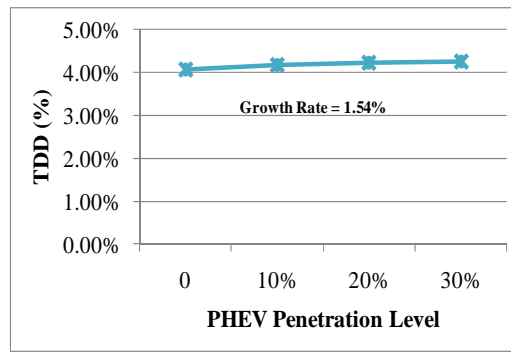
(b) TDD
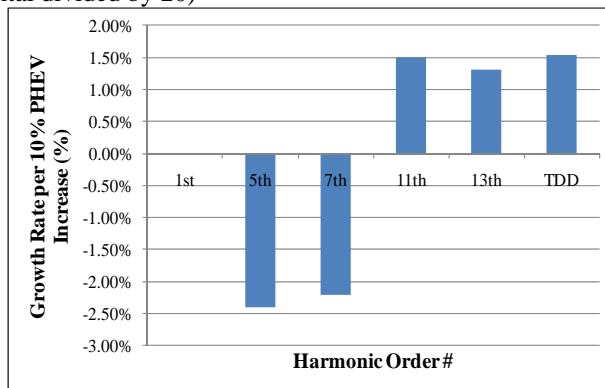
(c) Average growth rate per 10% PHEV increase

Figure 5.51 PHEV Growth characteristics of dominant sequence currents in the primary system.

183

(a) Zero sequence harmonic current

(b) Average growth rate per 10% PHEV increase
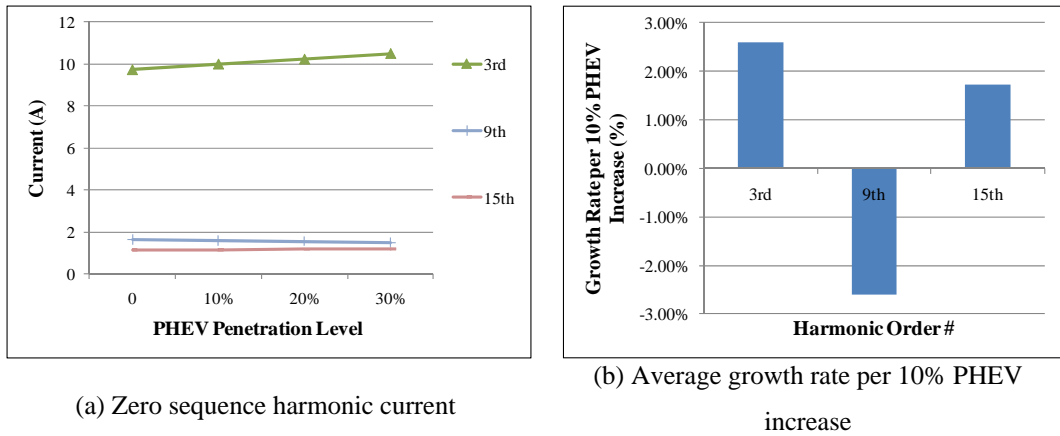
Figure 5.52 PHEV Growth characteristics of zero sequence currents in the primary system.

The harmonic growth rate is not notable at primary system, either. The growth rate per 10% PHEV increment of voltage THD_V and current TDD are 1.57% and 1.54%, respectively, which means the harmonic growth issue caused by PHEV in the primary system does not represent a concern.

II. Telephone interference in the form of IT factors

The growth of IT levels and voltage induced on a parallel conductor are shown in Figure 5.53 and Figure 5.54, respectively. It is found that total IT level and induced voltage will only increase at the rate of 2%, mainly due to the growth of 15th harmonic component, which is consistent with dominant sequence harmonic voltage/current level.

(a) Individual and total IT level   (b) Average growth rate per 10% PHEV increase
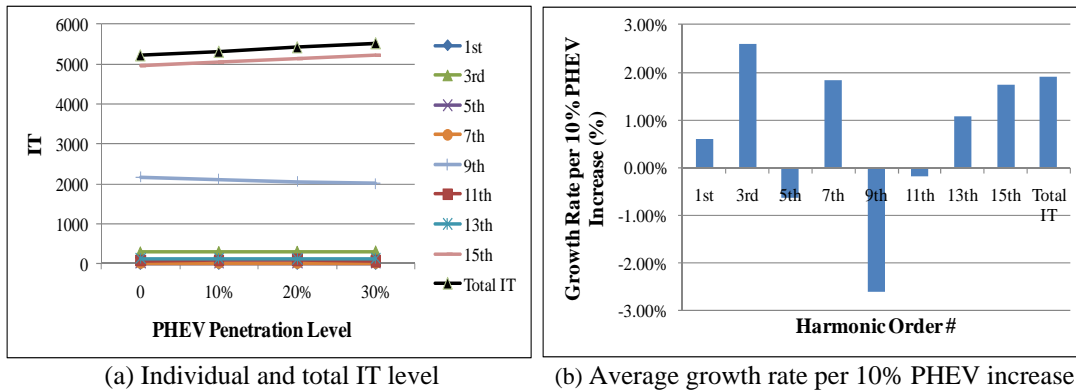
Figure 5.53 PHEV Growth characteristics of IT index in the primary system.

(a) Induced voltage   (b) Average growth rate per 10% PHEV increase
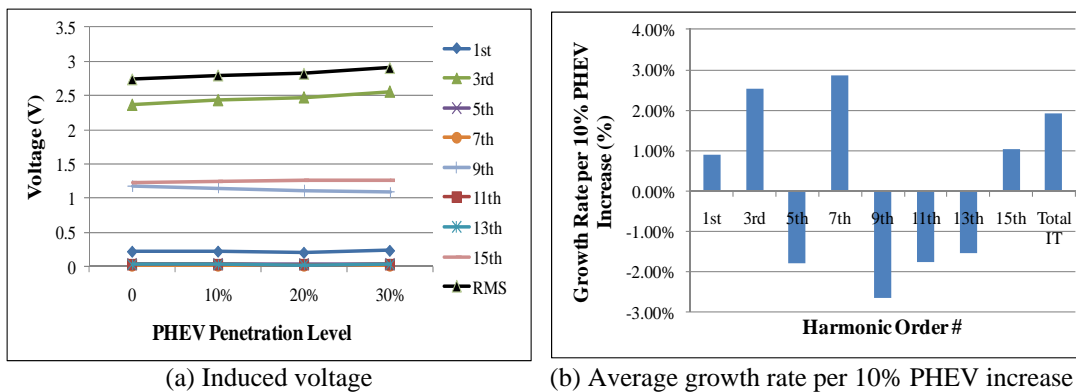
Figure 5.54 PHEV Growth characteristics of induced voltage on a parallel conductor.

III. Neutral Conductor Current & Voltage Rise

The results of neutral voltage and current growth are shown in Figure 5.55 and Figure 5.56 respectively. The results indicate that there is almost no impact of neutral voltage and current at primary system while the growth of PHEV.
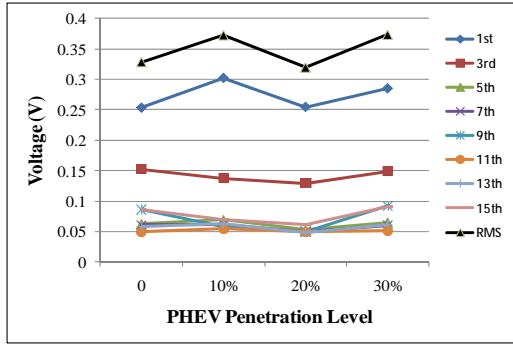
(a) Neutral harmonic voltage
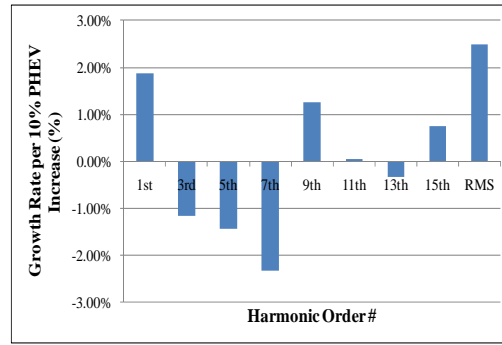
(b) Average growth rate per 10% PHEV increase

Figure 5.55 PHEV Growth characteristics of neutral voltage in the primary system.
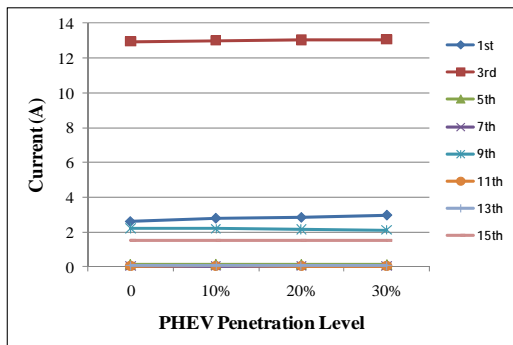
(a)) Neutral harmonic current (fundamental and RMS divided by 10)
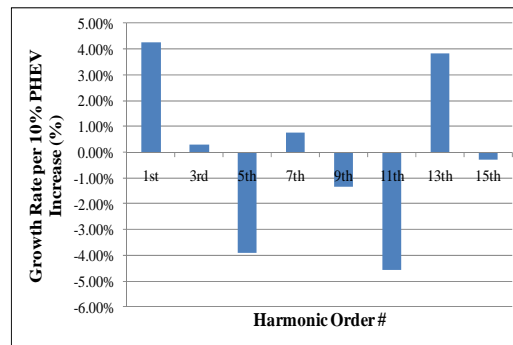
(b) Average growth rate per 10% PHEV increase

Figure 5.56 PHEV Growth characteristics of neutral current in the primary system.

IV. Primary System Power Losses

The PHEV growth characteristics of various loss components are shown in Figure 5.57 and Figure 5.58. As discussed in the secondary system section, due to the high growth rate of fundamental power losses for phase conductors, there would be almost 14% additional total power losses when increasing PHEV penetration level with 10%, which is also a great concern to primary distribution system operation.

186
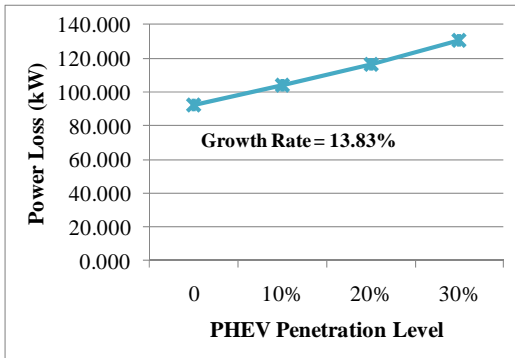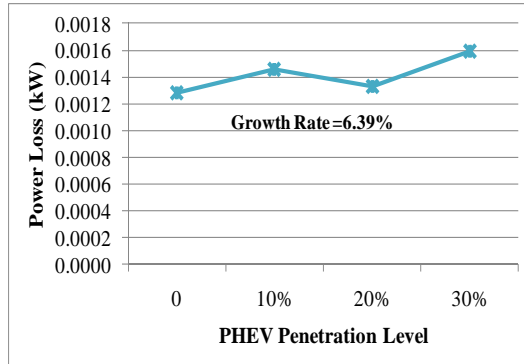
(a) Phases conductors power loss   (b) Neutral conductors power loss

Figure 5.57 Fundamental power losses at primary system respect to increasing PHEV penetration.
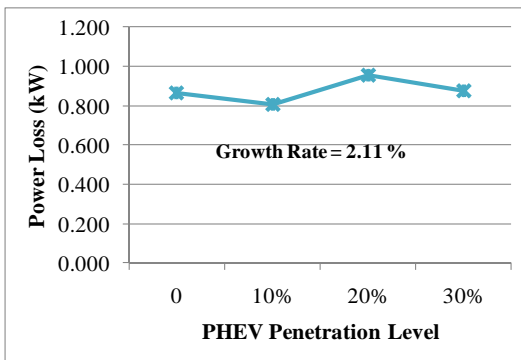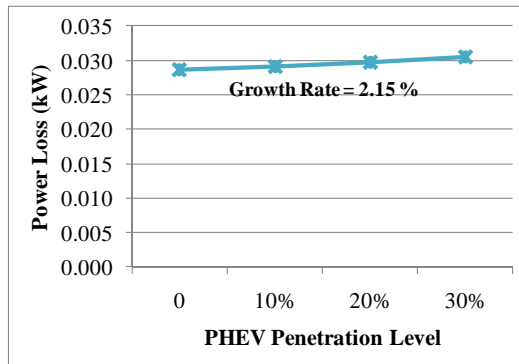
(a) Phases conductors power loss   (b) Neutral conductors power loss

Figure 5.58 Harmonic power losses at primary system respect to increasing PHEV penetration.

V. Voltage Violation at Primary System

Figure 5.59 shows the minimum voltage at Node 15, which is also the minimum node voltage in the primary distribution system, respect to increasing PHEV penetration level under uncontrolled charging. The minimum node voltage would

drop linearly with increasing PHEV penetration, and the most severe voltage drop

is 10.2% at 30% PHEV penetration.
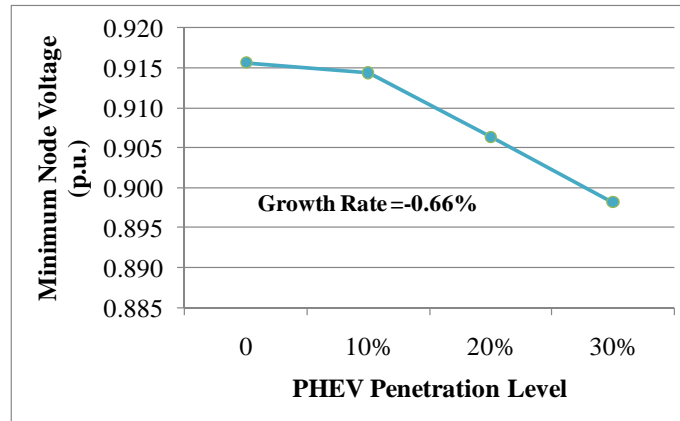
Figure 5.59 Minimum node voltage at primary system respect to increasing PHEV penetration.

5.5 Summary

This chapter proposed a model for PHEV charging load, which is based on the probabilistic modeling of vehicles' charging pattern and deterministic modeling of their charging characteristics.

Through this model, the impacts of PHEV penetration at different level on both secondary and primary distribution system are evaluated in several aspects. The following summarizes the findings and conclusions:

- **Harmonic voltage and current distortion levels:**
  The cases with Level 2 chargers and under controlled charging strategy have the highest harmonic voltage & current distortion level. However, the growth

rate of voltage THD_V and current TDD per 10% PHEV increment are both less than 2%, which makes the absolute value of these harmonic indices within 5% even with 30% PHEV penetration for both secondary and primary distribution system. Hence the conclusion is harmonic growth caused by PHEVs does not represent a concern.

- **The impact of charging harmonics on service transformer K-factor:**

It is not a concern for service transformer k-factor seems to not increase but decrease for PHEV widely adoption.

- **Telephone interference problems in primary distribution system:**

Similar as harmonic voltage and current distortion levels, PHEV seems not to bring severe telephone interference problems.

- **Neutral conductor voltage/current rise:**

The neutral to ground voltage rise due to PHEV loads is not significant for both secondary and primary distribution system.

- **Distribution system power losses:**

For integration PHEV loads into both secondary and primary distribution system, uncontrolled charging cause considerably expansive additional power losses while the reduction in additional losses over uncontrolled by smart charging is very significant. With high PHEV penetration level (e.g. 30%), up to 30% of total losses can be saved from uncontrolled case by employing smart charging.

- **Service transformer overloading:**

Uncontrolled charging and Level 2 charger are the most challenging to service transformer loading. Under uncontrolled charging of PHEV, additional 2 to 4.5 kVA loads will be added to transformer peak load every 10% PHEV penetration increase. Controlled charging has the potential to create new peak

during the evening while smart charging is the best to solve transformer overloading problems.

- **Voltage violations at distribution system:**

Uncontrolled charging of PHEVs will cause the minimum voltage reach an unacceptable level (e.g. <0.9 p.u.). However, controlled charging and smart charging would not bring out voltage problems.

According to the results, charging strategies have the most major impact of PHEV charging on distribution system. Basically, expansive additional distribution system power losses, service transformer overloading as well as unacceptable voltage drop are caused by uncontrolled charging strategy, while harmonics related problems are the most serious if under controlled charging strategy. However, once smart charging is employed, all aspects of above impacts can be simply minimized. Due to this reason, more sophisticated 'smart' charging algorithm based on smart metering and communication needs to be developed in the future.

Chapter 6

Conclusions and Future Work

6.1 Conclusions

The proliferation of energy-efficient appliances and modern consumer electronics has resulted in significant harmonic distortions in residential distribution systems. In order to determine the cumulative harmonic impact of these new harmonic sources, this thesis proposed a probabilistic bottom-up technique to model their random and distributed nature. By modeling the residential distribution systems with this technique, it is possible to estimate how serious the harmonic impacts become when more nonlinear appliances penetrate into the residential loads.

The major conclusions and contributions of this thesis are as follows:

- An extensive survey and analysis of customer market research data was conducted to establish the adoption or usage trends of key residential nonlinear appliances. This appliance adoption trend model could be essential for predicting the impact of future residential loads, including appliance addition and replacement.

- By investigating the voltage and the current correlation with the V x I plot, this thesis developed a useful but simple method for verifying if a household appliance is a linear or nonlinear load.

- This thesis developed a probabilistic method to model the random harmonic generations of home appliances by simulating the random operating statuses of the appliances. This modeling was done by determining the switching-on probability and operation duration of an appliance based on realistic factors such as the appliances' usage pattern as well as the number of occupants and their activities.

- One of the attractive characteristics of the proposed method is its bottom-up approach. As a result, one can simulate the effect of market trends or policy changes. For example, the harmonic impact of compact fluorescent lights can be studied by simply adjusting the composition of lighting fixtures in the appliance database.

- Based on the probabilistic bottom-up technique, a residential distribution system model was proposed to evaluate the harmonic impact of the distributed nonlinear residential loads on the secondary distribution system. This study could demonstrate the usefulness of our proposed methods. If our assumption of residential loads addition or replacement situation matches with the future trend, the typical annual growth rates of phase harmonic voltage and current are in the range of 10% to 15%, which could make the THD_V index exceed the IEEE limit of 5% in several years. This problem should be a major concern for utility companies.

- The power quality impact of charging plug-in hybrid vehicles (PHEV) on residential distribution networks was also investigated by using the same framework. Harmonic related issues do not represent a major concern, but the overloading of service transformers, expensive power losses, and unacceptable voltage drops are all problems that will result from the massive adoption of PHEVs. Since charging strategies have a significant impact on the above concerns, a more sophisticated 'smart' charging algorithm needs to be developed in the future.

6.2 Suggestions for Future Work

The following future work is suggested for the extending and modifying this thesis:

- To improve the accuracy of the simulation results, a more sophisticated harmonic model of appliances could be introduced in Chapter 2, in order to consider the harmonic current attenuation/amplification effect. Once this model is employed, the harmonic iterative method will become essential for harmonic power flow solutions. However, finding a generally accepted method to obtain such a model based on the measurement data is currently quite difficult.

- More realistic considerations can be added into the probabilistic bottom-up residential house model proposed in Chapter 3. For example, this thesis already considered the number of occupants and their activities when modeling residential loads, but the impact of other factors such as the season and weather was not taken into account. Additionally, more complicated mathematical tools can be introduced in order to better model the random nature of appliances' operation.

- As our aim was to derive a general evaluation of the impact of nonlinear appliances on residential distribution systems, a simple and hypothetical topology of distribution network was adopted. In order to give more specific results, the simulation can be extended to realistic distribution system once the detailed topology information is known.

References

[1]   "Tutorial on Harmonics Modeling and Simulation", IEEE Power Engineering Society, 98TP125-0, 1998.

[2]   "Modeling and simulation of the propagation of harmonics in electric power networks. I. Concepts, models, and simulation techniques," *Power Delivery, IEEE Transactions on,* vol. 11, pp. 452-465, 1996.

[3]   Dugan, R. C., McGranaghan, M. F., Beaty, H. W., Electrical Power Systems Quality,1996, McGraw-Hill.

[4]   R. Carbone*, et al.*, "Some considerations on the iterative harmonic analysis convergence," *Power Delivery, IEEE Transactions on,* vol. 8, pp. 487-493, 1993.

[5]   A. V. Oppenheim and R. W. Schafer, "Discrete-Time Signal Processing", Prince-Hall, Inc., Englewood Cliffs, NY, 1989.

[6]   "IEEE Recommended Practices and Requirements for Harmonic Control in Electrical Power Systems," *IEEE Std 519-1992,* p. 0_1, 1993.

[7]   W. Xu, "Status and future directions of power system harmonic analysis," in *Power Engineering Society General Meeting, 2004. IEEE*, 2004, pp. 756-761 Vol.1.

[8]   X. Daozhi and G. T. Heydt, "Harmonic Power Flow Studies Part I - Formulation and Solution," *Power Apparatus and Systems, IEEE Transactions on,* vol. PAS-101, pp. 1257-1265, 1982.

[9]   V. Sharma*, et al.*, "An iterative approach for analysis of harmonic penetration in the power transmission networks," *Power Delivery, IEEE Transactions on,* vol. 6, pp. 1698-1706, 1991.

[10]   W. Xu*, et al.*, "A multiphase harmonic load flow solution technique," *Power Systems, IEEE Transactions on,* vol. 6, pp. 174-182, 1991.

[11]   A. Cavallini*, et al.*, "Gaussian modeling of harmonic vectors in power systems," in *Harmonics And Quality of Power, 1998. Proceedings. 8th International Conference on*, 1998, pp. 1010-1017 vol.2.

[12]   Y. Baghzouz*, et al.*, "Time-varying harmonics. II. Harmonic summation and propagation," *Power Delivery, IEEE Transactions on,* vol. 17, pp. 279-285, 2002.

[13]   IEA, Light's Labour's Lost, International Energy Agency, OECD, Paris, 2006.

[14]   ESource, Who's Buying CFLs? Who's Not Buying Them? Findings from a Large-Scale, Nationwide Survey, 2008 ACEEE Summer Study.

[15]   V. Letschert, Potential Impact of Adopting Maximum Technologies as Minimum Efficiency Performance Standards in the U.S. Residential Sector, eScholarship, 2010.

[16]   LCD TV Market Growing Despite Weakness in North America; LED-Backlit Set to Take Lead in 2011, available online at: http://www.displaysearch.com/.

[17]   The Economist, Pocket World in Figures 2006 and 2010.

[18]   World Development Indicators, World Bank Group, 2010.

[19]   Canadian laptop ownership, IPSOS, 2009, available online at http://www.ipsos-na.com/news-polls/.

[20]   2008 could be the year laptop sales eclipse desktops in US, January 2008, available online at: http://arstechnica.com.

[21]   Gartner Says Worldwide PC Market Grew 13 Percent in 2007, January 2008, available online at: http://www.gartner.com/it/page.jsp?id=584210.

[22]   Natural Resources Canada, Energy Consumption of Major Household Appliances Shipped in Canada-Trends for 1990-2006, December 2008.

[23]   A. M. Jungreis and A. W. Kelley, "Adjustable speed drive for residential applications," *Industry Applications, IEEE Transactions on,* vol. 31, pp. 1315-1322, 1995.

[24]   IEEE Standard Definitions for the Measurement of Electric Power Quantities Under Sinusoidal, Nonsinusoidal, Balanced, or Unbalanced Conditions, IEEE Std 1459-2010 (Revision of IEEE Std 1459-2000) , vol., no., pp.1-40, March 19 2010.

[25]   A. Nassif, Modeling, measurement and mitigation of power system harmonics, PhD Thesis. University of Alberta, Fall 2009.

[26]   Clément C. Lefebvre, Electric Power: Generation, Transmission And Efficiency, Nova Science Publishers, Inc, 2008.

[27]   A. Capasso*, et al.*, "A bottom-up approach to residential load modeling," *Power Systems, IEEE Transactions on,* vol. 9, pp. 957-964, 1994.

[28]   I. Richardson*, et al.*, "Domestic electricity use: A high-resolution energy demand model," *Energy and Buildings,* vol. 42, pp. 1878-1887, 2010.

[29]   C. Walker and J. Pokoski, "Residential load shape modelling based on customer behavior," *Power Apparatus and Systems, IEEE Transactions on,* pp. 1703-1711, 1985.

[30]   Ipsos-RSL and Office for National Statistics, United Kingdom Time Use Survey, 3rd ed., UK Data Archive, Colchester, Essex, September 2003.

[31]   R. Hendron, Building America Research Benchmark Definition, Technical Report NREL/TP-550-40968, January 2007.

[32]   M. Armstrong, M. Swinton, H. Ribberink, I. Beausoleil-Morrison and J. Millette, Synthetically derived profiles for representing occupant driven electric loads in canadian housing, Building Performance Simulation, vol. 2, pp. 15–30, 2009.

[33]   Bell, M. Swinton, M.C. Entchev, E. Gusdorf, J. Kalbfleisch, W. Marchand, R.G. Szadkowski, F., Development of Micro Combined Heat and Power Technology Assessment Capability at the Canadian Centre for Housing Technology, pp. 48. 2003-12-08.

[34]   CSA, Energy Consumption Test Methods for Household Dishwashers, CSA Standard CAN/CSA-C373-92, 1992.

[35]   CSA, Test Method for Measuring Energy Consumption and Drum Volume of Electrically Heated Household Tumble-Type Clothes Dryers, CSA Standard CAN/CSA-C361-92, 1992.

[36]   Natural Resources Canada, Photovoltaic Systems – A Buyer's Guide, ISBN 0-662-31120-5, 2002.

[37]   Natural Resources Canada, Micro-Hydropower Systems – A Buyer's Guide, ISBN 0-662-35880-5, 2004.

[38]   Statistics Canada, Selected dwelling characteristics and household equipment, available online at: http://www40.statcan.gc.ca/l01/cst01/famil09b-eng.htm.

[39]   I.T. Jolliffe, Principal Component Analysis, by Springer-Verlag New York Inc, 1986.

[40]   J. R. Acharya, *et al.*, "Temporary Overvoltage and GPR Characteristics of Distribution Feeders With Multigrounded Neutral," *Power Delivery, IEEE Transactions on,* vol. 25, pp. 1036-1044, 2010.

[41]   Electric Power Distribution Handbook T. A. Short CRC Press 2003.

[42]   [30]   Hopkinson, F. H., "Approximate Distribution Transformer Impedances," General Electric Internal Memorandum, 1976. As cited by Kersting, W. H. and Phillips, W. H., "Modeling and Analysis of Unsymmetrical Transformer Banks Serving Unbalanced Loads," Rural Electric Power Conference, 1995.

[43]   J. Acharya, Power Quality Characteristics of MGN Distribution Systems, PhD Thesis. University of Alberta, Fall 2010.

[44]   R. Arseneau, *et al.*, "Application of IEEE standard 519-1992 harmonic limits for revenue billing meters," *Power Delivery, IEEE Transactions on,* vol. 12, pp. 346-353, 1997.

[45] "IEEE Recommended Practice for Establishing Transformer Capability When Supplying Non-sinusoidal Load Currents," *IEEE Std C57.110-1998,* p. i, 1998.

[46] "IEEE Guide for the Application of Neutral Grounding in Electrical Utility Systems, Part IV - Distribution," *IEEE Std C62.92.4-1991,* p. 0_1, 1992.

[47] J. Burke and M. Marshall, "Distribution system neutral grounding," in *Transmission and Distribution Conference and Exposition, 2001 IEEE/PES*, 2001, pp. 166-170 vol.1.

[48] M. K. Meyers, K. Schneider, R. Pratt, "Impacts Assessment of Plug-in Hybrid Vehicles on Electric Utilities and Regional US Power Grids Part 1: Technical Analysis," Pacific Northwest National Laboratory, Nov 2007.

[49] M. J. Scott, M. K. Meyers, D. B. Elliott, W. M. Warwick, "Impacts Assessment of Plug-in Hybrid Vehicles on Electric Utilities and Regional US Power Grids Part 2: Economic Assessment," Pacific Northwest National Laboratory, Nov 2007.

[50] S. W. Hadley, A. Tsvetkova, "Potential Impacts of Plug-in Hybrid Electric Vehicles on Regional Power Generation," ORNL/TM-2007/150, Jan 2008.

[51] J. Taylor*, et al.*, "Evaluation of the impact of plug-in electric vehicle loading on distribution system operations," in *Power & Energy Society General Meeting, 2009. PES '09. IEEE*, 2009, pp. 1-6.

[52] R. C. Green*, et al.*, "The impact of plug-in hybrid electric vehicles on distribution networks: a review and outlook," in *Power and Energy Society General Meeting, 2010 IEEE*, 2010, pp. 1-8.

[53] "Environmental Assessment of Plug-in Hybrid Electric Vehicles Volume 1: Nationwide Greenhouse Gas Emissions," EPRI TR-1015325, July 2007.

[54] "Environmental Assessment of Plug-in Hybrid Electric Vehicles Volume 2: United States Air Quality Analysis Based on AEO-2006 Assumptions for 2030," EPRI TR-1015326, July 2007.

[55] K. Clement*, et al.*, "Stochastic analysis of the impact of plug-in hybrid electric vehicles on the distribution grid," in *Electricity Distribution - Part 2, 2009. CIRED 2009. The 20th International Conference and Exhibition on*, 2009, pp. 1-1.

[56] S. Shengnan*, et al.*, "Challenges of PHEV penetration to the residential distribution network," in *Power & Energy Society General Meeting, 2009. PES '09. IEEE*, 2009, pp. 1-8.

[57] U.S. Department of Transportation, http://www.dot.gov/.

[58] U.S. Department of Transportation Federal Highway Administration, http://www.fhwa.dot.gov/ctpp/jtw/contents.htm.

[59] P. Mohseni and R. G. Stevie, "Electric vehicles: Holy grail or Fool's gold," in *Power & Energy Society General Meeting, 2009. PES '09. IEEE*, 2009, pp. 1-5.

[60] Q. Kejun*, et al.*, "Modeling of Load Demand Due to EV Battery Charging in Distribution Systems," *Power Systems, IEEE Transactions on,* vol. 26, pp. 802-810, 2011.

[61] Day-ahead Electricity Prices for Ameren Illinois Rate Zone I, https://www2.ameren.com/ RetailEnergy/realtimeprices.aspx.

[62] K. Clement-Nyns*, et al.*, "The Impact of Charging Plug-In Hybrid Electric Vehicles on a Residential Distribution Grid," *Power Systems, IEEE Transactions on,* vol. 25, pp. 371-380, 2010.

[63] E. Sortomme*, et al.*, "Coordinated Charging of Plug-In Hybrid Electric Vehicles to Minimize Distribution System Losses," *Smart Grid, IEEE Transactions on,* vol. 2, pp. 198-205, 2011.

[64] J. A. Orr*, et al.*, "Current Harmonics Generated by a Cluster of Electric Vehicle Battery Chargers," *Power Apparatus and Systems, IEEE Transactions on,* vol. PAS-101, pp. 691-700, 1982.

[65] Society of Automotive Engineers; Craig B. Toepfer, "SAE Electric Vehicle Conductive Charge Coupler, SAE J1772", California Air Resources Board, 2001-09-27.

[66] H. E. Mazin*, et al.*, "A Study on the Harmonic Contributions of Residential Loads," *Power Delivery, IEEE Transactions on,* vol. 26, pp. 1592-1599, 2011.

[67] Society of Automotive Engineers; Craig B. Toepfer, "SAE Electric Vehicle Conductive Charge Coupler, SAE J1772", California Air Resources Board, 2001-09-27.

Appendix A

Measurement Results of Home Appliances

This appendix presents the harmonic spectrum data of various home appliances that were referred through this thesis. Twelve compact fluorescent lamps commonly available in the Canadian retail stores were selected for investigation. They are all designed to operate at 60Hz, 120V, and have power consumption ratings of 5W to 30W. The lamps are listed in Table A.1. Note that the lamps are assigned with a code for easy identification. The lamps' powers are the last two numeric digits of their names and codes.

Table A.1 The twelve measured CFLs.

No.	Code	CFL Brand/Name	No.	Code	CFL Brand/Name
1	CFL P 15	Compact Phillips 15W	7	CFL S 30	Compact Sylvania 30W
2	CFL G 13	Compact Greenlight 13W	8	CFL G 10	Compact GE 10W
3	CFL N 09	Compact NOMA 9W	9	CFL G 26	Compact GE 26W
4	CFL G 23	Compact Globe 23W	10	CFL P 05	Compact Phillips 5W
5	CFL S 13	Compact Sylvania 13W	11	CFL P 27	Compact Phillips 27W
6	CFL S 27	Compact Sylvania 27W	12	CFL P 14	Compact Phillips 14W

The spectrum is presented in Table A.2.

Table A.2 Detailed harmonic currents absorbed by the measured CFLs (all values in amperes).

H	CFL P 15	CFL G 13	CFL N 09	CFL G 23	CFL S 13	CFL S 27	CFL S 30	CFL G 10	CFL G 26	CFL P 05	CFL P 27	CFL P 14
1	0.156	0.133	0.094	0.260	0.111	0.288	0.288	0.086	0.270	0.047	0.240	0.131
3	0.125	0.096	0.067	0.172	0.088	0.205	0.208	0.066	0.191	0.037	0.189	0.101
5	0.091	0.060	0.042	0.095	0.064	0.123	0.128	0.043	0.118	0.027	0.132	0.067
7	0.070	0.052	0.034	0.050	0.054	0.079	0.084	0.036	0.101	0.022	0.100	0.057
9	0.050	0.039	0.024	0.029	0.051	0.031	0.037	0.033	0.072	0.015	0.070	0.051
11	0.030	0.020	0.011	0.049	0.041	0.030	0.025	0.022	0.034	0.010	0.037	0.035
13	0.020	0.017	0.011	0.044	0.030	0.036	0.034	0.015	0.032	0.006	0.027	0.025
15	0.018	0.014	0.009	0.040	0.026	0.035	0.031	0.015	0.024	0.005	0.025	0.023
17	0.013	0.012	0.008	0.032	0.027	0.036	0.034	0.012	0.023	0.004	0.021	0.018
19	0.012	0.013	0.009	0.028	0.025	0.030	0.028	0.010	0.025	0.004	0.024	0.015
21	0.014	0.012	0.008	0.028	0.022	0.025	0.025	0.010	0.022	0.003	0.026	0.014
23	0.015	0.013	0.009	0.035	0.021	0.017	0.019	0.007	0.027	0.003	0.027	0.010
25	0.018	0.016	0.009	0.041	0.020	0.017	0.014	0.006	0.028	0.004	0.029	0.007
27	0.018	0.013	0.007	0.034	0.018	0.023	0.017	0.006	0.024	0.004	0.026	0.006
29	0.018	0.012	0.007	0.025	0.017	0.027	0.018	0.005	0.023	0.004	0.024	0.006

The following traditional lamps were selected for measurements:

- Electronic Ballast Tube Phillips cool white 15W – EBc P 15

- Electronic Ballast Tube Phillips ALTO 15W – EBa P 15

- Electronic Ballast Tube Phillips soft white 15W – EBs P 15

- Magnetic Ballast Tube Phillips ALTO 15W – MBa P 15

- Incandescent Phillips 60W – Inc P 60

Table A.3 shows the magnitude and angle characteristics of the five measured lamps. This table also provides information such as THD_I and measured input total RMS power.

Table A.3 Characteristics of the measured lamps.

Appliances	EBc P 15		EBa P 15		EBs P 15		MBa P 15		Inc P 60	
Operating Power (W)	17		17		16		33		59	
THD$_I$ (%)	145.36		133.7		138.22		7.86		3.73	
	Mag. (A)	Angle (deg)	Mag. (A)	Angle (deg)	Mag. (A)	Angle (deg)	Mag. (A)	Angle (deg)	Mag. (A)	Angle (deg)
H1	0.153	21.2	0.154	21.7	0.143	21.1	**0.731**	**-67.4**	**0.494**	**-0.05**
H3	0.124	53.9	0.123	56.6	0.117	53.7	0.057	144.0	0.012	-128.9
H5	0.087	105.5	0.088	106.7	0.083	101.5	0.004	178.7	0.011	-162.5
H7	0.069	169.4	0.068	170.2	0.067	165.1	0.005	-131.3	0.003	147.9
H9	0.067	-134.8	0.067	-132.4	0.066	-134.4	0.002	-46.2	0.002	143.3
H11	0.054	-84.2	0.053	-82.7	0.055	-80.1	0.003	-40.9	0.003	-47.4
H13	0.039	-21.8	0.039	-24	0.039	-25.3	0.001	18.7	0.002	70.1
H15	0.031	51.1	0.032	49.7	0.025	31.8	0.000	79.3	0.003	-78.4
H17	0.031	118.6	0.032	115.3	0.027	87.4	0.001	90.3	0.001	173.9
H19	0.026	-172.7	0.026	174.5	0.029	165.2	0.001	163.7	0.001	74.4
H21	0.019	-95.7	0.022	-118.1	0.025	-132.6	0.000	163.4	0.002	-112.6
H23	0.024	-31.5	0.023	-52	0.015	-87.8	0.001	-42.7	0.001	62.0
H25	0.025	61.8	0.02	14.9	0.023	-19.7	0.001	-56.8	0.001	-44.1
H27	0.025	142.1	0.016	82.3	0.012	37.7	0.001	117.6	0.001	-29.0
H29	0.02	-124.9	0.015	163.1	0.012	77.2	0.002	-7.9	0.001	-38.2

Three desktop computers were measured for this thesis:

- PC1: Intel Core 2 quad with dedicated video card and 4GB ram

- PC2: Intel Pentium IV HT, with 2 GB ram

- PC3: Intel Pentium IV, with 1 GB ram

PCs were measured under many typical conditions (reading DVDs, browsing internet, executing software, idling, etc – gaming and 3D tasks were not recorded). It was observed that, among the recorded conditions, the operating power did not vary significantly. Therefore, a random operating condition was selected to be presented here.

Table A.4 Characteristics of the measured PCs.

Appliances	PC 1		PC 2		PC 3	
Operating Power (W)	94		87.7		71.9	
THD$_I$ (%)	99.5		106		105	
	Mag. (A)	Angle (deg)	Mag. (A)	Angle (deg)	Mag. (A)	Angle (deg)
H1	0.823	0.5	0.759	4.1	0.623	9.6
H3	0.65	1.6	0.633	12.7	0.514	16.1
H5	0.407	3.6	0.425	23.5	0.338	28.3
H7	0.161	8.6	0.202	42.7	0.157	61.1
H9	0.099	58.1	0.033	116.6	0.058	148
H11	0.12	168.7	0.074	-172.9	0.089	-160
H13	0.118	178	0.084	-148.5	0.085	-133
H15	0.05	-170.2	0.045	-116.5	0.045	-79.7
H17	0.05	-64.8	0.012	-28.2	0.025	10.4
H19	0.07	-17.7	0.038	20.5	0.037	32.2
H21	0.041	-7.9	0.036	46.9	0.034	80.5
H23	0.025	12.6	0.015	89.4	0.02	145.5
H25	0.031	144.6	0.013	166.2	0.023	-154
H27	0.031	161.6	0.022	-154.7	0.027	-104
H29	0.011	171	0.017	-127.7	0.018	-75.8

Three of the five measured LCD monitors are presented in this section. They are:

- 22" wide-screen

- 19" full-screen

- 17" full-screen

Table A.5 shows the characteristics of the measured LCD monitors

Table A.5 Characteristics of the measured LCD monitors.

Appliances	LCD Monitor 1		LCD Monitor 2		LCD Monitor 3	
Operating Power (W)	31.2		24.9		38.8	
THD$_I$ (%)	118		104		96	
	Mag. (A)	Angle (deg)	Mag. (A)	Angle (deg)	Mag. (A)	Angle (deg)
H1	0.279	14.4	0.218	15	0.260	16.8
H3	0.230	34.7	0.170	32.7	0.201	40.5
H5	0.159	63.5	0.105	59.6	0.115	75.9
H7	0.100	108.7	0.051	103.5	0.042	135.6
H9	0.073	167.6	0.044	163.3	0.035	-156.2

H11	0.068	-141.7	0.047	-142.5	0.039	-104.8
H13	0.065	-105.5	0.041	-100.7	0.025	-65.4
H15	0.047	-59.8	0.024	-40.6	0.017	-5.37
H17	0.031	1.2	0.022	35.2	0.026	57.1
H19	0.032	44	0.024	74.9	0.016	104.9
H21	0.026	88.5	0.017	117.6	0.011	151.6
H23	0.018	139.6	0.010	175.5	0.014	-138.4
H25	0.012	-167.6	0.011	-120.6	0.013	-69.7
H27	0.011	-97.8	0.011	-64.4	0.009	-16.7
H29	0.009	-55.2	0.007	4.7	0.009	69.7

All the three laptop computers measured for this thesis can operate in two conditions, as described below. Condition 1 is a condition of higher power consumption, higher harmonic generation, and typically more time in operation. Therefore, the calculated indices were obtained for this condition.

- Condition 1: turned on and charging;

- Condition 2: turned off and charging.

Table A.6 Characteristics of the measured laptops.

Appliances	Laptop 1		Laptop 2		Laptop 3	
Operating Power (W)	55.5		68.9		70.7	
THD$_I$ (%)	127		133		151	
	Mag. (A)	**Angle (deg)**	**Mag. (A)**	**Angle (deg)**	**Mag. (A)**	**Angle (deg)**
H1	0.496	16.2	0.614	16.4	0.647	20.6
H3	0.397	47.1	0.502	51.6	0.512	65.7
H5	0.256	89.1	0.343	97.6	0.346	125.5
H7	0.173	154.1	0.253	161.9	0.292	-158.1
H9	0.172	-135.9	0.250	-136.4	0.313	-92.4
H11	0.178	-82.9	0.240	-86.5	0.298	-34.2
H13	0.149	-37.4	0.197	-36.9	0.264	27.3
H15	0.124	21.3	0.156	20.4	0.245	90.4
H17	0.116	77.4	0.135	78	0.225	150.3
H19	0.095	134	0.110	131.9	0.192	-149.1
H21	0.081	-171.7	0.083	-169.5	0.164	-84.8
H23	0.067	-110.1	0.067	-105	0.145	-21.8
H25	0.063	-50.6	0.060	-43.9	0.123	38.9
H27	0.055	6.11	0.046	13.5	0.097	102.4
H29	0.043	68.3	0.035	83.4	0.079	168.2

There is a variety of TVs available in the market today, e.g. LCD, Plasma, and CRT. All technologies are available in different resolutions (from 480i to 1080p). LCD TVs were measured because they are becoming the most popular technology in the Canadian market nowadays. Four of the measured LCD HDTVs are listed below. It was observed that their operating power almost does not change as the TV operates continuously, and therefore a random condition was chosen for analysis.

Table A.7 Characteristics of the measured LCD TVs.

Appliances	LCD TV 1		LCD TV 2		LCD TV 3		LCD TV 4	
Operating Power (W)	95.3		207		293		137	
THD$_I$ (%)	6.24		5.27		10.61		10.89	
	Mag. (A)	Angle (deg)	Mag. (A)	Angle (deg)	Mag. (A)	Angle (deg)	Mag. (A)	Angle (deg)
H1	0.797	4	1.740	9.5	2.646	6.1	1.186	2.97
H3	0.027	-22.2	0.067	47.4	0.218	51.4	0.101	172.4
H5	0.019	-155.6	0.054	-133.5	0.156	-150.2	0.026	-123.25
H7	0.017	-24.3	0.020	-161.9	0.046	-172.9	0.036	-9.63
H9	0.022	-148.5	0.005	-92	0.018	3.1	0.054	167.03
H11	0.004	3.75	0.005	26.6	0.021	14.4	0.029	-26.19
H13	0.009	-162	0.003	175.6	0.028	179.7	0.017	113.02
H15	0.009	56.2	0.004	25.5	0.030	3.5	0.007	-55.1743
H17	0.002	146.7	0.003	-147.6	0.016	-168.3	0.005	26.56824
H19	0.003	40.5	0.007	10.2	0.007	-31.4	0.006	-83.0711
H21	0.005	-61.4	0.010	-73.2	0.008	-143.1	0.005	-164.283
H23	0.004	-99.3	0.007	34.8	0.007	9.1	0.007	137.632
H25	0.002	-81.6	0.004	-79.8	0.003	152.4	0.008	-10.7418
H27	0.003	148.3	0.005	-178.8	0.008	59	0.001	115.4616
H29	0.004	124	0.002	-146.5	0.009	-89.5	0.006	-51.565

Two CRT TVs were measured for obtaining the results presented in Chapter 2. The production of CRT TVs is currently being superseded by the production of TVs of newer technologies, such as Plasma, LCD and LED. This device was studied because it is still in use in many typical residences, but it is likely that it will no longer be available in the future.

Table A.8 Characteristics of the measured CRT TVs.

Appliances	CRT TV 1		CRT TV 2	
Operating Power (W)	48.5		132	
THD$_I$ (%)	145.8		87.05	
	Mag. (A)	Angle (deg)	Mag. (A)	Angle (deg)
H1	0.398	5.2	1.082	-2.97
H3	0.356	10.8	0.813	-10.48
H5	0.309	18.4	0.411	-17.53
H7	0.246	26	0.046	-19.89
H9	0.184	33.5	0.141	144.45
H11	0.123	43.1	0.141	134.69
H13	0.066	55.2	0.044	111.92
H15	0.022	81.1	0.049	-42.4251
H17	0.011	-174.5	0.071	-62.7979
H19	0.022	-136.2	0.031	-93.4818
H21	0.024	-118.5	0.025	134.7567
H23	0.018	-112.9	0.041	102.6796
H25	0.008	-101.1	0.022	69.74248
H27	0.001	-112.5	0.015	-43.6578
H29	0.007	84.6	0.025	-87.8368

During the measurement of microwave ovens, it was observed that they exhibit primarily two states: on and off. What makes a difference among the different power levels is the time they are on; for example, when they are performing at 100%, their magnetron is on all the time; for lower power levels, the time when the magnetron operates is adequately timed. Three microwave ovens were measured.

Table A.9 Characteristics of the measured microwaves.

Appliances	Microwave 1		Microwave 2		Microwave 3	
Operating Power (W)	1097		999		1170	
THD$_I$ (%)	41.3		26.6		26.2	
	Mag. (A)	Angle (deg)	Mag. (A)	Angle (deg)	Mag. (A)	Angle (deg)
H1	9.770	-11.4	8.570	0.7	10.501	-4.07
H3	3.808	43.4	2.097	39.8	2.658	12.69
H5	1.130	-72.6	0.752	-64.1	0.442	-49.35
H7	0.417	156.3	0.366	132.3	0.454	74.4

H9	0.257	85	0.186	50.9	0.185	-17.07
H11	0.131	-4.9	0.125	-63.9	0.142	-174.91
H13	0.071	-102.8	0.080	-167	0.082	60.98
H15	0.061	-169.2	0.052	98.1	0.063	-75.476
H17	0.037	75.1	0.045	-4.4	0.050	-175.542
H19	0.041	-21.1	0.034	-121.2	0.034	51.08047
H21	0.039	-123.4	0.027	133.9	0.032	-77.1846
H23	0.033	131.8	0.022	30	0.024	135.0022
H25	0.030	50.9	0.021	-75.4	0.023	33.68759
H27	0.028	-42.6	0.020	179	0.019	-110.168
H29	0.025	-138.3	0.015	70.6	0.019	137.5356

Three ASD-based high-end refrigerators were measured. They were measured for over 6 hours in order to capture their whole operating cycle. It was observed that they show typically 4-5 duty cycles, and that they repeat every 2-3 hour periods when no human interaction with the device exists. The results are shown below.

Table A.10 Characteristics of the measured ASD-based fridges.

Appliances	ASD Fridge 1		ASD Fridge 2		ASD Fridge 3	
Operating Power (W)	275		272		350	
THD$_I$ (%)	5.8		6.5		7.19	
	Mag. (A)	**Angle (deg)**	**Mag. (A)**	**Angle (deg)**	**Mag. (A)**	**Angle (deg)**
H1	2.32	-7.0	2.27	-0.9	2.95	-12.0
H3	0.09	-131.3	0.08	-118.2	0.14	-128.6
H5	0.06	-131.1	0.12	-134.6	0.07	-123.2
H7	0.08	64.4	0.06	100.8	0.11	97.2
H9	0.02	-3.0	0.01	172.2	0.03	54.5
H11	0.01	-88.5	0.01	-101.9	0.01	45.6
H13	0.03	-4.2	0.01	51.6	0.03	64.4
H15	0.01	-51.5	0.01	-111.0	0.01	71.9
H17	0.00	-44.6	0.00	-13.4	0.01	137.5
H19	0.00	1.2	0.01	167.9	0.01	147.9
H21	0.00	-12.9	0.01	-41.5	0.01	165.4
H23	0.00	32.52	0.00	124.5	0.01	176.0
H25	0.00	-55.8	0.01	-99.5	0.00	-154.5
H27	0.00	52.6	0.00	93.0	0.00	-113.3
H29	0.00	47.9	0.00	-149.5	0.00	-50.7

Sample results of two of the measured regular refrigerators are presented in this subsection. The regular refrigerators are, however, will be reduced in production to give place to the newer technology ASD-based refrigerators. Today, they still represent the majority of refrigerator loads in most typical customers. The measurements results for a freezer are also presented.

Table A.11 Characteristics of the measured regular fridges and freezer.

Appliances	Regular Fridge 1		Regular Fridge 2		Freezer	
Operating Power (W)	150		110		114	
THD$_I$ (%)	18		26.5		19.6	
	Mag. (A)	Angle (deg)	Mag. (A)	Angle (deg)	Mag. (A)	Angle (deg)
H1	1.275	-19.7	1.033	-26.66	1.101	-29.22
H3	0.060	-131.6	0.163	-153.83	0.175	-128.22
H5	0.170	173.5	0.183	-147.97	0.097	-169.94
H7	0.076	34.4	0.100	134.34	0.068	113.99
H9	0.007	5	0.045	94.61	0.029	79.26
H11	0.034	-129	0.047	-126.11	0.026	-128.5
H13	0.022	76	0.013	-26.5	0.007	4.06
H15	0.004	145.1	0.016	-142.526	0.011	-136.549
H17	0.012	-37.9	0.012	-134.182	0.007	-141.829
H19	0.007	146	0.004	101.9487	0.005	84.33337
H21	0.002	-155.3	0.007	21.23837	0.005	14.2711
H23	0.004	34.4	0.004	-48.7149	0.001	-56.4178
H25	0.002	-126.1	0.002	-83.9743	0.002	-15.1549
H27	0.001	-100.6	0.001	-161.192	0.001	163.0479
H29	0.002	179.2	0.004	154.139	0.002	107.9156

The results of the measurements regarding one washer are shown below. It has been measured in different operating conditions: filling water, washing, rinsing, rinsing off, spinning, and fast spinning. It has been observed that the "rinsing" condition is the one that consumes the highest amount of power and it is as well the condition where the highest amount of harmonics is injected. The measured normalized spectrum is shown in Table A.12 shows the characteristics of one measured washer.

Table A.12 Characteristics of the measured washer.

Appliances	Washer	
Operating Power (W)	189	
THD$_I$ (%)	75.4	
	Mag. (A)	Angle (deg)
H1	2.310	-63.6
H3	1.538	164.5
H5	0.528	19.2
H7	0.289	126.1
H9	0.380	-19.7
H11	0.118	174.3
H13	0.180	-76.5
H15	0.192	147.5
H17	0.042	-91.1
H19	0.122	88.6
H21	0.105	-41.1
H23	0.021	25.6
H25	0.082	-101.9
H27	0.057	-63.5
H29	0.019	164.4

The characteristics of an ASD-based laundry dryer are shown below. The input voltage for the dryer is 240V, for this device is connected between the two hot conductors of the single-phase distribution transformers typically used in North America.

Table A.13 Characteristics of the measured ASD-based dryer.

Appliances	ASD Dryer	
Operating Power (W)	3600	
THD$_I$ (%)	1.55	
	Mag. (A)	Angle (deg)
H1	4.235	-168.5
H3	1.293	-65.7
H5	1.141	11.2
H7	0.988	88.2
H9	0.796	166.8
H11	0.590	-113.4
H13	0.415	-30.2
H15	0.259	57.7

H17	0.163	155.0
H19	0.120	-96.3
H21	0.104	8.3
H23	0.091	101.5
H25	0.070	-169.9
H27	0.044	-78.7
H29	0.023	32.8

Table below shows the characteristics of one measured dryers. Differently from the ASD-based case, the regular dryers do not have an ASD, and no significant harmonics were noticed in their measurements.

Table A.14 Characteristics of the measured regular dryer.

Appliances	Regular Dryer	
Operating Power (W)	4180	
THD$_I$ (%)	1.37	
	Mag. (A)	**Angle (deg)**
H1	20.2	38.7
H3	0.1936	110.1
H5	0.1673	-176.1
H7	0.0504	-101.7
H9	0.0060	-26.6
H11	0.0544	49.9
H13	0.0464	129.9
H15	0.0060	-145.7
H17	0.0181	-51.4
H19	0.0121	52.6
H21	0.0101	153.6
H23	0.0121	-115.3
H25	0.0121	-30.8
H27	0.0121	57.1
H29	0.0101	157.9

One installed fully-operating heat pump was measured at the service panel of one house. Its normalized spectra are shown below. The presented results are for the condition that it consumed the largest observed amount of power.

Table A.15 Characteristics of the measured furnace.

Appliances	Furnace	
Operating Power (W)	535	
THD$_I$ (%)	10.5	
	Mag. (A)	**Angle (deg)**
H1	5.160	-33
H3	0.505	-159.4
H5	0.199	78.6
H7	0.049	141.5
H9	0.027	-30.8
H11	0.020	-131.7
H13	0.006	-78.7
H15	0.004	125.7
H17	0.006	-0.1
H19	0.002	-179.2
H21	0.001	45
H23	0.003	-120.9
H25	0.001	94.1
H27	0.004	55
H29	0.001	-3.1

The results of the measurements regarding two vacuum cleaners are shown below.

Table A.16 Characteristics of the measured vacuum cleaners.

Appliances	Central Vacuum		Vacuum	
Operating Power (W)	1391		1237	
THD$_I$ (%)	18.9		13.7	
	Mag. (A)	**Angle (deg)**	**Mag. (A)**	**Angle (deg)**
H1	11.899	-11.64	10.512	-10.52
H3	2.175	-52.9	1.374	-45.02
H5	0.426	-151.68	0.283	-165.33
H7	0.310	108.53	0.251	106.28
H9	0.159	57.18	0.138	61.16
H11	0.063	-52.39	0.044	-65.05
H13	0.042	-93.63	0.043	-134.5
H15	0.021	178.1405	0.036	149.9256
H17	0.009	115.7534	0.027	52.77027
H19	0.005	61.45979	0.003	-51.9998

H21	0.006	-23.4564	0.009	87.38214
H23	0.010	-51.5998	0.005	95.82058
H25	0.020	175.1229	0.009	71.12443
H27	0.023	-179.332	0.025	7.814747
H29	0.004	-176.768	0.022	-11.1674

The results of the measurements regarding a garage door are shown below.

Table A.17 Characteristics of the measured garage door.

Appliances	**Garage Door**	
Operating Power (W)	472	
THD$_I$ (%)	14	
	Mag. (A)	**Angle (deg)**
H1	4.768	-30.776
H3	0.589	-85.8419
H5	0.301	163.0407
H7	0.017	22.70653
H9	0.082	92.86342
H11	0.032	-162.285
H13	0.026	-1.61705
H15	0.026	-164.442
H17	0.012	-118.912
H19	0.012	100.6087
H21	0.010	44.38272
H23	0.007	30.89911
H25	0.007	-119.932
H27	0.002	166.9353
H29	0.005	147.7294

The results of the measurements regarding two blender models, one bread maker and one food processor are shown below.

Table A.18 Characteristics of the measured appliances.

Appliances	Blender 1		Blender 2		Bread Maker		Food Processor	
Operating Power (W)	157		80.7		80.1		193	
THD$_I$ (%)	10		10		12.4		15.8	
	Mag. (A)	Angle (deg)	Mag. (A)	Angle (deg)	Mag. (A)	Angle (deg)	Mag. (A)	Angle (deg)
H1	1.313	-13.6535	0.681	-13.9013	0.936	-45.508	1.616	-11.2292
H3	0.119	-54.903	0.062	-69.8059	0.110	-104.759	0.233	-54.3451
H5	0.047	-170.71	0.025	-154.567	0.029	162.25	0.076	-160.517
H7	0.017	100.1323	0.010	120.7956	0.017	91.34587	0.068	121.5488
H9	0.015	55.72739	0.009	50.28692	0.013	24.95229	0.018	59.52841
H11	0.002	-68.5596	0.002	-45.8056	0.003	-48.5822	0.011	-48.5992
H13	0.005	-94.0848	0.003	-128.602	0.003	-112.668	0.005	-135.05
H15	0.002	-2.93683	0.003	166.2576	0.001	141.3312	0.005	-144.892
H17	0.002	163.6169	0.004	73.22285	0.002	136.4195	0.004	178.4611
H19	0.001	-83.4848	0.003	160.1062	0.002	-126.746	0.002	-19.9077
H21	0.004	86.86527	0.003	-72.7618	0.000	86.95087	0.002	71.69211
H23	0.003	-95.9076	0.001	-99.2194	0.001	-91.599	0.007	28.16899
H25	0.004	-74.727	0.002	-41.6223	0.001	-1.68401	0.004	-41.9755
H27	0.002	40.38974	0.001	-45.4804	0.001	-40.409	0.004	-14.503
H29	0.002	98.07048	0.001	95.84152	0.001	54.85701	0.003	69.53433

Appendix B

V x I Plot of Home Appliances

In this appendix, the correlation between supply voltage and current consumed by each appliance (V x I plot) analyzed in this thesis is presented in the following figures.
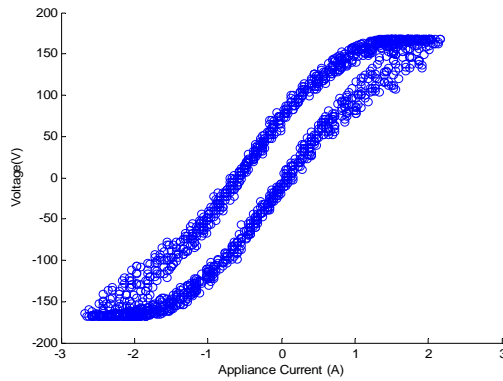
Blender V x I plot
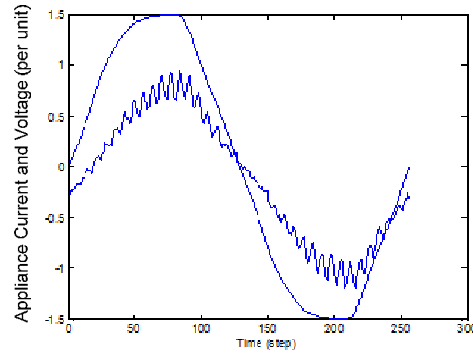
Blender V and I waveforms.
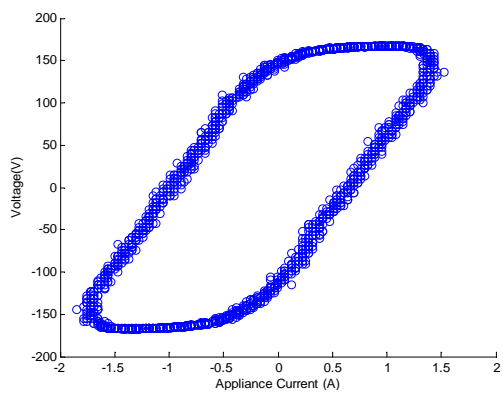
Bread maker V x I plot
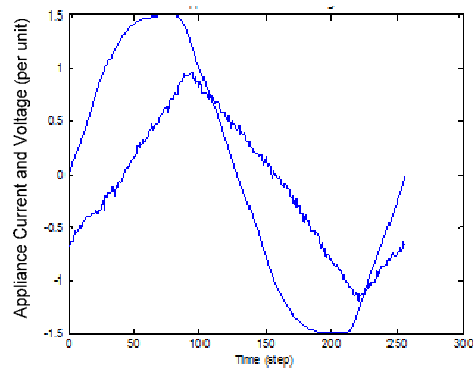
Bread maker V and I waveforms.
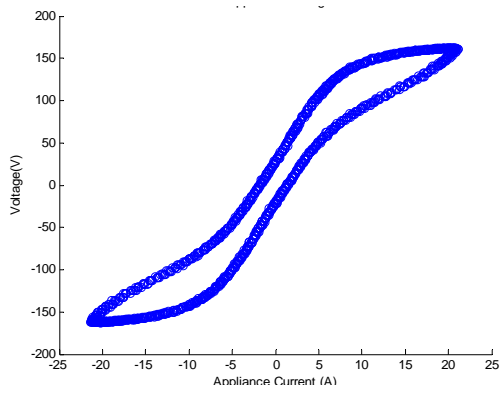
Central vacuum V x I plot
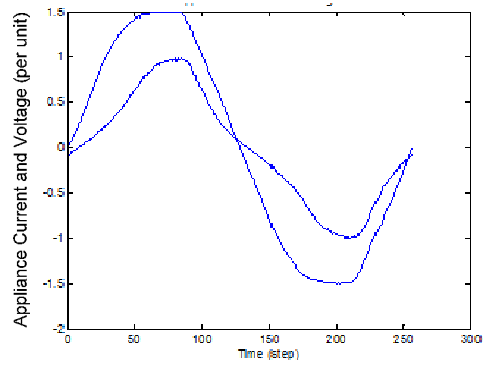
Central vacuum V and I waveforms.
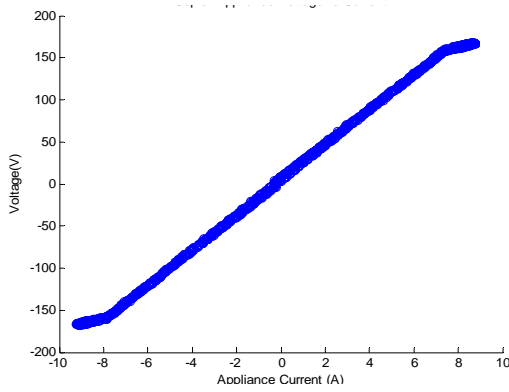

Copier V x I plot
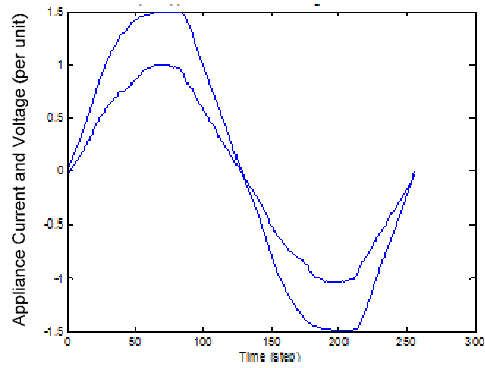
Copier V and I waveforms.
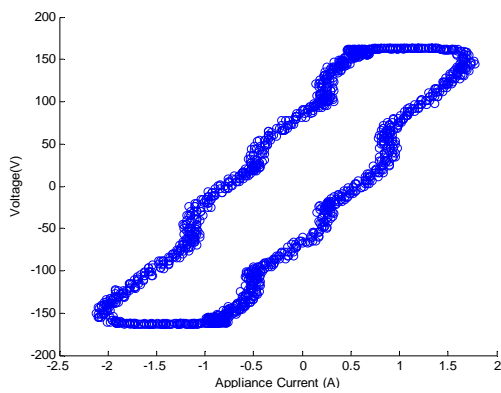
Freezer V x I plot
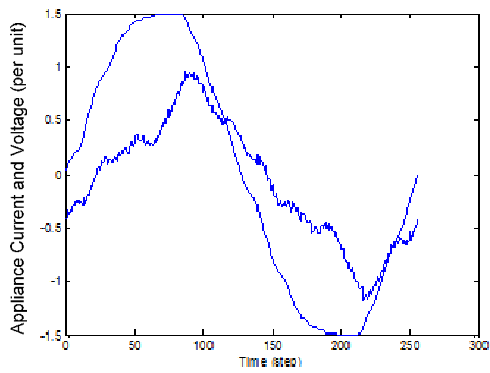
Freezer V and I waveforms.
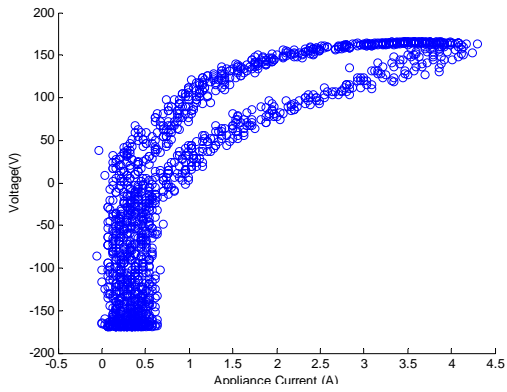
Food processor V x I plot
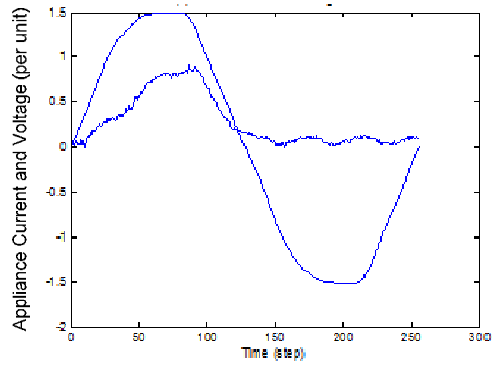
Food processor V and I waveforms.
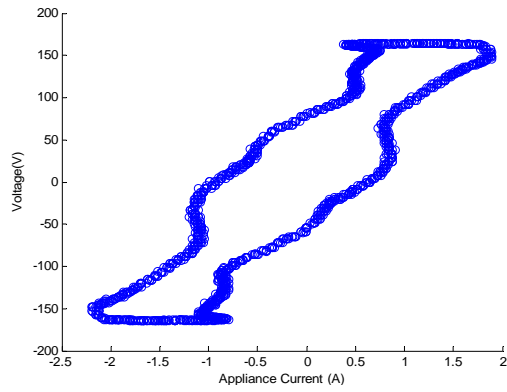
Fridge V x I plot
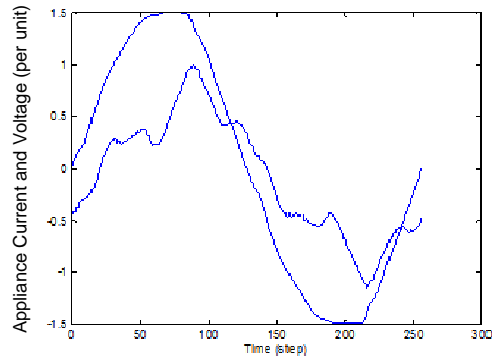
Fridge V and I waveforms.
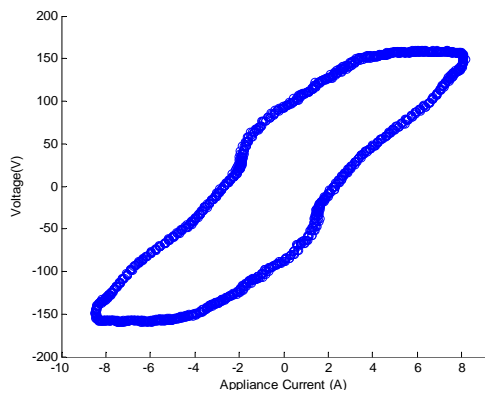
Garage door V x I plot
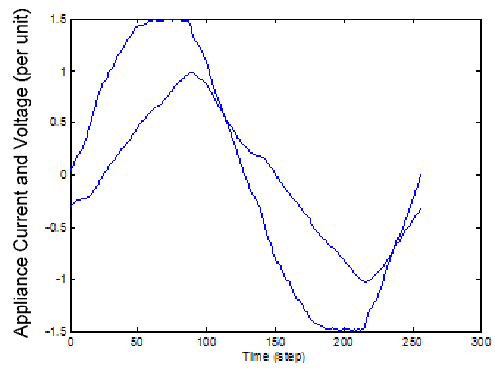
Garage door V and I waveforms.

218
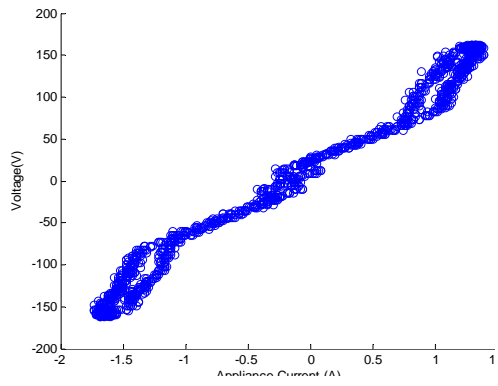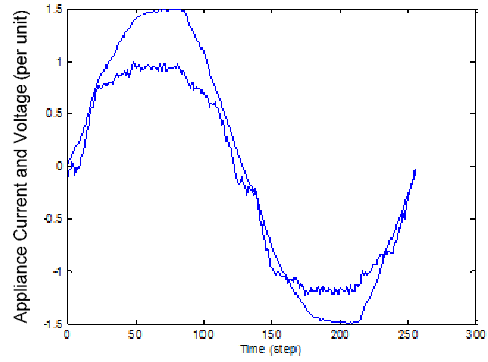
LCD TV V x I plot

LCD TV V and I waveforms.
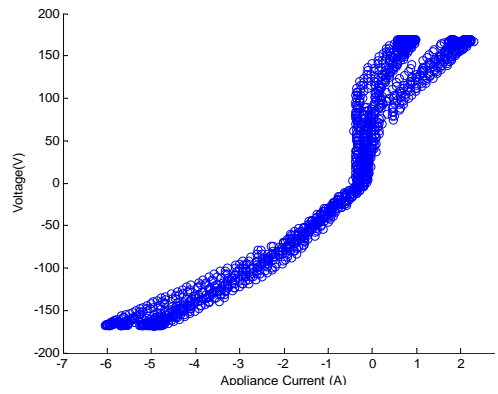
Printer V x I plot
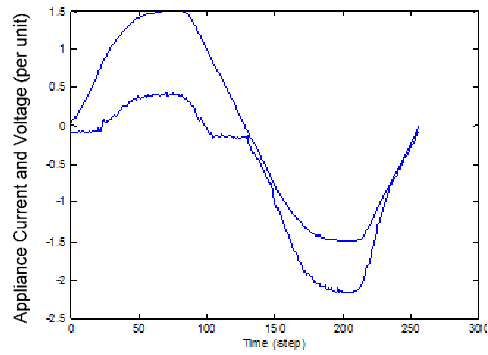
Printer V and I waveforms.
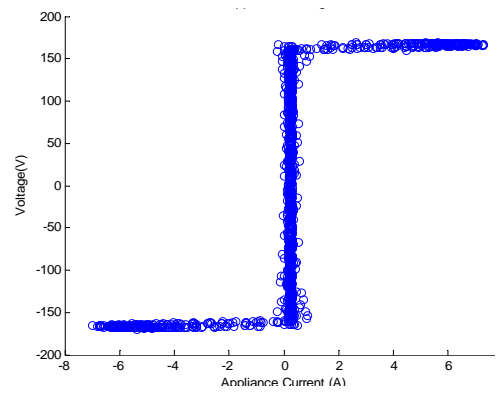
Treadmill V x I plot
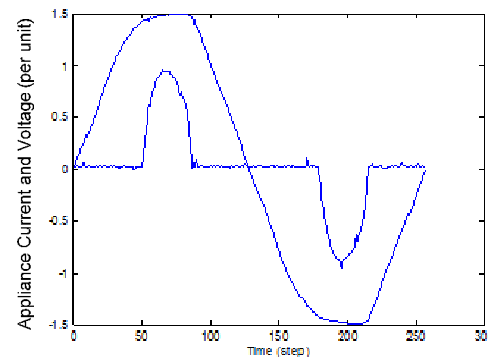
Treadmill V and I waveforms.
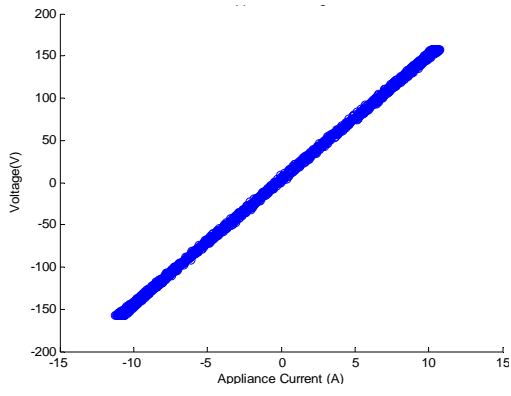
Waffle iron V x I plot
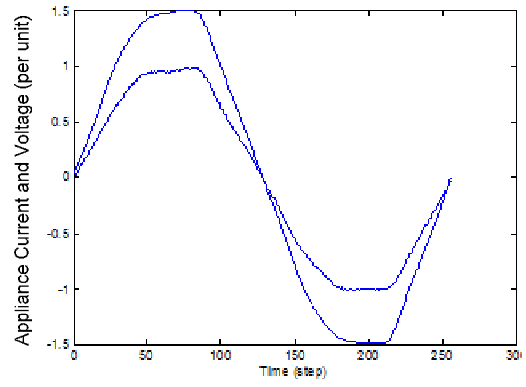
Waffle iron V and I waveforms.

Appendix C

Single House Equivalent Circuit Model

The appliances are essentially connected in a random fashion in the circuits, and this arrangement makes it difficult to represent in the modeling. To determine the harmonic contributions of the customer at the revenue meter point, the equivalent circuit model shown in Figure C.1 is used ([66]). On the load side, appliances are supplied with phase-to-neutral 120V (modeled by Z_1, Ic_1 and Z_2, Ic_2) and phase-to-phase 240V (modeled by Z_3). Normally, phase-to-phase connected loads are linear. Therefore, in this thesis, there are no current sources connected between phases.
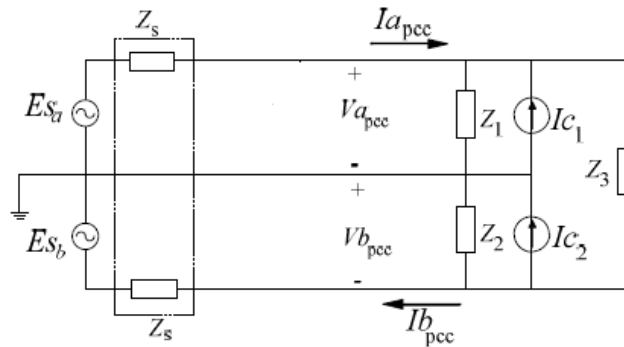
Figure C.1 Harmonic source equivalent model for three-wire single-phase systems.

In practical cases, voltage and current measurements are available only at the utility-interface point, so that only the phase currents Ia_{pcc} and Ib_{pcc} can be accessed, but not the currents flowing through the impedances Z_1, Z_2 and Z_3. This problem increases the complexity of estimating the customer side load impedances. In order to overcome this difficulty, a new equivalent model for the

two-branch load was developed in ([66]) and is presented in Figure C.2(a). Z_3 can be separated into two parts, as shown in Figure C.2.
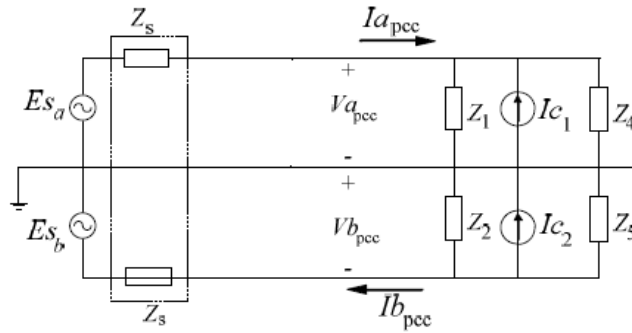
$$Z_4 = \frac{Va_{pcc}}{Va_{pcc} + Vb_{pcc}} \times Z_3$$

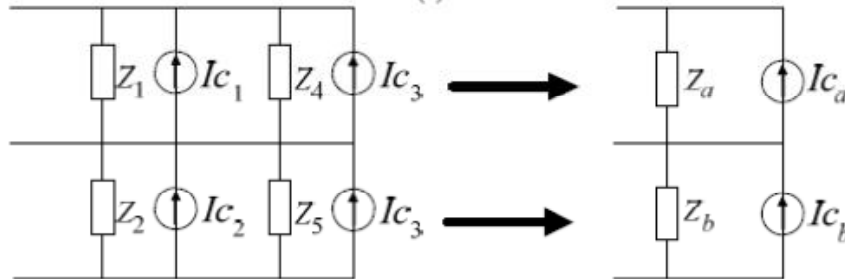$$Z_5 = \frac{Vb_{pcc}}{Va_{pcc} + Vb_{pcc}} \times Z_3$$

(D.1)

The load impedances for this system can be represented by two equivalent phase-to-neutral impedances, Z_a and Z_b, which can be calculated by using following equations:

$$Z_a = Z_1 // Z_4$$
$$Z_b = Z_2 // Z_5$$

(D.2)

(a) Approximation of the actual circuit

(b) Final equivalent circuit for customer side

Figure C.2 Proposed equivalent model for a single-phase two- branch system.

222

As a result, the entire house can be studied using a simple single-phase circuit shown in Figure C.3. In each simulation step, the connected linear appliance impedances are paralleled as new linear impedance $Z_{total}(h)$, and non-linear appliance current sources added up together as a new current source. As shown in Figure C.3, the outputs of interest from the simulation are $I_{total}(h)$, $I_{NL}(h)$ in both fundamental and harmonic and linear impedance of the house $Z_{total}(h)$.
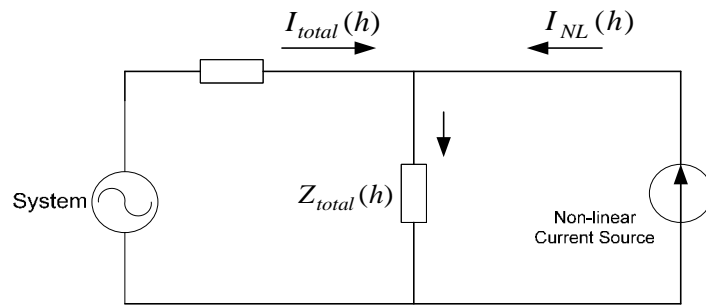

Figure C.3 Electrical system to simulate the harmonic load output from several appliances.

Appendix D

Service Transformers Field Measurements

Figures below show the fundamental and harmonic currents magnitude measured from 10 service transformers.
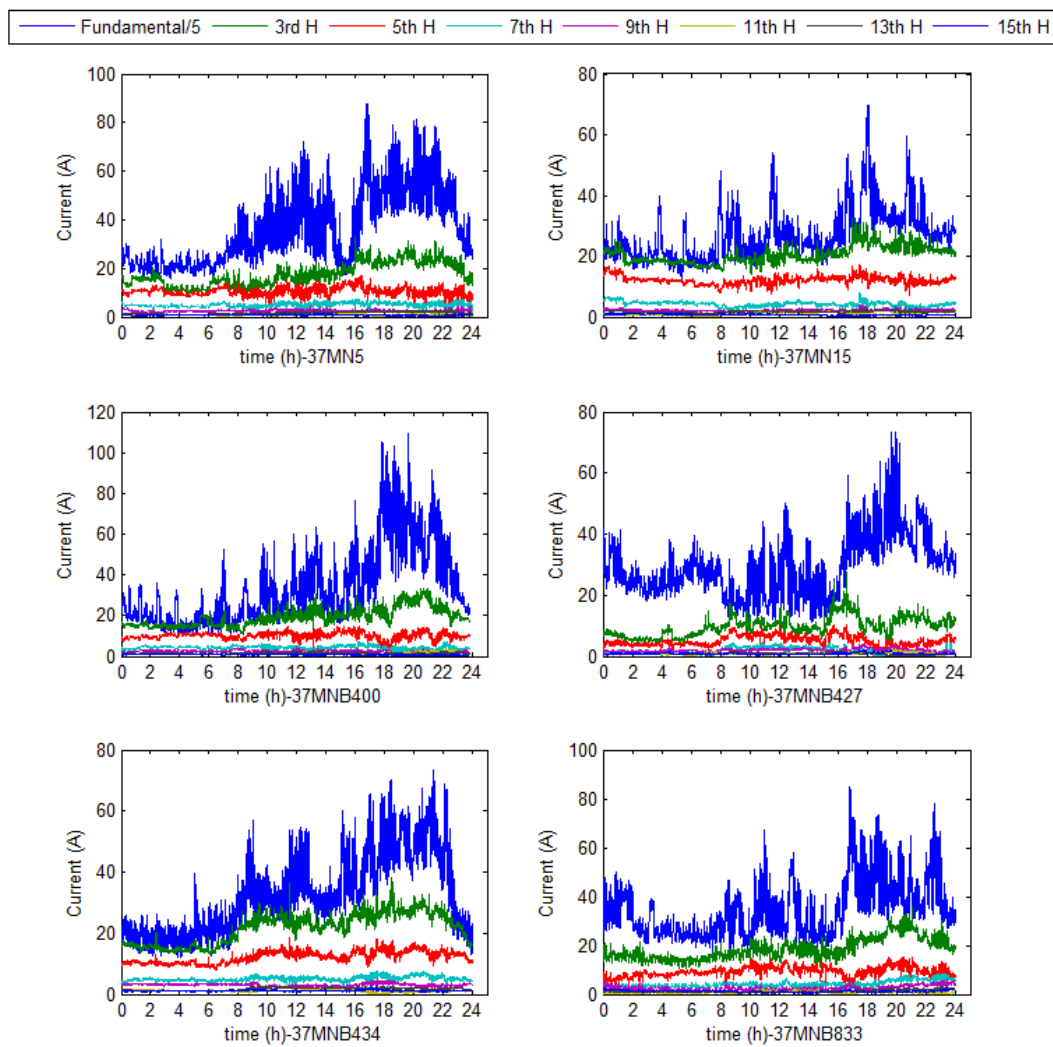
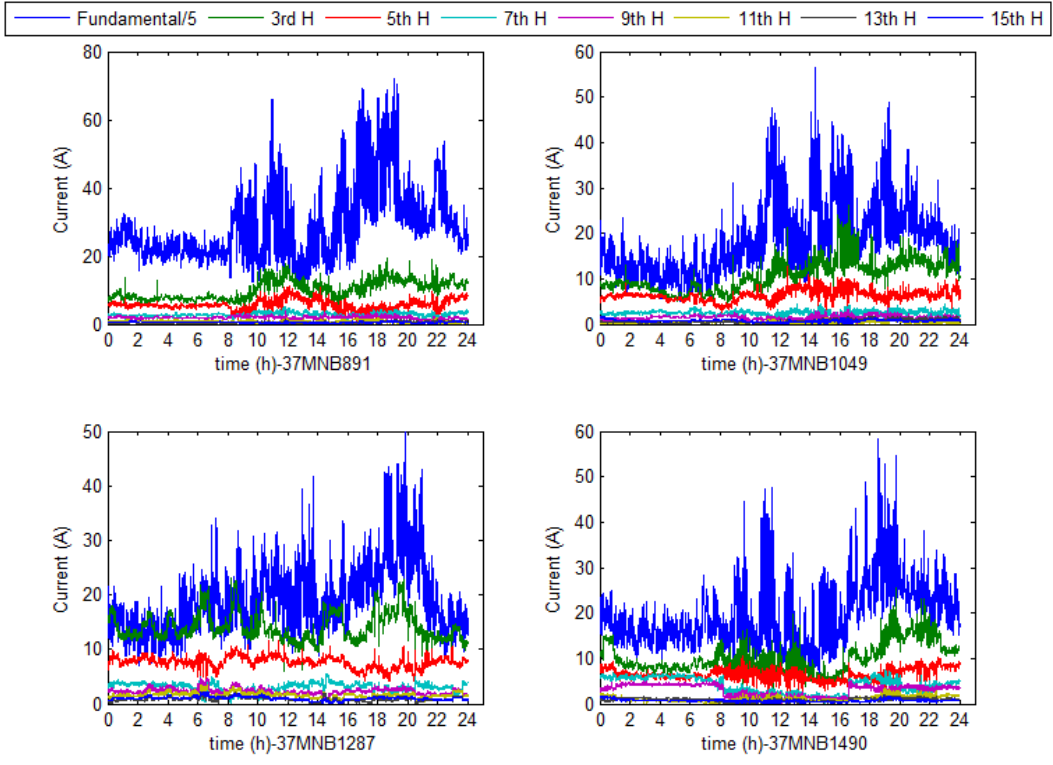Figure D.1 Field measurement results for 6 different service transformers.

Figure D.2 Field measurement results for 4 different service transformers.

Appendix E

Sensitivity Study for Market Trend Variation

The purpose of this sensitivity study is to verify the impact of varying market trends on load evolution study results. **Personal computer** market trends are assumed to be scaled based on the customer trend model proposed in Chapter 2, while the market trends for other appliances remain the same. Three PC market trends are applied in the study:

- **Case 1**: The annual growth rate of computers is 1.98%.
  The annual growth rate of laptops is 3.7%.
- **Case 2**: The annual growth rate of computers is 3.97%.
  The annual growth rate of laptops is 7.4%.
- **Case 3**: The annual growth rate of computers is **5.95%**.
  The annual growth rate of laptops is **11.1%**.

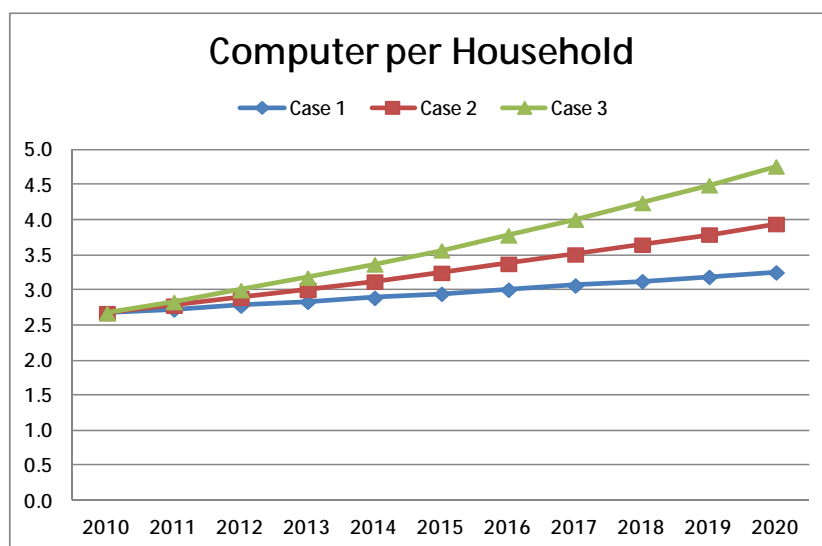Figures below show these different trends for computer related appliances:

Figure E.1 Different trends on the number of computers per household.
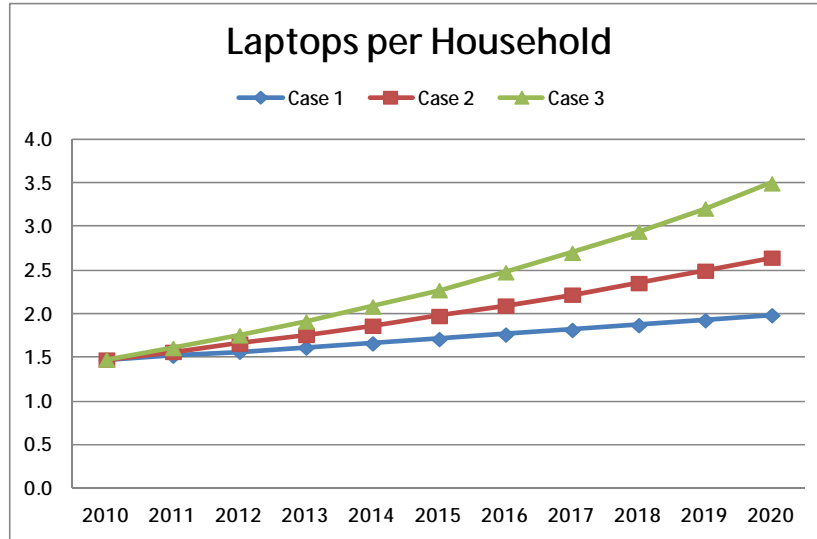
Figure E.2 Different trends on the number of laptops per household.
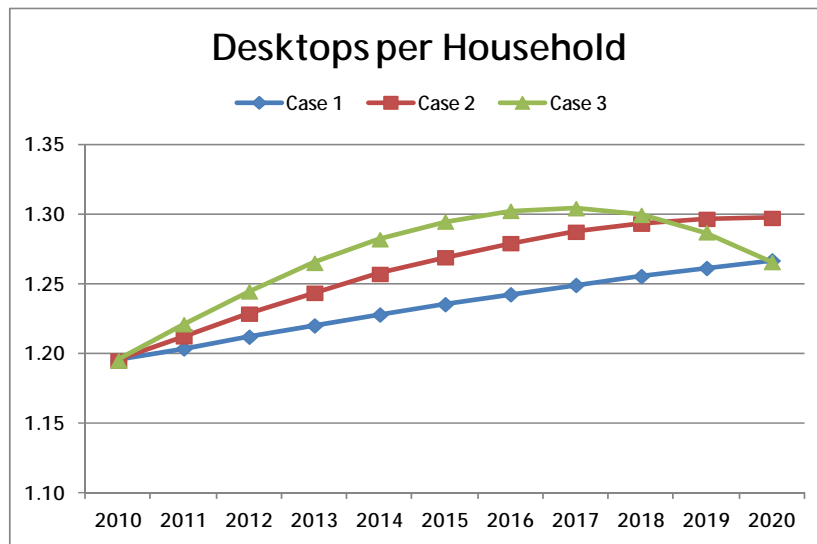

Figure E.3 Different trends on the number of desktops per household.

In the following step, the appliance loads are "evolved" or "grown" according to the market data, different PC market trends will be considered separately. The same as in Chapter 4, two load evolution scenarios are studied:

- *Natural Load Evolution.* This case considers the evolution or change of all home appliances per the market trend.
- *PC Load Evolution.* This case considers the situation where only PC related appliances are changed. Again this is a hypothetical case useful to understand the specific impact of PC loads.

As illustration purpose, we only show the impact of varying computer market trends on harmonic voltage and current distortion levels. The average annual growth rates associated to individual harmonic voltage/current and THDv/TDD at secondary houses with various PC market trends are shown in the following figures. Figure E.4 and Figure E.6 show harmonic voltage and current situation for the *Natural Load Evolution* scenario, while Figure E.5 and Figure E.7 are for the *PC Load Evolution* scenario.
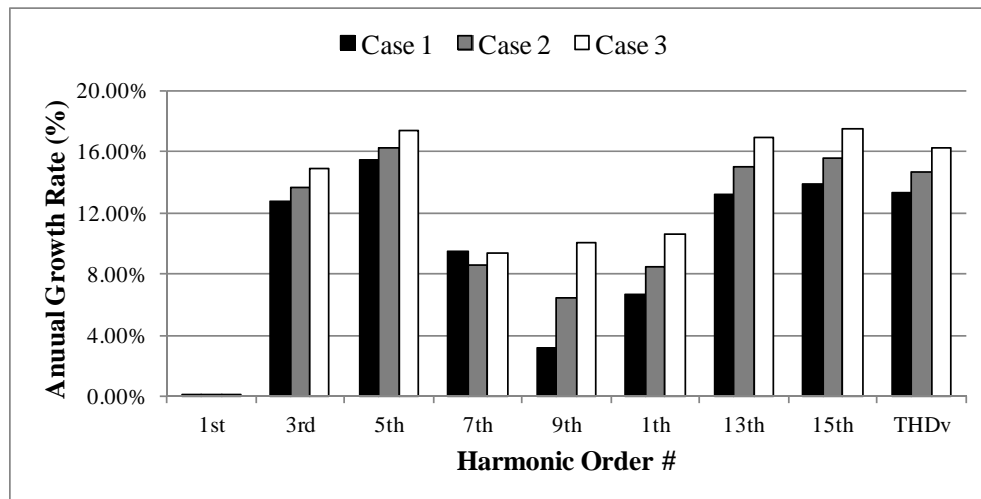
I. Harmonic Voltage Distortion Levels

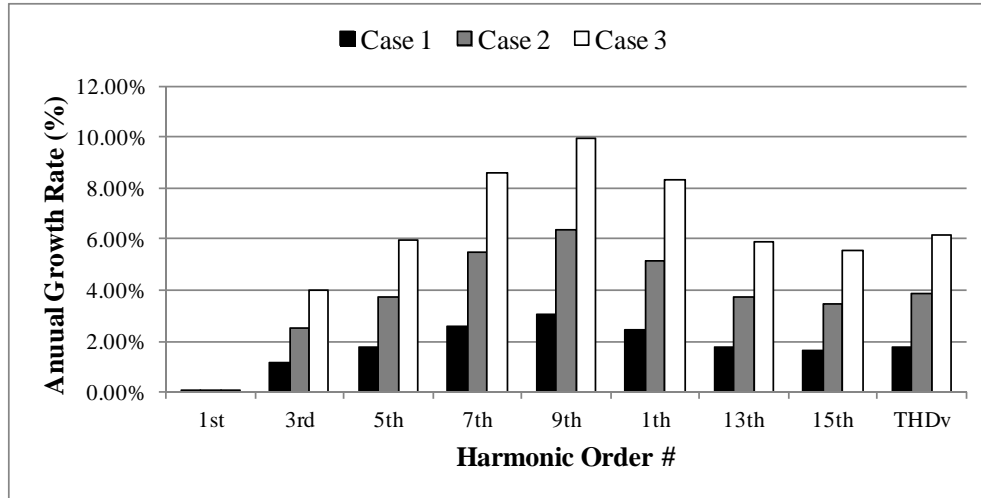Figure E.4 The annual growth rate of harmonic voltage for *Natural Load Evolution*

228

Figure E.5 The annual growth rate of harmonic voltage for *PC Load Evolution*
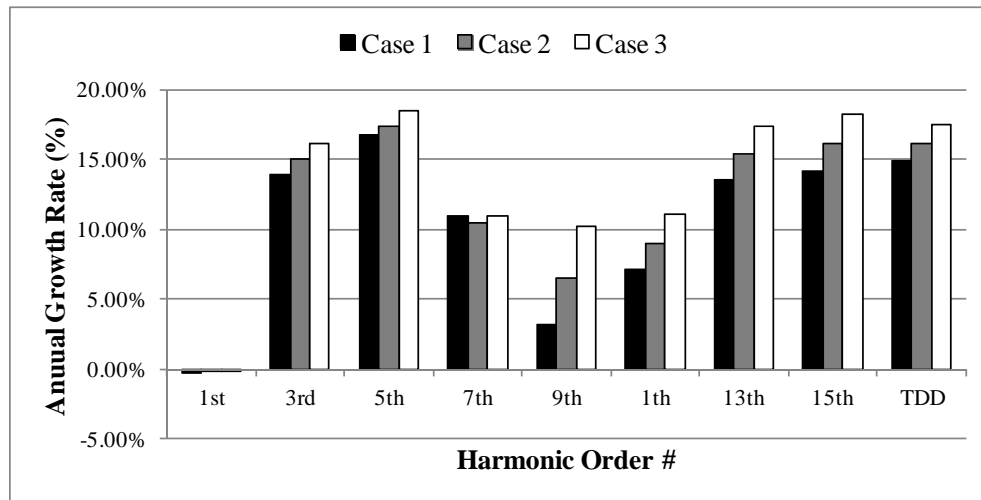
II. Harmonic Current Distortion Levels

Figure E.6 The annual growth rate of harmonic current for *Natural Load Evolution*
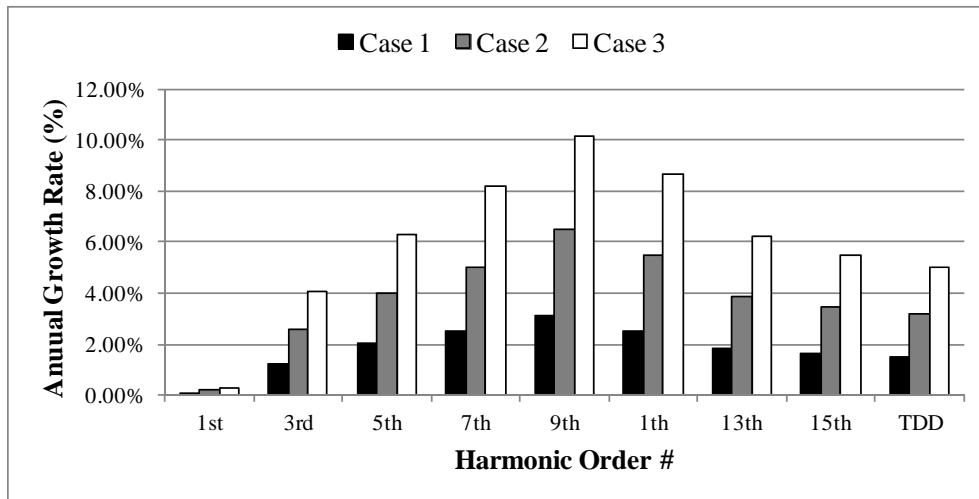
Figure E.7 The annual growth rate of harmonic current for *PC Load Evolution*